

July 28, 2008

Mr. Reginald Tyler
U.S. Department of Energy
Golden Field Office
1617 Cole Boulevard
Golden, CO 80401-3305

Dear Mr. Tyler:

Subject: EERC Center for Biomass Utilization[®] 2004–2005 Final Technical Report
DOE Agreement No. DE-FC36-03-GO13055

Please find enclosed the subject final report for the work performed by the Energy & Environmental Research Center (EERC) under DOE Agreement No. DE-FC36-03-GO13055. An electronic copy was uploaded to the Project Management site.

If you have any questions or comments, please contact me by phone at (701) 777-5123, by fax at (701) 777-5181, or by e-mail at czygarlicke@undeerc.org.

Sincerely,

Chris J. Zygarlicke
Deputy Associate Director for Research

CJZ/jre

Enclosure

c: Katherine Anagnost, EERC

EERC CENTER FOR BIOMASS UTILIZATION 2004–2005

Final Technical Report

(for the Period of Performance from June 1, 2005, through March 31, 2008)

Prepared for:

Reginald Tyler

U.S. Department of Energy
Golden Field Office
1617 Cole Boulevard
Golden, CO 80401-3305

DOE Agreement No. DE-FC36-03-GO13055

Prepared by:

Christopher J. Zygarlicke
Edwin S. Olson
Ted R. Aulich
Chad A. Wocken
Darren D. Schmidt
Kerryanne M. Leroux
Kirk D. Williams

Energy & Environmental Research Center
University of North Dakota
15 North 23rd Street, Stop 9018
Grand Forks, ND 58202-9018

EERC DISCLAIMER

LEGAL NOTICE This research report was prepared by the Energy & Environmental Research Center (EERC), an agency of the University of North Dakota, as an account of work sponsored by the U.S. Department of Energy (DOE) National Energy Technology Laboratory. Because of the research nature of the work performed, neither the EERC nor any of its employees makes any warranty, express or implied, or assumes any legal liability or responsibility for the accuracy, completeness, or usefulness of any information, apparatus, product, or process disclosed, or represents that its use would not infringe privately owned rights. Reference herein to any specific commercial product, process, or service by trade name, trademark, manufacturer, or otherwise does not necessarily constitute or imply its endorsement or recommendation by the EERC.

DOE DISCLAIMER

This report was prepared as an account of work sponsored by an agency of the United States Government. Neither the United States Government, nor any agency thereof, nor any of their employees makes any warranty, express or implied, or assumes any legal liability or responsibility for the accuracy, completeness, or usefulness of any information, apparatus, product, or process disclosed or represents that its use would not infringe privately owned rights. Reference herein to any specific commercial product, process, or service by trade name, trademark, manufacturer, or otherwise does not necessarily constitute or imply its endorsement, recommendation, or favoring by the United States Government or any agency thereof. The views and opinions of authors expressed herein do not necessarily state or reflect those of the United States Government or any agency thereof.

This report is available to the public from the National Technical Information Service, U.S. Department of Commerce, 5285 Port Royal Road, Springfield, VA 22161; phone orders accepted at (703) 487-4650.

ACKNOWLEDGMENT

This report was prepared with the support of the U.S. Department of Energy (DOE), Golden Field Office Cooperative Agreement No. DE-FC36-03-GO13055. However, any opinions, findings, conclusions, or recommendations expressed herein are those of the author(s) and do not necessarily reflect the views of DOE.

TABLE OF CONTENTS

LIST OF FIGURES	v
LIST OF TABLES	ix
EXECUTIVE SUMMARY	xiii
INTRODUCTION	1
Year 2004	1
Year 2005	2
GOAL	2
OBJECTIVES	2
YEAR 2004 – ACTIVITY 1 – ETHANOL PROCESSING FOR HYDROGEN PRODUCTION – SYSTEM INTEGRATION	3
Introduction	3
Goals and Objectives	3
Experimental Reactions	4
Description of Materials, Instrumentation, and Equipment	4
Sample Collection and Parametric Testing	4
Economic Evaluation	5
Results and Discussion	5
Conclusions	11
References	12
YEAR 2004 – ACTIVITY 2 – BIOJET FUEL COLD-FLOW IMPROVEMENT	13
YEAR 2004 – ACTIVITY 3 – BIOMASS III ENERGY AND PRODUCTS WORKSHOP	13
Introduction	13
Goals and Objectives	14
Experimental	14
Results and Discussion	14
Conclusions	16
References	16
YEAR 2004 – ACTIVITY 4 – BIOMASS GASIFICATION AND DISTRIBUTED POWER PRODUCTION	16
Introduction	16
Goals and Objectives	17
Experimental	17
Results and Discussion	19

Continued . . .

TABLE OF CONTENTS (continued)

Conclusions 26
References 26

YEAR 2004 – ACTIVITY 5 – ECONOMICALLY OPTIMIZED BIODIESEL
PRODUCTION FROM LOW-VALUE FEEDSTOCKS 27
 Introduction 27
 Goals and Objectives 28
 Experimental 28
 Results and Discussion 29
 Conclusions 35
 References 36

YEAR 2004 – ACTIVITY 6 – MANAGEMENT AND STRATEGIC STUDIES 36
 Introduction 36
 Goals and Objectives 37
 Experimental 37
 Results and Discussion 37
 Conclusions 39
 References 39

YEAR 2005 – ACTIVITY 1 – MANAGEMENT AND STRATEGIC STUDIES 39
 Introduction 39
 Goals and Objectives 39
 Experimental 40
 Results and Discussion 40
 Conclusions 43
 References 44

YEAR 2005 – ACTIVITY 2 – BIOMASS GASIFICATION AND DISTRIBUTED
POWER PRODUCTION 44
 Introduction 44
 Goals and Objectives 44
 Experimental 45
 Procedure 45
 Results and Discussion 50
 Conclusions 55
 References 56

YEAR 2005 – ACTIVITY 3 – NOVEL HIGH-CETANE OXYGENATES FROM WASTE
GLYCEROL FROM BIODIESEL PLANTS 56
 Introduction 56
 Goals and Objectives 57

Continued . . .

TABLE OF CONTENTS (continued)

Experimental	57
Results and Discussion.....	61
Conclusions	63
References.....	64
YEAR 2005 – ACTIVITY 4 – UTILIZATION OF CUPHEA OILS FOR BIODIESEL PRODUCTION.....	
Introduction	64
Goals and Objectives.....	65
Experimental	66
Results and Discussion.....	70
Economics	75
Conclusions	77
References.....	77
YEAR 2005 – ACTIVITY 5 – PROCESS INTEGRATION FOR ECONOMIC HYDROGEN PRODUCTION FROM ETHANOL	
Introduction	79
Goals and Objectives.....	79
Experimental	80
Results and Discussion.....	82
Conclusions	89
References.....	89
YEAR 2005 – ACTIVITY 6 – BIOJET FUEL COLD-FLOW IMPROVEMENT.....	
Introduction	90
Environmental Issues	91
Crop Oil.....	92
JP-8 and Its Specifications	94
Cold-Flow Impacts/Cold-Flow Properties	95
Goals and Objectives.....	96
Experimental	99
Results and Discussion.....	104
Conclusions	113
References.....	114
YEAR 2005 – ACTIVITY 7 – UREA FERTILIZER PRODUCTION FROM ETHANOL COPRODUCT CARBON DIOXIDE	
Introduction	116
Goals and Objectives.....	117
Experimental	117
Results and Discussion.....	118

Continued . . .

TABLE OF CONTENTS (continued)

Conclusions 121
References 122

YEAR 2005 – ACTIVITY 8 – CHEMICAL FEEDSTOCKS FROM LIGNOCELLULOSIC
PYROLYSIS 122
 Introduction 122
 Goals and Objectives 123
 Experimental 123
 Results and Discussion 124
 Conclusions 130
 References 130

YEAR 2005 – ACTIVITY 9 – LANDFILL METHANE FOR MICROTURBINE POWER ... 131
 Introduction 131
 Goals and Objectives 136
 Experimental 137
 Basic Assessment of the Landfill Site 139
 Results and Discussion 150
 Comprehensive LFG Gas Analyses 156
 Major Gas Contaminant Removal Systems 158
 Basic LFG Economics 163
 Project Revenues 164
 Site Energy Demand 167
 Preliminary Economic Assessment 168
 LFG Production Barriers 171
 Follow-Up Project Concepts 174
 Future Research Directions 174
 Future Project Financial Resources 175
 Conclusions 176
 ORC Technologies 177
 Microturbine Materials Development 178
 Innovative Gas Pretreatment Technologies 178
 References 178

YEAR 2005 – ACTIVITY 10 – BIODIESEL EDUCATION AND OUTREACH 182
 Introduction 182
 Goals and Objectives 182
 Experimental 182
 Results and Discussion 183
 Conclusions 184
 References 185

DETAILED GAS SAMPLING AND ANALYSIS Appendix A

PRELIMINARY ECONOMIC ANALYSIS Appendix B

LIST OF FIGURES

1	Shakedown testing, reforming ethanol Sample 4 with 46% wt water to hydrogen	6
2	Overall conversion of feed to product.....	7
3	Hydrogen yield from ethanol reforming	8
4	Product gas composition at a feed rate of 2.0 mL/min.....	9
5	Product gas composition at a feed rate of 3.3 mL/min.....	9
6	Hydrogen production costs from various technologies.....	12
7	Portable gasifier test setup.....	18
8	Process flow diagram	18
9	Diesel engine and dynamometer	19
10	Gas control and measurement	19
11	Gas piping from gasifier trailer to engine located in the building	20
12	Gas piping to turbo intake	20
13	Diesel fuel pump and governor	20
14	Wood chips (left) and sunflower hulls (right).....	22
15	Aspen wood pellets	23
16	Mixture of chunk wood and sawdust	23
17	Shredded wood bark.....	24
18	Corn stover before reduction in size (left) and after size reduction (right).....	25
19	Wild rice husks.....	25
20	Switchgrass before size reduction (left) and after size reduction (right)	25
21	Ankur fluidized-bed gasifier (FBG) and stratified gasifier reduction zones.....	44

Continued . . .

LIST OF FIGURES (continued)

22	Process and instrumentation diagram.....	46
23	Assembled gasification trailer.....	47
24	Gas piping.....	47
25	Wood pellets.....	48
26	Wheat straw.....	48
27	Corn silage.....	49
28	Sawdust.....	49
29	Wood chips.....	50
30	Day 1 process temperatures firing wood chips with an average flow rate of approximately 45 scfm.....	52
31	Day 2 process temperatures firing pellets and sawdust with an average flow rate of 35 scfm for the first half of the run and 16 scfm for the second half.....	52
32	Day 3 process temperatures firing wheat straw, corn silage, and sawdust with an average flow rate of approximately 60 scfm.....	53
33	Correlation of tar vapor content with toluene measurements.....	54
34	Tar condensation in the process blower.....	56
35	Formation of esters from cyclic acetyls.....	59
36	Formation of dioxolane ester from glycerol monoester.....	60
37	Formation of cyclic acetyls from glycerol.....	62
38	Schematic of the autoclave system used for the screening tests.....	68
39	Schematic of the autoclave system used for the bulk production runs.....	68
40	Comparison of cuphea and soybean oil carbon chain length compositions.....	71

Continued . . .

LIST OF FIGURES (continued)

41	Refractive index of cuphea oil and cuphea methyl esters	73
42	Simulated distillation of cuphea oil and cuphea methyl esters with respect to temperature.....	74
43	Simulated distillation of cuphea oil and cuphea methyl esters with respect to time.....	74
44	Process flow diagram of the ethanol-reforming apparatus.....	80
45	Photograph of the ethanol-reforming apparatus.....	81
46	Profit per gallon of ethanol converted to anhydrous ammonia as a function of ethanol value and sale price of anhydrous ammonia	86
47	Profit per gallon of ethanol converted to urea as a function of ethanol value and sale price of urea	86
48	Contributing factors to savings from ethanol-to-hydrogen integration.....	88
49	Cost of H ₂ production from various feedstocks for comparable system size.....	88
50	Structure of a typical triglyceride molecule	93
51	Biojet fuel process.....	98
52	Schematic of thermal cracking apparatus.....	102
53	Photo of thermal cracking apparatus.....	102
54	The generation of biojet fuel from soybean oil and SME	109
55	Schematic diagram of an electrolysis cell.....	118
56	Polarization curves measured at 5 mV s ⁻¹ for a gold microelectrode.....	120
57	Proposed conversion of HA to dialkylethanolamines	125
58	Conversion of HA to poly(N,N-diethylammoniumethylene glycol)(VII) and/or poly(hydroxymethyl-N,N-diethylethyleniminium)(VIII)	125
59	Conversion of HA to poly(N-hydroxyethanolamine)	127

Continued . . .

LIST OF FIGURES (continued)

60	Interconversion of hydrophobically modified polymers.....	130
61	Facility layout.....	133
62	Closure elevation contour map.....	143
63	Potentiometric surface map.....	144
64	Planned biogas collection system.....	147
65	Existing elevation contour map.....	152

LIST OF TABLES

1	Summary of Feedstock Characteristics	6
2	Estimated Savings for an Integrated Ethanol–Hydrogen System	11
3	Sponsors and Exhibitors.....	15
4	Composition of Biomass Fuels During Run	22
5	Gas Compositions, Dry Gas HHV (Btu/scf), Efficiency	26
6	Contaminant Levels in Producer Gas.....	27
7	Yields of Esters from Oleic Acid and Alkylating Agent RX.....	30
8	Conversions to Esters from Canola Oil and Alkylating Agent RX.....	31
9	Conversions to Methyl Esters from Canola Soapstock and Alkylating Agent RX.....	32
10	Yields of Esters from Oleic Acid and Methylating Agent CH ₃ X with Solid Acid Catalysts	33
11	Conversions to Esters from Soy Oil and Methylating Agent CH ₃ X with Solid Acid Catalyst.....	34
12	Conversions to Esters from Soy Oil and Methanol with Solid Acid Catalysts.....	34
13	Conversions to Esters with Solid Acid Catalysts Using Lower Methanol Concentrations.....	35
14	Schedule of Operation.....	50
15	Ultimate and Proximate Analysis of Biomass Fuels.....	51
16	Summary of Gas Analysis.....	53
17	Comparison of Fuel Performance	55
18	Fuel Properties of Cyclic Acetyls.....	61
19	Analyses Performed on Cuphea Seed Oil	66

Continued . . .

LIST OF TABLES (continued)

20	Analyses Performed on Cuphea Biodiesel	67
21	Screening Tests Conducted in the EERC Autoclave at 71.1°C (160°F) with 75 mL Methanol and 100 mL Cuphea Oil.....	69
22	Crude Cuphea Oil Profile	71
23	Cuphea Biodiesel Analysis Results.....	72
24	Mass Balances of Production Runs.....	75
25	Comparison of Fuel Cloud Points	76
26	Comparison of Cuphea Biodiesel to Soy Diesel and ASTM Standards	76
27	Comparative Biodiesel Production Cost for Varying Feedstocks.....	76
28	Parameters Utilized to Determine Optimum Ethanol-Reforming Conditions	82
29	Experimental Results from a Continuous Ethanol-Reforming Reactor	83
30	Regression Results from Ethanol-Reforming Data.....	83
31	Results from High-Pressure Reforming of Ethanol and Water in a Modified Reactor.....	84
32	Change in Economics for the Estimation of Ethanol-to-Hydrogen Integration Savings	87
33	Chemical Structure of Common Fatty Acids	93
34	Fatty Acid Composition of Soybean Oil	93
35	Typical Properties of JP-8 Aviation Fuel.....	94
36	Typical JP-8 Composition.....	95
37	ASTM D5972 Freezing Point of JP-8 Biodiesel (SME) Blends.....	96
38	Key Components of CME/SME and Canola/Soybean Oil.....	99
39	Composition of Alkane Standard	100

Continued . . .

LIST OF TABLES (continued)

40	Composition of FAME Standard.....	101
41	Design of Experimental Matrix for Thermal Cracking Optimization.....	105
42	Parameters in Experimental Matrix for the Cracking of CME	105
43	Parameters in Experimental Matrix for the Cracking of Canola Oil.....	105
44	Results from Experimental Matrix Tests for the Cracking of CME	106
45	Results from Experimental Matrix Tests for the Cracking of Canola Oil	106
46	Cold-Flow Properties of Biojet Fuel Produced from CME.....	108
47	Cold-Flow Properties of Biojet Fuel Produced from Canola Oil.....	108
48	The Composition of Crackates and Final Biojet Fuel Samples Generated from SME	110
49	The Composition of Crackates and Final Biojet Fuel Samples Generated from Soybean Oil.....	110
50	Results and GC Analysis of CME Crackates Using Column 1.....	111
51	Results and GC Analysis of CME Crackates Using Column 2.....	111
52	Results and GC Analysis of CME Biojet Fuel Using Column 2	113
53	Results and GC Analysis of Canola Oil Using Crackates Using Column 2	113
54	Results and GC Analysis of Canola Oil Biojet Fuel Using Column 2.....	113
55	Electrolysis Results for the Coreduction of NO and CO ₂	121
56	Viscosities (cps) of Partially Hydrolyzed PAM Solutions (0.5 wt%) Combined with Ammonium and Polyquat Solutions.....	128
57	Viscosities (cps) of Partially Hydrolyzed PAM Solutions (0.5 wt%) Combined with Polyquats Prepared under Different Conditions.....	128
58	Viscosities of Polycation Solutions.....	129

Continued . . .

LIST OF TABLES (continued)

59	Piezometer Biogas Velocity Measurements for Wells in Closure Phases I, III, and IV Taken Mid-2007	146
60	Common Siloxane Species and Their Current Detection Limits by GC-MS.....	149
61	Estimated Common Capital Costs for LFG Systems	149
62	Preliminary Economic Assessment of the Grand Forks Landfill Methane Collection and Energy Generation System	169
63	Measured Water Surface Elevations in the Three Piezometer Wells.....	172

EERC CENTER FOR BIOMASS UTILIZATION 2005

EXECUTIVE SUMMARY

The goal of the Energy & Environmental Research Center (EERC) Center for Biomass Utilization[®] (CBU[®]) project for years 2004 and 2005 was to develop economical, environmentally sound technologies to promote efficient biopower or bioenergy, transportation biofuels, and bioproducts such as marketable chemicals from biomass. This research was conducted under U.S. Department of Energy (DOE) Cooperative Agreement No. DE-FC36-03GO13055. This executive summary gives technical research highlights and results for the specific research activities undertaken in 2004 and 2005.

2004

Activity 1 – Ethanol Processing for Hydrogen Production – System Integration

Optimized integration of ethanol and hydrogen production processes was performed to try to significantly improve the economics of using ethanol as a hydrogen feedstock by 1) eliminating a large portion of the energy-intensive ethanol dehydration required in the production of fuel-grade ethanol and 2) eliminating intermediate steps required in a stand-alone hydrogen production process. The feasibility of reforming a dilute ethanol stream derived from an intermediate purification process was demonstrated at the laboratory scale. Various ethanol process streams were characterized from fermentation through distillation to determine the most appropriate process stream for hydrogen reforming. A bench-scale steam reforming system was designed and built to test five different ethanol–water mixtures from Chippewa Valley Ethanol Company (CVEC). Testing helped determine the effectiveness of hydrogen production and define operational parameters necessary to demonstrate at the pilot scale. Results of the testing were coupled with economic data to show that integration of a steam reforming system with an ethanol facility for hydrogen production may reduce the cost of hydrogen \$0.30/kg over distributed steam reforming of fuel-grade ethanol. Further, these savings would be in addition to future improvements and cost savings associated with less expensive ethanol production and gas processing technologies to purify hydrogen for fuel cell use. Partners for this activity included the Minnesota Corn Growers Association and CVEC.

Activity 2 – BioJet Fuel Cold-Flow Improvement

In partnership with Wright–Patterson Air Force Base (WPAFB) in Dayton, Ohio, a vegetable oil-based “biojet” fuel was developed using soybean and other triglyceride oils with the goal of meeting JP-8 specifications such cold-flow, pour point, energy density, and other critical properties that comply with values specified for U.S. military-grade jet fuel. The activity focused primarily on designing and building a batch 2-gallon bench-scale reactor as well as a companion batch distillation unit. This equipment would allow researchers to generate fuel quantities sufficient for testing in a microturbine modified slightly for a lighter renewable biodiesel fraction. Bench-scale methods were designed for thermal cracking of primarily soybean oil to shorter molecular-chain-length molecules, as compared to longer-chain methyl esters in biodiesel. Further cracking process technology and parametric testing were reserved for a follow-

up project in the EERC CBU 2005 project. Cost share for the project was provided by the North Dakota State Board of Agriculture and Research and Education (NDSBARE), the University of North Dakota (UND), and the North Dakota Soybean Council.

Activity 3 – Biomass III Energy & Products Workshop

A third annual biomass workshop was organized to disseminate useful information derived, in part, from activities within the EERC CBU project relating to converting biomass to heat, power, transportation fuels, and biochemicals. The workshop format provided opportunities for innovative research with potential new industry partners to advance innovative applications of biomass. Biomass III Energy and Products Workshop was held in conjunction with the Renewable Energy Conference held February 23 and 24, 2005, in Grand Forks, North Dakota, at the Alerus Center, a large civic conferencing center. There were over 500 participants in the conference, with 25 exhibitors. The conference focused primarily on wind and biomass energy-related topics. Well over 400 of the participants attended at least one of the biomass-related sessions, which included biomass resources, biomass-to-ethanol, biopower, biorefineries, biodiesel, small biomass power electrical transmission, renewable legislation, production tax credits, renewable energy credit systems, renewable hydrogen production, and commercial demonstrations of biopower systems. Marilyn Brown, Director of the Energy Efficiency and Renewable Energy Program at Oak Ridge National Laboratory, was one of several keynote speakers at the conference.

Activity 4 – Biomass Gasification and Distributed Power Production

A 150-kWe distributed biomass gasification power plant was designed and constructed for producing biobased electricity. The system was designed to be portable and was mounted on a semitrailer. Wood residue biomass was the primary feedstock, and the system included simple, yet effective, producer gas cleanup. Over 200 hours of testing was performed on municipal chipped woody biomass after the system was constructed and shaken down. Cleaned producer or syngas was fed to a 200-hp John Deere internal combustion engine. This type of system had not been developed in the United States. The EERC partnered with the Biomass Energy Resource Center (BERC) in Vermont. Economics for the integrated gasification system were determined for electric power markets of less than 1 MWe where low-cost biomass wood be realized from residues and the forest products industry, such as the vast resources of the northeastern United States.

Activity 5 – Economically Optimized Biodiesel Production from Low-Value Feedstocks

An innovative method for producing methyl ester-based biodiesel or higher-cetane additives from feedstocks with significantly lower value than soybean oil and other traditional biodiesel feedstocks was investigated. Biodiesel process by-products include oils high in free fatty acid (FFA). A proprietary nonalcohol alkylating agent in a column reactor packed with a solid acid catalyst was used process the FFA to a higher-cetane additive for use in diesel engines. High-FFA-content oil was provided by Archer Daniels Midland (ADM) Company, and biodiesel and additive yields were over 90% for the process technology. The proposed project focused on

1) assessment and improvement of process economics via optimization of reaction conditions, reactor configuration, and catalyst type and configuration and 2) process evaluation and optimization with a variety of different feedstocks. The North Dakota Soybean Council and ADM were collaborating sponsors in this activity.

Activity 6 – Management and Strategic Studies

The objective of this task was to provide efficient project management for technical projects and to direct select strategic studies that define emerging environmental, economic, and technological issues with respect to new or cutting-edge technologies in biomass power, transportation biofuels, and marketable bioproducts. Deliverables were quarterly and final topical reports; internal project review meetings; implementation of quality assurance/quality control measures, including a midproject review meeting to gauge project status and quality; communication with DOE on important national initiatives and the overall direction of the EERC Biomass Utilization Program and its individual subtask projects; developing a Web site to showcase biomass-related research within the EERC Biomass Utilization Program, including the individual subtask projects described herein; attendance and dissemination of information generated through the CBU at international biomass-related conferences and meetings with commercial industry clients interested in biomass technologies; developing biomass promotional materials; and aiding in the annual Biomass: Energy & Products Workshop (Biomass III Energy and Products Workshop, February 2005).

2005

Activity 1 – Management and Strategic Studies

Overall project management included administration activities for the DOE Golden Field Office and DOE administrators in Washington, D.C.; preparing all project application documents; preparing all quarterly, final topical, hazardous substance, and milestone reports; assembling an annual project review presentation; ensuring quality assurance/quality control for all activities; and facilitating kickoff, midproject review, and bimonthly renewables/biomass informational meetings with individual activity leaders. Strategic studies activities included facilitating sessions related to bioenergy/bioproducts at an annual renewable energy conference, attending and participating in strategic conferences related to biomass utilization, and conducting forward planning for cutting-edge biomass utilization research in accordance with DOE plans and objectives. Finally, in the area of education and outreach, a workshop was held in May 2006 at the EERC drawing nearly 200 participants. The event focused mostly on using biomass as a fuel for automobiles (including cellulosic ethanol and biodiesel) and new technologies in biomass gasification for heat, energy, and chemicals. Over 136 organizations participated along with four countries (the United States, Canada, New Zealand, and the United Arab Emirates), 25 states, and seven Canadian provinces. The demographics were 46% industry; 21% research/academia; 17% government; 7% community and economic developers; and 9% financial organizations, landowners, and media.

Activity 2 – Biomass Gasification and Distributed Power Production

A small (<150-kW) biomass gasifier which can operate as a stationary distributed-energy system or as a mobile (trailer-mounted) system was designed, built, and tested at the EERC. Biomass processing, handling, and feeding; gasifier power performance; producer gas quality/gas cleanup; char handling; and wastewater cleanup were evaluated for a range of biomass fuels, including switchgrass, wheat straw, flax straw, sunflower hulls, nut shells, wood residues, and a blend of biomass and stoker-grade coal. The gasifier proper and all feed and gas cleanup components were mounted on a 14-ft trailer. Gas cleaning includes a simple venturi wet scrubber and a filter system. Several hours of testing showed tars in the 250–500 ppm range. Soot and other contaminant levels were slightly higher than expected but certainly in the range of optimization. Overall, producer gas quality was adequate, showing 1:1 ratios of CO:H₂ and about 2% methane. Capital costs were low (<\$1500/kW), and this system represents a significant opportunity to utilize biomass residues and provide electricity generation at attractive prices.

Activity 3 – Novel High-Cetane Oxygenates from Waste Glycerol from Biodiesel Plants

The quality of diesel fuels can be significantly improved by the addition of certain organic compounds containing oxygen (oxygenates). These oxygenates typically reduce particulate emissions and improve the ignition quality of the fuel, as measured in a relative cetane number (CN) scale. The oxygenate compounds vary greatly in their ability to increase or decrease the CN of the base fuel with which they are mixed. For diesel fuels, methanol, ethanol, and other small alcohols have a deleterious effect on the ignition quality with very low CNs, whereas ethers offer a significant improvement in fuel quality. The goal of this project was to determine if processing of by-product glycerol from biodiesel plants can yield oxygenates with high blending CN characteristics at a minimal cost of production. A low production cost for producing a high-cetane additive to diesel fuel could be an important factor in the stimulation and development of biomass refineries where a variety of fuels and chemicals are produced from vegetable oil resources.

New synthetic methods for ether and ester derivatives were developed to prepare cyclic acetyls (dioxolane–dioxane structures) from the starting glycerol and other glycols. Four of the target compounds prepared were ether derivatives with the cyclic acetyl structures. Two of the target compounds were ester derivatives of the cyclic acetyl structures. Liter quantities of fuel blends were prepared. Derivatives from the glycols resulted in extremely high blending cetane numbers (BCNs). Testing of the four soluble target compounds derived from glycerol gave only mediocre BCNs. The results rejected the hypothesis that increasing either linkage by converting the three hydroxyls of glycerol to ether functionalities or mixed ether–ester functionalities will increase the BCNs. There are likely steric hindrances in the cyclic compounds that destabilize transition states of the cyclic molecules during reactions with oxygen radicals in the combustion process. One glycerol-derived cyclic ether was tested for octane enhancement qualities for a gasoline additive. This branched derivative exhibited a high blending octane number as well as high solubility in gasoline. This was the most encouraging fuel additive prepared in the project. Testing of the glycerol and glycol derivatives for cold-flow filter plugging points (CFPPs) gave the expected improvements. Most of the cyclic acetyls significantly lowered the CFPP; however,

this and other general benefits of using oxygenate blends of glycerol derivatives would not likely be cost-effective for producing high-performance fuels owing to the recent upward trend in glycerol prices.

Activity 4 – Utilization of Cuphea Oils for Biodiesel Production

The U.S. DOE-sponsored EERC CBU, Technology Crops International, and the Agricultural Utilization Research Institute (AURI) collaborated on this project to investigate the potential feedstocks for development of a biodiesel with cold-flow properties equivalent to or better than those of petroleum diesel. Challenges yet to be overcome for widespread biodiesel utilization include a high cloud point that causes it to gel in colder climates and high cost relative to petroleum diesel fuel. Research conducted on short-chain oils and triglycerides suggests that they may provide an improvement in the cold-flow properties of biodiesel. Rising prices in current conventional biodiesel feedstocks, such as soybean oil, create an opportunity to consider other agricultural oils for biodiesel production.

The primarily medium-carbon-chain cuphea seed oil proved technically viable for biodiesel production, exhibiting superior cold-flow properties to winterized diesel in addition to biodiesel from soybean and canola oil feedstocks. The cuphea biodiesel product had a measured cloud point of -19°C (-2°F). Other advantages of cuphea include agricultural benefits for current U.S. crop rotations, greater oil yield per acre, and low viscosity and sulfur content.

Although cuphea biodiesel is not, at this time, economically feasible, it may become viable in the next decade, especially if petroleum diesel continues its significant price growth or if used as a blend with canola biodiesel to improve cold-flow properties as well as economics. Future work should consist of optimizing process parameters and separation methodology and conducting engine testing of cuphea biodiesel as a fuel.

Activity 5 – Process Integration for Economic Hydrogen Production from Ethanol

Pilot-scale testing was conducted to evaluate the effectiveness of generating hydrogen from partially distilled ethanol product for fuel cell applications. Results from previous studies were used to select several feedstocks best suited to reforming applications for hydrogen production. Parametric testing was conducted to quantify operational parameters for optimal hydrogen production and to identify process conditions required to address characteristics of a partially distilled ethanol product. Data collected are being used to evaluate integration strategies and associated economics.

Activity 6 – Biojet Fuel Cold-Flow Improvement

A thermocatalytic cracking process designed and constructed at the pilot scale in EERC CBU 2004 was further developed and optimized for converting not only soybean but also canola vegetable oils and/or esterified vegetable oils to a jet fuel that meets military cold-flow and other key performance specifications. Biodiesel or “green” diesel investigations included parametric testing of the first-order thermocatalytic cracking process to remove oxygen from feedstocks to yield a paraffinic fuel with a volumetric energy content similar to that of petroleum-derived JP-8.

Evaluation of the fuel was to be conducted at WPAFB Fuels Research Laboratory, but to save time and costs and to lower the risk of impacts of such an experimental fuel on the WPAFB test turbine system, an SR-30 Minilab microturbine power system (Turbine Technologies Ltd.) was used. An extensive series of experiments were performed on the small lab-scale thermal cracking unit to obtain the optimum conditions for fuel production, to better understand the design issues affecting commercialization, and to produce data required for the commercial feasibility study. Consistent biojet fuel product yields were 86% of the feed input to the process. Intermediate and final product composition cloud and pour points of the liquids were very close to JP-8. Fuel energy content, as measured by higher heating values, were determined to be 15,500 Btu/lb for biojet fuel produced from SME and 17,400 Btu/lb when produced from soybean oil. These compare to a JP-8 value of 19,700 Btu/lb and biodiesel values of around 16,100–16,900 Btu/lb. Computer simulations of the process were developed and used to design a facility capable of processing 3,000,000 gallons of feed soybean oil per year. The capital costs and economics were found to be comparable and competitive with a biodiesel plant of the same size.

Activity 7 – Urea Fertilizer Production from Ethanol Coproduct Carbon Dioxide

Electrochemical processes that utilize inputs of carbon dioxide (CO₂), nitric oxide (NO), hydrogen, and electricity for production of ammonia, urea, and ammonium nitrate (AN) fertilizers were developed and preliminarily evaluated for economic viability, with the objective of commercializing one or more of the processes based on the use of low-cost electricity, ethanol coproduct CO₂, and NO recovered from coal combustion oxides of nitrogen (NO_x) emissions. The economic viability assessment, which included integration of NO recovery at a coal-fired power plant with fertilizer production, indicated that, of the three processes, the AN process showed the greatest commercial potential by virtue of its low hydrogen input requirement versus the other two processes. Commercialization of the processes would improve the economics of utility NO_x emission control by turning NO_x into a revenue stream and enable development of a non-natural gas-based economically competitive domestic fertilizer production industry. Process optimization is ongoing with support from a consortia of commercial partners, including regional corn grower associations.

Activity 8 – Chemical Feedstocks from Lignocellulosic Pyrolysis

Fast pyrolysis of biomass yields primary products that include a wide variety of sugars and anhydrosugars. In a separate thermochemical conversion technology development project, processes were developed that utilized fast-pyrolysis bio-oil-extracted hydroxyacetaldehyde (HA) as a feedstock for production of polyamines and polyquaternary ammonium salts or “polyquats.” Several types of polyamines and polyquaternary ammonium salts were produced from HA that have the unique property of modifying the structure and consequently lowering the viscosity of other high-molecular-weight anionic polymers so that they can be pumped without shearing. Compositing, viscosity, and phase partition testing results showed that the polymers could be separated in situ and the high viscosity that is needed for “polymer-flood” enhanced oil recovery (EOR) was restored. The EERC is pursuing acquisition of commercial EOR agent cost data for use in evaluating this technology.

Activity 9 – Landfill Methane for Microturbine Power

A prefeasibility energy study of the Grand Forks municipal landfill site was completed in cooperation with, and with matching funds from, the City of Grand Forks to determine potential biogas-to-energy applications of the landfill gas (LFG) from the site. LFG samples were collected and analyzed for total volatile organic compounds (VOCs), the complete siloxane series, hydrogen sulfide species, gas constituents, and heating value.

Results from this energy study indicate the Grand Forks municipal landfill site may have a gross power generation capacity around 2 megawatts (MW), which could be equivalent to an annual electricity generation potential of more than 10,000 megawatt hours (MWh) after parasitic loads are accounted for, assuming an 80% capacity factor. The duration of this level of power generation is estimated to be about 20 years, assuming ideal conditions for the age, moisture, depth, and quantity of waste at this site. This preliminary energy assessment determined that this site, under ideal conditions, could produce enough energy to offset on-site electrical costs as well as provide a large portion of the heat and power requirements for the nearby city-owned wastewater treatment facility.

Economical electricity and heat generation in a typical Carnot combustion cycle looks promising for this municipal location. However, because of the nonscalable nature and high cost of current biogas treatment technologies, it was recommended that further research be considered utilizing Organic Rankine Cycle (ORC) technology coupled with an innovative biogas pre-treatment system that could offer a more cost competitive LFG-to-energy package at this site and similar landfill sites with gross power generation potential below 4 MW.

Activity 10 – Biodiesel Education and Outreach

Biodiesel education and outreach workshops were held in cooperation with the North Dakota Department of Agriculture, the South Dakota Soybean Research and Promotion Council, the Red River Valley Clean Cities Coalition, and several collaborating agencies from Minnesota, North Dakota, and South Dakota. The workshops focused on the basics of establishing biodiesel use in a community or municipality, including biodiesel production, distribution, blending, cold-flow issues, engine performance impacts, emission impacts, promotion, public awareness, financial incentives, and local economic impacts. Over 140 attendees participated in the two workshops which were held in March and April of 2007 in Fargo, North Dakota, and in Sioux Falls, South Dakota. Presentations were made by EERC personnel and several other biodiesel experts and fleet managers from around the country.

EERC CENTER FOR BIOMASS UTILIZATION 2004–2005

INTRODUCTION

Biomass utilization is one solution to our nation's addiction to oil and fossil fuels. What is needed now is applied fundamental research that will cause economic technology development for the utilization of the diverse biomass resources in the United States. This Energy & Environmental Research Center (EERC) applied fundamental research project contributes to the development of economical biomass utilization for energy, transportation fuels, and marketable chemicals using biorefinery methods that include thermochemical and fermentation processes. The fundamental and basic applied research supports the broad scientific objectives of the U.S. Department of Energy (DOE) Biomass Program, especially in the area of developing alternative renewable biofuels, sustainable bioenergy, technologies that reduce greenhouse gas emissions, and environmental remediation. Its deliverables include 1) identifying and understanding environmental consequences of energy production from biomass, including the impacts on greenhouse gas production, carbon emission abatement, and utilization of waste biomass residues and 2) developing biology-based solutions that address DOE and national needs related to waste cleanup, hydrogen production from renewable biomass, biological and chemical processes for energy and fuel production, and environmental stewardship. This project serves the public purpose of encouraging good environmental stewardship by developing biomass-refining technologies that can dramatically increase domestic energy production to counter current trends of rising dependence upon petroleum imports. Decreasing the nation's reliance on foreign oil and energy will enhance national security, the economy of rural communities, and future competitiveness. Although renewable energy has many forms, such as wind and solar, biomass is the only renewable energy source that can be governed through agricultural methods and that has an energy density that can realistically compete with, or even replace, petroleum and other fossil fuels in the near future. It is a primary domestic, sustainable, renewable energy resource that can supply liquid transportation fuels, chemicals, and energy that are currently produced from fossil sources, and it is a sustainable resource for a hydrogen-based economy in the future.

Year 2004

- Activity 1 – Ethanol Processing for Hydrogen Production – System Integration
- Activity 2 – Biojet Fuel Cold-Flow Improvement
- Activity 3 – Biomass III Energy and Products Workshop
- Activity 4 – Biomass Gasification and Distributed Power Production
- Activity 5 – Economically Optimized Biodiesel Production from Low-Value Feedstocks
- Activity 6 – Management and Strategic Studies

Year 2005

- Activity 1 – Management and Strategic Studies
- Activity 2 – Biomass Gasification and Distributed Power Production
- Activity 3 – Novel High-Cetane Oxygenates from Waste Glycerol from Biodiesel Plants
- Activity 4 – Utilization of Cuphea Oils for Biodiesel Production
- Activity 5 – Process Integration for Economic Hydrogen Production from Ethanol
- Activity 6 – Biojet Fuel Cold-Flow Improvement
- Activity 7 – Urea Fertilizer Production from Ethanol Coproduct Carbon Dioxide
- Activity 8 – Chemical Feedstocks from Lignocellulosic Pyrolysis
- Activity 9 – Landfill Methane for Microturbine Power
- Activity 10 – Biodiesel Education

Ethanol is the one form of biomass-derived renewable fuel production that has a widely expanding market in the United States and worldwide. About 3 billion gallons of ethanol will be produced in the United States in 2004. Federal initiatives within DOE and the current administration are being directed toward using hydrogen as a next-generation energy carrier and transportation fuel. The problem with hydrogen as a fuel is that near-term feedstocks for its production include mostly fossil fuels such as methanol and natural gas. Using ethanol as a domestically produced biomass feedstock for hydrogen production is a renewable solution. Logistically, ethanol plants also serve to help develop a hydrogen production and dispensing infrastructure, since the plants are already scattered throughout the midwestern United States. An innovative EERC activity under the EERC Center for Biomass Utilization[®] (CBU[®]) Program explored the feasibility of converting a hydrogen production line within an existing ethanol plant.

GOAL

The goal of the EERC CBU[®] project, which was carried out as two successive projects in 2004 and 2005, was to develop economical, environmentally sound technologies to promote efficient biopower or bioenergy, transportation biofuels, and bioproducts such as marketable chemicals.

OBJECTIVES

Specific objectives for the EERC CBU Program for 2004 to 2005 are addressed in each individual activity.

YEAR 2004 – ACTIVITY 1 – ETHANOL PROCESSING FOR HYDROGEN PRODUCTION – SYSTEM INTEGRATION

Introduction

The use of fuel cells as a source of electricity continues to be an area of interest as a means of reducing dependency on fossil fuels, providing reliable distributed energy generation, and offering an alternative for transportation applications. To support further development of fuel cell technologies, hydrogen production methods also must be developed that reduce the use of fossil fuels and are compatible with a hydrogen and fuel cell infrastructure.

Ethanol has several inherent characteristics that make it an excellent source for hydrogen production. As a biomass-derived renewable fuel, it not only reduces fossil fuel use, but can be produced domestically and is relatively nontoxic, readily biodegradable, and considered CO₂-neutral. Another major advantage to ethanol is the absence of sulfur compounds. Sulfur, which is a major fuel cell contaminant, can poison reformers and shift catalysts, resulting in costly sulfur removal unit operations upstream of fuel-processing and fuel cell equipment. In many other fuels being investigated and evaluated for use as hydrogen carriers, sulfur is either inherent to the fuel, like gasoline, diesel, and naphtha, or added as an odorant, as is the case for natural gas and propane. By eliminating the need for sulfur removal unit operations, the size, operational conditions, and cost associated with reforming are greatly improved over applications for other fuels.

Two other characteristics of ethanol work to further simplify the reforming process: its miscibility with water and the presence of oxygen in the molecular structure. Water is a necessary component of the reforming process that improves hydrogen yield and reduces coke formation. Ethanol's miscibility with water eliminates the need for separate water storage and handling equipment and alleviates the need for freeze protection in cold climates. The oxygen atom contained in ethanol further reduces the size and complexity of reforming operations by reducing the volume of air and water needed to obtain the same hydrogen yield. This reduction in airflow translates to a reduced nitrogen input, which is advantageous because nitrogen is an energy-free diluent that increases system size and related costs.

The fermentation based ethanol production process contains many synergies with hydrogen production. By integrating the operation, efficiencies in process operation, energy use, and distribution can be realized.

Goals and Objectives

The goal of this project was to integrate the hydrogen and ethanol processes. The objective was, therefore, to evaluate the feasibility and economics of integrating hydrogen production with an ethanol-processing plant.

Experimental Reactions

Reforming ethanol can follow several reaction pathways and result in numerous products depending upon the water content, catalyst, and operating conditions. Optimization of conditions is critical to maximize hydrogen production. A few of the possible reactions involved in reforming ethanol, ignoring reversibility, are shown below. Reactions 1–3 would be optimal for hydrogen production, while Reactions 8–10 result in undesired carbon deposition on the reforming catalyst, which translates to reduced efficiency of the reforming process:

1. $\text{C}_2\text{H}_5\text{OH} + 3\text{H}_2\text{O} \longrightarrow 2\text{CO}_2 + 6\text{H}_2$
2. $\text{C}_2\text{H}_5\text{OH} + 1.5\text{O}_2 \longrightarrow 2\text{CO} + 2\text{H}_2\text{O} + \text{H}_2 \longrightarrow 2\text{CO}_2 + 3\text{H}_2$
3. $\text{C}_2\text{H}_5\text{OH} + 0.5\text{O}_2 + 2\text{H}_2\text{O} \longrightarrow 2\text{CO}_2 + 5\text{H}_2$
4. $\text{C}_2\text{H}_5\text{OH} + \text{Energy} \longrightarrow \text{CO} + \text{CH}_4 + \text{H}_2$
5. $\text{C}_2\text{H}_5\text{OH} + \text{Energy} \longrightarrow \text{H}_2\text{CO} + \text{CH}_4$
6. $\text{C}_2\text{H}_5\text{OH} + \text{Energy} \longrightarrow \text{CH}_3\text{CHO} + \text{H}_2$
7. $2\text{CO} + \text{H}_2 \longrightarrow \text{CH}_4 + \text{O}_2$
8. $\text{C}_2\text{H}_5\text{OH} + \text{Energy} \longrightarrow \text{H}_2\text{CO} + \text{C} + 2\text{H}_2$
9. $\text{C}_2\text{H}_5\text{OH} + 1.5\text{O}_2 \longrightarrow \text{CO}_2 + 2\text{H}_2\text{O} + \text{C} + \text{H}_2$
10. $\text{C}_2\text{H}_5\text{OH} + 0.5\text{O}_2 \longrightarrow 2\text{C} + 2\text{H}_2\text{O} + \text{H}_2 \longrightarrow 2\text{CO} + 3\text{H}_2 \longrightarrow \text{CO}_2 + \text{C} + 3\text{H}_2$

Description of Materials, Instrumentation, and Equipment

The bench-scale reforming system used for project experimentation is located at the EERC and consists of a feed system, reactor, furnace, condenser, and online gas analyzer. An ISCO Model 314 high-pressure syringe pump, capable of rates up to 3.3 cm³/min, fed a metered stream of ethanol–water mixture to the reformer system. The reactor, a 71-cm-thick-walled stainless steel tube with I.D. of 0.81 cm (O.D. 1.9 cm), was housed within a Lindberg Type 50344 tube furnace to provide the necessary heat input. Additional heat was supplied to the system using a Thermolyne Type 21100 tube furnace preheater. System pressure, temperature, gas composition, and total gas volume were recorded during each test.

Approximately 18 g of catalyst was contained in the reactor to promote the reforming process. A 2-L autoclave acted as a condensing vessel to collect unreacted liquid. A Rockwell International R-200 gas meter measured total gas flow. Gas composition was determined online with a Sick/Maihak S715 gas analyzer. At steady-state conditions, a gas sample was collected in a gas bag and analyzed with a refinery gas chromatograph (GC) to measure methane concentrations that exceeded the range measured with the Maihak analyzer.

Sample Collection and Parametric Testing

Several samples of ethanol were collected from an ethanol production process. Each sample was analyzed via GC by Chippewa Valley Ethanol Company (CVEC) personnel. The results of this sample characterization were used to evaluate their potential as a reforming feedstock.

Initial shakedown testing was conducted to evaluate operational constraints of the bench-scale system. The high latent heat of water and heat input limitations of the bench-scale furnace likely limited the heat available to reform the feed stream. To evaluate the effect of additional thermal input to the feed prior to reforming, some samples were tested both with and without an additional preheat coil, raising the feed temperature prior to its entering the reformer.

Following bench-scale shakedown experiments, parametric testing was conducted at the EERC to compare hydrogen yield and product gas composition from reforming five ethanol samples obtained from CVEC. Tests were conducted at different feed rates for each sample to compare the effect of residence time on product gas composition. Pressure, temperature, gas composition, and total gas volume were recorded during each test. Although testing was not conducted under optimized conditions for hydrogen production from ethanol, these experiments provided an opportunity to evaluate the relative feasibility of integrating hydrogen and ethanol production processes.

Economic Evaluation

The economic benefit of producing hydrogen through integration with the ethanol production process was quantified, assuming feedstocks of ethanol and water fed at a carbon-to-oxygen ratio of 1:2 on a molar basis (the stoichiometric ratio of ethanol and water for hydrogen production is 1:3 ethanol:water). The cost of hydrogen production from ethanol was calculated based on the cost of production taking into account savings associated with elimination of unnecessary operations (capital and operating cost), transport to a reforming facility, tankage, and thermal integration. This hydrogen production cost was then compared to the cost of hydrogen production from fuel-grade ethanol in a distributed application, water electrolysis from wind-generated electricity, and traditional steam methane reforming.

Results and Discussion

Ethanol Feedstock Characterization

Through collaboration with CVEC, the properties of ethanol were characterized via GC by CVEC. Eight samples were collected during two rounds of sampling, and the results are summarized in Table 1. Samples 1–3 were collected during the first round and underwent GC analysis only. Samples collected during the second round (Samples 4–8) were analyzed via GC and tested at the EERC. Coproduct concentration ranged from about <0.1 to 4.3 wt%.

Hydrogen Production

The limited shakedown experiments that were conducted on Sample 4 showed widely varying hydrogen production on a basis of moles of hydrogen produced per mole of ethanol feed. Results from six shakedown tests indicated that the greatest hydrogen yield occurred at 258°C and 1100 psi and at 276°C and 2400 psi, as illustrated in Figure 1. Based on these data, the lower temperature and pressure conditions were selected for testing the remaining ethanol samples at two feed rates, 2 and 3.3 mL/min.

Table 1. Summary of Feedstock Characteristics

Component	GC Samples			Bench-Scale Test Samples				
	1	2	3	4	5	6	7	8
Coproducts, ppm								
Acetaldehyde	–	–	–	21	362	24	84	50
Ethyl Acetate	–	–	–	7	64	11	76	92
Methanol	<1	<1	14	20	73	21	44	36
<i>n</i> -Propanol	35	53	512	1,165	316	1,798	349	451
<i>iso</i> -Butanol	10	61	813	1,655	150	2,902	47	211
1-Butanol	<1	4	250	427	16	570	<1	18
Active Amyl Alcohol	13	26	2,536	2,972	134	3,056	3	136
<i>iso</i> -Amyl Alcohol	85	220	18,360	31,309	759	34,745	<1	720
<i>n</i> -Amyl Alcohol	<1	5	12	14	273	13	<1	5

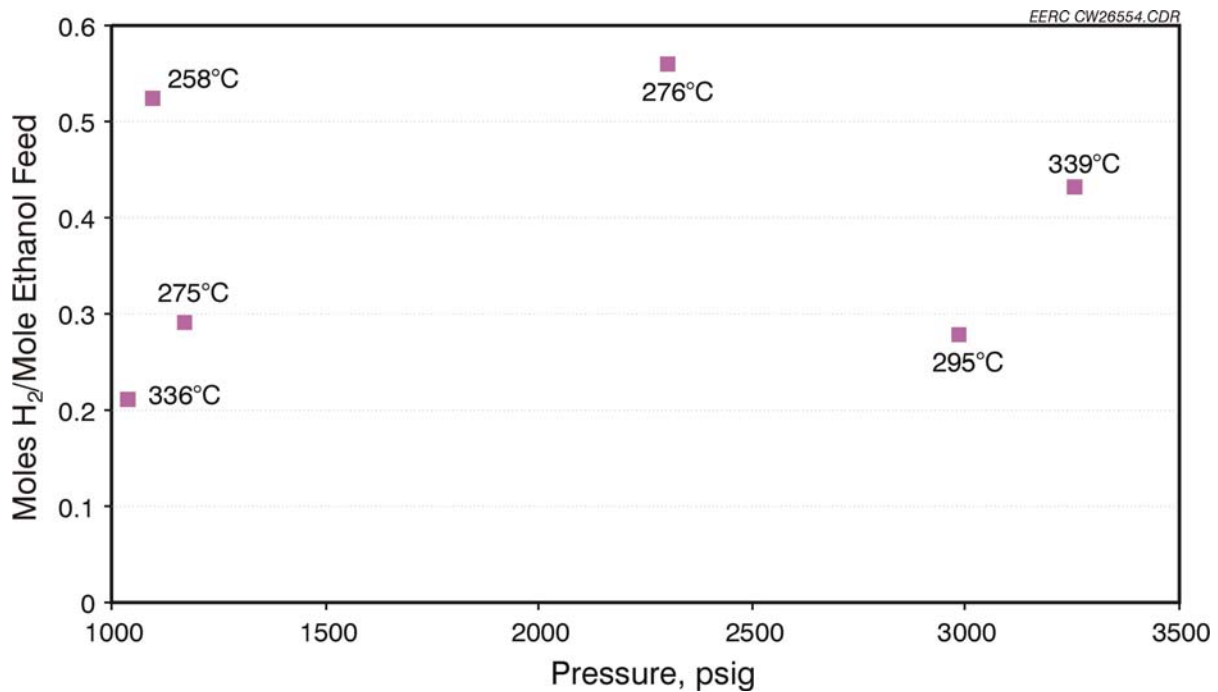


Figure 1. Shakedown testing, reforming ethanol Sample 4 with 46% wt water to hydrogen.

Three criteria were used to evaluate and compare the relative feasibility of reforming the five ethanol samples for hydrogen: overall conversion of the ethanol and water feed to product gas, hydrogen production on a mole H₂/mole ethanol feed basis, and product gas composition. Each of the five ethanol samples was tested with different quantities of water to test various carbon-to-oxygen ratios in an integrated system. Water is a necessary component in steam reforming to release hydrogen while forming CO₂ among other products. Insufficient water results in the formation of carbon, which precipitates on surfaces, and often reduces catalyst effectiveness. Excess water requires additional energy input to obtain the desired hydrogen product. Results from testing the five samples were used to evaluate the impact of coproducts on hydrogen production in an integrated system.

The greatest overall conversion of feed to product occurred with tests conducted as illustrated in Figure 2. The Sample 4 tests showed very low conversion to product gas, which could be attributed to the large fraction of water that passed unreacted across the reactor. However, Sample 6, with similar water feed rate, demonstrated substantially better conversion, at the same temperature and pressure. One significant difference between Samples 4 and 5 was the presence of nearly 3.5% more coproduct (large hydrocarbon molecules) in Sample 4. Additional tests of Sample 4, both with and without additional preheat suggest that there was insufficient temperature to reform samples with higher coproduct content and greater water addition.

Sample 5, in addition to demonstrating nearly 60% conversion to product, also resulted in the greatest hydrogen production at the lower feed rate of 2.0 mL/min. At this feed rate, the greatest fraction of hydrogen (moles of hydrogen per mole of ethanol fed to the reactor) was generated from Samples 5, 6, and 4 (with preheat). The relatively low hydrogen yield from Samples 7 and 8 can be attributed to insufficient oxygen and subsequent coke formation in the reactor. Although the conversion of feed to product was high in these samples, insufficient oxygen resulted in coking, which was observed by visual inspection following each test. A summary of the hydrogen yield from the ten experiments is provided in Figure 3. These results do not represent optimized conditions for hydrogen production, but rather a screening of actual ethanol product with various levels of coproduct and water addition that can be investigated further to develop an optimal integration strategy.

The last parameter used to compare the possible feedstock was the product gas composition. Gas chromatography and online gas analysis were used to measure hydrogen,

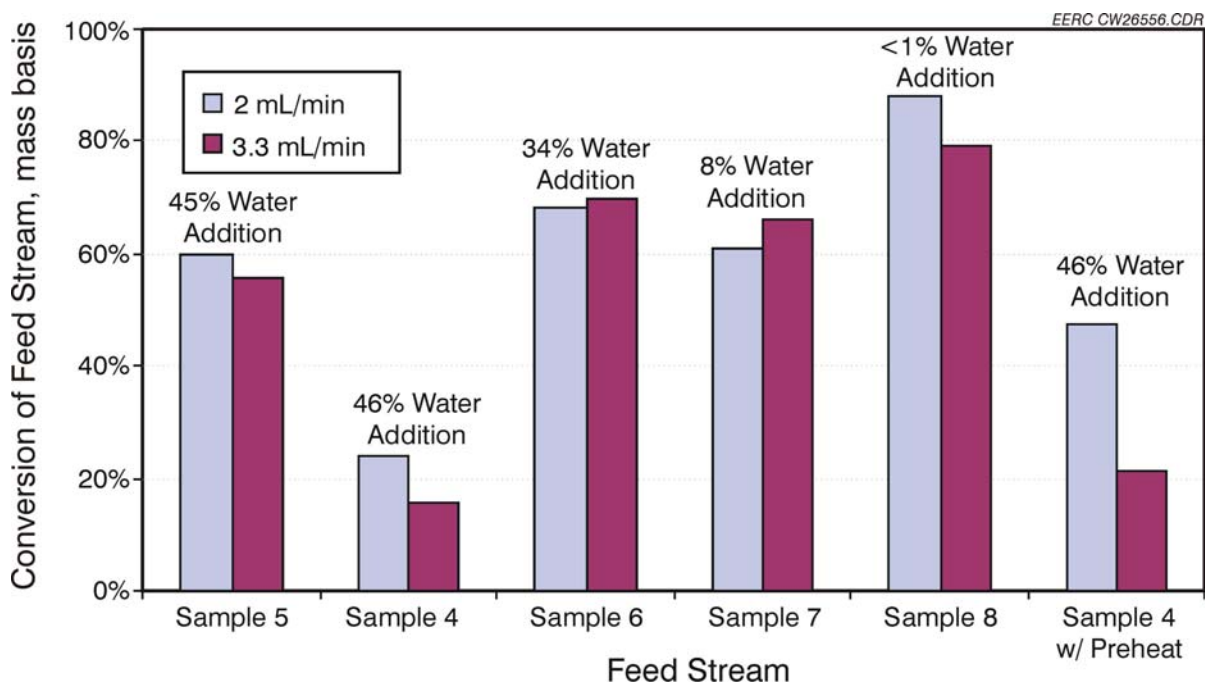


Figure 2. Overall conversion of feed to product.

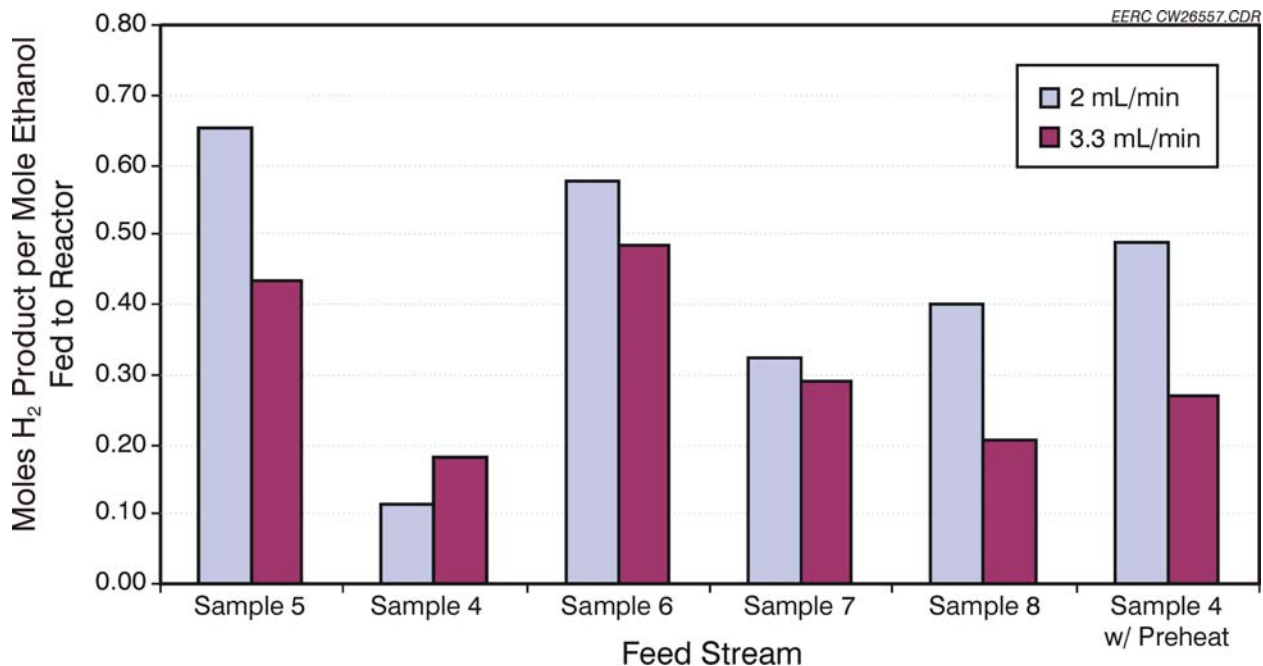


Figure 3. Hydrogen yield from ethanol reforming.

methane, carbon dioxide, carbon monoxide, and other hydrocarbons in product gas streams. In general, the percentage of hydrogen in the product gas was very similar for all of the samples, as illustrated in Figures 4 and 5.

A significant amount of methane was generated during the experiments, which was expected at the relatively low operating temperature (below the reforming temperature of methane: $>750^{\circ}\text{C}$). It is anticipated that, at higher reactor temperatures, methane reforming would be enhanced to produce additional hydrogen and CO_2 .

The greatest variability in product gas was in the fraction of methane and carbon dioxide. Results from tests of Samples 7 and 8 at 2.0 mL/min show very low levels of methane production; however, at the higher feed rate (shorter residence time), a greater fraction of methane was produced.

Preliminary Economic Analysis

A review of the economic impacts of integrated ethanol processing and hydrogen production was conducted to quantify the potential cost savings associated with lower capital equipment, reduced transportation, and lower energy input. Analysis was conducted on the basis of a new ethanol plant designed and constructed for hydrogen production. The improved economics of an integrated system were based specifically on reducing the cost of feedstock production. Fuel-grade ethanol storage and transportation costs are eliminated, and energy consumption is reduced through thermal integration.

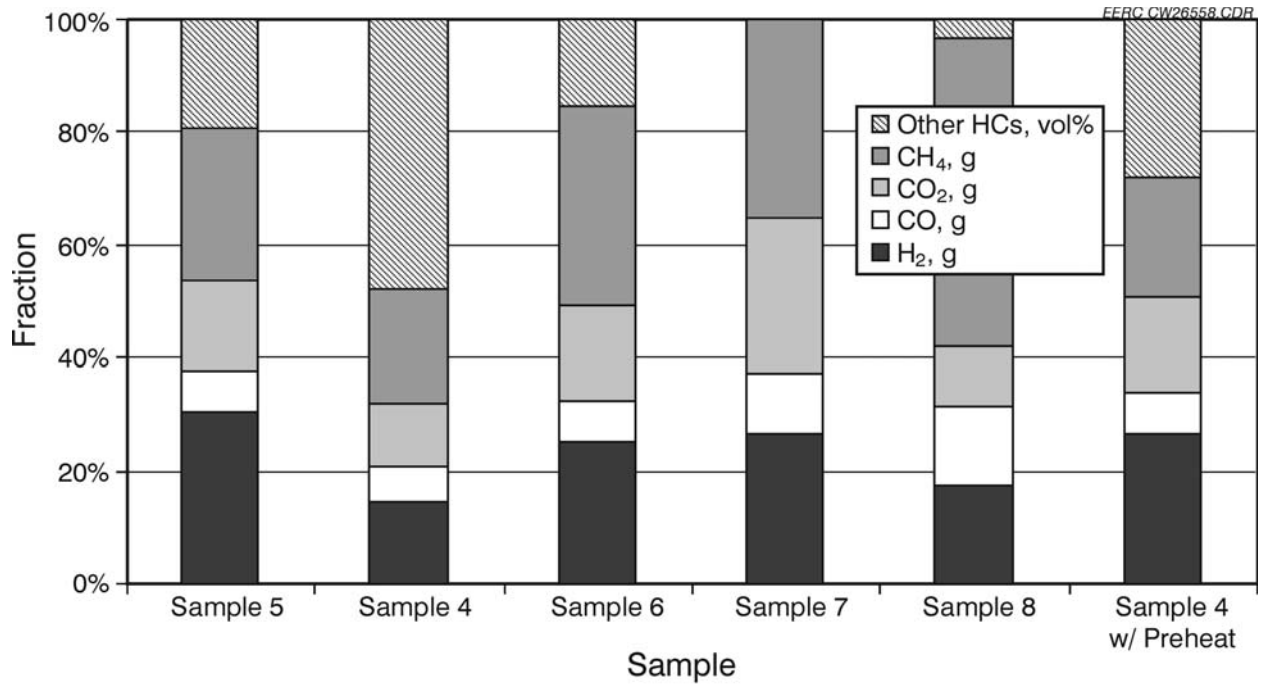


Figure 4. Product gas composition at a feed rate of 2.0 mL/min (HCs [hydrocarbons]).

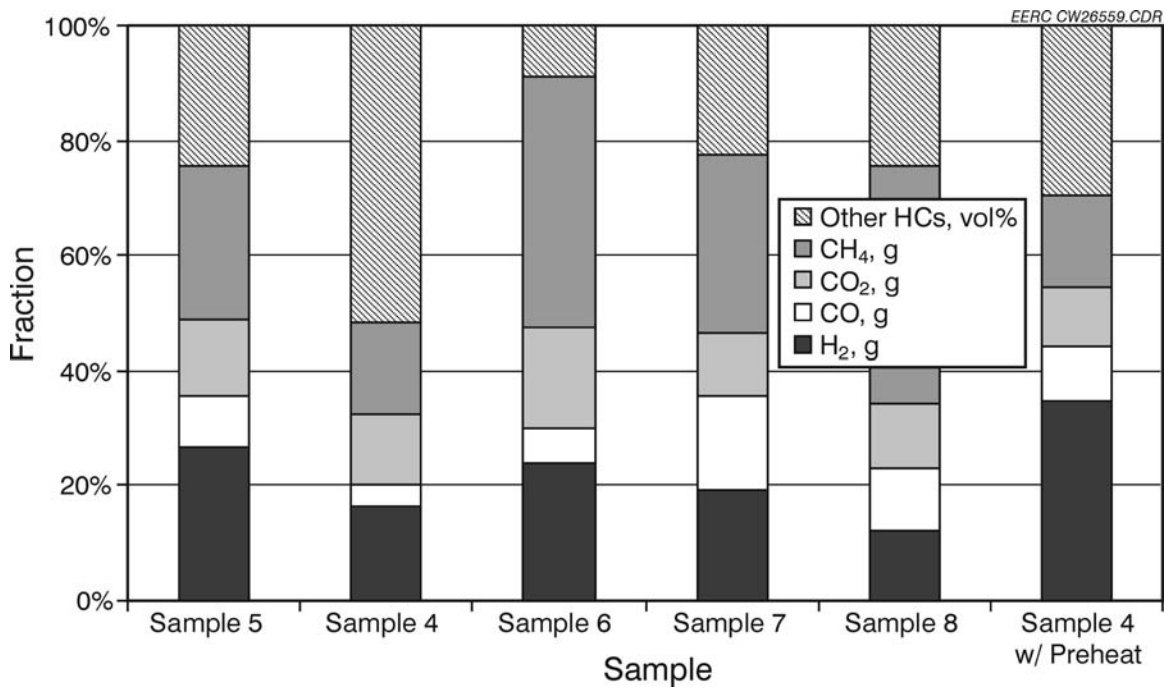


Figure 5. Product gas composition at a feed rate of 3.3 mL/min.

The cost of production of hydrogen was based on integration with a 20-million-gallon dry mill ethanol plant. The production cost of hydrogen assumes complete conversion of that ethanol feedstock annually. Approximately 15.6 million kg of H₂ would be produced under this assumption.

Ethanol Production

Comparative savings to the ethanol–water feedstock cost were estimated by first quantifying savings to a typical fuel ethanol facility. The capital cost of a 20-million-gallon dry corn mill ethanol plant was estimated to be \$29.5 million with annual production costs of \$43.0 million and dried distiller grains with solubles (DDGS) revenue of \$14.5 million. DDGS is a high-value by-product of ethanol production, sold at about \$97/ton DDGS (Paustian, 2004) as livestock meal for dairy, beef, swine, and poultry industries. These values were also based on the capital cost of various ethanol plants (Quentin Burdick Center for Cooperatives, 2003; Barbieri, 2005) amortized over 20 years and a wholesale ethanol cost of \$1.50/gal (Finnerty, 2005).

According to the methods of Peters and Timmerhaus (1980), implemented for the ease of comparison, the cost of equipment is approximately 16% of the total installed capital cost, estimated at \$4.7 million. The capital savings incurred by the integration of the ethanol and reforming facilities, such as elimination of fuel-grade ethanol storage, was calculated to be \$1.4 million. The revised capital cost becomes \$28.1 million for ethanol production in an integrated facility. Amortized over the assumed 20-year service life, annual savings were estimated to be about \$70,000 per year. Specific capital equipment eliminated from the process is considered confidential as it defines the process integration required to achieve feedstock cost reduction.

Transportation and Thermal Integration

Components of the annual production cost of ethanol affected by an integrated system include raw material, utilities, and transportation expenses. Typically up to 90% of the water used to produce ethanol is recycled. In an integrated facility, a significant amount of water would be required to convert ethanol to hydrogen via steam reforming. This would result in an increase of 17.5 million gallons of water annually. However, the same amount of water would be required for hydrogen reforming in a stand-alone facility. Therefore, no net change in raw material costs was included.

Natural gas comprises ~80% of the utility cost for ethanol production. It was estimated that approximately 457,000 MMBtu annually could be saved through system integration. With the cost of natural gas during this project at \$6.88/MMBtu (Natural Gas Navigator, 2005), an estimated \$3.15 million is anticipated in annual savings.

Transportation expenses were calculated using a cost of 7.7¢/gal ethanol (Mann, 2002). This would no longer be necessary in an integrated system, reducing annual feedstock costs for hydrogen production by approximately \$1.54 million.

Overall Savings

The total annual savings for the integrated ethanol–hydrogen system is estimated at \$4.76 million, as shown in Table 2. This cost reduction equates to a savings of \$0.30/kg of H₂ over the cost of reforming a fuel-grade ethanol product off-site.

The effect of capital cost on the overall integration is small, only 1.5% of the savings is attributed to reduced capital equipment. Therefore, since the primary savings come from operational savings, it can be concluded that integrating a hydrogen production process into an existing ethanol facility could result in similar economic benefits.

The analysis presented here is based on preliminary empirical data and a general economic analysis in order to determine if additional investigation is warranted. More research is indeed necessary to better characterize the synergies of an integrated system and to better understand the operational conditions of an integrated hydrogen production and ethanol production operations facility. It should be noted that the savings generated through integration are additive to any advances that reduce the cost of ethanol production (e.g., cellulose biomass fermentation) or improvements in catalysts that reduce the cost of reforming ethanol to hydrogen.

According to studies conducted by H2Gen Innovations, Inc. (Thomas, 2004), the cost of producing hydrogen from distributed fuel-grade ethanol via steam reforming is estimated at \$4.36/kg H₂. Based on this analysis, the cost of an integrated process would be \$4.06/kg. A comparison of the cost of several hydrogen production technologies is provided in Figure 6. Steam reforming of natural gas is the most widely used commercial technology today. However, increasing demands on natural gas and the increased emphasis on reducing CO₂ emissions will likely impact these cost estimates. With the exception of biomass-derived hydrogen, ethanol provides the next most cost-effective form of renewable hydrogen and provides a viable alternative in the development of both distributed and regional hydrogen infrastructure.

Conclusions

Results from reforming the five ethanol samples illustrated that hydrogen can be generated from ethanol with various levels of coproduct. The highest yield of hydrogen was achieved from Sample 5. The highest fraction of hydrogen in the product gas was observed in Sample 4, processed with additional preheat. Optimization of operating conditions is still necessary to maximize hydrogen production. Additional bench- and pilot-scale experiments will be conducted

Table 2. Estimated Savings for an Integrated Ethanol–Hydrogen System, millions of dollars

<u>Item</u>	<u>Savings</u>
Amortized Capital	0.07
Thermal Integration	3.15
Transportation	1.54
Total Savings	4.76

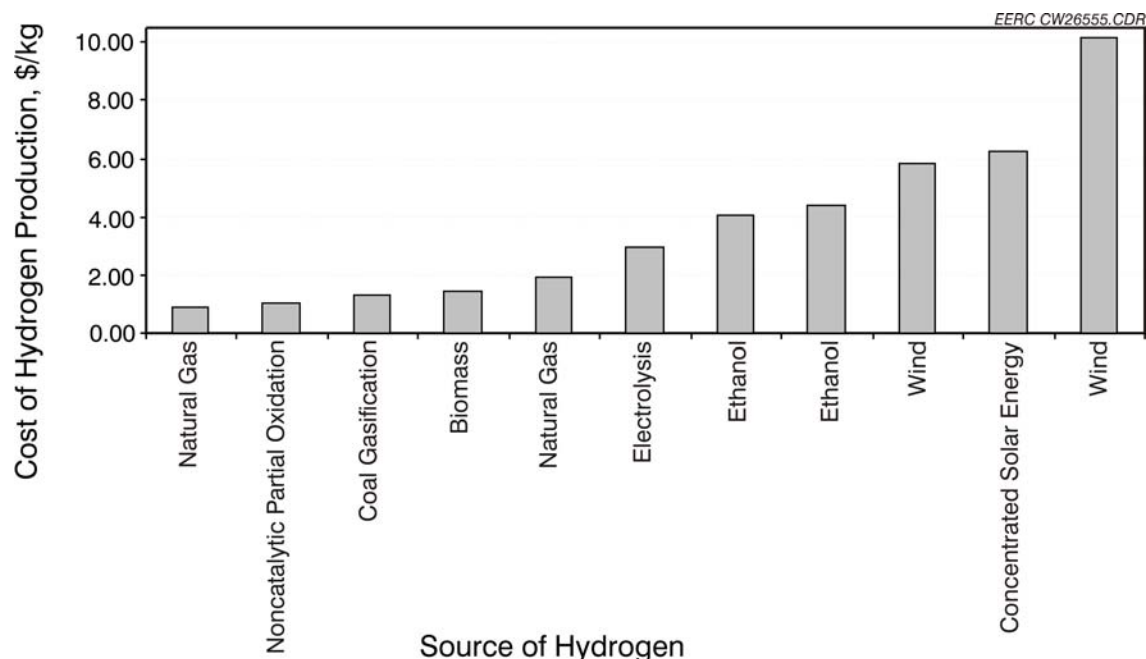


Figure 6. Hydrogen production costs from various technologies (Padró and Putsche, 1999; Thomas, 2004).

in the upcoming year to evaluate the effects of temperature, pressure, residence time, and catalyst on hydrogen yield. Additionally, limited equilibrium modeling will be conducted to develop a test matrix to prioritize the parameters to be tested.

It is suggested from preliminary economic analyses that integration of a steam-reforming system to an ethanol facility for hydrogen production may reduce the cost of hydrogen by \$0.30/kg. These savings are estimated based on a reduction in equipment and energy requirements, transportation of fuel-grade ethanol, and subsequent reforming. The savings are additive to the cost savings associated with future improvements in ethanol manufacture as well as reforming processes.

References

- Barbieri, J. Wells Ethanol Plant Aimed. *The News-Banner*, May 12, 2005, www.news-banner.com/index/news-app/story.1332 (accessed Aug 2, 2005).
- Finnerty, L. Ethanol Spells Price Relief. *Farm Bureau News*, American Farm Bureau Federation, May 2, 2005, www.fb.org/views/focus/fo2005/fo0502.html (accessed Aug 2, 2005).
- Mann, A. Review of Transportation Issues and Comparison of Infrastructure Costs for a Renewable Fuels Standard. Office of Integrated Analysis and Forecasting, Energy Information Administration, Department of Energy, Sept 2002, www.eia.doe.gov/oiaf/servicerpt/fuel/rfs.html (accessed Aug 2, 2005).

Natural Gas Navigator. U.S. Natural Gas Prices. Energy Information Administration, Department of Energy, May 2005, http://tonto.eia.doe.gov/dnav/ng/ng_pri_sum_dc_u_nus_.htm (accessed Aug 11, 2005).

North Dakota State University. Farmer-Owned Ethanol Plants. Quentin Burdick Center for Cooperatives, North Dakota State University, 2003, www.ag.ndsu.nodak.edu/qbcc/HomePage/ethanol%20plants1.htm (accessed Aug 2, 2005).

Padró, C.E.G.; Putsche, V. *Survey of the Economics of Hydrogen Technologies*; National Renewable Energy Laboratory, NREL/TP-570-27079, Sept 1999.

Paustian, P. 2004 National Distillers Grains Marketing Surveys. Iowa Ag Innovation Center, Iowa Department of Agriculture and Land Stewardship, Nov 2004, www.ams.usda.gov/tmd/FSMIP/FY2002/IA0354Present04.pdf (accessed August 2, 2005).

Peters, M.S.; Timmerhaus, K.D. *Plant Design and Economics for Chemical Engineers*, 3rd Ed.; McGraw-Hill Book Company: New York, 1980.

Thomas, C.E. An Affordable Hydrogen Entry Pathway. H2Gen Innovations, Inc., Presented to the 15th Annual National Hydrogen Association Meeting, Los Angeles, CA, April 29, 2004.

YEAR 2004 – ACTIVITY 2 – BIOJET FUEL COLD-FLOW IMPROVEMENT

See Year 5, Activity 6 – Biojet Fuel Cold-Flow Improvement.

YEAR 2004 – ACTIVITY 3 – BIOMASS III ENERGY AND PRODUCTS WORKSHOP

Introduction

Disseminating information through a workshop promotes the use of biomass for heat and power and value-added products. The workshop format provides opportunities for innovative research with potential new industry partners to advance innovative applications of biomass.

The first annual Biomass Energy for Heat and Power workshop was held on June 11, 2002, in Grand Forks, North Dakota. The first workshop focused on heat and power only, while the second (November 13, 2003) and the third workshop included additional topic areas such as biorefineries. The following organizations served as sponsors in 2002 and 2003: the North Dakota Department of Commerce Division of Community Services (DCS), Great River Energy, Montana–Dakota Utilities Resources Foundation, North Dakota Forest Service, Otter Tail Power Company, and Xcel Energy. In 2003, Basin Electric Power Cooperative and the North Dakota Forest Service were added as sponsors.

Although the federal dollars for biomass have decreased significantly in recent years, industry interest and sponsor financial support are strong and growing. For the 2003 workshop, the diversity of our speakers increased immensely. The geographical area represented by our speakers included Colorado, Kansas, North Dakota, Minnesota, Alabama, Georgia, Pennsylvania, Wyoming, Michigan, California, and Manitoba. There was strong support from both the sponsors and the speakers to launch another workshop, and the direction of 2004–2005 workshops was designed to meet the needs of the target audience.

Goals and Objectives

The overall goal was to continue the success and momentum of the first and second Biomass Workshops. Specific objectives included:

1. Add two new sponsors.
2. Increase participation from 2002 levels by 35% to 100 participants.
3. Improve workshop by implementing suggestions from prior year's evaluations.

Involve stakeholders and sponsors in the planning of the workshop, which is an additional goal from previous years.

Experimental

This activity did not have a research component to detail in this section.

Results and Discussion

Originally, the Biomass III Energy and Products Workshop was planned to be held in the fall of 2004; however, the opportunity arose for the workshop to be held as a track within the Renewable Energy Conference in Grand Forks, North Dakota.

The Conference on Renewable Energy in the Upper Midwest was held on February 23–24, 2005, at the Alerus Center in Grand Forks, North Dakota. The conference was hosted by U.S. Senator Byron Dorgan, the University of North Dakota EERC, and the North Dakota Department of Commerce Division of Community Services. More than 520 people from 25 states, the District of Columbia, and five Canadian provinces attended, representing more than 295 organizations.

The 2-day event included the entire Upper Midwest region. The opening session from 8:30 a.m. to noon on February 23, 2005, was offered free to the general public. The public had an opportunity to hear opening session keynote speakers and attend two sessions covering information on the current status of renewable energy in the region and legislation related to renewable energy projects. Attendees also had unlimited access to the exhibit hall during that time.

The Renewable Energy in the Upper Midwest Conference included numerous sponsors and exhibitors related to biomass (Table 3) from around the nation.

Table 3. Sponsors and Exhibitors

Name	Status
Ballard Power Systems	Sponsor
ND DCS	Sponsor
DH Blattner & Sons, Inc.	Sponsor
EAPC	Sponsor and Exhibitor
EERC	Sponsor and Exhibitor
EERC CBU	Sponsor
EERC POWER	Sponsor and Exhibitor
Energy Maintenance Service	Sponsor and Exhibitor
enXco	Sponsor
Farm Credit Services	Sponsor
Farmers Union	Sponsor
Izaak Walton League	Sponsor
MDU Resources	Sponsor
Midwest ISO	Sponsor
Missouri River Energy Services	Sponsor
North Dakota Forest Service	Sponsor
ND Touchstone Cooperatives	Sponsor
Otter Tail Power	Sponsor and Exhibitor
SW REAP and Champion Alliance	Sponsor
Ulteig Engineers – Eric Michel	Sponsor and Exhibitor
Wanzek Construction	Sponsor and Exhibitor
WAPA	Sponsor and Exhibitor
Xcel Energy	Sponsor
Total Sponsorships	
The Affordable House	Exhibitor
Agricultural Utilization Research Institute (AURI)	Exhibitor
BBI International	Exhibitor
Biopower Technologies, Inc.	Exhibitor
Consulting Engineers Group (CEG)	Exhibitor
High Plains Consortium, Inc. (HPC)	Exhibitor
Maxim Technologies Inc.	Exhibitor
New Bio E Systems, Inc.	Exhibitor
Northwest Manufacturing Inc.	Exhibitor
North Dakota Seed	Exhibitor
NRG Systems, Inc.	Exhibitor
Port of Milwaukee	Exhibitor
Red River Valley Research Corridor	Exhibitor
The Rommesmo Companies	Exhibitor
Society for Energy Alternatives	Exhibitor
University of Minnesota – Initiative for Renewable Energy and the Environment (IREE)	Exhibitor
Wanzek Construction	Sponsor and Exhibitor
Westwood Professional Services, Inc.	Exhibitor
Zeltinger Geotechnical Engineering	Exhibitor

The event featured keynote presentations from the nation's top renewable energy officials. Keynote speakers included U.S. Senator Byron Dorgan (D-ND); Marilyn Brown, Director of the Energy Efficiency and Renewable Energy Program, Oak Ridge National Laboratory; North Dakota Governor John Hoeven; and Patrick Wood III, Chairman of the Federal Energy Regulatory Commission.

The Renewable Energy Conference was attended by more than 520 participants from 25 states, the District of Columbia, and five Canadian provinces. The demographic breakdown of attendees is as follows: industry (25%), government (9%), research/academia (16%), utility (16%), finance (2%), development group (14%), landowners (7%), media (2%), and others (9%).

The conference was well-received by attendees. Some representative attendee comments were as follows:

- “Great opportunity to meet and interact with major stakeholders including developers, constructors, manufacturers, policy makers, etc.” – Sudershan Srinivasan, Teshmont Consultants
- “This is a very informative and valuable conference to all involved in renewable energy in our region. Keep up the good work.” – Bob Swenson, Moorhead Public Service.
- “Extraordinary conference! From the knowledgeable, well-spoken presenters and the helpful, efficient organizers to the excellent materials and the A/V that actually worked (and well). Kudos all around!” – Katherine McGuire, Harford Community College

Conclusions

This activity met and then exceeded its proposed objectives. The interest in biomass remains high in the region, and upcoming workshops are planned.

References

None.

YEAR 2004 – ACTIVITY 4 – BIOMASS GASIFICATION AND DISTRIBUTED POWER PRODUCTION

Introduction

Many industries can benefit from the utilization of biomass residues and the production of electric power. However, producing electric power at scale conducive to industry (1 MWe) is cost-prohibitive with conventional technology. The typical approach involves a combustion-based steam cycle plant where continuous attention of a certified (high-pressure steam) boiler operator is required. The economics of such a system typically do not prove attractive. Gasification presents an economic solution. Biomass can be converted to a gas and fired in a

reciprocating/piston engine. The process is performed at low pressure and eliminates the requirement of attended operation, thus reducing operating cost and improving economics. In addition, the equipment is simpler and cheaper to install and can be automated. The combination of these factors enables economically attractive scenarios for biomass conversion to electric power at 1 MWe and less. Many small biomass gasifiers have been constructed and studied; however, commercial-based demonstrations have yet to be completed to prove the technology in the market. This project is focused on overcoming the market barriers.

Goals and Objectives

The goal of the activity is to complete research and demonstration to further the development of a successful power plant demonstration/installation in a commercial setting. Specific objectives include:

- Obtaining gas quality analysis produced from downdraft gasification and performance of various gas-cleaning devices. Tar and particulate are the primary contaminants of concern for piston engines.
- Ascertaining the potential engine life for firing of low-Btu product gas from biomass.
- Demonstrating the commercial aspects (operation and maintenance) of gasification system operation.

Experimental

A portable gasification system constructed at the EERC was provided for testing. The gasifier, gas-cleaning system, and automatic controls are mounted to a 45-ft trailer, as shown in Figure 7. A general process flow diagram is provided in Figure 8. The process flow is as follows. Fuel is loaded into a platform feeder, conveyed, and introduced to the gasifier through a lock hopper. Fuel feed is automated and monitored for alarm conditions with level detection and timers. A programmable logic controller (PLC) provides the control. A single-stage centrifugal blower provides suction on the gasifier and draws gas through a venturi scrubber and filtration. The pressure side of the blower forces gas to a flare or safety filter. The safety filter was bypassed during testing, and primarily all of the gas was flared. Charcoal exiting the bottom of the reactor is carried out in a water slurry. This slurry is combined with scrubbed particulate from the venturi scrubber and condensed water from the coarse filter. The solids are separated using a nylon bag filter downstream. Charcoal is collected in drums, and filtered water is collected in a tank and pumped to two locations. Water is circulated to the bottom of the gasifier for charcoal removal, and water is circulated to the scrubber. Prior to the scrubber, water is filtered, and heat is exchanged from a cooling tower.

Data were collected for gas composition (H_2 , CO , CO_2 , O_2 , CH_4), gas contaminants (particulate and tar), temperatures, pressures, flow rates, and operational parameters. Temperature, pressure, and flow rate data are supplied in 1-min intervals to DASYS Lab software through an Iotech data acquisition module. Gas compositions were recorded in 15-min intervals and supplied from a slipstream (1/4-in. tubing) located between the discharge of the blower and



Figure 7. Portable gasifier test setup.

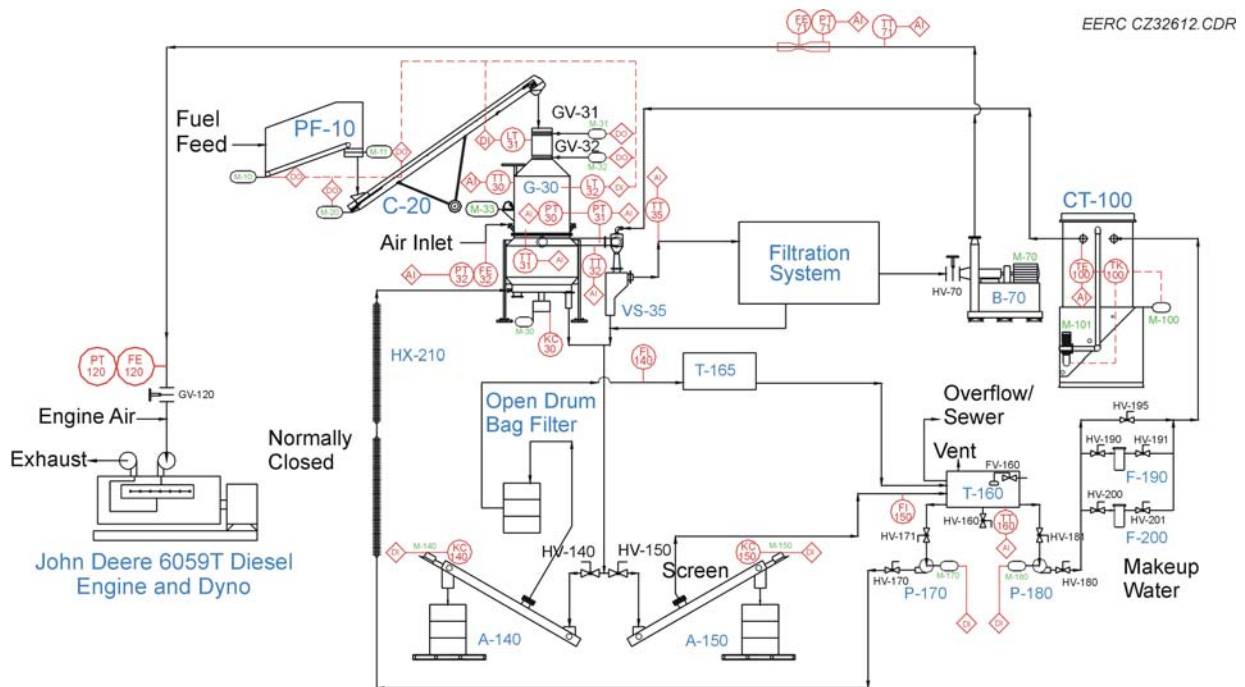


Figure 8. Process flow diagram.

inlet of the flare. Contaminant samples were collected over periods of approximately 5 hr from the same location. Gas was filtered and condensed through a typical impingement train, and the collected material was quantified. A laboratory notebook was used to record major events during each test run to provide a written record of operational data, such as water production/use, fuel consumption, spot measurements, and visual observations. Fuel consumption was measured by recording volumetric loadings of wood chips into the platform feeder and noting the lock hopper cycles. Water production/use was measured by noting the water level change in the tanks over time and the volume of discharges collected. Tests included measuring the performance of a diesel engine connected to a dynamometer, as shown in Figure 9. An existing John Deere 6059T (approximately 100 hp) turbocharged diesel engine and dynamometer were available at the EERC to complete preliminary assessment for operation of the engine with producer gas. Gas flow rate, air flow rate, horsepower, diesel fuel flow rate, and emissions (NO_x, CO, HC) were measured. Gas flow to the engine was controlled manually with a gate valve and measured with a pitot tube (Figure 10). Piping was provided from the gasifier to the engine as shown in Figure 11. The final connect was applied at the inlet of the turbocharger in Figure 12. As gas was introduced to the engine, the diesel fuel was automatically backed off at the governor or fuel pump, shown in Figure 13.

Results and Discussion

BERC Results

Gas production test runs were completed for the Biomass Energy Resource Center (BERC) on August 23–25 and September 20–22, 2004. The gasifier is nominally designed to produce 269 scfm of gas at 127–141 Btu/scf, which is enough energy to produce 100 kW from a spark-ignited piston engine generator or 200 kW from a dual-fuel diesel generator. Test results indicate an average system performance at lower levels than stated by the manufacturer but within acceptable limits. The majority of testing was purposely conducted below the nominal design (269 scfm dry gas production) at an average production of 198 scfm. Since specific operation of the gasifier is usually not with wood chips, steady-state conditions were achieved at less than



Figure 9. Diesel engine and dynamometer.



Figure 10. Gas control and measurement.



Figure 11. Gas piping from gasifier trailer to engine located in the building.



Figure 12. Gas piping to turbo intake.



Figure 13. Diesel fuel pump and governor.

nominal output prior to ramping up to full output and resulted in a lower average production over the course of testing. Correspondingly, all process parameters were lower than stated by the manufacturer. The average measured performance over a 72.1-hr operation period is as follows: gasification efficiency, 68.4%; fuel feed rate, 280 lb/hr; wood heating value, 6426 Btu/lb; wood moisture, 25.2%; product gas heating value, 103.6 Btu/scf; charcoal production rate, 11 lb/hr; and condensate production rate, 0.09 gpm.

Clean gas is critical to engine operation. Particulates and tar content were measured downstream of the gas scrubber and wood-based filters. The average results were 42.5 mg/Nm³

and 484 mg/Nm³, respectively, which is within reasonable expectations for successful engine operation. The cleaned gas was fired in a diesel engine to collect performance data. Although air-to-fuel ratio was not optimized, power, efficiency, and emissions data were obtained. Performance data were collected at 86 hp and 1490 rpm, with the engine operating at a total efficiency of 12%. The equivalence ratio (A/F [air/fuel] ratio actual/A/F ratio stoichiometric) was 0.4 versus 2.1 for baseline diesel operation, which indicates a fuel-rich operation. The diesel substitution rate was 56%. Compared to diesel baseline measurements, hydrocarbon emissions increased from 16 to 25 ppm, carbon monoxide increased from 0.01% to 0.26%, carbon dioxide increased from 7.2% to 15.7%, and NO_x decreased from 1102 to 56 ppm. Baseline diesel fuel efficiency is 39.9%. Further testing is required to optimize the A/F ratio when producer gas and diesel are fired, which will optimize the efficiency and emission data. Testing proved that the engine was capable of producing power from producer gas, and consistent power levels were achieved. The emission data are more indicative of fuel-rich operation than the result of firing producer gas. Emission data from diesel engines firing producer gas can be found in literature where, at optimum conditions, hydrocarbons are expected to remain constant, CO is expected to increase by a factor of 3–5, CO₂ is expected to double, and NO_x is expected to decrease by half.

Several concerns relative to installation at Heyes Forest Products were identified. The primary concern is relative to products of the process: 1) process water, 2) charcoal, 3) filter media, and 4) fuel drying. Every gasification process must cool the product gas down to 140°F prior to firing an engine. Gas cooling produces hydrocarbon-based condensate. Since testing concluded that the gasification process was a net producer of water, condensate becomes a disposal issue. A leaching test was performed to determine the hazardous nature of process water, charcoal, and filter media. The charcoal and filter media were nonhazardous; however, the process water indicated benzene levels exceeding the HazMat (hazardous materials) threshold by a factor of 5.2. Strategies to mitigate benzene concentrations in the process water will require evaluation. Also, economic disposal strategies for charcoal and water must be determined. Filter media can be recycled to the gasifier with no special handling requirements. The processing of charcoal and condensate will affect the design for removal from the process, where the current arrangement is not suitable for Heyes Forest Products. Wood chip moisture content is largely responsible for the quantity of water produced from the system. Limiting fuel moisture can decrease tar production in the gas and minimize the volume of water production; therefore, fuel drying is recommended. Wood chips fired during this test were dried from 45% down to 25% moisture. Since wet wood is expected at Heyes Forest Products, forced drying will most likely be required.

Pembina RC&D Results

Table 4 provides the composition of the biomass fuels during the gasification runs. The composition was obtained from the proximate and ultimate analysis of the fuels. The proximate analysis shows the weight percentages of moisture, volatiles, and fixed carbon. The ultimate analysis shows the weight percentages of hydrogen, carbon, nitrogen, sulfur, oxygen, and ash. The heating value is measured.

In general, the woody fuels operated better than the grassy fuels. The chunk wood and sawdust mixture gave the best performance overall, in spite of it being relatively moist to the touch. This is in contrast to the wood chips, which had to be air-dried over a 3-day period to

Table 4. Composition of Biomass Fuels During Run

Type	Moisture, wt%	Volatiles, wt%	Fixed Carbon, wt%	Hydrogen, wt%	Carbon, wt%	Nitrogen, wt%	Sulfur, wt%	Oxygen, wt%	Ash, wt%	Heating Value, Btu/lb
Wood Chips	18.3	67.9	12.9	6.0	40.7	0.3	0.1	52.1	0.9	6651
Aspen Pellets	9.7	69.8	15.5	5.7	44.3	0.4	0.0	44.6	5.0	7530
Chunk Wood and Sawdust	46	44.4	9.3	7.9	27.3	0.2	0.0	64.3	0.4	4628
Wood Bark	6.1	74.8	13.3	5.5	44.3	0.6	0.1	43.9	5.8	6346
Sunflower Hulls	18.9	62.3	15.6	5.9	40.3	0.6	0.1	50.0	3.2	6813
Corn Stover	15.5	66.8	14.2	5.6	40.9	0.6	0.1	49.4	3.5	6448
Rice Husk	9.2	76.1	11.5	5.9	45.0	1.1	0.1	44.7	3.2	7569
Switchgrass	9.4	69.7	18.2	6.0	42.3	0.6	0.1	46.7	4.3	7044

gasify properly. The wood pellets performed extremely well. The sunflower hulls also handled and gasified very well.

The shredded wood bark, corn stover, wild rice hulls, and switchgrass gave mixed results. In general, these fuels were of lower bulk density and higher surface area than the woody fuels. These fuels were highly reactive and tended to gasify well when they reached the combustion zone of the gasifier. Feeding to the gasifier was not a problem. However, once in the gasifier, both intermittent and catastrophic bridging occurred.

The gasification runs were started on wood chips (Figure 14), which were air-dried over an 8-hour period. These runs were generally unsuccessful, producing a combustion gas with very little CO and H₂ content. The wood chips were then dried over a 3-day weekend and the runs



Figure 14. Wood chips (left) and sunflower hulls (right).

attempted again. The runs with the drier wood chips were successful and without problems. Feeding and handling of the wood chips, both wet and dry, presented no problems. Nor were there any indications of bridging within the gasifier. Moisture analysis of the wood chips indicated 37.3% and 18.3% moisture, respectively, for these two runs. This indicates that the moisture level for wood chips should be below 20% by weight to gasify properly.

The aspen pellets (Figure 15) and wood blocks–sawdust mixture (Figure 16) were run next. Both of these fuels provided very stable gas compositions, flow rates, and gasifier temperatures. Feeding and handling were without problem, and there was no indication of bridging with either of these fuels.

The shredded wood bark (Figure 17) was run fourth and the sunflower hulls (Figure 14) run fifth. The physical characteristics of the wood bark were a mixture of chunky pieces of bark and fibrous chips. The wood bark was received wet and allowed to air dry over a 3-day weekend to 6% moisture by weight before testing. Feeding and handling of the wood bark were without



Figure 15. Aspen wood pellets.



Figure 16. Mixture of chunk wood and sawdust.



Figure 17. Shredded wood bark.

problem. Visual observation of the combustion zone confirmed the high reactivity of the fibrous chips. This was further confirmed by a decrease in the feeding intervals, to about one-third that of chunk wood. This indicated that the wood bark was gasifying at a faster rate than typical wood chunks. The wood bark was run over 2 days. Throughout the runs, the temperature at the top of the reactor cycled from normal to high. This may have been an indication of intermittent bridging in the gasifier. Longer-term runs are needed to determine the severity of the bridging tendency. A possible solution to the bridging tendency is to reduce the size of the bark before feeding. The sunflower hulls ran very well. They exhibited no feed issues and gasified very well.

The corn stover (Figure 18), wild rice hulls (Figure 19), and switchgrass (Figure 20) were run last over a period of 2 weeks because of the need to shut down, cool off, and provide maintenance to the reactor after each of these runs. The corn stover and switchgrass were reduced prior to testing to below $\frac{1}{2}$ in. In general, these fuels had very low bulk density and relatively high surface area, making them highly reactive. Feeding and handling to the reactor were without problem. Once in the reactor, however, signs of catastrophic bridging occurred within the first 2 hours of the runs. Each of these runs was shut down prematurely. Visual inspection of the gasifier after cooling confirmed the bridging.

The dry gas composition during the steady-state gasification condition is presented in Table 5. The gasification efficiency was estimated from a carbon balance between the gas composition data and proximate/ultimate data. The efficiency calculation neglected the amount of char removed during gasification because it was not possible to differentiate the effect each fuel had on the char bed in such short-term runs. Longer-term runs are necessary to take into account the char conversion efficiency specific to each fuel. The total char removed during the gasification runs was less than 3%, by weight, of the total fuel fed. The efficiency calculation must be lowered by approximately 3%. As an example, the efficiency for the wood chips is between 53% and 56%. For the sunflower hulls, the efficiency during the steady gasification condition is between 69% and 72%.



Figure 18. Corn stover before reduction in size (left) and after size reduction (right).



Figure 19. Wild rice husks.



Figure 20. Switchgrass before size reduction (left) and after size reduction (right).

Table 5. Gas Compositions, Dry Gas HHV (Btu/scf), Efficiency

Type	CO, vol%	CO ₂ , vol%	CH ₄ , vol%	H ₂ , vol%	N ₂ , vol%	HHV, Btu/scf	Energy Efficiency, %
Wood Chips	10.75	19.71	1.46	13.50	54.59	86.2	56
Aspen Pellets	17.50	17.59	2.77	15.69	46.45	125.2	66
Wood Sawdust	14.92	15.95	0.90	14.94	53.29	97.7	62
Wood Bark	12.15	19.64	1.74	14.98	51.50	97.5	69
Sunflower Hulls	15.17	16.79	1.88	19.61	46.56	121.7	72
Corn Stover*	14.04	15.44	1.09	15.83	53.60	99.6	70
Rice Husk*	17.39	13.45	0.77	21.02	47.37	122.1	68
Switchgrass*	13.31	16.12	0.92	16.05	53.60	96.4	65

* Incomplete runs.

Engine generators require relatively clean gas to prevent premature top-end failures. Gas contaminants include particulate and tar, which cause erosion and intake fouling. Particulate and tar were measured over approximately a 1-hour period. The results are included in Table 6. Particulate concentrations varied from 1.4 to 192 mg/Nm³. The relative tar levels varied from 300 to 6000 mg/Nm³. The wood chunk–sawdust mixture provided the cleanest producer gas overall, with tar and particulate levels of 338 and 4.6 mg/Nm³, respectively.

Conclusions

Research was conducted to help further the commercial advancement of biomass gasification for power generation (<1 MWe). The results of the project support the project objectives as follows:

- Gas quality data were obtained from gasification of various fuels. Gas-cleaning equipment appears to be adequate for cleanup relative to firing in a piston engine. Wet fuels tend to cause higher tar levels in the product gas.
- Engines firing producer gas can experience short-term operation issues due to tar deposits on engine intake surfaces. The diesel engine used in the experiment did not exhibit tar deposits, and gas quality measurements show low particulate levels in the product gas, suggesting better long-term engine life.

Fuels that have good gravity flow characteristics and are relatively dry perform the best in a fixed-bed downdraft gasifier. Fuels that have very low bulk densities or are prone to bridging because of their geometry can be problematic. General process maintenance is relatively low; however, advancements regarding process residuals will need improvement to ensure a commercially attractive product.

References

None.

Table 6. Contaminant Levels in Producer Gas

Type	Tar, mg/Nm ³	Particulate, mg/Nm ³
Wood Chips	6250	192
Aspen Pellets	6150	165
Wood and Sawdust	338	4.6
Wood Bark	820	1.4
Sunflower Hulls	867	7.2
Corn Stover*	700	6.4
Rice Husk*	700	21.2
Switchgrass*	1000	18.2

* Notes incomplete runs.

YEAR 2004 – ACTIVITY 5 – ECONOMICALLY OPTIMIZED BIODIESEL PRODUCTION FROM LOW-VALUE FEEDSTOCKS

Introduction

Vegetable oils and their derivatives have been used as diesel fuels for over 100 years. Some of the first diesel engines preferred peanut oil derivatives for fuel. However, the high viscosity of the vegetable oils resulted in severe gumming and deposition, so the transition to petroleum hydrocarbon fuels ensued, despite the serious particulate and sulfur emission problems from the compression ignition engines using the hydrocarbon fuels. To achieve lower emission vehicles, fuels were formulated with varying amounts (blends) of lower viscosity methyl esters (biodiesel) prepared from the vegetable oils. Ethanol is also used to prepare the corresponding ethyl esters of the fatty acids, or E-diesel.

In addition to reduced particulate, CO, organic, and sulfur emissions obtained using these fuel blends, the biodiesel is a renewable resource fuel. Being renewable, it contributes less to global warming than the petroleum fuels. Produced from U.S. crop oils (mostly soy oil in the United States and rapeseed oil in Europe), biodiesel can help to decrease the dependence on foreign oil or, at least, level out the fluctuations in supply so as to keep fuel prices stable. Some of the biodiesel is produced from waste grease, animal fats, and frying oils. Another advantage of biodiesel is the lubrication property. This is important in blends with hydrocarbon fuels with very low sulfur content.

Disadvantages of biodiesel are its slightly higher NO_x emission, problems with gelling and clouding in cold climates, and relatively high cost. Although the process utilized to produce commercial biodiesel is relatively inexpensive, the per-gallon cost of soy and other vegetable oil feedstocks translates to a biodiesel market cost that is usually significantly higher than that of petroleum diesel. So usually a blend with petroleum hydrocarbon diesel is used, rather than 100% biodiesel.

Most biodiesel is produced via the transesterification reaction of methanol with vegetable oil that has been minimally refined, that is mainly the triglyceride form. The reaction is catalyzed by adding NaOH, and after a short time, the biodiesel ester separates from the glycerol–water

layer containing the NaOH. If, however, free fatty acid (FFA) is present in the oil, the catalyst is converted to an inactive soap, and the process does not complete. This is a problem especially with using waste oils and with by-product soapstock oils from vegetable oil refining plants, since these contain free acids and the process must be done in two stages.

A concept was devised at the EERC for producing methyl ester-based biodiesel from feedstocks with significantly lower value than soybean oil and other traditional biodiesel feedstocks. One option for cheaper biodiesel involves its production from soapstock by-products from the vegetable oil processing industry that are high in FFA content. In a project funded through the EERC's National Alternative Fuels Laboratory (NAFL), a method was recently developed for processing high FFA-content oil to biodiesel. The method is based on the solid acid-catalyzed reaction of the soapstock oil with a proprietary nonalcohol alkylating agent. In preliminary tests with commercial oleic acid (a major component of the by-product oil), yields of nearly 100% methyl ester were achieved. With commercial high FFA-content soy soapstock oil provided by Archer Daniels Midland Company (ADM), a high yield of biodiesel esters was obtained. Further work was needed to complete the conversion of the glycerides present in the soapstock oil into methyl esters and to develop an acceptable product isolation scheme for removing by-products from the methyl esters.

Goals and Objectives

The objectives of project are the following:

- Assessment and improvement of process economics via optimization of reaction conditions, reactor configuration, and catalyst type and configuration.
- Process evaluation and optimization with a variety of different feedstocks.

Experimental

The project objective is the development of an innovative method for economically converting high fatty acid-content vegetable oil to methyl (or ethyl) esters. As stated previously, oils high in FFAs are inexpensive, but are difficult to process because FFAs consume catalyst. The processing method employed here is based on the use of a proprietary nonalcohol alkylating agent that utilizes a solid acid catalyst.

The EERC has pioneered the development of a proprietary alkylation process that not only represents a novel method of driving the transesterification reaction, but also utilizes a reagent (CH_3X) that is worth less than the biodiesel coproduct (HX) shown in the generic reaction:



The corresponding transesterification reaction with the glycerides present in the oil is represented in Reaction 2, where $\text{R}'\text{X}$ is a by-product from the glycerin. This is a more general equation of the methanol reaction with the glyceride, where $\text{X} = \text{OH}$ and $\text{R}'\text{X} = \text{glycerol}$.



Key advantages of this approach versus the traditional methanol (alkylation agent) and sodium hydroxide (catalyst) biodiesel process include 1) compatibility with continuous (versus batch) processing; 2) required use of only a catalytic amount (versus a stoichiometric amount) of catalyst to ensure quantitative transesterification of triglycerides and FFAs, 3) elimination of the need for sodium hydroxide neutralization; 4) possible elimination of the need to separate biodiesel from water and reaction residues, which means no dealing with salts and emulsions; and 5) generation of a high-value coproduct from the glycerin by-product (R'X) from oil transesterification.

Results and Discussion

Preparation of Solid Acid Catalysts for Biodiesel Methyl Ester Production

Solid acid catalysts for transesterification of vegetable oils and acidulated soapstocks obtained from vegetable oil refining were selected and prepared in the initial phase of the project. Solid acid catalysts have many economic advantages over the conventional base catalysts for biodiesel. An acid catalyst is not impacted by FFA present in the substrate, such as acidulated soapstock, whereas a base catalyst is neutralized and destroyed. A solid catalyst does not require a neutralization step, since it is easily removed from the products of a batch reaction by decanting or filtering, and it allows continuous reactions to be performed using a bed of the solid catalyst. A disadvantage of solid catalysts is that the reactions are considerably slower and, therefore, require higher temperatures to optimize the yields of methyl esters from these feedstocks using solid acid catalysts in a reasonable time period. The solid acid catalysts were selected on the basis of prior experience with a variety of reactions conducted at elevated temperatures. Both proprietary and conventional catalysts were utilized in this investigation.

Evaluation of Catalysts for Transesterification

Several solid acid catalysts were investigated for their activity for production of biodiesel from raw vegetable oil and oil refining by-products. Liquid-phase acid catalysts were also utilized to provide a comparison of the activities. Batch and flow-through reactions were evaluated under various process conditions to determine which process configurations will be economically preferable and which conditions produce highest yields. Using the catalysts, two series of catalytic batch tests were conducted on four biodiesel precursor substrates, viz., raw vegetable oils (canola and soy), acidulated soapstock, and oleic acid. Oleic acid is the major fatty acid of canola soapstock and several other vegetable oil soapstocks. The initial series of tests utilized an inexpensive methylating reagent that was expected to produce high conversions of the methyl ester because of its ability to shift the equilibrium and also produce a higher-value by-product from the reaction of the agent with a carboxylic acid. The second series of tests used methanol.

Reactions of the Alternative Methylating Agent with Oleic Acid

Reactions of the alternative methylating agent (CH_3X) with oleic acid were conducted in a Parr pressure reactor with acid catalyst using various molar ratios of the reactants and several temperature–pressure conditions. The yields of methyl ester are shown in Table 7.

In the first set of reactions, the catalyst was the H^+ form of a cation exchange resin, and the molar ratio of reactants and operating pressure were varied. Reactions using the molar ratio of CH_3X / oleic acid = 1 at relatively low pressure (50 psi) and low temperature (100°C) gave a poor yield of methyl ester. Increasing the pressure to 700 psi by adding nitrogen pressure increased the yield to 49%, but this was still not satisfactory, even with the long reaction time. When the ratio of CH_3X /oleic acid was increased to 4, the yield improved to 72% for reaction time of 6 hr at 600 psi. Increasing the pressure to 700 psi for the reactant ratio of 4 resulted in a 79% yield. An attempt to drive the reaction with added additional molecular sieves to absorb the water by-product gave only a 19% yield of methyl ester under the same conditions.

A comparison of the reaction with a soluble liquid catalyst (sulfuric acid) with the solid acid catalyst was conducted. The reaction of the 1:4 mixture of oleic and CH_3X with sulfuric acid catalyst at 700 psi gave a small improvement in the yield of methyl ester to 82%.

The effect of temperature was demonstrated with a reaction at 125°C and pressure of 700 psi. The yield data show that the higher temperature conditions are much superior (92%) to the yields at lower temperatures (100°C) at comparable pressure (79%).

Table 7. Yields of Esters from Oleic Acid and Alkylating Agent RX

RX	Catalyst	RX/ Oleic Acid	Pressure, psi	Temp., $^\circ\text{C}$	Time, hr	Yield, %
CH_3X	IR-120	1	50	100	22	32
CH_3X	IR-120	1	700	100	22	49
CH_3X	IR-120	4	600	100	6	72
CH_3X	IR-120	4	700	100	3	79
CH_3X + Mol. Sieve	IR-120	4	650	100	3	19
CH_3X	H_2SO_4	4	700	100	3	82
$\text{CH}_3\text{CH}_2\text{X}$	IR-120	4	550	100	3	2
CH_3X	IR-120	4	700	125	3	92
CH_3X	MSA	4	900	125	3	96

A second soluble (homogeneous) catalyst (MSA) was tested at the 125°C conditions. This catalyst provided slightly better yield (96%) compared to the solid acid catalyst.

Reactions of the Alternative Methylating Agent with Canola Oil

Reactions of the alternative methylating agent (CH₃X) with canola oil were conducted in a Parr pressure reactor with solid acid catalyst using various molar ratios of the reactants and several temperature–pressure conditions. Several fatty glycerides are present in the canola oil but it was mainly oleate. The conversions of the canola triglyceride to the methyl ester mixture are shown in Table 8.

With the H⁺ form of a cation exchange resin as catalyst and the molar ratio of CH₃X/canola oil at 4.5, a poor conversion of canola oil to methyl ester was obtained at 100°C during the short time period. Increasing the time period to 22 hr increased the yield to 63%. But this conversion compares poorly with the reaction of oleic acid under the same conditions. Thus it is more difficult to react the triglyceride than the acid forms. The temperature limitation of the resin acid is actually less than 100°C for long-term use. To run the reactions at the higher temperatures requires a liquid-phase catalyst in a batch reaction or a solid inorganic acid. Both options were pursued in this project.

Reactions of the alternative methylating agent (CH₃X) with canola oil were conducted in a Parr pressure reactor with liquid acid catalyst (MSA) using a molar ratio of the reactants of 4 at 125°C. The conversions of the canola soapstock to the methyl ester mixtures are shown in Table 8. Owing to the low reactivity of the di- and triglycerides, the yield was mediocre. The reaction with canola oil conducted at 150°C gave a very high conversion to the methyl ester (98%). The alkylating reagent decomposes above this temperature.

Reactions of an Analogous Ethylating Agent (CH₃CH₂X) with Oleic Acid and Canola Oil

The reaction of the analogous ethylating agent (CH₃CH₂X) with oleic acid (molar ratio = 4) using the ion exchange resin catalyst gave a very poor yield of ethyl ester (Table 7). The

Table 8. Conversions to Esters from Canola Oil and Alkylating Agent RX

RX	Catalyst	RX/ *FAeq	Pressure, psi	Temp., °C	Time, hr	Yield, %
CH ₃ X	IR-120	4.5	700	100	3	23
CH ₃ X	IR-120	4	700	100	22	63
CH ₃ CH ₂ X	IR-120	4	700	100	3	0
CH ₃ X	MSA	4	875	125	3	70
CH ₃ X	MSA	4	900	150	3	98

* FAeq is the fatty acid equivalent of the triglyceride or moles/3.

reaction with canola oil gave no conversion to ethyl ester (Table 8). Thus it is very difficult to react the ethyl analog of the alkylating agent with the fatty acids or triglycerides.

Reactions of the Methylating Agent with Canola Soapstock

Reactions of the alternative methylating agent (CH_3X) with acidulated canola soapstock were conducted in a Parr pressure reactor with liquid acid catalyst (MSA) using a molar ratio of the reactants of 4 at 125°C . The conversions of the canola soapstock to the methyl ester mixtures are shown in Table 9. Even though the oleic acid present in the feed was expected to give a high yield of methyl ester, the mediocre conversion is likely due to the low reactivity of the di- and triglycerides present in the acidulated soapstock.

A reaction with the canola soapstock was conducted at 150° and 750 psi using the MSA catalyst. This reaction gave the highest conversion to esters (99.7%).

Continuous Reaction on Solid Acid Catalyst Bed

A bed of the solid acid ion exchange resin (IR-20) was placed in a tube reactor, and a solution of the acidulated soapstock feed in the methylating agent (ratio = 1:4) was pumped through the bed at 82°C . However, a poor conversion (25%) of soapstock to methyl ester was obtained at this low temperature and low pressure (Table 9). It was difficult to run the tube at higher temperature and pressure conditions.

Solid Inorganic Acid Catalysts for Transesterification of Crude Soy Oil

Several proprietary inorganic acid catalysts were prepared and investigated for the transesterification reactions of vegetable oils. These were mixed metal oxides with strong acidic properties. The rationale for this change was that the soapstock will not actually be produced in the large amounts needed for the potential demand for biodiesel. If we find an acidic catalytic system that works well with the triglyceride forms, it will work better with the acidulated soapstock, since the latter is much more reactive.

The tests used the methylating agent initially and then methanol in later tests. The rationale for this is that the methylating reagent is less reactive than methanol and will require higher

Table 9. Conversions to Methyl Esters from Canola Soapstock and Alkylating Agent RX

RX	Catalyst	RX/ Oleic Acid	Pressure, psi	Temp., $^\circ\text{C}$	Time, hr	Yield, %
CH_3X	MSA	4	875	125	3	80
CH_3X	MSA	4	900	150	3	98
CH_3X	IR-20 Continuous	4	400	82	0.3	25

temperatures and pressures. The methylating reagent is also unstable at the higher temperatures that may be required for very high conversions in a short time. The higher pressure requirement makes it more difficult to use in a continuous reactor. The glycerol-derived by-products from the alkylating agent reaction are more difficult to separate from methyl biodiesel than is glycerol obtained from the methanol reaction. This would not be a big problem if there were good markets for the derivatives, but these do not yet exist.

Reactions of the methylating reagent with oleic acid using the ZA catalyst gave excellent yields of methyl ester at 200°C, but dropped off considerably at 250°C, owing to decomposition of the methylating agent and formation of gas, which increased the pressure (Table 10). The catalyst at 150°C was not active enough to generate good yields of ester.

The reactions of a soy triglyceride oil with the alkylating agent were also investigated using a solid inorganic acid (AL), and the results shown in Table 11. Reactions at 150°C gave poor yields with 5% fresh AL catalyst. Using recovered catalyst at 10% load at 150°C improved the conversion to 53%. The reaction at 200°C gave a quantitative yield of ester, but all the excess alkylating reagent was decomposed at the high temperature, and the pressure increased drastically. The catalyst may help decompose the methylating reagent at the high temperature. When only 1% loading of catalyst was used, less decomposition occurred, as demonstrated by the lower operating pressure observed. Unfortunately, a much lower conversion (72%) was obtained for this experiment.

Methanol Reactions

The reactions of the soy oil with methanol were carried out with several solid inorganic acids. For comparison, the uncatalyzed reaction with the methanol reactant in large excess gave 45% conversion at 200°C for 16 hr (Table 12). Both the AL and ZT catalysts under similar conditions gave 100% conversion to esters. Reactions with the AL catalyst for 2 hr gave a 90% conversion to esters. The reaction conducted at 175°C with AL also gave 100% conversion to esters at 16 hr, but dropped to 43% conversion for a 1-hr reaction at 175°C. Reducing the temperature further to 150° (4 hr) lowered the conversion substantially (78%). So it is clear that both temperature and reaction time have a major impact on the conversion. The AL catalyst was recovered and reused, giving 100% conversion to esters.

Table 10. Yields of Esters from Oleic Acid and Methylating Agent CH₃X with Solid Acid Catalysts

RX	Catalyst	RX/ Oleic Acid	Pressure, psi	Temp., °C	Time, hr	Yield, %
CH ₃ X	ZA	4	300	150	6	42
CH ₃ X	ZA	4	500	200	6	97
CH ₃ X	ZA	4	2500	250	6	72

Table 11. Conversions to Esters from Soy Oil and Methylating Agent CH₃X with Solid Acid Catalyst

RX	Catalyst	RX/ FAeq	Pressure, psi	Temp., °C	Time, hr	Conversion, %
CH ₃ X	AL 5%	3.7	325	150	16	40
CH ₃ X	AL 5%	3.7	2500	200	16	100
CH ₃ X	AL 1%	3.7	630	200	16	72
CH ₃ X	AL recov. 10%	3.7	630	150	16	53

Table 12. Conversions to Esters from Soy Oil and Methanol with Solid Acid Catalysts

RX	Catalyst	RX/ FAeq	Pressure, psi	Temp., °C	Time, hr	Conversion, %
CH ₃ OH	None	28	550	200	16	45
CH ₃ OH	AL	28	600	200	16	100
CH ₃ OH	ZT	28	600	200	16	100
CH ₃ OH	AL	28	600	200	2	90
CH ₃ OH	AL	28	500	175	16	100
CH ₃ OH	AL	28	400	175	1	43
CH ₃ OH	AL	28	300	150	4	78
CH ₃ OH	AL recov.	28	600	200	16	100
CH ₃ X + CH ₃ OH	AL	28	650	150	16	66
CH ₃ OH	ZD	28	300	150	16	100
CH ₃ OH	ZD	28	250	150	4	100
CH ₃ OH	DS	28	250	150	4	100

Since lower conversions at 150°C were observed for vegetable oils using the methylating agent in the reactions discussed above, the reaction of a mixture of methanol with the methylating agent was attempted with the AL catalyst at 150°C. Unfortunately, the methanol did not promote the reaction of the methylation reagent at the lower temperature and only 66% yield was obtained.

Reactions of methanol with soy oil were performed using two other solid inorganic acid catalysts, ZD and DS. These reactions were conducted at a lower temperature (150°C), but also gave 100% conversion at the lower reaction time period (4 hr). A problem of these two catalysts

was that they partially dissolved in the reaction media. Thus part or all of the reaction may have occurred with the solubilized portion (homogeneous reaction). This would explain the very high reactivity at 150°C, but may make it difficult to recover the catalyst.

The final set of reactions was conducted with methanol at a lower concentration; that is, methanol/fatty acid equivalent = 7.3. The reaction times were also reduced to 1 hr or less. The reactions were conducted at 200°C, since there is no issue of decomposition at this temperature. The reaction of methanol with soy oil using the DT catalyst gave a very good conversion to ester (91%) for a 1-hr time period. However, the catalyst recovered from the reaction performed poorly when it was reused in a subsequent reaction. A catalyst with similar chemistry (DB) was less catalytically reactive, giving 57% conversion for 1-hr and 48% for 0.5-hr reaction times.

Interestingly, the recovered DB catalyst performed much better in a subsequent test using the same conditions. It is likely the catalyst was actually slowly transformed into a better catalyst during heating in the methanol–oil mixture in the course of the reaction. Further work is needed to prove this point. In any case, longer reaction periods are needed to optimize reactions with this catalyst.

Two more catalysts were also tested with lower methanol concentrations and short reaction times (Table 13). Both the ZN and SU catalysts performed poorly in the transesterification under these conditions. The number of catalysts tested under these conditions was not as comprehensive as we had originally planned; however, one of the most active catalysts (DT) was tested. Further work will be performed at somewhat longer reaction times.

Conclusions

A novel process was demonstrated for production of methyl esters from vegetable oil refining by-products such as soapstock or other waste oils with high FFA content. These

Table 13. Conversions to Esters with Solid Acid Catalysts Using Lower Methanol Concentrations

RX	Catalyst	RX/ FAeq	Pressure, psi	Temp., °C	Time, hr	Conversion, %
CH ₃ OH	DT	7.3	550	200	1	91
CH ₃ OH	DT recov.	7.3	450	200	1	13
CH ₃ OH	DB	7.3	525	200	1	57
CH ₃ OH	DB	7.3	500	200	0.5	48
CH ₃ OH	DB recov.	7.3	550	200	1	71
CH ₃ OH	ZN	7.3	450	200	1	20
CH ₃ OH	SU	7.3	500	200	1	30

substrates are not converted in high yields using the conventional base-catalyzed process. With the methylating reagent in the novel processing, the conversion of these acid substrates (soapstock or oleic acid) to methyl ester using several liquid and solid acid catalysts were exceptionally high (99%). Conversions of the raw or refined vegetable oil were lower, however, owing to the slower kinetics for the triglyceride forms, and the operating temperatures were limited by the decomposition of the reagent in the presence of the catalyst. A preliminary assessment of availability showed that the high acid soapstock supply is limited and could not make up a significant piece of the biodiesel market. Furthermore, no market currently exists for the glyceryl derivative formed in the new process, so its value could not be assessed. Thus emphasis in the project shifted to the use of methanol with the highly active solid acid catalysts that produce methyl esters with glycerol as the by-product from the triglycerides.

Thus to find an optimal solid acid catalyst to use with methanol and raw oil, a second series of tests evaluated the use of methanol with the various solid acid catalysts for the conversion of a raw soy oil. Quantitative conversions to methyl ester biodiesel were obtained from the raw oil using several of the catalysts. Even with reaction times as short as 1 hr and low ratio of methanol to oil, good yields were obtained. Recovery of the catalyst was by filtration or decantation, giving a significant advantage over previous catalytic systems. Since the solid catalyst was easily recovered, it was reused in some cases with excellent results. Catalyst recovery and reuse provide a significant advantage over previous liquid catalytic systems where acid was neutralized and destroyed. Thus the solid acids can be utilized in a fixed bed in a continuous reactor. Glycerol by-product settled out upon evaporation of the methanol; thus it can be obtained without any neutralization and subsequent contamination by the salt.

Because of the change in focus from methylating agent to methanol, the economic evaluation has, therefore, been slowed, but should be much easier to accomplish in the near future, since we are not producing any new by-product and not using any new reagent or the soapstock, whose value has been highly questionable. Nevertheless, the new process is different from the conventional base catalysis process, so the economic evaluation needs to be performed.

References

None.

YEAR 2004 – ACTIVITY 6 – MANAGEMENT AND STRATEGIC STUDIES

Introduction

Disseminating information through a workshop promotes the use of biomass for heat and power and value-added products. The workshop format provides opportunities for innovative research with potential new industry partners to advance innovative applications of biomass.

The first annual Biomass Energy for Heat and Power workshop was held on June 11, 2002, in Grand Forks, North Dakota. The first workshop focused on heat and power only, while the second (November 13, 2003) and the third workshop included additional topic areas such as

biorefineries. The following organizations served as sponsors in 2002 and 2003: North Dakota Department of Commerce Division of Community Services, Great River Energy, Montana–Dakota Utilities Resources Foundation, North Dakota Forest Service, Otter Tail Power Company, and Xcel Energy. In 2003, Basin Electric Power Cooperative and the North Dakota Forest Service were added as sponsors.

Although the federal dollars for biomass have decreased significantly in recent years, industry interest and sponsor financial support are strong and growing. For the 2003 workshop, the diversity of our speakers increased immensely. The geographical area represented by our speakers included Colorado, Kansas, North Dakota, Minnesota, Alabama, Georgia, Pennsylvania, Wyoming, Michigan, California, and Manitoba. There was strong support from both the sponsors and the speakers to launch another workshop, and the direction of 2004–2005 workshop was designed to meet the needs of the target audience.

Goals and Objectives

The goal of this task was to provide efficient project management, direct any select strategic outreach or studies, and continue success and the momentum of the first and second Biomass Workshops. Specific objectives included:

- Providing overall management of the EERC CBU 2004 project.
- Implementing a quality assurance and quality review process for all research activities and spending, including periodic internal project review meetings.
- Spearheading all necessary DOE reports, including NEPA, quarterly, final, and other report types.
- Developing a Web site to showcase biomass-related research within the project.
- Promoting attendance and dissemination of information generated through the project at international biomass-related conferences and meetings.
- Networking with commercial industry clients and peers.
- Aiding in the annual Biomass: Energy and Products Workshop.

Experimental

This activity did not have a research component to detail in this section.

Results and Discussion

Efficient project management and quality control were provided for all five technical project activities, with individual review meetings held with each project activity manager. In these meetings, the status of project results, milestones, timetables, and budgets were reviewed.

In addition, periodic internal meetings were held for all research activity managers to discuss project results and project status and to discuss results with other peers not directly involved in these activities but working in similar biomass technology areas. Also at these meetings, a 30–40-minute presentation was usually given by either a researcher from an academic department of the University of North Dakota (UND), from the EERC, or from a visiting agency. The presentations were very informal but centered on utilizing biomass for energy and fuels. Presenters included Dr. Kline Ileligi from Purdue University, who discussed biomass slurry-heat treatment as a processing method for biorefinery technologies; Dr. Chuanbin Liu from Washington State University, who gave a talk on fermentative production of bioenergy and bioproducts; Chris Zygarlicke and Darren Schmidt from the EERC, who gave an overview of distributed electricity production using small-scale biomass gasification technology; and Dr. Dinyi Ye from the EERC, who spoke on applied and environmental microbiology.

Activity 6 also aided in putting together speakers and technical content for the Biomass III Energy and Products Workshop, held in conjunction with the Renewable Energy Conference on February 23 and 24, 2005, in Grand Forks, North Dakota, at the Alerus Center, a large civic conferencing center. There were over 520 participants in the conference with 25 exhibitors. The conference focused primarily on wind and biomass energy-related topics. Well over 400 of the participants attended at least one of the biomass-related sessions which included sessions on biomass resources, biomass-to-ethanol, biopower, biorefineries, biodiesel, small biomass power electrical transmission, renewable legislation, production tax credits, renewable energy credit systems, renewable hydrogen production, and commercial demonstrations of biopower systems. Marilyn Brown, Director of the Energy Efficiency and Renewable Energy Program at Oakridge National Laboratory, was one of several keynote speakers at the conference.

In the area of strategic studies and forward planning for future biomass research and development, several meetings were held and presentations made regarding biomass utilization. A visit was made to the DOE Office of Energy Efficiency and Renewable Energy headquarters in Washington, D.C., in January 2005 to give a technical review and progress report presentation on all the individual activities that were ongoing. The meeting included Chris J. Zygarlicke, overall project manager of the EERC CBU[®] project and John Ferrell and Larry Russo from the Biomass office of DOE Energy Efficiency and Renewable Energy (EERE). Director of the DOE EERE Office of Biomass, Douglas Kaempf, was invited but did not attend. Ferrell and Russo were both in charge of biorefinery project development efforts, including projects from federal solicitations and congressionally directed projects like the EERC CBU[®] 2004. They acknowledged the need for the project activities, especially those pertaining to biorefinery-biobased products like the production of succinic acid and alkanolamines from biomass and cetane from glycerin. They were impressed with EERC work in developing distributed power from biomass gasification. Also discussed were important national initiatives and the overall direction of the EERC CBU Program. They gave input on the future direction of the EERC project.

Several meetings and conferences were attended to publish and disseminate results generated from the EERC CBU Program through the presentation of papers, sitting on discussion panels, and attending colleague meetings at these venues: the Harvesting Clean Energy Conference V on January 20–21, 2005, in Great Falls, Montana; the National Ethanol

Conference in Scottsdale, Arizona, on February 7–9, 2005; PowerGen Renewables in Las Vegas, Nevada, on March 1–3, 2005; the National Hydrogen Association’s Annual International Hydrogen Conference in Washington, D.C., March 29 – April 1; the International Technical Conference on Coal Utilization and Fuel Systems (Clearwater Conference) in Clearwater, Florida, on April 17–21, 2005; the Second Annual World Congress on Industrial Biotechnology and Bioprocessing, held in Orlando, Florida, on April 20–22, 2005; the 27th Symposia on Biotechnology for Fuels and Chemicals in downtown Denver, Colorado, sponsored by the National Renewable Energy Laboratory; a DOE EERE review meeting in Denver, Colorado, on June 8, 2005, where the EERC presented on biodiesel research projects (Activities 2 and 5); a seminar on June 16, 2005, related to Agri-Based Energy and Fuels presented at the Biobased Products Institute on the Montana State University campus at Bozeman, Montana; and a poster presentation made at the DOE Peer Review in Arlington (Washington, D.C.) on November 14–16, 2005.

Conclusions

This activity met and then exceeded its proposed objectives. The interest in biomass remains high in the region, and upcoming workshops are planned.

References

None.

YEAR 2005 – ACTIVITY 1 – MANAGEMENT AND STRATEGIC STUDIES

Introduction

The Management and Strategic Studies task involves general management duties that include administering contractual obligations for the DOE administrators in Washington, D.C.; preparing all project application documents; preparing all quarterly, final topical, hazardous substance, and milestone reports; assembling an annual project review presentation; ensuring quality assurance/quality control for all activities; and facilitating kickoff, midproject review, and bimonthly renewables/biomass informational meetings with individual activity leaders. Strategic studies activities include facilitating sessions related to bioenergy/bioproducts at an annual renewable energy conference; attending and participating in strategic conferences related to biomass utilization; and conducting forward planning for cutting-edge biomass utilization research in accordance with DOE plans and objectives.

Goals and Objectives

The goal of this task was to provide efficient project management and to direct strategic outreach activities. Specific objectives included:

- Providing management for the EERC CBU 2005 project.

- Implementing a quality assurance and quality review process for all research activities and spending, including periodic internal project review meetings.
- Spearheading all necessary DOE reports, including NEPA, quarterly, final, and other report types.
- Promoting attendance and dissemination of information generated through the project at a 2-day regional technical workshop on biomass in Grand Forks and also at international biomass-related conferences and meetings.
- Networking with commercial industry clients and peers to provide sound applied and fundamental research.

The overall goal of the Biomass for Energy and Products Workshop IV, entitled Biomass '06: Power, Fuels, and Chemicals Workshop, was to promote the use of biomass in the region for both energy uses and value-added products. Building upon the success and the momentum of the prior workshops with the Biomass for Energy for Products workshops with a third annual event is the means toward achieving that overall goal.

One activity objective was to include sponsors and stakeholders in planning the event. This year, we plan to recruit two new sponsors from regional utilities and foundations. Involving our stakeholders and sponsors helps create an event with timely and relevant topics. The topics are generally focused on biomass issues relevant to the upper Great Plains region. We also plan to incorporate suggestions from the prior year's evaluation.

A second activity objective is to promote partnerships and project ideas toward the end of utilizing biomass for energy and products. Growing participation levels in the workshop over the past 2 years is encouraging toward this objective. For the upcoming workshop, we hope to increase participation by another 20%. Ongoing communication and interaction with the sponsors and participants through all phases of the workshop promote partnerships and project ideas.

Experimental

This activity did not have a research component to detail in this section.

Results and Discussion

Project management and quality control were provided for all nine of the project's technical activities. Final negotiations with DOE's EERE in Golden, Colorado, were completed, and a final official contract was signed off with DOE in August 2005. An internal project kickoff meeting was held on August 10, 2005. At this meeting, activity managers described the scope of work for their project to an audience that included other researchers and project managers at the EERC working within and outside of CBU projects. The meeting also served to explain reporting requirements, deadlines, milestones, environmental issues, and quality assurance/quality control project reviews. Quarterly meetings were held thereafter where the status of project results,

milestones, timetables, and budgets were reviewed. In addition, the quarterly internal meetings served as a venue for listening to cutting edge research from other researchers. A 30–40-minute presentation was usually given by either a researcher from an academic department of the UND, from the EERC, or from a visiting agency. The presentations centered on utilizing biomass for energy and fuels. Presenters included Dr. Michael Mann, professor and Chemical Engineering Department Chairman at the UND, discussed a research effort centered on cracking vegetable oils to make smaller-chain renewable additive transportation fuels; Ted Aulich from the EERC spoke on renewable jet fuel production; and Philip Hutton spoke on an integrated biomass gasifier–solid oxide fuel cell system.

With respect to reporting, all quarterly reports and milestone activity logs were written and submitted to DOE. All projects within EERC CBU 2005 were reviewed and project managers queried on deliverables, milestones, and remaining objectives and budgets. Preparation of presentation materials was done for the 2007 DOE Biomass Program Review meeting in Golden, Colorado. Dr. Bruce C. Folkedahl presented materials related to the EERC CBU project at the review meeting on August 15–16, 2007. Criticisms of the EERC CBU project were addressed in writing using the rebuttal process prescribed by DOE. Overall, the peer review was an excellent exercise in engaging with DOE and other researchers and an excellent guide for future research in the field of biomass.

Through the strategic studies portion of this activity, several meetings and conferences were attended or arranged related to forward planning of future biomass research, pathways forward to biomass-driven energy and fuels, and dissemination of applied biomass research results. Such events attended included a 1-day workshop related to biobased opportunities, held at Ames Iowa and hosted by Iowa State University; a poster presentation that described biomass gasification in the small 150-kW gasifier developed under Activity 2 at the 14th European Biomass Conference and Exhibition – Biomass for Energy, Industry and Climate Protection, Palais des Congrès, Paris, France; a review meeting for the EERC CBU program at the November 14–16, 2005, EERE, Office of the Biomass Program (OBP) biennial Program Peer Review at the Hyatt Arlington, in Washington, D.C.; a meeting held at the Pacific Northwest National Laboratory (PNNL) to discuss potential future collaborations in research related to EERC and PNNL work in developing biochemicals and fuels from seed-vegetable oil and woody or herbaceous biomass; a meeting held at Siemens Power Generation at its headquarters for Power Generation in Orlando, Florida, to discuss potential partnership opportunities particularly with respect to production of syngas from biomass for applications in power technologies owned by Siemens; presentations and meetings related to the biomass activities and biomass sessions chaired at the 31st International Technical Conference on Fuel Technology in Clearwater, Florida, May 21–26, 2006; discussions held with interested industry representatives for technologies being developed in the project at the PowerGen Renewable Conference on April 10–12, 2006 in Las Vegas, Nevada; a meeting attended and the state of biomass gasification and fermentation to ethanol and chemicals discussed at the North Dakota Biomass Taskforce final meeting in Jamestown, North Dakota, in December 2006; a working-group discussion on biomass utilization as related to agricultural economies attended and participated in at the Midwest Ag-Energy Network meeting in St. Paul, Minnesota, in December 2006; a meeting with several engineering groups building biomass gasification systems for the thermochemical conversion of biomass to ethanol at the Western Fuels Symposium in Denver, Colorado, in

October 2006; discussions with staff from the Office of Science Biological and Environmental Research (BER) program office in Germantown, Maryland, related to biomass utilization for fuels, chemicals, and energy in conjunction with attendance and discussions with other DOE officials on the state of biofuels research at the Cellulosic Ethanol Summit in Washington, D.C., in October 2007; meetings held with DuPont at the EERC to discuss potential use of CBU research results on converting biomass residues to biobased chemical feedstocks; meetings attended at a workshop sponsored by the University of Minnesota in St. Paul, Minnesota, in July 2007, where discussions were centered on biomass energy crops development and impacts on land use, water, and wildlife; and finally several meetings with several individuals from Barkley Ag Enterprises, WestBred LLC, the Montana State University Institute for Biobased Products, whereby the discussion was related to biojet fuel and green diesel production with a particular focus on camelina as a feedstock.

As a result of interaction and discussion in formal peer review meetings and other more informal meetings with DOE personnel and biomass industry experts, specific areas related to biofuels and bioenergy were identified and targeted as great needs to the United States and as relevant areas needing federal assistance to perform higher-risk applied research or demonstration. Some of these areas include indirect liquefaction of wood wastes integrated with small-scale syngas reactors for methanol/ethanol or distributed hydrogen production; low-temperature catalytic reforming of glycerol to hydrogen using improved catalysts; high-pressure electrolysis of biobased glycerol and biobased alcohols for on-demand hydrogen production; well-integrated gas turbine biomass gasifier power plants for distributed power production; gasification of wet biomass utilizing supercritical hydroconversion; mitigation of hydrogen sulfide concomitant enhancement of methane production; thermal conversion of torrefied-biomass pellets; integrating fermentation ethanol and crop oil in processing that creates ethyl biodiesel and glycerol-based products; production of formic acid-based chemicals and hydrogen via gasification of cellulosic biomass; and developing robust microgasification technology for municipal solid waste.

This activity also helped to conduct and host a small biomass workshop in Grand Forks and two separate biodiesel workshops. As an educational and outreach tool, a regional technical biomass workshop was organized and hosted in Grand Forks. Several presentations and poster/booth displays on CBU-related biomass utilization projects were facilitated at the Biomass '06 Workshop: Power, Fuels, and Chemicals held at the EERC in Grand Forks, North Dakota, on July 18–19, 2006. There were 188 attendees, 136 organizations, four countries (the United States, Canada, New Zealand, and United Arab Emirates), 25 states, and seven Canadian provinces represented. Demographics of workshop attendees were 46% industry; 21% research/academia; 17% government; 7% community and economic developers; and 9% financial organizations, landowners, and media.

The Biomass '06: Power, Fuels, and Chemicals Workshop, July 18–19, 2006, in Grand Forks, North Dakota, at the Energy & Environmental Research Center focused on key advances in technologies for making power, chemicals, and transportation fuels from biomass (or agricultural products such as straw, corn, and wood residue). Advances in conventional and new methods for production of biodiesel and ethanol were highlighted as well as the production of hydrogen from biomass.

The workshop featured top industry representatives from companies such as Cargill, Great River Energy, Xethanol, Archer Daniels Midland Company, Siemens Power Generation, and the North Dakota Department of Commerce.

Evidence of the success of the workshop is found in comments from participants such as:

- “The best organized workshop I have attended in at least a decade.”
- “A very impressive line-up of presenters, an exciting look into the future, in a first-class facility.”
- “A nice blend of industry and research focusing on a single issue.”

The organizing sponsors included DOE and the EERC. The collaborating sponsor was the North Dakota Department of Commerce Division of Community Services State Energy Program, Bismarck, North Dakota. Partnering Sponsors included Fagen, Inc., Granite Falls, Minnesota; Great River Energy, Elk River, Minnesota; MDU Resources Group, Inc., Bismarck, North Dakota; Minnesota Power, Duluth, Minnesota; North Dakota Department of Agriculture, Bismarck, North Dakota; North Dakota Forest Service, Bottineau, North Dakota; Otter Tail Power Company, Fergus Falls, Minnesota; the Touchstone Energy Cooperatives of North Dakota (Basin Electric Power Cooperative, Bismarck, North Dakota; Minnkota Power Cooperative, Inc., Grand Forks, North Dakota; and North Dakota Association of Rural Electric Cooperatives, Mandan, North Dakota); and Wanzek Construction, Inc., Fargo, North Dakota

There were ten exhibitors as follows: EERC; Agricultural Utilization Research Institute, Crookston, Minnesota; BBI International, Grand Forks, North Dakota; Bio-Renewable Group, Fargo, North Dakota; Fremont Industries, Inc., Shakopee, Minnesota; Initiative for Renewable Energy and the Environment (IREE), St. Paul, Minnesota; Pinnacle Engineering, Inc., Maple Grove, Minnesota; Vidir Biomass Inc., Arborg, Manitoba, Canada; Wanzek Construction, Inc., Fargo, North Dakota; and Zeton, Inc., Burlington, Ontario, Canada.

Finally, this activity aided Activity 10 – Biodiesel Education and Outreach in finding speakers and presentation material on new technologies in biodiesel and green diesel production for two biodiesel workshops. The workshops were focused on grower issues, the refining process, transportation issues, marketing and incentives, and the implementation of biodiesel fuel in fleet vehicles such as city and school buses or state and other government vehicles. There were over 140 attendees for the two workshops which were held in March and April of 2007 in Fargo, North Dakota, and in Sioux Falls, South Dakota. Presentations were made by EERC personnel and several other biodiesel experts and fleet managers from around the country.

Conclusions

This activity met and then exceeded its proposed objectives. The interest in biomass remains high in the region, and upcoming workshops are planned.

References

None.

YEAR 2005 – ACTIVITY 2 – BIOMASS GASIFICATION AND DISTRIBUTED POWER PRODUCTION

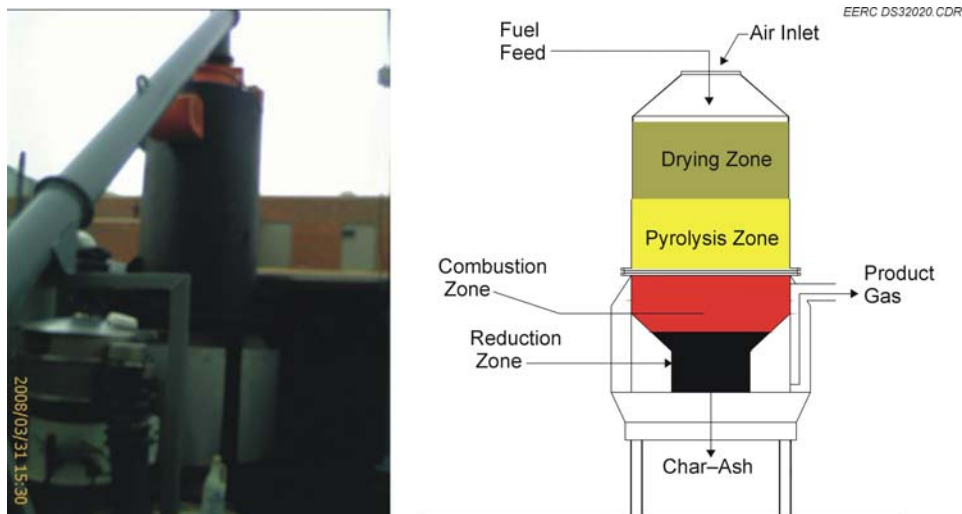
Introduction

Distributed electrical generation produced from piston engines firing low-Btu gas from biomass gasification is an economical solution for industrial loads of 100 kWe – 1 MWe. The gas must be cleaned to levels acceptable for engine operation. The EERC has been testing downdraft biomass gasifiers and is exploring the range of biomass fuels that can be successfully gasified using downdraft technology. This project was completed to publish gas-quality data produced from downdraft gasification.

Ankur Scientific (www.ankurscientific.com) is a company that has been supplying biomass gasifiers in the small 5-hp irrigation pump size to 500-kW electric generator size for approximately 20 years in India. Publications suggest that gasifiers from Ankur can produce clean gas (contaminants below 10 ppm) (1). Ankur Scientific donated a gasifier to the EERC for the completion of this project. The gasifier is its fine biomass gasifier (FBG) model and is commercially utilized to gasify rice hulls. The gasifier is a stratified, or “open top,” downdraft gasifier, shown in Figure 21.

Goals and Objectives

The goal is to publish gas-quality data from various biomass fuels.



Project objectives included the following:

- Procure gasification system
- Install and conduct testing
- Publish results in journals and present at a major conference

Experimental

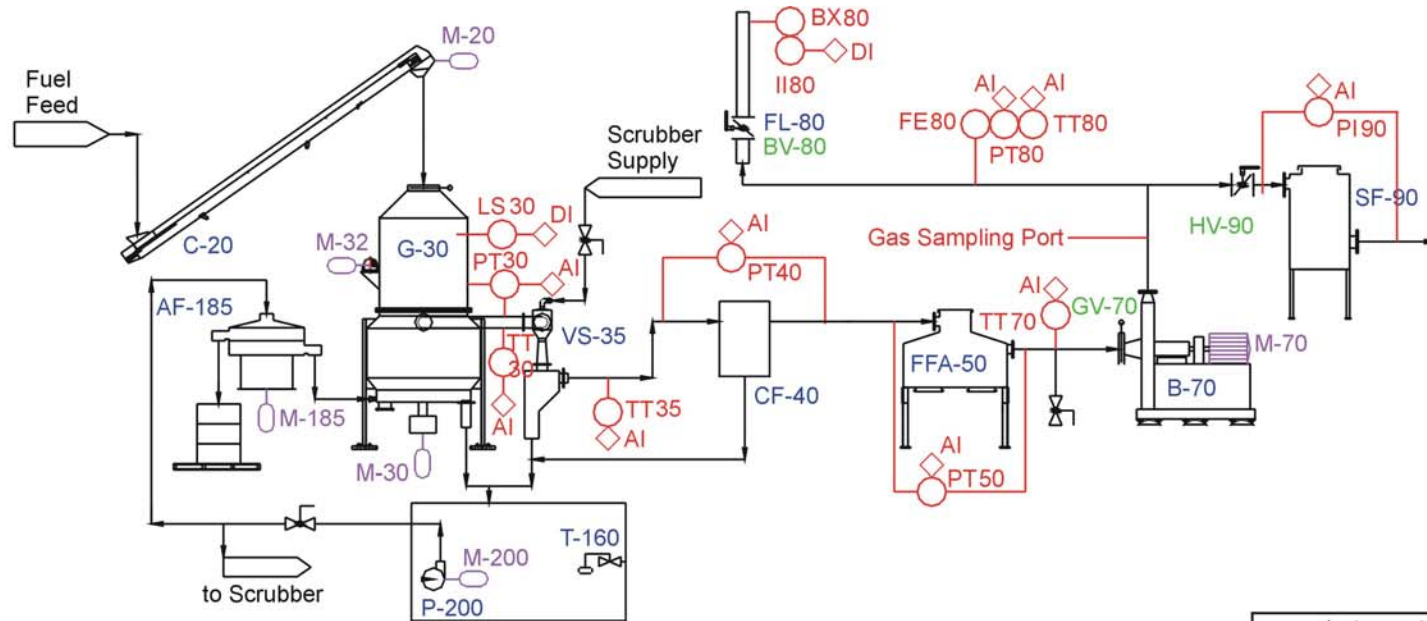
An Ankur FBG gasifier was donated and assembled on a trailer. A process and instrumentation diagram is provided in Figure 22. The system included an auger feed, gasifier, gas-cleaning system (however, scrubbing and filtration were not used during testing), blower, flare, and process controls. Data collection included process temperatures, differential pressures, flow rates, and gas and fuel samples. Proximate and ultimate analysis was conducted on the fuel samples. Gas chromatography was used to analyze gas samples, and Dräger tubes were utilized to sample trace contaminants in the product gas. The experimental setup is shown in Figures 23 and 24. Although the process includes a scrubber and filtration system, the gas-cleaning equipment was not used during testing, and gas sampling included collection of raw (unprocessed) gas from the gasifier.

Procedure

A series of tests were run using five different fuels: wood chips, wood pellets, sawdust, wheat straw, and corn silage. Tests were conducted over the course of a week, and each fuel was fired for approximately 1 to 2 hours. Steady-state conditions were kept during gasification. Gas flow rates varied between tests but were maintained constant during gasification. The fuels are shown in Figures 25–29. The wood pellets are $\frac{3}{8}$ -in.-diameter pellets produced from Aspen and supplied in 40-lb bags. The wheat straw material is residue from a particleboard company that grinds rejects from wheat straw board manufacture. The corn silage was provided by a farmer, and the material included stover, leaves, corn cobs, and corn kernel residues. The sawdust and wood chips are sourced from a supplier of pine. The sawdust was ground from the wood chip material. The wood chip material includes chips no larger than $\frac{1}{4}$ in. which is relatively fine and small. All of the above fuels were selected based on the fact that the FBG gasifier is designed to gasify rice hulls; therefore, fuels that had a relatively fine size characteristic were chosen, with the exception of the leafy consistency for some of the corn silage. The total weight and bulk density of the various fuels fired in the gasifier are as follows:

- Wood chips – 124 lb, 9.4 lb/ft³
- Sawdust – 126 lb, 9.6 lb/ft³
- Wood pellets – 160 lb, NA
- Wheat straw – 58 lb, 8.8 lb/ft³
- Corn silage – 33 lb, 5.1 lb/ft³

Tests were segregated into 3 days of testing which included firing wood chips on the first day; pellets and sawdust on the second day; and wheat straw, corn silage, and sawdust on the third day. Table 14 provides the schedule of operation relative to fuel type.



46

Signal Input to PLC, Output from PLC		Notes:	Instrument Letter Code	
			First Letter	Second Letter
◇ AI	Analog Input	All motors have manual control from PLC. All motors provide status indication to PLC.	B	Burner
◇ AO	Analog Output		F	Flow
◇ DI	Discrete Input		H	Hand
◇ DO	Discrete Output		I	Current
			J	Power
			K	Time
			L	Level
			P	Pressure
			T	Temperature
			Z	Position
			C	Control
			E	Element
			I	Indicator
			K	Control Station
			Q	Totalizer
			R	Recorder
			S	Switch
			T	Transmitter
			X	Igniter

Figure 22. Process and instrumentation diagram.



Figure 23. Assembled gasification trailer.



Figure 24. Gas piping.



Figure 25. Wood pellets.



Figure 26. Wheat straw.



Figure 27. Corn silage.



Figure 28. Sawdust.



Figure 29. Wood chips.

Table 14. Schedule of Operation

Date	Time	Fuel
3/25/2008	10:00–13:30	Wood chips
3/26/2008	9:30–9:40	No fuel
3/26/2008	9:40–11:35	Wood pellets
3/26/2008	11:35–12:42	Sawdust
3/27/2008	10:00–11:00	No fuel
3/27/2008	11:00–11:45	Wheat straw
3/27/2008	11:45–12:30	Corn silage
3/27/2008	12:30–13:32	Sawdust
3/27/2008	1:32–13:43	Wheat straw

Results and Discussion

Fuels were submitted for proximate and ultimate analysis. Table 15 includes the results of analysis. All of the fuels were relatively dry at <10% moisture. Notably, the wood chips and sawdust differ from the other fuels in that they are very dry at <4% moisture, have volatile matter contents of at least 10% greater than the other fuels, and have ash contents 5–8 orders of magnitude less than the other fuels. The ultimate analysis yields typical results for biomass fuels. Heating values for the wood chips and sawdust are notably higher than the other fuels as a result of low moisture content. The wheat straw has notably higher ash content at 8.5%.

Table 15. Ultimate and Proximate Analysis of Biomass Fuels, wt%

	Wood Pellets	Wood Chips	Sawdust	Wheat Straw	Corn Silage
Proximate Analysis					
Moisture	9.7	3.5	3.8	5	6
Volatile Matter	69.8	83.7	84.24	68.04	74.81
Fixed Carbon	15.5	12	11.46	18.43	15.11
Ash	5	0.8	0.5	8.53	4.08
Ultimate Analysis					
Hydrogen	5.7	7.1	7.26	6.8	6.72
Carbon	44.3	47.1	47.28	45.45	42.41
Nitrogen	0.4	0.27	0.28	1.36	1.26
Sulfur	0	0.03	0.01	0.14	0.08
Oxygen	44.6	44.7	44.67	37.72	45.45
Ash	5	0.8	0.5	8.53	4.08
HHV ¹	7530	8623	8740	8464	7607

¹ Higher heating value.

Process temperatures were recorded for each day of testing. Figures 30–32 provide the results. Figure 30 was recorded on March 25, 2008. The gasification outlet temperature (TT30) remained relatively constant throughout the test with several spikes. The temperature spikes can be attributed to bridging of the fuel in the reactor. Upon realization of a temperature spike, the operator used a tool to poke the gasifier fuel bed, which subsequently lowered the gasification outlet temperature. The variations in the scrubber outlet temperature (TT35) were specific to water flow adjustments through the scrubber. The scrubber was not used at the end of the test, revealing higher temperatures. Process gas temperatures (blower inlet and outlet) remained steady between 150° and 200°F.

Figure 31 provides data collected on March 26, 2008. Gas outlet temperatures were initially at 850°F, dropped, and remained steady at 700°F. Gas flow was reduced at 11:45, and gasifier outlet temperatures dropped accordingly to less than 500°F. Figure 32 provides temperature data for testing on March 27, 2008. Gas flows were consistent at approximately 60 scfm, and gas outlet temperatures averaged approximately 650°F. Process gas temperatures (TT70, TT80) were higher than previous tests, near 200°F.

Gas bags were collected and analyzed using a gas chromatograph for bulk gas composition, and a Dräger tube sampling device was used to measure trace quantities of petroleum hydrocarbons, benzene, toluene, and xylene. The results are summarized in Table 16, and a detailed log is provided in Appendix A. Highlighted in Table 16 are points of interest. Wood pellets and corn silage produced reasonably high hydrogen contents (15%), while wheat straw and wood pellets produced high CO levels (20%). Wood pellets and sawdust fuels produced high methane content and light tar vapor (lower molecular weight than benzene) content. Nitrogen contents were low for wood pellets and sawdust, producing high heating

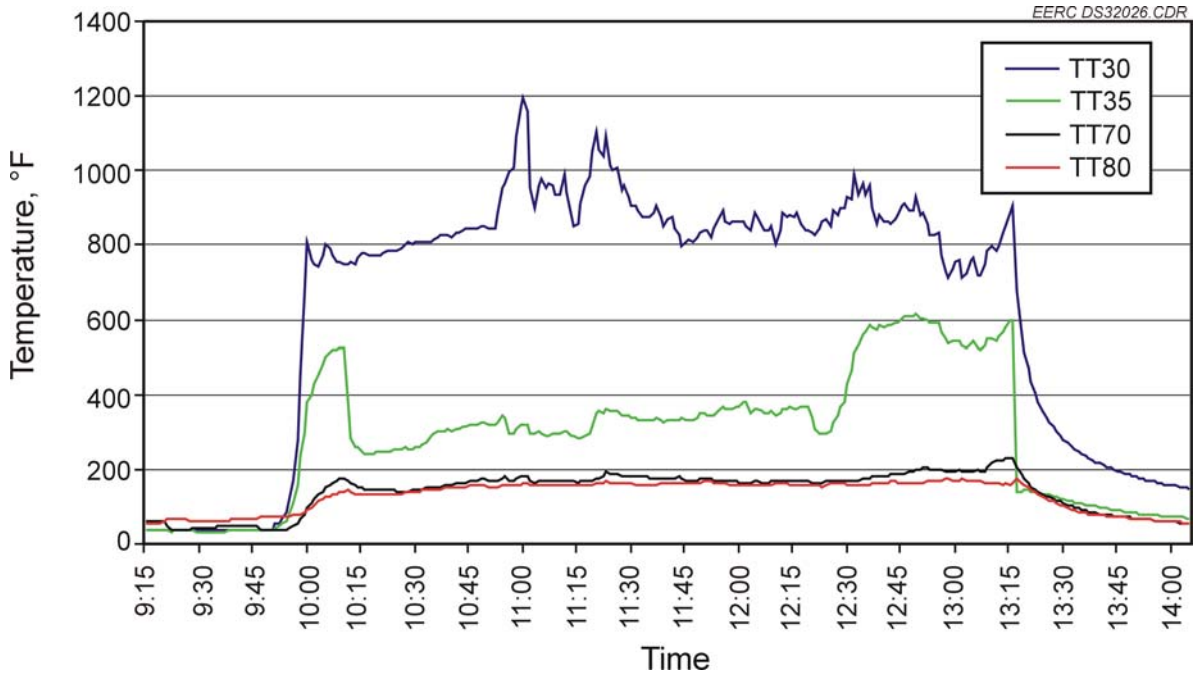


Figure 30. Day 1 process temperatures firing wood chips with an average flow rate of approximately 45 scfm.

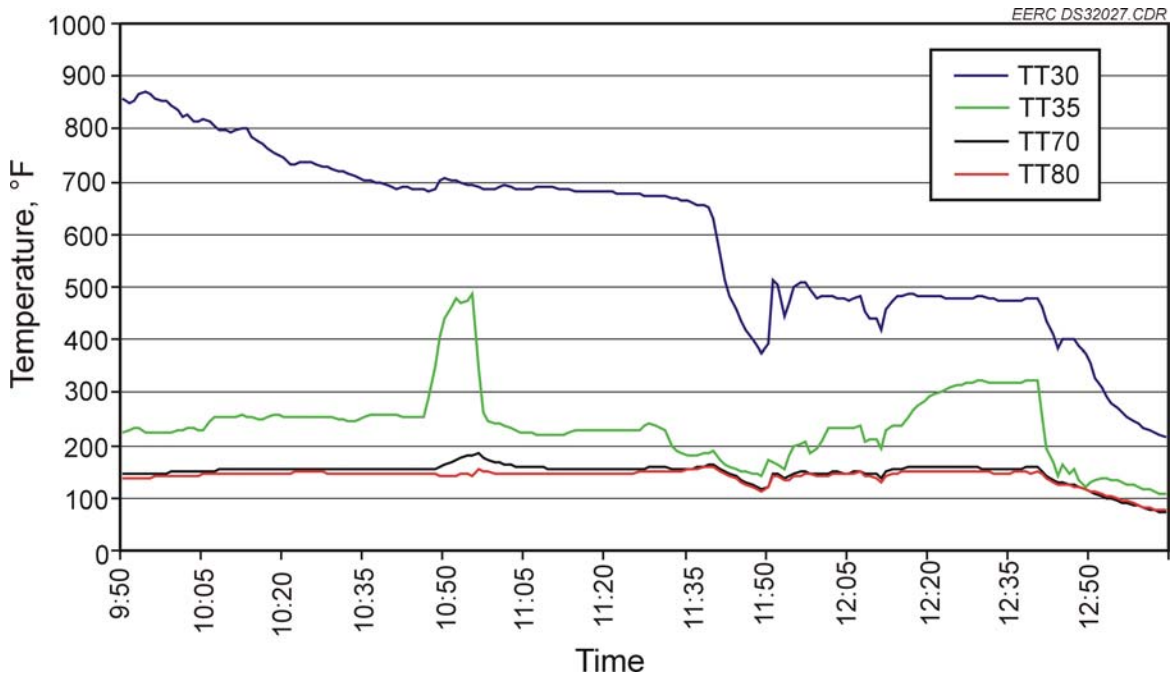


Figure 31. Day 2 process temperatures firing pellets and sawdust with an average flow rate of 35 scfm for the first half of the run and 16 scfm for the second half.

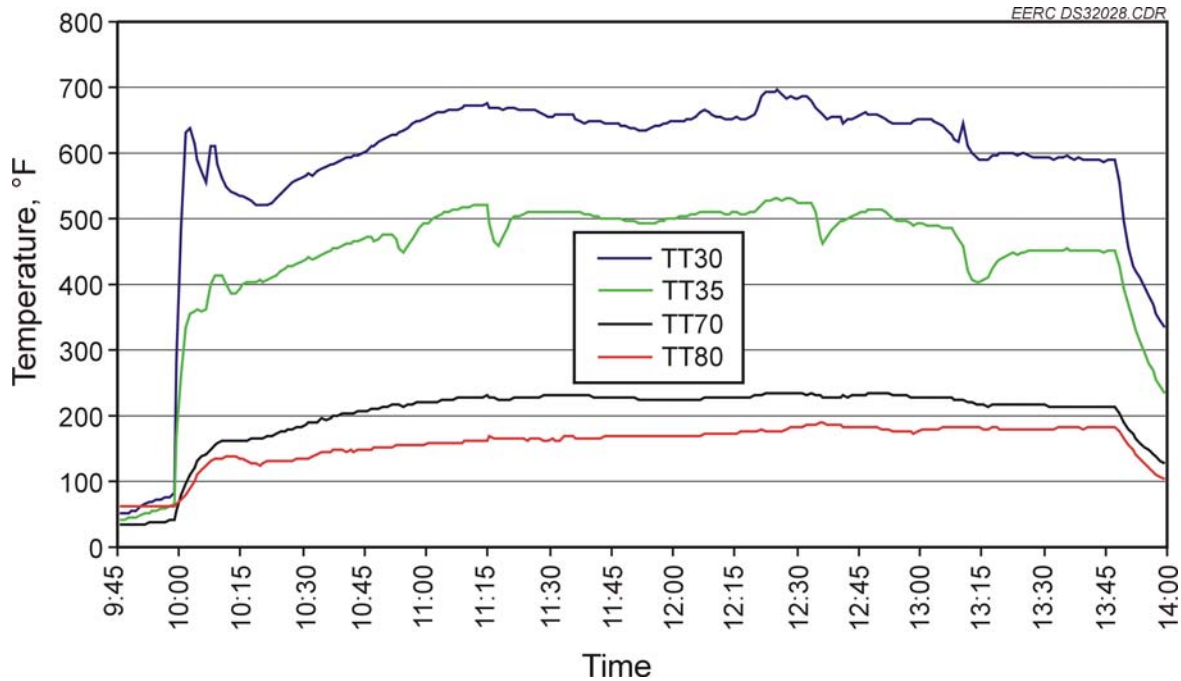


Figure 32. Day 3 process temperatures firing wheat straw, corn silage, and sawdust with an average flow rate of approximately 60 scfm.

Table 16. Summary of Gas Analysis

Gas Bag Sample No.	1	3	4	5	6	7	8	9	10	11
Fuel:	Wood Chips	Wood Pellets	Wood Pellets	Sawdust	Sawdust (char)	Wheat Straw	Wheat Straw	Corn Silage	Sawdust	Sawdust
Hydrogen	1%	11%	15%	14%	15%	12%	12%	15%	10%	13%
Carbon Monoxide	3%	15%	19%	15%	18%	21%	12%	11%	9%	10%
Methane	1.1%	2.9%	3.7%	4.7%	2.4%	1.1%	1.7%	1.7%	3.2%	2.6%
Tar Vapors	0.1%	0.9%	1.0%	1.2%	0.4%	0.1%	0.2%	0.5%	1.0%	0.6%
Carbon Dioxide	15%	15%	15%	19%	11%	9%	15%	16%	15%	16%
Nitrogen	74%	54%	46%	45%	52%	55%	57%	54%	57%	54%
Drager Tubes, toluene ppm	25	400	400	400	100	50	100	50	200	300
MW	30.1	27.4	26.1	27.0	25.7	26.3	27.1	26.7	27.9	27.1
HHV, Btu/scf	24.3	126.4	161.6	162.3	136.9	120.4	98.9	109.9	110.6	110.9
Sp. Gravity	1.04	0.94	0.9	0.93	0.89	0.91	0.94	0.92	0.96	0.94

values (160 Btu/scf). In Appendix A, it can be seen that the gas produced from sawdust consistently produced more butene vapors than that of wood pellets. High tar vapor content correlated well with toluene measurements, as shown in Figure 33. The low-heating-value result of Sample 1, wood chips, was primarily due to an air leak discovered in the scrubber. The leak

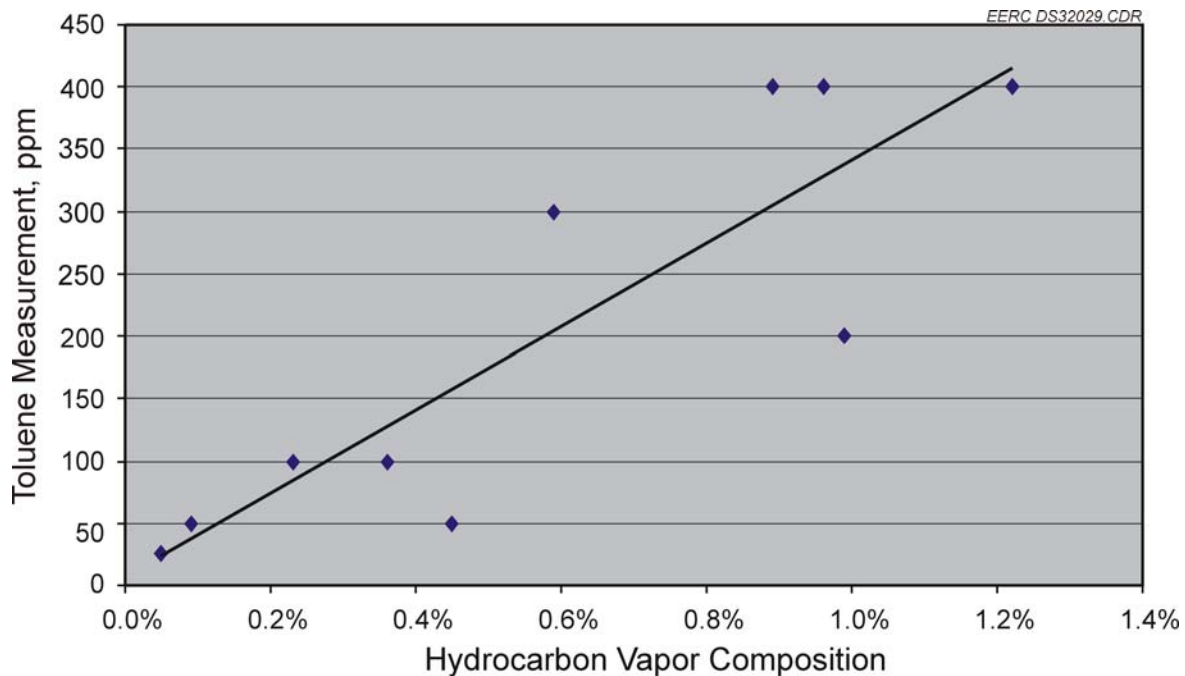


Figure 33. Correlation of tar vapor content with toluene measurements.

was fixed for subsequent runs. However, as shown in Appendix A, high oxygen values were repeated for sawdust in Samples 10 and 11.

The testing conducted by the EERC was to primarily compare various performances of biomass fuels in a stratified downdraft gasifier provided by Ankur Scientific. The test included measuring the gas composition and trace contaminant levels from firing various fuels. The primary issues with small gasification systems used for distributed generation include gasifier performance, ability to handle solids, and contaminant levels (tars) found in the product gas.

The gas analysis provided in Appendix A and Table 16 reveals that the highest-heating-value gases were produced firing wood pellets and sawdust. However, these gases also contained significant levels of tar vapors. The heavy hydrocarbons (higher molecular weight than benzene) are typically problematic in engine generators and gas-cleaning systems. Dräger tube sampling revealed that tars are most likely greater than 1000 ppm for the gas produced directly from the gasifier and that the dry sawdust fuel was more conducive to producing higher amounts of tar. The factors that contribute to the high tar production include low moisture, high volatile matter, small particle size, and bridging in the reactor. It appears that although the sawdust fuel has a high heating value and should burn hotter, temperature and time are not sufficient to crack hydrocarbons and reduce tar formation.

The lowest tar levels were produced from wheat straw and corn silage; however, gas heating values were also low (120–100 Btu/scf, respectively). Gases below 100 Btu/scf do not perform well in combustion devices. The wheat straw and corn silage seemed to produce a relatively clean gas with the minimum requirements for operation in an engine generator. The

best-performing fuel including high heating value, medium tar level, and consistency in the gasifier was wood pellets.

Conclusions

Fuels that offer advantages to downdraft gasification include fuels that will produce low tar levels in the gas, produce gas in a heating value range of 100 to 150 Btu/scf, do not present solids-handling problems for the gasifier, and can maintain reasonable temperatures relative to tar cracking and clinker formation. The fuels are compared in Table 17.

The best-performing fuel was wood pellets; although tar levels appeared high none of the problematic butenes was formed as with sawdust gasification. Sawdust gasification runs resulted in shutdown of the system because of tars binding up the gas blower (example shown in Figure 34). None of the other fuels seemed to have caused tar condensation in the blower, and the analytical data support the lower formation of tar compounds from fuels other than sawdust.

Wheat straw and corn silage produced low tar and low-heating-value gas. Gasifier efficiency was not easily measured during operation because of the amount of fuel in the gasifier in the form of charcoal prior to start-up. Rough calculations of efficiencies seem to support that the best gasifier performance was on March 27, 2008, when wheat straw and corn silage were the primary fuels. The overall calculated gasifier efficiency for the entire test period was 63.1%, and the gasifier efficiency excluding the first day (because of the air leak) was 79.4%. Gasifier efficiencies of 80% to 85% were typical.

The tests conducted for this project revealed the following:

- Dry, high-volatility sawdust is a problematic fuel for stratified downdraft gasifiers and is not recommended without improved air distribution and solids handling.
- Wheat straw and corn silage can be advantageous fuels for a stratified downdraft gasifier. The silica content in wheat straw has been known to clinker and should be further evaluated. Gas heating values can be lower for these fuels than other higher-volatility fuels.
- Wood pellets are an excellent gasification fuel, producing high heating value, reasonable tar levels, and excellent fuel-handling characteristics.

Table 17. Comparison of Fuel Performance

Fuel	Tar Level	Heating Value, Btu/scf	Fuel-Handling Characteristics
Wood Chips	N/A	N/A	Bridging in gasifier
Sawdust	High	110–160	Bridging in gasifier
Wood Pellets	Medium to high	125–160	Excellent
Wheat Straw	Low	100–120	Excellent (clinker not evaluated)
Corn Silage	Low	110	Excellent (clinker not evaluated)



Figure 34. Tar condensation in the process blower.

References

1. Wen, H.; Lausten, C.; Pietruszkiewicz, J.; Delaquil, P.; Jain, B.C. Advances in Biomass Gasification Power Plants. Presented at the American Power Conference, 1998.

YEAR 2005 – ACTIVITY 3 – NOVEL HIGH-CETANE OXYGENATES FROM WASTE GLYCEROL FROM BIODIESEL PLANTS

Introduction

The quality of diesel fuels can be significantly improved by the addition of certain organic compounds containing oxygen (oxygenates). These oxygenates typically reduce particulate emissions and improve the ignition quality of the fuel. The cetane number (CN) is used to characterize the ignition quality of a diesel fuel. The CN is obtained by test engine comparison at known conditions of a fuel's performance to that of a standard mixture of hexadecane (cetane) and heptamethylnonane. The blending cetane number (BCN) of the oxygenate is determined for a mixture or several mixtures of the oxygenate with a base diesel fuel with a known CN. The BCN is the proportional contribution of the oxygenate to the cetane number of the blend.

Many oxygenated compounds are available from petroleum processing, but many can also be obtained from biomass sources using some combination of fermentation, extraction, pyrolysis, and other chemical processes. The oxygenate compounds vary greatly in their ability to increase or decrease the CN of the base fuel with which they are mixed. For diesel fuels, methanol, ethanol, and other small alcohols have a deleterious effect on the ignition quality, with very low

(2–25) CNs and BCNs (1). Glycerol is not soluble in diesel fuel, but it could be predicted that the alcohol functionalities would result in very low BCNs. Ethers offer a significant improvement in fuel quality, and the BCNs of a number of petroleum-derived ethers were reported (2). Long-chain esters exhibit good CNs; however, most short-chain esters have low CNs.

The goal of this project was to determine if processing of waste glycerol from biodiesel plants can yield oxygenates with high BCN characteristics at a minimal cost of production. The value of the crude glycerol from vegetable oils is continuously dropping as new biodiesel plants are coming online, offering the potential for feedstock costs of less than \$0.10/lb. A low production cost for producing a high-cetane additive to diesel fuel could be an important factor in the stimulation and development of biomass refineries where a variety of fuels and chemicals are produced from vegetable oil resources.

Goals and Objectives

The objective of the project was to convert glycerol to several ether and mixed ether–ester derivatives and determine whether the resulting derivatives containing the multiple ether functionalities exhibit high BCN values. The effects of derivatization on the flow characteristics of the blend were also to be determined. Identification of the ignition quality and flow characteristics represents the first step in developing a new consumer fuel and must be followed by emission and toxicity testing.

Experimental

Preparation of Ether Derivatives of the Cyclic Acetyls

Several routes were explored for preparation of the alkyl ethers of the cyclic acetyls having structures III and IV where R_a is alkyl or hydrogen and R_b is an alkyl group. Both acid and basic catalysts were employed, depending on the reagents and reactions being employed for the syntheses. Reactions with alcohols or olefins employed a solid or liquid acid catalyst, whereas reactions with alkyl halides employed a basic catalyst (Williamson reaction).

Reactions of the cyclic acetyls with n-alcohols were extensively explored. Using a liquid or solid acid catalyst produced low yields of ether product mixtures. Several of the reaction products were produced via opening of the acetyl ring. While some of the products may have been suitable as oxygenates (high cetane, good solubility), the mixtures retained much hydroxyl functionality, and separation was impossible. Were this successful, it would represent the most direct and inexpensive route to the desired primary ethers, since methanol, ethanol, and butanol could be utilized.

Reactions of the cyclic acetyls with olefins were also carried out with acid catalysts. The reaction with 1-butene was only partially successful, giving only a moderate yield of an ether product, corresponding to structures III and IV, and the product mixture was difficult to separate. Another problem with this product, however, is that the ether linkage forms at the secondary carbon, resulting in a branched structure (isobutyl ether) that would not have the desired positive effect on CNs that would be obtained from a straight-chain alkyl ether.

In contrast, the acid-catalyzed reaction of the cyclic formal with isobutylene proceeded readily to completion to form the tertiary butyl ether in high yield. Although this product was a pure ether mixture, corresponding to structures III and IV, the BCN is expected to be low.

The reactions of primary alkyl halides with the cyclic acetyls gave high yields of the desired primary alkyl ethers. This reaction was previously reported in the Russian literature (3), but fuel properties were not determined. A proprietary method was used to form the alkoxide using inexpensive alkali hydroxides as bases. It was not necessary to use the more expensive NaH as in the Delfort patent, to react with the alcohol group of the glycerol cyclic acetyl to form the alkoxide intermediate that subsequently reacted with the diethyl carbonate. The alkyl halide reagents were derived from simple alcohols or from glycerol by proprietary routes. An alternative preparation of hexyl iodide by a literature method from sorbitol failed to give much monoiodo product and was abandoned.

The final product mixtures, comprising n-butyl and allyl ether derivatives of the dioxolane III and 1,3-dioxane IV, where R_b = n-butyl and allyl, were purified by simple distillation. The alkyl ethers with both the formal and butyral rings (R_a = H and propyl, respectively) were completely soluble in diesel oil.

An alternative route to the alkyl ether V was also investigated. This route used the Williamson synthesis from the 4-chloromethyl-substituted cyclic acetyls. These are conveniently prepared via acetyl formation from glycerol monochlorohydrin, which is easily obtained by the reaction of glycerol with HCl (4). The chloromethyl derivative of glycerol is well known in the Russian literature.

In either of the Williamson routes, there are several steps, and halogen must be introduced and eventually exited as alkali halide. Methods are available for regenerating the halide, such as thermal conversion of the iodide, but these involve more steps, making the production less likely to be accomplished at small, dispersed biodiesel biorefineries.

Preparations of Ester Derivatives from the Cyclic Acetyls

Several methods for preparing esters from the cyclic acetyls were investigated. The acyl group to be added to the cyclic acetyl structure was selected to meet the requirement that it did not contain alpha hydrogens on the carbon adjacent to the carbonyl group. The simple Fischer esterification of glycerol formal with the selected carboxylic acids was carried out using p-toluenesulfonic acid as the catalyst. This gave approximately 50% yields of the desired cyclic acetyl esters, as described in the Russian literature (5). However, a considerable portion of the product had undergone ring-opening reactions of the cyclic acetyl to form linear acetyl esters (VI) as shown in Figure 35, where Ac_b represents the acyl group added from the carboxylic acid.

Furthermore, the desired ester mixture from the formal ring was not soluble in diesel fuel unless the acyl chain was long (and expensive). The most desired formal ester product (R_a = H) was not soluble and so was not further explored. The butyral esters (R_a = propyl) are soluble in diesel fuel, so they will be candidates for testing, provided the yield of V and VII can be improved.

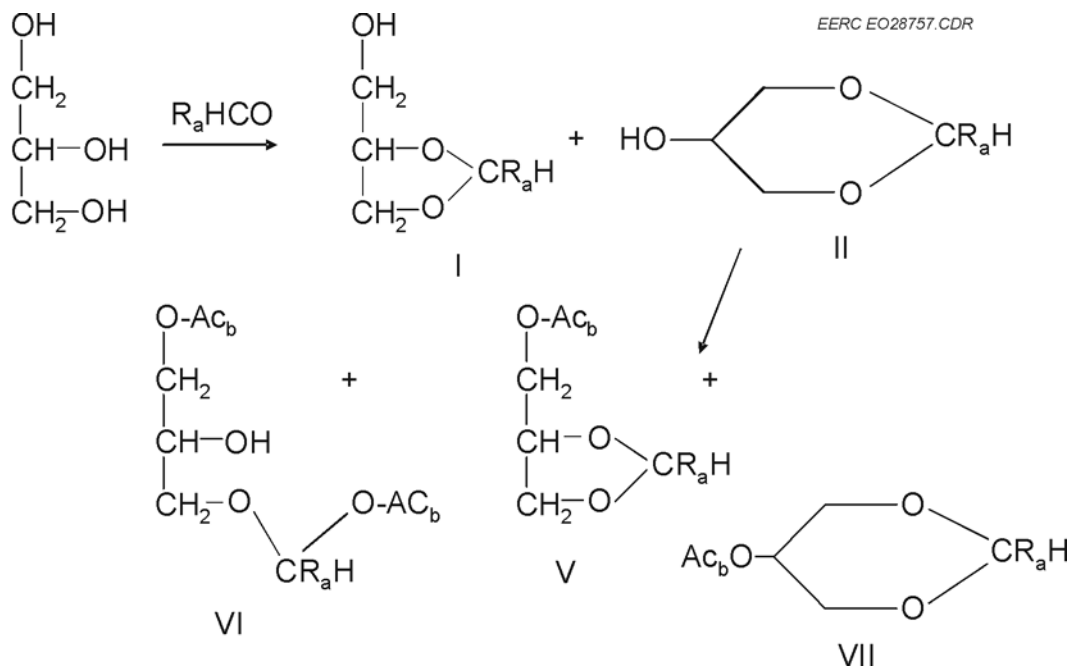


Figure 35. Formation of esters from cyclic acetyls.

Additional studies with other acylating reagents produced similar mixtures of products, and it was difficult to convert all the hydroxyl groups. The use of a solid acid catalyst did not improve the yields.

The conversion of glycerol esters to cyclic acetyls was also investigated. An impure glycerol monoformate ester (IX) was prepared by direct esterification of glycerol. This intermediate reacted with butyraldehyde to form the dioxolane ester (X) as shown in Figure 36. However, the starting material contained di- and triesters, so the yield of dioxolane ester was lower.

An alternative but similar route to a glycerol monoester utilized a triolein precursor. Reaction of triolein with two moles of glycerol with a basic catalyst gave a product mixture consisting of mainly glycerol monooleate. The monoglyceride reacted with paraformaldehyde and a sulfuric acid catalyst to give the mixture of cyclic acetyl (dioxolane and dioxane) oleate esters, which was highly soluble in diesel oil.

Further work is in progress to improve this route or improve the feedstock purity. Equilibration of the esters and butyraldehyde may not be a viable answer to obtaining good yields of dioxolane ester, since linear acetyls are likely to form via ring opening. It may be possible to get out some soluble mixture that will improve the ignition quality. Although the monoester could be obtained in relatively pure form by the reaction of glycerol monochlorohydrin with the salt of the desired acid, this is a longer route than the direct esterification described above. The corresponding reaction of the salt of the desired acid with the 4-chloromethyldioxolane is also considered to be a viable alternative.

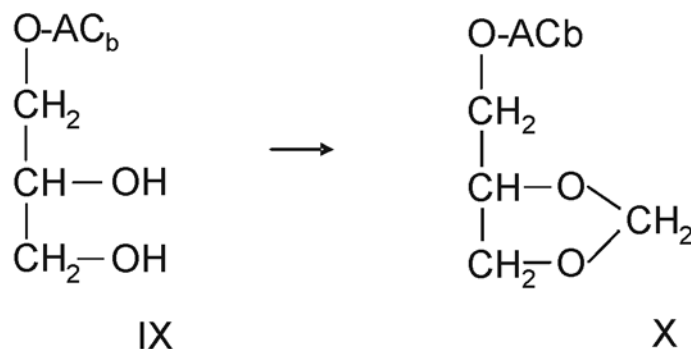


Figure 36. Formation of dioxolane ester from glycerol monoester.

Ether Cetane Numbers

The addition of ethers to diesel fuels to improve ignition and CNs was previously demonstrated and patented several decades ago (6). Aliphatic straight-chain ethers and polyether blends reported in the Lipkin patent gave high CNs, differing somewhat from those reported by Pecci et al. (2). But BCNs in the range of 70–117 clearly demonstrate that the ether oxygen is promoting the ignition in all of the straight-chain ether oxygenates and blends.

Similar high values were reported for glycol ethers. When branching occurs on only one side of the ether, the BCN drops only a little; for example, 103 was reported for 2-methylbutyl pentyl ether (2). The cost of production of the glycol ethers has always been a problem for fuel applications, owing to the high cost of ethylene glycol, and ethylene oxide is also very toxic. The toxicity of the ethylene oxide and the glycol ethers is also a serious problem. The diethyleneglycol diethyl ether is teratogenic. Some of the straight-chain glycol ethers are too hydrophilic and absorb water easily. The straight-chain glycol ethers also raise the cloud point and cold-flow plugging point and, thus, have a deleterious effect on the cold-flow properties of the blends. These considerations will likely inhibit the development of this type of ether fuel.

The BCNs for acetyls typically range from 57 to 97, depending on the chain length and branching. Both our previous results (7) and the literature results (2) showed very high BCNs for the straight-chain formals.

Fuel properties of several of blends of the target glycerol-derived cyclic acetyls ethers and esters were tested as 10% blends with a base diesel fuel with CN = 42.6. For comparison, two additional cyclic acetyls derived from glycols (not glycerol) were tested also as 10% blends. Blending cetane numbers and cold filter plugging points of the 10% blends are given in Table 18.

Table 18. Fuel Properties of Cyclic Acetyls

Cyclic Acetyl Additive	BCN ¹	CFPP, ² °F
4-Ethyl-1,3-Dioxolane	53	-36
2-Propyl-1,3-Dioxolane	66	-36
Allyl Glycerylformal Ether	36.6	-33
Butyl Glycerylformal Ether	43.6	-36
Glycerylformal Oleate Ester	45.6	-4
Base Diesel Fuel	42.6	-27

¹ BCN = 10 [CN_{blend} - 0.9CN_{base}]

² CFPP + cold filter plugging point of the 10% blend

The results show that the glycol-derived cyclic butyral derivative (2-propyl-1, 3-dioxolane) has moderately high BCN of 66, but this is significantly lower than the BCN of most of the straight-chain glycol ethers and straight-chain formal derivatives discussed above. The cyclic formal ether 4-ethyl-1,3-dioxolane is lower (BCN = 53). Instead of increasing the BCN as expected for the addition of another ether functionality, the results from target glycerol-derived compounds showed even lower results. Thus adding the allyl glycerol formal ether actually would decrease the cetane number of the blend, since the BCN is below the base fuel cetane number (42.6). The BCN of the glycerol formal oleate ester was similar to that of other fatty oleate esters, such as those used in methyl biodiesel fuels.

Most of the cyclic acetyls had a positive effect on the cold-flow filter plugging point (CFPP), decreasing the CFPP from -27 to -36°F. The exception was the oleate ester, which raised the CFPP. Again, this is typical for fatty esters.

Since these BCNs of the glycerol acetyl ethers and esters exhibit little cetane-enhancing effect, one must consider all other benefits from oxygenate additives. Various patents (8–10) and applications (11) describe fuel additives containing glycol monoethers and polyethers. In addition to lower emissions, these are shown to provide lubrication, prevent gum and deposit formation, inhibit smoke production, and condition the fuel. They also serve as a vehicle for the addition of peroxides and nitrates that enhance the CNs. It is, however, likely that adding the glycerol derivatives to a diesel blend for these purposes would not seem to be economical. The glycerol derivatives may have a cost advantage over the ethylene glycol-derived compounds, but this may be only temporary. The straight-chain ethers and acetyls appear to have a much greater potential, owing to their high BCNs.

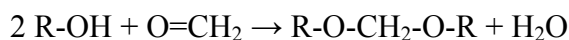
Results and Discussion

The objective in this project is to produce ethers and esters from glycerol that will result in high CNs. Previous testing in an EERC project demonstrated that dibutyl ether and dibutyl formal have exceptionally high blending cetane values at 10% blends in No. 2 diesel fuel (7).

These can be produced from butanol, which in turn can be prepared easily from ethanol via the Guerbet reaction in impure form. In general, the CNs of the corresponding butyl alcohol blends were exceptionally low (negative BCNs!). Short-chain ester (methyl, ethyl, butyl) CNs were also disappointing. The conclusions from a number of studies of this kind were that n-alkyl

ether groups or other functional groups with hydrogens attached to a carbon that also contains one or two oxygens confer high reactivity in diesel combustion and result in oxygenate additives with high cetane ratings. Alternately, compounds with hydrogen directly attached to oxygen (alcohols) or hydrogen attached to carbons adjacent to a carbonyl (esters) have a large negative or moderate negative effect, respectively, on the CNs.

Acid-catalyzed reactions of a simple alcohol (2 moles) with an aldehyde give an acetyl structure which is a diether with its two oxygens attached to the former aldehyde carbon:



Reaction of a diol with an aldehyde gives a cyclic diether. In the case of a 1,2-diol, the product is a five-membered ring heterocyclic compound, 1,3-dioxolane, whereas a 1,3-diol forms a six-membered 1,3-dioxane. Glycerol, a 1,2,3-triol forms the mixture of dioxolane and dioxane ring structures with one remaining hydroxyl (Figure 37). Thus conversion of low-cost impure glycerol to acetyls with aldehydes is relatively easy and should presumably result in higher ignition reactivity. Formaldehyde gives the formals, and other aldehydes or ketones give alkyl-substituted products. Etherification or esterification of the remaining hydroxyl group can give suitable candidates for testing.

This approach was previously used in French Patents 2833606 and 2833607 (12). The mixture of cyclic acetyls from the reaction of glycerol with butyraldehyde was reacted with sodium hydride and an excess of dialkyl carbonate to form the mixture of carbonate esters of the acetyls in good yield. The cyclic acetyl mixture was also reacted with diethoxymethane to form the monoethyl acetyls of the two cyclic acetyls. Mixtures of the products with a diesel fuel

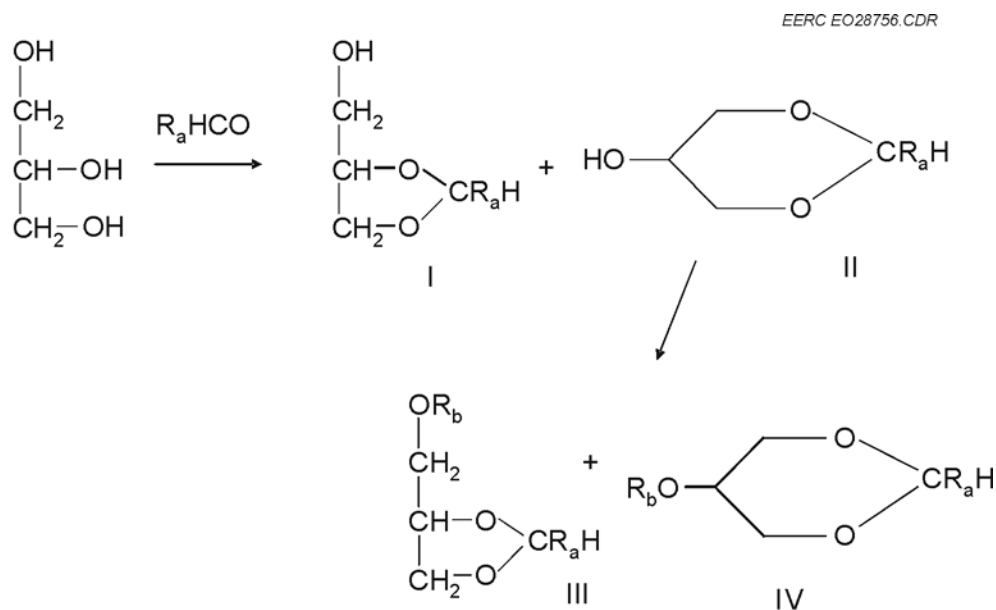


Figure 37. Formation of cyclic acetyls from glycerol.

resulted in lowering the particulate emissions of the fuel, but no cetane value was determined for either fuel mixture.

The approach in the current project was to use similar cyclic acetyl mixtures since they are easy to prepare, even from an impure starting glycerol containing salt and water. Different derivatives are prepared from the cyclic acetyls, however. Rather than the acetyl and carbonate derivatives that would infringe the Delfort patents, other ether and ester derivatives were selected based on our previous experience in identifying functional groups with high cetane potential. It is important that the ether groups introduced on the cyclic acetyl not be of the branched isoalkyl type since these result in lower ignition activity and lower CNs.

Likewise, the ester groups introduced should not contain hydrogens on the alpha carbons adjacent to the carbonyl group. We also focused on producing the ethers from reagents that could be prepared from biomass sources such as carbohydrate, glycerol, or fermentation products. However, some minimal work was conducted using inexpensive olefin commodities from the petrochemical industry.

One important obvious factor is that the resulting derivative must be oil-soluble to be of use as a diesel oxygenate additive. Thus butyl or other longer alkyl chains must be incorporated into the structure to promote oil solubility. Therefore, one way to promote oil solubility is to use butanal instead of formaldehyde to make the cyclic acetyls.

Conclusions

As a result of previous testing of blends of diesel fuel and acetyls and ether additives for improved ignition quality (cetane numbers), several target compounds to be derived from glycerol were identified. The target compounds include mixtures of 1,3-dioxolanes and 1,3-dioxanes prepared from glycerol feedstock. Several intermediate mixtures of the dioxolanes and dioxanes were synthesized using a liquid acid catalyst, and further conversions of the intermediates to oxygenate additives were conducted with appropriate reagents using liquid and solid acid catalysts. Four of the target compounds prepared were ether derivatives of the dioxolane–dioxane structures. Two of the target compounds were ester derivatives of the dioxolane–dioxane structures, but only one was soluble in diesel fuel.

Testing of the four soluble target compounds for cetane numbers gave only mediocre BCNs for the glycerol-derived acetyl ethers and esters. The results rejected the hypothesis that increasing either linkages by converting the three hydroxyls of glycerol to ether functionalities or mixed ether-ester functionalities will increase the BCNs. There are likely steric hindrances in the cyclic compounds that destabilize transition states of the cyclic molecules during reactions with oxygen radicals in the combustion process.

Testing of the glycerol derivatives for CFPPs gave the expected improvements. Most of the cyclic acetyls significantly lowered the CFPP; however, this and other general benefits of using oxygenate blends of glycerol derivatives would not likely be cost-effective for producing high performance fuels. Other uses for the glycerol derivatives are currently being investigated.

References

1. Abou-Rashid, H; Marrouni, K.E.; Kaliaguine, S. *J. Molecular Struct.(Theochem)* **2003**, *631*, 241.
2. Pecci, G.C.; Clerici, M.G.; Giavazzi, F.; Ancillotti, F.; Marchionna, M.; Patrino, R. *IX Int. Symp, Alcohol Fuels* **1991**, *1*, 321.
3. Teregulova, G.T; Ismagilova, L.A; Rol'nik, L.Z.; Zlotskii, S.S.; Rakhmankulov, D.L. *Izvestiya, Vysshikh Uchebnykh Zavedenii, Khimiya i Khimicheskaya Tekhnologiya* **1989**, *32* (1), 35–38; CAN 111:194641.
4. Niviere, J. *Bull. Soc. Chim.* **1914**, *13*, 893–894.
5. Khaikina, M.B.; Vinokurov, D.M. *Izvestiya, Vysshikh Uchebnykh Zavedenii, Khimiya i Khimicheskaya Tekhnologiya* **1966**, *9* (3), 418–420; CAN 66:10536.
6. Lipkin, D. U.S. Patent 2,221,839, 1940.
7. Olson, E.S.; Sharma, R.K.; Timpe, R.C.; Aulich, T.R. High-Cetane Diesel Fuels from Biomass. In *Proceedings of the 27th Symposium on Biotechnology for Fuels and Chemicals*; Denver, CO, May 1–4, 2005.
8. Nelson, M.L.; Nelson, Jr., O.L. U.S. Patent 4,753,661, 1988.
9. Colwell, A.T. U.S. Patent 2,563,101, 1951.
10. Liotta, Jr., F.J.; Kesling, Jr., H.S. U.S. Patent 5,314,511, 1992.
11. Kesling, Jr., H.S.; Karas, L.J.; Liotta, Jr., F.J. U.S. Patent 5,308,365, 1993.
12. Delfort, B.; Durand, I.; Jaecker, A.; Lacombe, T.; Montagne, X.; Paille, F. Fr. Patent 2833606, 2003; Fr. Patent 2833607, 2003.

YEAR 2005 – ACTIVITY 4 – UTILIZATION OF CUPHEA OILS FOR BIODIESEL PRODUCTION

Introduction

Through the collaborative efforts of the U.S. DOE-sponsored EERC CBU, Technology Crops International (TCI), and the AURI, this project was conducted to investigate the potential feedstocks for development of a biodiesel with cold-flow properties equivalent to or better than those of petroleum diesel. CBU, which is cofunded by DOE and various corporate partners, promotes research and development in converting biomass to energy, fuels, and marketable products. TCI is a global leader in high-value specialty oilseed crops, such as cuphea, planting

the first commercial crops in 2004. Created and supported by the Minnesota State Legislature, AURI is a nonprofit corporation which develops new uses and new markets for agricultural products and is actively involved in the research and promotion of biodiesel. Biodiesel is the only alternative fuel to have fully satisfied the health effects testing requirements of the 1990 Clean Air Act Amendments (1). Its use reduces U.S. dependence on fossil fuels as well as imported fuels while providing economic benefit to the agriculture industry. Challenges yet to be overcome for widespread biodiesel utilization include a high pour or cloud point that causes it to gel in colder climates (2) and high cost relative to petroleum diesel fuel.

High cloud point results from a fuel made of mono-alkyl esters of fatty acids derived primarily from long-chain vegetable oils, such as soybean or canola oil. Conventional biodiesel thus consists of longer hydrocarbon chains (predominantly C18). One method of decreasing these temperatures would be to reduce the size of the molecules making up the fuel. A source of shorter-chained compounds is the cuphea plant, an annual with small seeds (3) that are rich in short- and medium-chain triglycerides (4). Research conducted on short-chain oils and triglycerides suggests that they may provide an improvement in the cold-flow properties of biodiesel (5).

Cuphea is highly desirable because it produces the high-value fatty acids caprylic, capric, lauric, and myristic that are currently available only in imported coconut and palm kernel oils (6). Efforts to commercialize cuphea production are being performed by researchers at Western Illinois University, Oregon State University, the U.S. Department of Agriculture Agricultural Research Service (USDA-ARS), the University of Georgia (3), and AURI in Minnesota (7). TCI, in partnership with USDA-ARS, Procter and Gamble, and the Universities of Oregon and Western Illinois, planted the first commercial crops in 2004 (8).

Biodiesel produced from a medium-chain feedstock, exhibiting lower pour point characteristics without additives, could significantly improve the economics of biodiesel, its marketability and, thus, consumption in colder climates. Additives are currently being used to overcome limitations of biodiesel flow properties at low temperatures. As cuphea oil is not only reported to be shorter-chained but lower in unsaturates as well, esterification of the oil may produce a more stable fuel than from conventional feedstocks. Environmental benefits of increased utilization of biodiesel are reduced particulate matter and greenhouse gas emissions.

Goals and Objectives

The goal of this project is to develop a biodiesel with cold-flow properties equivalent to or better than those of petroleum diesel. The objectives outlined to meet this goal include the following:

- Characterize cuphea seed oil.
- Produce and characterize biodiesel made from cuphea seed oil feedstock.

- Evaluate cuphea biodiesel by comparing results of the cuphea biodiesel analyses with properties of other biodiesels (e.g., soy diesel), as well as ASTM International biodiesel specifications.
- Conduct a preliminary economic analysis of cuphea biodiesel.

Experimental

The work was divided into four tasks: procurement and characterization of cuphea oil, production and analysis of cuphea biodiesel, data reduction and analysis, and information dissemination.

Procurement and Characterization of Cuphea Oil

TCI provided a cuphea seed oil sample for analysis and processing, and subsequent characterization of the sample was conducted to determine if any treatment of the oil prior to processing was required, such as degumming.

Approximately 4 gallons from this batch were sent to AURI in Marshall, Minnesota, for characterization (Table 19). Three separate batches of crude cuphea oil were received and combined to form a homogeneous single batch. The crude cuphea oil was dark green in color, presumably because it contained chlorophyll.

Production and Analysis of Cuphea Biodiesel

Mass and material balances for the run were performed and the liquid product characterized according to the parameters listed in Table 20. A single-stage, base-catalyzed process was used to transesterify the cuphea oil.

Transesterification Method and Equipment

Base-catalyzed transesterification is commonly used to produce biodiesel because it is an economical process. It is performed at low temperatures and pressures and typically results in a 98% conversion to biodiesel (9). Existing autoclave systems at the EERC were utilized for processing.

The transesterification process is the reaction of a triglyceride (a fat or oil) with an alcohol to form esters and glycerol, as shown in Equation 1. During this process, the alcohol reacts with

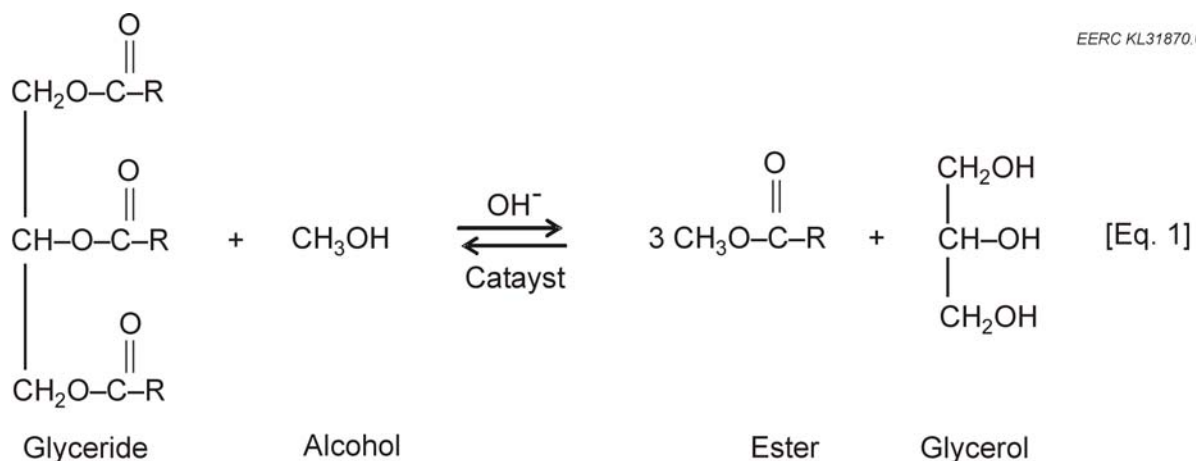
Table 19. Analyses Performed on Cuphea Seed Oil

Ash	CFPP	Sulfur
Btu/gal	Distillation (ASTM D1160)	Total glycerin
Carbon–Hydrogen–Nitrogen	Flash point	FFAs
Cetane Number	Free glycerin	Phospholipids
Cloud Point	Kinematic viscosity, 40°C	Karl Fischer water

Table 20. Analyses Performed on Cuphea Biodiesel

Ash	Distillation (D1160)	Acid number
Btu/gal	Flash point	Carbon residue, 100% sample
Carbon–Hydrogen–Nitrogen	Free glycerin	Copper strip corrosion
Cetane Number	Kinematic viscosity, 40°C	Phosphorus content
Cloud Point	Sulfur	Sulfated ash
Cold-Filter Plugging Point	Total glycerin	Water and sediment

the fatty acids on the triglyceride to form the monoalkyl ester (i.e., biodiesel) and crude glycerol. Methanol or ethanol typically serve as the alcohol, producing methyl esters or ethyl esters, respectively. The base used to catalyze the reaction is usually potassium hydroxide (more suitable for ethyl ester biodiesel production) or sodium hydroxide. Reaction takes place at just above the boiling point of the alcohol (about 71°C, or 160°F), for between 1 and 8 hr.



Two autoclave systems were used during the performance of this work. A small system was used for the tests in which reaction conditions were screened, while a larger system was utilized for the bulk production runs. A schematic of the smaller system is shown in Figure 38, while a schematic of the larger autoclave system is shown in Figure 39.

Reaction Condition Screening Tests

Processing of the cuphea oil began with base-catalyzed transesterification at 160°F for 8 hr, conditions that are typically used in biodiesel production from soybean oil. For transesterification of the cuphea oil, methanol served as the alcohol, and sodium hydroxide was used as the catalyst.

Four screening tests were performed to determine the appropriate reaction time within the range of 1 to 8 hr as well as the ratio of alkaline catalyst to oil feedstock, summarized in Table 21. All of the tests were performed in a small autoclave system, a schematic of which is shown in Figure 38. For each test, methoxide was prepared by mixing NaOH with 75 mL of

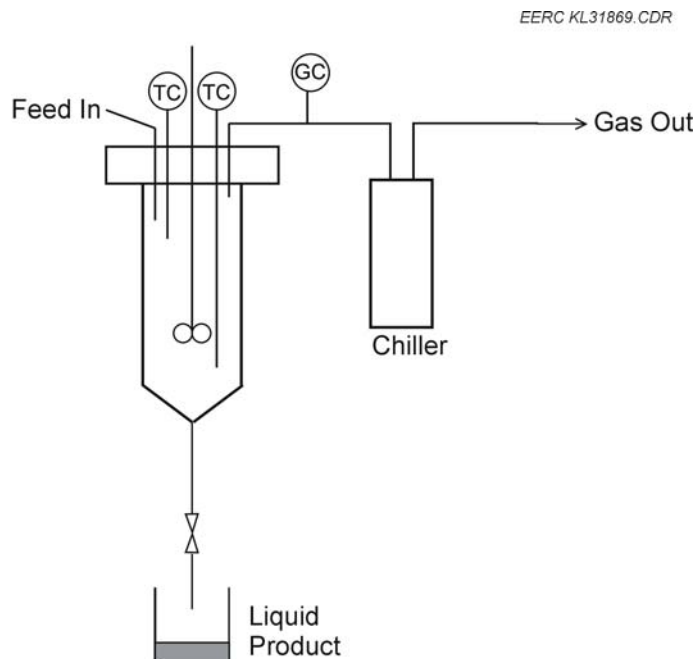


Figure 38. Schematic of the autoclave system used for the screening tests.

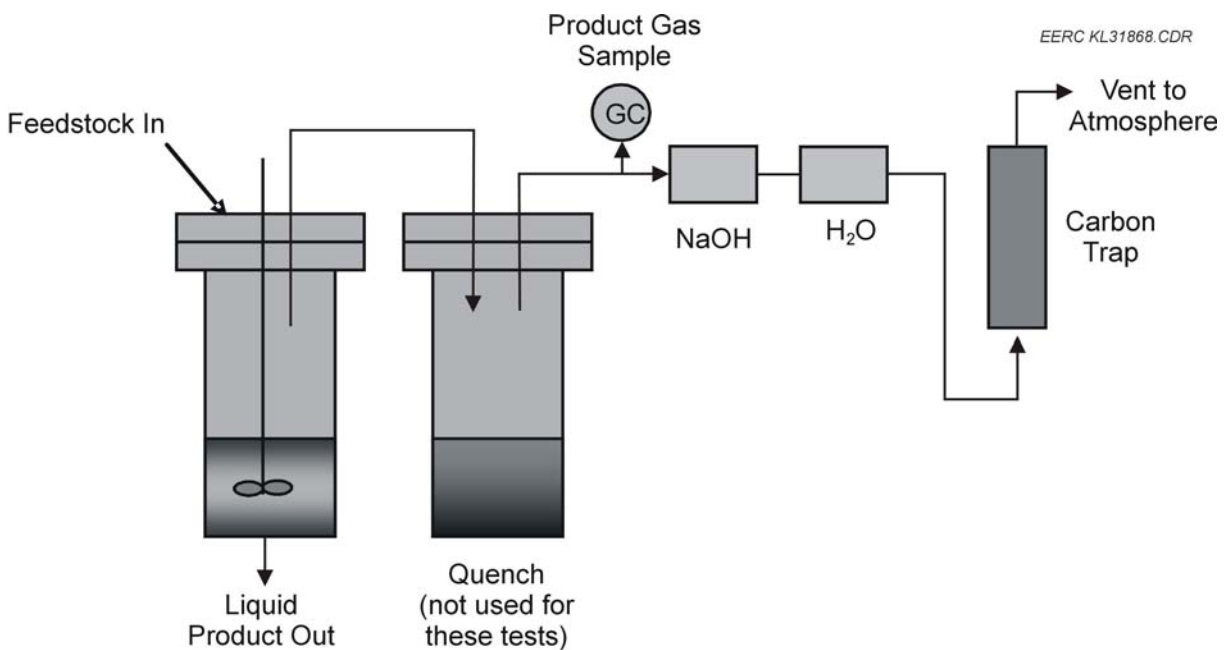


Figure 39. Schematic of the autoclave system used for the bulk production runs.

Table 21. Screening Tests Conducted in the EERC Autoclave at 71.1°C (160°F) with 75 mL Methanol and 100 mL Cuphea Oil

Test No.	NaOH, g	Residence Time, hr
1	0.5	1
2	2.0	1
3	2.0	8
4	2.0	4

methanol. One hundred mL of crude cuphea oil was introduced to the reactor and heated to the reaction temperature of 71.1°C (160°F) while the NaOH and methanol were mixing. The methoxide was added to the heated cuphea oil and the stirrer set at 325 rpm to provide vigorous agitation. The reactor was heated back to the reaction temperature and held there for the duration of the test, after which the liquid product was collected. As a means to determine similarities between the products of the screening tests and to ensure that the apparent change in viscosity was not simply due to dilution with methanol, refractive indices and distillation analyses were performed on the methyl ester products.

Bulk Processing Tests

Following screening for operating parameters, production of the cuphea biodiesel sample was conducted using 2.0 g NaOH per 100 mL cuphea oil and a residence time of 4 hours. The product was separated and analyzed.

Four identical bulk production tests were performed. For these tests, methoxide was prepared by mixing 44.4 g NaOH with 1665 mL methanol. While this was stirring, 2220 mL cuphea oil was warmed to 68°C, and the autoclave was heated to 71.1°C. The methoxide and warm cuphea oil were added to the heated autoclave, the system sealed, and the stirrer set to 325 rpm. The system was heated back up to 71.1°C and held for 4 hr. After cooling, the liquid product was collected and weighed.

Because of the relatively small quantities of product, the separation of the water and methanol from the methyl ester was performed in the laboratory. Approximately 1 gallon of cuphea methyl ester was treated by adding at least 600 mL of deionized water to the ester in a 4-L separatory funnel. After vigorous shaking, portions of HCl were added with shaking until pH paper showed that the mixture had a pH of about 4. The mixture was allowed to separate into water and oil phases overnight. The following day, the aqueous phase was slowly drawn off in 1-L portions and neutralized with Na₂CO₃ to achieve a pH of about 6 to 7. This was allowed to stand overnight while oil trapped in the water phase separated. Approximately 10–20 mL of methyl ester separated and was collected using a small separatory funnel. The oil phase was neutralized with aqueous Na₂CO₃. Additional deionized water was added and the mixture shaken vigorously and allowed to stand to separate. The water fraction was drawn off. To facilitate removal of any remaining methanol, saturated NaCl solution was added with shaking and allowed to separate. This was repeated several times until no additional water separated from the methyl ester. The cleaned oil phase was then combined with the previous similarly cleaned oil.

Cuphea Biodiesel Evaluation and Economics

The results of the cuphea biodiesel product analysis were utilized for comparison to conventional biodiesel feedstocks and standards for subsequent evaluation of the technical and economic viability of cuphea biodiesel.

Comparisons were made between the properties of cuphea biodiesel and other biodiesel fuels as well as biodiesel industry standards. The product properties were compared to those of typical soybean biodiesel and the ASTM B100 biodiesel specifications. The comparison assisted in determining suitability for use in diesel engines.

Preliminary economic analyses were performed to provide an indication of the cost of producing biodiesel from cuphea relative to the cost of producing it from other oils. TCI assisted with the projected cost of cuphea since it is still in the process of commercialization. This price was used with general biodiesel production costs to estimate a cuphea biodiesel price.

Results and Discussion

The mostly medium-carbon-chain cuphea seed oil proved technically viable for biodiesel production, displaying a low cloud point of -19°C (-2°F) when using a refined feedstock; albeit economic feasibility may take many years to achieve. Other advantages of cuphea include agricultural benefits for current U.S. crop rotations and greater oil yield per acre. Utilization of refined cuphea oil was required to determine the cold-flow properties for cuphea biodiesel. Improvements over other biodiesel feedstocks are low cloud point, viscosity, and sulfur. Cuphea biodiesel could potentially become viable economically by the year 2015.

Cuphea Oil Characterization

Advantages of cuphea oil include lower-carbon-chain composition and compatibility with U.S. crops. As expected, the cuphea oil sample had high medium-carbon-chain content. The cuphea seed plant could also provide benefits to current domestic crops.

The results of the unrefined cuphea oil analysis are presented in Table 22, showing a high cloud point, viscosity, and medium-carbon-chain content as well as low sulfur. A cloud point of 10°C (50°F) was identified for the oil sample. Kinematic viscosity was determined to be over 5 cSt/s, and sulfur content was 3 ppm. The sample contained about 70% C10 fatty acids, in contrast to soybean oil which contains over 80% C18:0–3, as shown in Figure 40. Considerable differences in cuphea biodiesel were thus anticipated over soybean diesel.

Cuphea could also prove to be a valuable new crop in U.S. agriculture, providing higher oil yield and compatibility with current domestic crops. Economic benefits to the industry are expected as some cuphea species may generate more than twice the oil per acre as soybeans (10, 11). Cuphea has also been touted as a rotation crop for soybeans and corn to control corn rootworms, decreasing pesticide costs while maintaining production yield in biodiesel feedstocks (12).

Table 22. Crude Cuphea Oil Profile

Analysis	Cuphea Oil	Analysis	Cuphea Oil
Heat of Combustion, Btu/lb	15,615	Flash Point, °C	
Btu/gal (est.)	117,122	Smoke	144.5
Carbon–Hydrogen–Nitrogen		Flash	256.0
Carbon	72.82%	Fire	289.5
Hydrogen	11.46%	Karl Fischer water, by vol	0.08%
Nitrogen	0.01%	Phospholipids	
Oxygen	15.71%	Phosphatidyl choline	0.021%
Cetane	–*	Phosphatidyl ethanolamine	0.035%
Cloud Point, °C	10	Phosphatidyl inositol	<0.005%
Cold-Filter Plugging Point, °C	14	Phosphatidyl serine	<0.005%
Distillation (D1160)	–	Sulfur, ppm	3
Nitrogen by Chemilumin, mg/kg	95.1	Sulfated ash, by wt	–
Calculated Acid Number, as oleic (18:1)	10.12%	Free fatty acids (FFAs)	5.09%
Free Glycerin	–	Kinematic viscosity, cSt/s @ 100°C	5.54
		Total glycerin	–
Fatty Acid Composition			
C8:0	0.58%	C18:1	7.79%
C10:0	69.35%	C18:2	6.39%
C12:0	2.66%	C20:0	0.11%
C14:0	3.76%	C20:1	0.72%
C16:0	5.79%	C22:0	0.11%
C18:0	0.93%	C24:0	0.09%

* Not available.

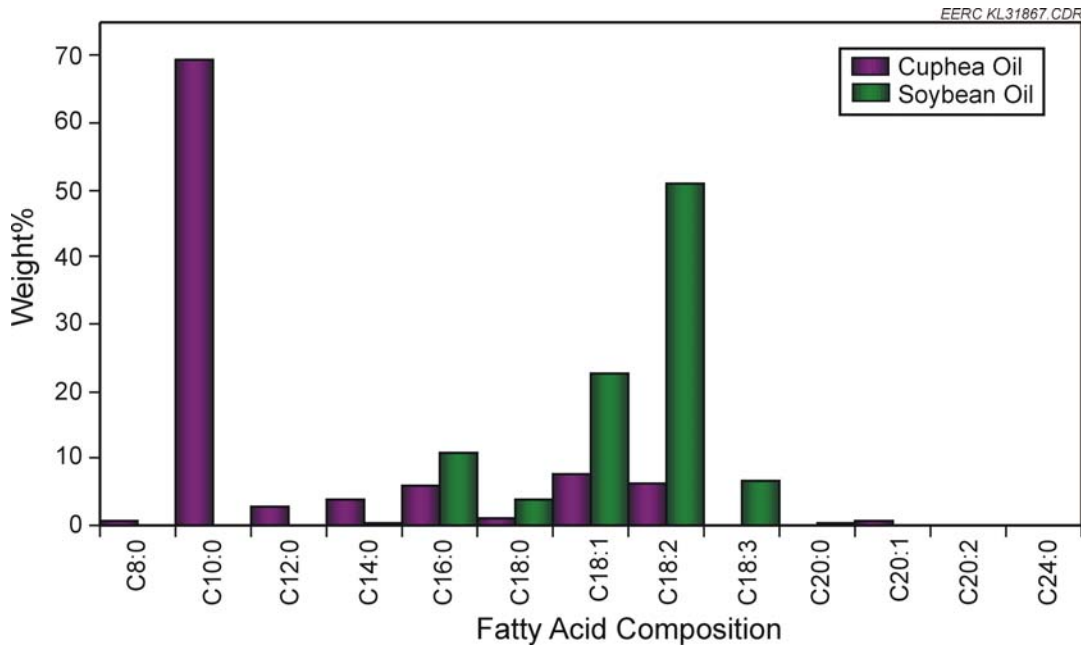


Figure 40. Comparison of cuphea and soybean oil carbon chain length compositions.

Cuphea Biodiesel

Although the crude oil sample converted readily to a biodiesel product, a product sample from refined oil was required to determine cold-flow properties. Analysis of the cuphea biodiesel showed a low cloud point for a refined feedstock and high medium-chain content. The bulk processing tests were performed using the higher catalyst-to-feedstock ratio and the moderate residence time.

Table 23 displays the analysis of the produced cuphea biodiesel, showing a low cloud point and high medium-chain content. Heat of combustion is moderate at about 120,000 Btu/gal. The cloud point of the biodiesel produced from the crude cuphea oil was not determined because of the remaining solids. Therefore, a separate refined sample of cuphea oil was used to generate an additional biodiesel sample for cloud point analysis. The result was a cloud point of -19°C

Table 23. Cuphea Biodiesel Analysis Results

Analysis	Cuphea Biodiesel	Analysis	Cuphea Biodiesel
Acid Number, mg KOH/gram	18.23	Cetane	48.4
Heat of Combustion, Btu/lb	15,523	Copper strip corrosion	1a
Btu/gal (est.)	116,422	Flash point, $^{\circ}\text{C}$	144
Carbon residue, 100% sample by wt	0.350%	Kinematic viscosity, cSt/s @ 40°C	2.62
Carbon–Hydrogen–Nitrogen		Karl Fischer water, by vol.	1.67%
Carbon	70.28%	Phosphorus content, by wt	0.0013%
Hydrogen	11.36%	Specific gravity	0.8759
Nitrogen	0.00%	Sulfur, ppm	3
Oxygen	18.36%	Sulfated ash, by wt	0.316%
Nitrogen by Chemilumin, mg/kg	40.7	Total glycerin	0.341%
Cloud Point, $^{\circ}\text{C}$	-19^*	Monoglyceride	0.319%
Cold-Filter Plugging Point, $^{\circ}\text{C}$	8	Diglyceride	0.022%
Distillation (D1160)		Triglyceride	0.000%
ABP AET, $^{\circ}\text{C}$	226	Free glycerin	0.000%
5% Rec. AET	238	Fatty acid composition	
10% Rec. AET	239	C8:0	0.57%
20% Rec. AET	240	C10:0	70.49%
30% Rec. AET	242	C12:0	2.72%
40% Rec. AET	243	C14:0	3.83%
50% Rec. AET	244	C16:0	5.40%
60% Rec. AET	247	C18:0	0.76%
70% Rec. AET	266	C18:1	8.08%
80% Rec. AET	327	C18:2	6.42%
90% Rec. AET	350	C20:0	0.11%
95% Rec. AET	365	C20:1	0.72%
FBP AET	368	C22:0	0.11%
		C24:0	0.09%

* Refined cuphea oil feedstock.

(-2°F). The contradictorily high cold-filter plugging point of 8°C is representative of the crude cuphea biodiesel product. The low cloud point of the refined biodiesel sample is supported by the high C13 content over 10%.

The bulk processing tests were performed using 2.0 g NaOH for every 100 mL of cuphea oil and 75 mL of methanol at a temperature of 71.1°C for 4 hr based on the results of the screening tests. Figures 41–43 show little difference between the products of the 1-, 4-, and 8-hr tests in which the higher amount of NaOH was used. The difference in refractive indices between the raw and transesterified oils ensured that the observed change in viscosity was not the dilution with methanol and that the triglycerides had indeed been transesterified. A methyl ester made from refined cuphea oil is used as a base of comparison. It should be noted that there is little difference between the refined, filtered, or crude oil samples and between the methyl ester samples, the exception being the first screening test using a low catalyst concentration. Similar results were observed from the simulated distillation of the samples. When the simulated distillation signatures are plotted with respect to time, Figure 43, a residence time of 4 hours, appears to provide the best conversion rate. Good mass closure was achieved for all four tests, as can be seen in Table 24.

Cuphea Biodiesel Evaluation

Benefits of cuphea biodiesel over other biodiesel feedstocks are low cloud point, viscosity, and sulfur. Biodiesel from cuphea oil provides significant improvement in cold-flow properties

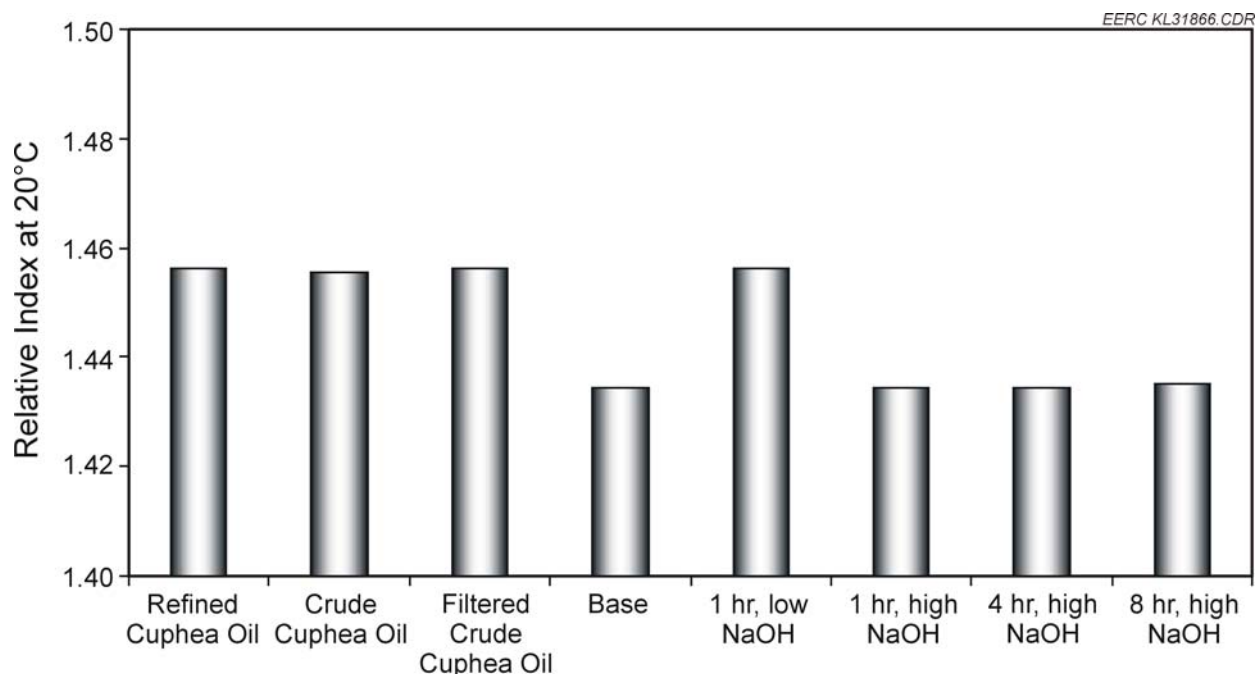


Figure 41. Refractive index of cuphea oil and cuphea methyl esters.

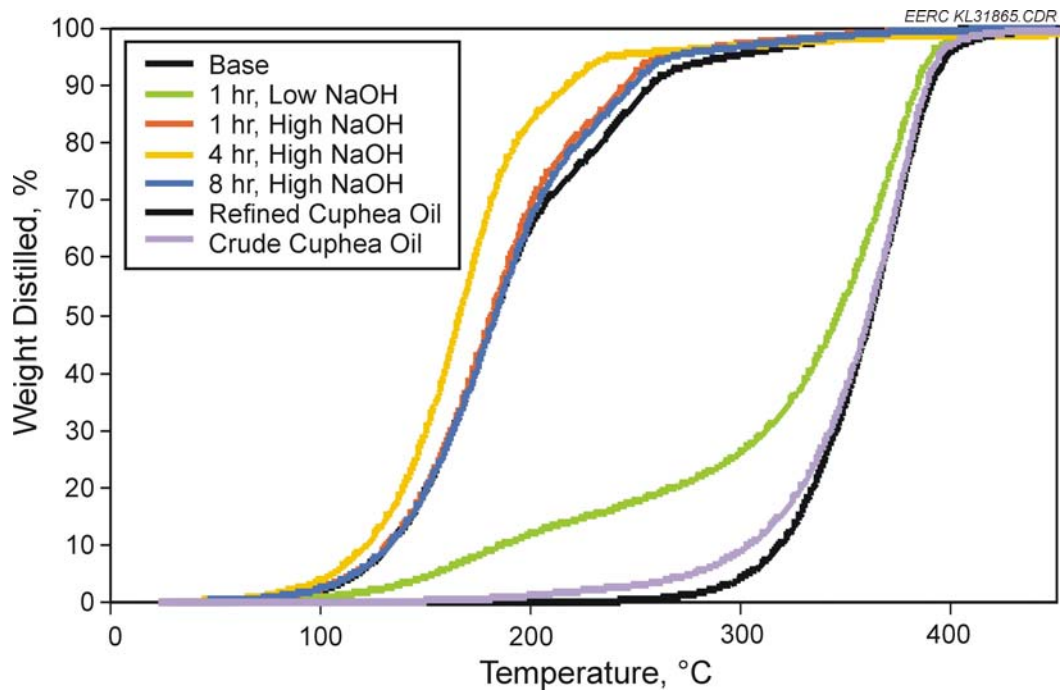


Figure 42. Simulated distillation of cuphea oil and cuphea methyl esters with respect to temperature.

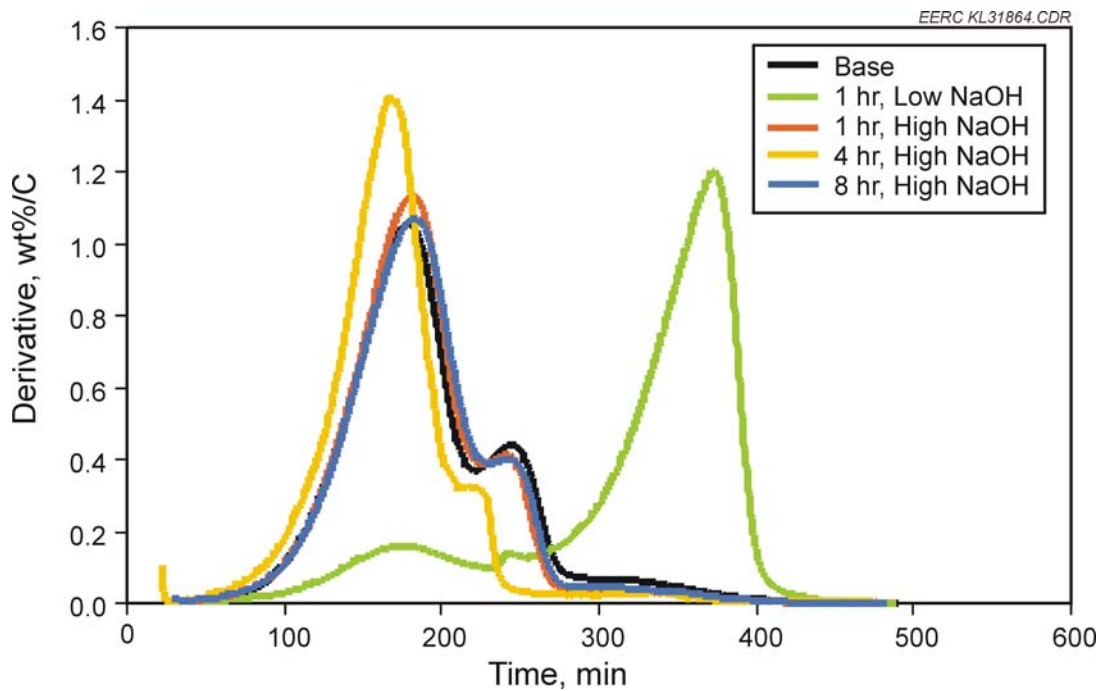


Figure 43. Simulated distillation of cuphea oil and cuphea methyl esters with respect to time.

Table 24. Mass Balances of Production Runs

Production Run Number	Mass Balance, %
1	95.67
2	97.94
3	99.18
4	98.50
Average	97.8

over winterized petroleum diesel. The production process requires optimization if all ASTM International (ASTM) requirements are to be met.

The cold-flow properties of cuphea biodiesel are significantly improved over winterized petroleum diesel or Diesel No. 2 and, thus, Diesel No. 1, as well as biodiesel from soybean and canola oils (Table 25). Soy diesel is similar to diesel, having a cloud point around the freezing point of water. Canola biodiesel is a slight improvement, with a cloud point of -3°C (26°F); however, the cloud point is still not as low as winterized diesel at about -8°C (18°F). Cuphea biodiesel could maintain engine operability at temperatures as low as -19°C (-2°F).

The cuphea biodiesel production process performed during experimentation requires optimization to meet all ASTM requirements. Table 26 compares properties of the cuphea biodiesel produced with biodiesel from soybean oil and ASTM regulations. Without optimization, cuphea biodiesel is similar to soy diesel and meets ASTM standards for kinematic viscosity, cetane, copper strip corrosion, FAA distillation, flash point, free glycerin, and sulfur. Advantages of cuphea biodiesel are a low viscosity of 2.6 cSt/s, nearly half that of soy diesel, and a sulfur content of 3 ppm, less than ultralow-sulfur diesel at 15 ppm. Properties requiring optimization to meet ASTM specifications are acid number, carbon residue, Karl Fischer water, sulfated ash, and total glycerin.

Cuphea biodiesel may become economically viable within the next decade. Feedstock cost can account for more than 90% biodiesel production costs, making cuphea biodiesel uneconomical until further progress is made with domestication and commercialization to lower the current cuphea oil price.

Economics

The price of refined cuphea oil is about \$3.00/lb, with potential to drop to \$1.00/lb with further genetic modification for domestication. For the year 2007, the price ranged from \$2.02 to \$3.90 per pound (13). Domestication efforts continue for large-scale commercialization of cuphea. Current yield is 30% of genetic potential; at 100% potential, achievable within the next 5–10 years, a price of \$1.00 per pound could be realized (13). The eventual goal for commercialized cuphea is to be interchangeable with specialty canola, bringing the competitive price down below \$0.60/lb (14, 15). However, this goal is several decades into the future.

Cuphea biodiesel will not be economically feasible for many years. Table 27 compares the relative price of petroleum diesel and biodiesel for soybean, cuphea, and canola oil feedstocks.

Table 25. Comparison of Fuel Cloud Points

Fuel	Cloud Point	
	°C	°F
Diesel No. 1	4	40
Soy Diesel	0–4	32–40
Canola Biodiesel	–3	26
Diesel No. 2 (winterized)	–9 to –7	15–20
Cuphea Biodiesel	–19	–2

Table 26. Comparison of Cuphea Biodiesel to Soy Diesel and ASTM Standards

Analysis	Soy-	Cuphea Biodiesel	ASTM
	Based Biodiesel		(D 6751-03a for B100)
Acid Number, mg KOH/gram	0.6	18.23	<0.80
Carbon Residue, 100% sample by wt	<0.01%	0.350%	<0.050%
Karl Fischer Water, by vol.	–*	1.67%	<0.050%
Sulfated Ash, by wt	<0.01%	0.316%	<0.020%
Total Glycerin	<0.20	0.341%	<0.240%
Phosphorus Content, by wt	<0.001	0.0013%	<0.001%
Kinematic Viscosity, cSt/s @ 40°C	4.6	2.62	1.9–6.0
Cetane	46–60	48.4	>47
Copper Strip Corrosion	1A	1A	<No. 3
90% Rec. AET, °C	–*	350	<360
Flash, °C	145	144	>130.0
Free Glycerin	<0.02	0.000%	<0.020%
Sulfur, ppm	<0.01%	3	<500 for S500, <15 for S15

* Not available.

Table 27. Comparative Biodiesel Production Cost for Varying Feedstocks

Feedstock Oil	Unit Price,	Biodiesel Cost,
	per lb oil	per gallon
Current Prices/Costs		
Biodiesel = Diesel	\$0.51	\$4.00
Soybean	\$0.61	\$4.78
Cuphea	\$2.96	\$22.20
Canola	\$0.59	\$4.65
Year 2015 Projections		
Diesel	–	\$7.00
Cuphea	\$1.00	\$7.75
Cuphea/Diesel (B60 for –9°C/15°F c.p.)	\$1.00	\$7.45*
Cuphea/Canola (2:3 for –9°C/15°F c.p.)	\$1.00/\$0.84	\$7.03

* Price would drop to \$6.85 if blending tax still available.

The current price for diesel is about \$4 per gallon, with an average annual escalation rate of 10% since 2000 (16). Diesel prices could thus reach \$6–\$8 per gallon by 2015. Biodiesel production without feedstock costs is estimated at \$0.25 per gallon biodiesel for a facility producing 10 million gallons annually (17). About 75 million pounds feedstock oil would be required for this facility. Current soybean oil prices average \$0.61 per pound, more than doubling over the last 2 years and producing an estimated \$4.78/gal biodiesel (18). Even the biodiesel blenders tax credit of \$1.00/gal biodiesel blended with petroleum diesel is not enough to offset increased prices, and many biodiesel facilities are halting production (19). Current cuphea prices would result in \$22/gal biodiesel. For the projected \$1/gal price around 2015, cuphea biodiesel would be about \$7.75/gal. A 60% blend of cuphea biodiesel with petroleum diesel (B60) to provide a cloud point of -9°C (15°F) gives a fuel price of \$7.45/gal. If the blenders tax credit was still available, the cuphea blend would be competitive at \$6.85/gal. Canola prices have been fairly stable, seeing an average escalation of 5% annually since 2000, potentially reaching \$0.84/lb by 2015 (15). Although canola is more economical than the other feedstocks, it has a higher cloud point than winterized diesel. Therefore, a 2:3 blend of cuphea and canola is suggested to maintain a cloud point of -9°C (15°F) and competitive biodiesel price of \$7/gal for B100 fuel in 2015.

Conclusions

A feedstock of high medium-chain-content provided a significantly lower cloud point than conventional biodiesel feedstocks, supporting past research efforts. Cuphea seed oil is a potential resource for medium-chain fatty acids, capable of producing an improved biodiesel for low-temperature applications. However, current high prices for cuphea oil inhibit implementation in the short term.

The cuphea seed oil is an excellent source of C10 fatty acids. However, separation of the final product was tedious and lengthy, a drawback of the higher presence of shorter carbon chains. The higher oxygen-to-carbon ratio creates a more water-soluble biodiesel product than that made from conventional products. Future work should consist of optimizing process parameters and separation methodology and engine testing of cuphea biodiesel as a fuel.

Cuphea biodiesel exhibits superior cold-flow properties to winterized diesel in addition to biodiesel from soybean and canola oil feedstocks. Although cuphea biodiesel is not, at this time, an economically viable feedstock for biodiesel production, it may become feasible in the next decade if used as a blend with canola biodiesel to improve cold-flow properties as well as economics, especially if petroleum diesel continues its significant price growth.

References

1. Biodiesel.org. www.biodiesel.org/resources/faqs/ (accessed Jan 2005).
2. World Energy Alternatives, LLC. www.worldenergy.net/product/operations.asp (accessed Jan 2005).
3. *Cuphea*. www.wiu.edu/AltCrops/cuphea.htm (accessed Oct 2004).

4. *Cuphea*. Interactive European Network for Industrial Crops and Their Applications. DG Research of the European Commission. www.ienica.net/crops/cuphea.pdf (accessed Sept 2004).
5. Chapman, E.; Hile, M.; Pague, M.; Song, J.; Boehman, A. Eliminating the NO_x Emissions Increase Associated with Biodiesel. *Prepr. Pap.—Am. Chem. Soc., Div. Fuel Chem.* **2003**, *48* (2), 639–640.
6. *Cuphea*; Ag Innovation News 12 (3); Agricultural Utilization Research Institute: Crookston, MN, July–Sept 2003.
7. Morrison, E.M. *Is Cuphea the Future? AURI Study Explores Industrial Markets for Minnesota Crop Components*; Ag Innovation News 12 (2); Agricultural Utilization Research Institute: Crookston, MN, April–June 2003.
8. Technology Crops International, Crops and End Products, www.techcrops.com/crops.htm (accessed Jan 2005).
9. Faupel, K.; Kurki, A. Biodiesel: A Brief Overview, Current Topic, ATTRA National Sustainable Agriculture Information Service, NCAT Agricultural Energy Specialists, May 2002, www.attra.org/attra-pub/biodiesel.html (accessed Oct 2004).
10. Selected New Industrial Crops. www.wws.princeton.edu/cgi-bin/byteserv.prl/~ota/disk1/1991/9105/910509.PDF (accessed Oct 2004).
11. McGraw, L. *Three New Crops for the Future – Cuphea, Milkweed, and Euphorbia lagascae*. U.S. Government Printing Office, Gale Group, Dec 1999, www.findarticles.com/p/articles/mi_m3741/is_12_47/ai_58576957 (accessed Sept 2004).
12. www.esru.strath.ac.uk/EandE/Web_sites/02-03/biofuels/what_biodiesel.htm (accessed April 2006).
13. Hebard, A. President, TCI. Personal communication, Oct 16, 2007.
14. TFC Commodity Charts. Canola: Monthly Price Chart. <http://tfc-charts.w2d.com/chart/CA/M> (accessed March 2008).
15. Canola Council. Seed, Oil and Meal Prices. www.canola-council.org/canolaprices.aspx (accessed March 2008).
16. Energy Information Administration. Weekly Retail Gasoline and Diesel Prices. March 17, 2008, http://tonto.eia.doe.gov/dnav/pet/pet_pri_gnd_dcus_nus_w.htm (accessed March 2008).
17. Haas, M.; McAloon, A.; Yee, W.; Foglia, T. A Process Model to Estimate Biodiesel Production Costs. *Bioresour. Technol.* **2006**, *97*, 671–678.

18. TFC Commodity Charts. Soybean Oil: Monthly Price Chart. <http://tfc-charts.w2d.com/chart/SO/M> (accessed March 2008).
19. Engstrom, T. SoyMor Stops Producing Biodiesel. *Albert Lea Tribune*, March 15, 2008, www.albertleatribune.com/articles/2008/03/15/news/news2.txt (accessed March 2008).

YEAR 2005 – ACTIVITY 5 – PROCESS INTEGRATION FOR ECONOMIC HYDROGEN PRODUCTION FROM ETHANOL

Introduction

As petroleum prices increase and the world's finite petroleum reserves continue to decline, industry and consumers are looking toward alternative energy solutions to help fill the inevitable energy gap. The so-called hydrogen economy refers to a society that will utilize hydrogen as a power source for emission-free fuel cells. Ironically, 95% of hydrogen used in the United States is currently produced by the reforming of natural gas (1). During natural gas reforming, 1 mole of carbon dioxide is formed for every 4 moles of hydrogen produced. Thus fuel cells operating on hydrogen derived from natural gas result in a net increase in global CO₂. Natural gas steam reforming also requires performing cleanup equipment to remove inherent sulfur compounds (2). As an alternative reforming feedstock, ethanol leads to an overall lower amount of CO₂ emissions because of CO₂ uptake by crops and does not require sulfur removal equipment.

High-pressure (>5000 psi) ethanol reforming was also investigated. Because of hydrogen's low energy density, the gas must be compressed prior to onboard vehicular storage. Hydrogen compression is expensive and energy-intensive. For high-pressure hydrogen dispensing, it has been estimated that the compression process consumes 18% to 32% of the lower heating value of the hydrogen being produced (3). A process that produces hydrogen at high pressure has the significant advantage of operating without gas compression, thereby improving process efficiency. Instead of producing hydrogen at low pressure and then compressing it, these experiments pumped liquid reactants to a high-pressure reformer, where they reacted to form a hydrogen-rich reformat at 5000 psi.

The EERC conducted ethanol-reforming screening tests at the bench scale. Experiments at the small pilot scale provided optimization data for catalyst amount, reactor temperature, reactor pressure, and water-to-ethanol mass ratio. Experiments reformed pure ethanol as well as unrefined "rectifier alcohol" (58 wt% ethanol) in a continuously fed catalytic reactor system.

Goals and Objectives

The primary objective of the proposed project was to demonstrate, on a pilot scale, the continuous production of a hydrogen gas stream from a partially distilled ethanol product. The continuous reactor system, considered to be pilot scale, typically reformed 6 lb/hr of an ethanol-water mixture. Data were to be obtained at various conditions in order to better characterize the feedstock handling, energy input, and operational conditions required to produce a hydrogen gas stream. An economic evaluation was proposed in order to evaluate the economic impact of

integrating hydrogen production at an ethanol facility. Hydrogen costs when reforming pure ethanol and unrefined ethanol were compared to hydrogen produced by conventional methods.

Experimental

Experiments were conducted in a continuous reactor system capable of operating at temperatures and pressures of 650°C and 12,000 psig, respectively. The reforming apparatus consisted of three subsystems: the feedstock storage system, the feedstock preparation system, and the reactor system. Figure 44 shows a process flow diagram for the reforming apparatus, and Figure 45 shows a photograph of the reforming apparatus.

The feedstock storage system consisted of two tanks and two pumps. An ethanol feedstock was pumped out of one storage tank, and water was pumped out of the other as needed to augment water addition to the reactor.

The feedstock preparation system mixed and heated feedstock streams. The feedstock preparation system had the ability to mix ethanol and water prior to the preheating coil (thereby preheating both liquids) or after the preheater (allowing ethanol to bypass the preheater).

The reactor system was a vertically oriented stainless steel vessel. A catalyst was positioned in the center of the reactor vessel. Reactor temperature and pressure were controlled remotely from a computer. A multicomponent gas analyzer, manufactured by Atmosphere Recovery, Inc., measured real-time product gas composition. Researchers collected gas bag samples and analyzed them via gas chromatography (GC) to verify real-time measurements.

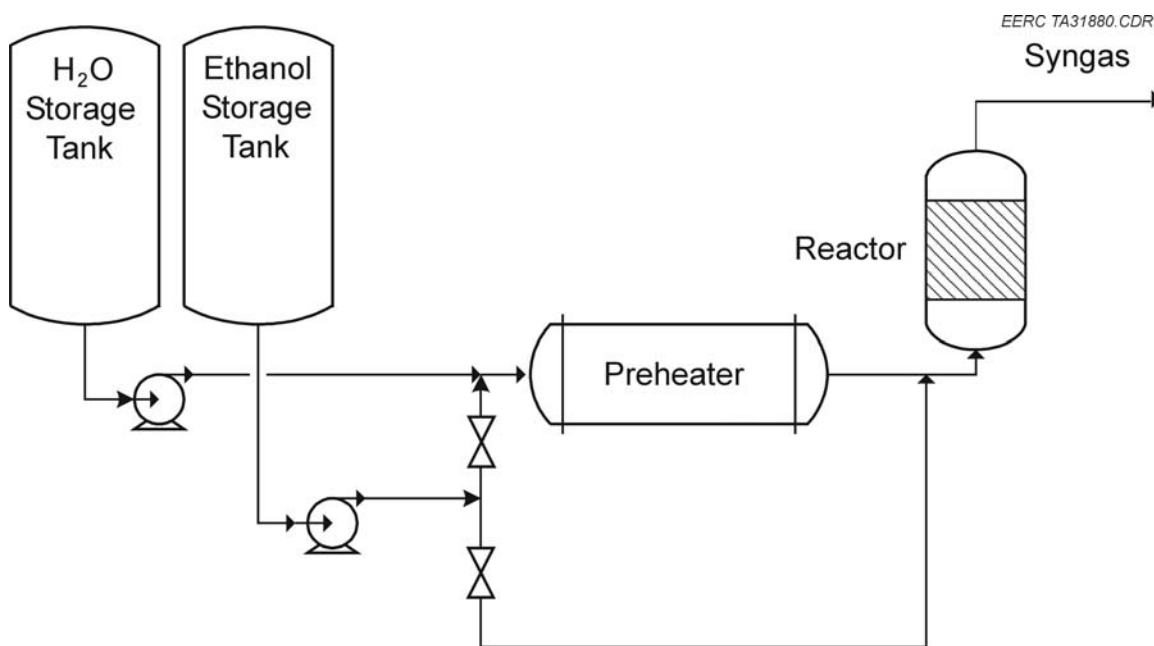


Figure 44. Process flow diagram of the ethanol-reforming apparatus.

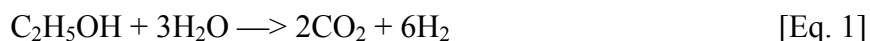


EERC TA27505

Figure 45. Photograph of the ethanol-reforming apparatus.

Experiments investigated the effect of the following parameters on hydrogen production: catalyst amount, reactor temperature, reactor pressure, water-to-ethanol mass ratio, and purity of ethanol feedstock.

The reforming reaction that maximizes hydrogen yield is shown below. The theoretical maximum hydrogen yield for ethanol reforming is 75 mol%, as calculated in Equation 1.



Additional reforming reactions occur simultaneously and have the potential to produce methane, carbon monoxide, and carbon coke. These additional reactions reduce the reformate's hydrogen concentration because they result in nonhydrogen products.

A condensate pot collected unreacted liquid products, and at the end of the test day, an alcohol meter measured the concentration of unconverted ethanol. An overall ethanol conversion number was calculated for each run as follows:

$$\frac{\text{Ethanol In (g)} - \text{Ethanol Out (g)}}{\text{Ethanol In (g)}} \times 100\% = \text{wt\% Ethanol Conversion} \quad [\text{Eq. 2}]$$

Results and Discussion

Parametric Screening Results

Catalyst amount, pressure, temperature, and water-to-ethanol mass ratio were investigated to determine their respective effects on product gas hydrogen concentration. Table 28 displays process parameters and the ranges over which they were studied.

Experimental results are shown in Table 29. The data are divided into three operating blocks. Block 1 shows data taken when temperature and pressure were below the supercritical temperature and pressure of ethanol. Block 2 shows data when temperature and pressure were above the supercritical temperature and pressure of ethanol but below the supercritical temperature and pressure of water. Block 3 shows data when temperature and pressure were above the supercritical temperature and pressure of water.

Experimental data were regressed to determine the coefficients for an equation to model product gas hydrogen concentration as a function of catalyst amount, reactor pressure, reactor temperature, and water-to-ethanol mass ratio. Table 30 shows regression results.

As Table 30 shows, the student's t statistic at a 95% confidence level with 7 degrees of freedom is 2.365. All four parameters had t statistics higher than 2.365 and were included in the model. Equation 3 shows the model equation that predicts product gas hydrogen concentration as a function of catalyst amount in grams (X_1), reactor pressure in psig (X_2), reactor temperature in degrees Celsius (X_3), and water-to-ethanol mass ratio (X_4):

$$H_2\% = 60.77 + (0.02)(X_1) - (0.011)(X_2) - (0.152)(X_3) + (6.22)(X_4) \quad [\text{Eq. 3}]$$

Where: X_1 = Catalyst amount in grams
 X_2 = Reactor pressure in psig
 X_3 = Reactor temperature in °C
 X_4 = Water-to-ethanol mass ratio

According to Equation 3, maximum product gas hydrogen concentration is predicted at a high-catalyst amount, low reactor pressure, low reactor temperature, and high water-to-ethanol mass ratio. Intuitively, most of these results make sense. A high-catalyst amount increases residence time, which would favor more complete conversion to hydrogen. Low reactor pressure favored hydrogen production, which is in agreement with LeChatelier's principle. Because sufficient water is necessary for maximum hydrogen yields and substoichiometric water in the

Table 28. Parameters Utilized to Determine Optimum Ethanol-Reforming Conditions

Parameter	Range
Catalyst Amount	985–1600 grams
Pressure	164–3835 psig
Temperature	304°–487°C
Water-to-Ethanol Mass Ratio	1.7–6.76

Table 29. Experimental Results from a Continuous Ethanol-Reforming Reactor ^{a, b}

Block	Run	Catalyst Weight, g	Ethanol Purity	Water-to-Ethanol Mass Ratio	T, °C	P, psig	CO	H ₂	CO ₂	CH ₄	Ethanol Conversion,
											wt%
1	14,1	985	Pure	4.0	342	298	0.3	49	26	24	90%
	14,3	985	Pure	4.0	352	321	0.4	49	24	25	90%
	17,2	1600	Pure	1.7	347	290	0.6	48	26	25	79%
	18,1	1600	Rectifier	1.7	349	164	0.9	47	25	26	100%
	18,2	1600	Rectifier	6.76	487	185	0.3	60	26	13	100%
2	14,2	985	Pure	4.0	304	970	0.2	49	26	24	90%
	15,1	1600	Pure	3.3	419	1002	0.6	36	26	37	94%
	15,2	1600	Pure	3.3	336	986	0.3	48	25	25	94%
	16,1	1600	Pure	3.0	383	1001	0.5	45	27	27	72%
	17,1	1600	Pure	1.7	317	999	0.6	49	24	25	79%
3	15	1600	Pure	3.3	420	3835		<i>10</i>		<i>90</i>	94%
	16,2	1600	Pure	3.0	390	3301		<i>10</i>		<i>90</i>	72%

^a Supercritical ethanol conditions (Block 2) are >240°C, >890 psig. Supercritical water conditions (Block 3) are >374°C, >3200 psig.

^b Data in normal font came from GC data. Block 3 data in italicized font came from real-time data.

Table 30. Regression Results from Ethanol-Reforming Data

Regression Statistics			
Multiple R	0.982		
R Square	0.965		
Adjusted R Square	0.945		
Standard Error	3.693		
Observations	12		
Degrees of Freedom*			
Regression	4		
Residual	7		
Total	11		
	Coefficients	Standard Error	t Stat (t*, 95% = 2.365)
Intercept	60.77	8.66	7.02
g	0.02	0.01	2.87
psig	-0.01	0.00	-11.40
°C	-0.15	0.05	-3.26
Ratio	6.22	1.62	3.83

* ANOVA.

reactor would lead to more coke deposits and less hydrogen production, it makes sense that hydrogen yield increases with water-to-ethanol mass ratio. Temperature's effect on product gas hydrogen concentration, however, is counter-intuitive. One would think that higher temperatures would favor hydrogen production because more available energy would drive reactions on the catalyst. However, these results suggest that lower temperatures are more favorable for

maximizing hydrogen concentration when this catalyst is used within the experimental temperature range.

In uncoded values, using the parameter ranges in Table 28, optimal product gas hydrogen concentration would occur when using 1600 g of catalyst, 164 psig, 304°C, and a water-to-ethanol mass ratio of 6.76. The experimental data point obtained while operating with conditions closest to these was run with 1600 g of catalyst, 194 psig, 489°C, and a water-to-ethanol mass ratio of 6.76. Hydrogen concentration at this point, measured by a real time gas analyzer, was 65 mol%. At the same condition, the model predicts a hydrogen concentration of 59 mol%, which equates to a relative difference of 9%.

At optimal conditions (1600 g of catalyst, 164 psig, 304°C, and a water-to-ethanol mass ratio of 6.76), the model predicts a hydrogen concentration of 87 mol%. Because the theoretical maximum hydrogen yield is 75 mol% (Equation 1), the actual hydrogen yield at optimal conditions would be less than predicted.

There was also a distinct change in process chemistry when temperature and pressure simultaneously exceeded the supercritical temperature and pressure of water. When the data in Table 29 are viewed as three operating blocks, it can be seen that hydrogen dropped to 10 mol% and methane increased to 90 mol% when operational temperature and pressure rose above the supercritical temperature and pressure of water (Block 3).

Improved Results at High Pressure

The original reactor system was modified in an attempt to achieve higher hydrogen yields at pressures greater than 5000 psi. Modifying the reactor system improved the percentage of hydrogen in the product gas from 10 to 50 mol%. Results from high-pressure reforming are shown in Table 31.

Table 31. Results from High-Pressure Reforming of Ethanol and Water in a Modified Reactor

Run	Water-to-Ethanol Mass Ratio	T (°C)	P (psig)	CO	H ₂	CO ₂	CH ₄	Ethanol Conversion (carbon balance) ^a	Ethanol Conversion (S.G.) ^{b,c}
1	10.8	395	4870	0.3	52.0	22.9	18.4	96%	
2	40.3	433	4860	0.3	51.9	23.1	18.5	99%	100%
3	6.2	436	4878	0.6	51.3	23.1	18.7	89%	100%
4	11.0	440	4844	0.4	52.1	23.1	18.4	87%	
5	9.8	440	5173	0.4	52.3	23.0	18.4	73%	100%
6	12.6	434	5359	0.4	52.8	22.5	18.1	95%	100%

^a $\frac{\text{Rate of Carbon Atoms Out}}{\text{Rate of Carbon Atoms In}} \times 100\% = \text{Ethanol Conversion}$

^b S.G. is specific gravity.

^c An ethanol meter calibrated for ethanol–water mixtures was utilized to determine the amount of unreacted ethanol in the condensate pot.

As Table 31 shows, the modified reactor produced a reformat with approximately 50 mol% hydrogen at 5000 psi and with conversions approaching 100%. These results are promising for a high-pressure, compressorless system to reform ethanol into high-pressure hydrogen.

Feasibility of Reforming a Partially Distilled Ethanol Feedstock

The motive behind reforming partially distilled ethanol was to reduce processing costs. Researchers hypothesized that the reforming catalyst used in experiments could tolerate impurities present in a partially distilled ethanol feedstock. Five gallons of “rectifier alcohol” was provided by the Chippewa Valley Ethanol Company. This partially distilled ethanol contained 58 wt% ethanol, along with liquid impurities. No changes in catalyst activity were noted when reforming rectifier alcohol. Regarding operational issues, the exit screen at the top of the reactor plugged one time while reforming rectifier alcohol, causing an elevated pressure drop across the reactor. The feed pump was manually shut off and then restarted. Restarting the feed pump dislodged the plugged material, and testing resumed without additional operational problems.

Table 29 shows that product gas hydrogen concentration data points, when reforming pure ethanol and rectifier alcohol at similar conditions, were within 1% of each other (Runs 17,2 and 18,1).

Utilization of Hydrogen for Fertilizer Production

An economic analysis was conducted to determine if and when the conversion of a reformed ethanol reformat into value-added fertilizer products would be a profitable venture. Figures 46 and 47 show economic analyses for anhydrous ammonia and urea fertilizer production. Profit, calculated in dollars per gallon of ethanol converted to fertilizer, is plotted as a function of foregone ethanol cost (\$/gal) and market value of fertilizer (\$/ton).

The model assumes that an ethanol feedstock is completely converted to a product gas that contains 64 mol% hydrogen (85% of the maximum theoretical hydrogen yield). Input cost breakdown was based on the process costs of steam methane reforming, as follows: feedstock = 55%, capital equipment = 28%, and operating and maintenance = 17% (4).

As Figure 46 shows, the current market value of ammonia (\$575/ton) would have to increase to \$1496/ton for the process to break even at a foregone ethanol price of \$1.50/gallon. As Figure 47 shows, the current market value of urea (\$425/ton) would have to increase to \$848/ton for the urea fertilizer process to become profitable (at a foregone ethanol price of \$1.50). This equates to a 260% increase in the market value of ammonia and a 200% increase in the market value of urea.

A declining ethanol price would also favor fertilizer production economics. Holding the market values of anhydrous ammonia and urea constant, the price of ethanol would have to drop

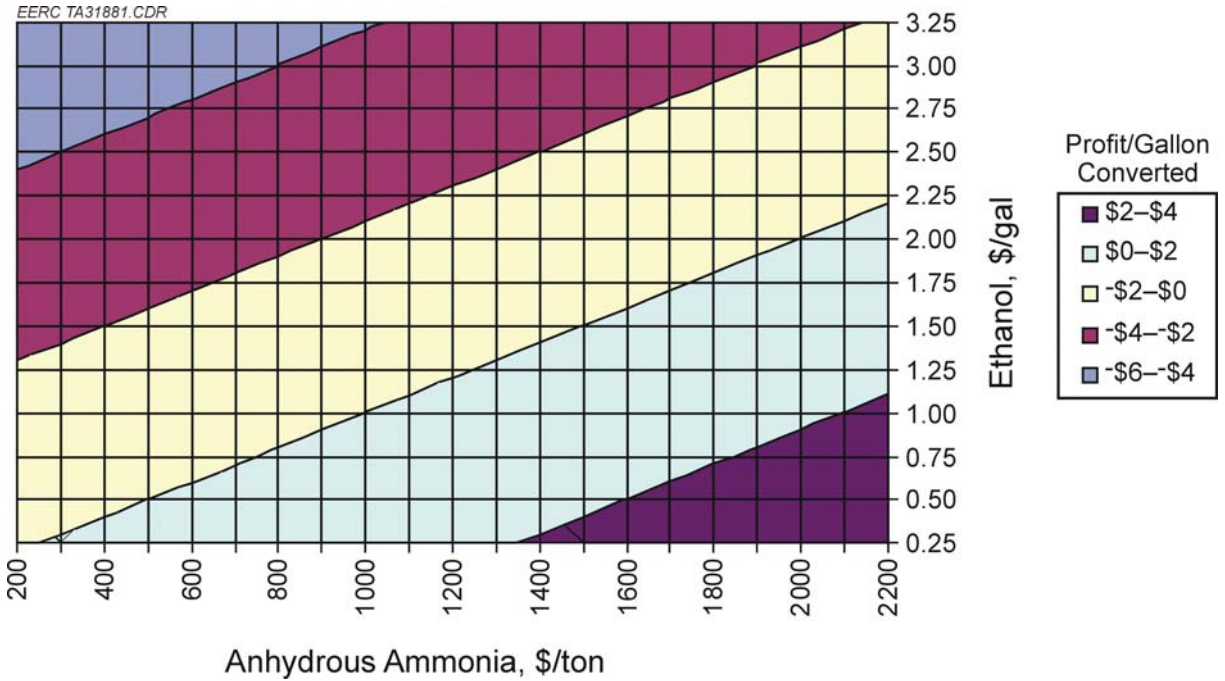


Figure 46. Profit per gallon of ethanol converted to anhydrous ammonia as a function of ethanol value and sale price of anhydrous ammonia.

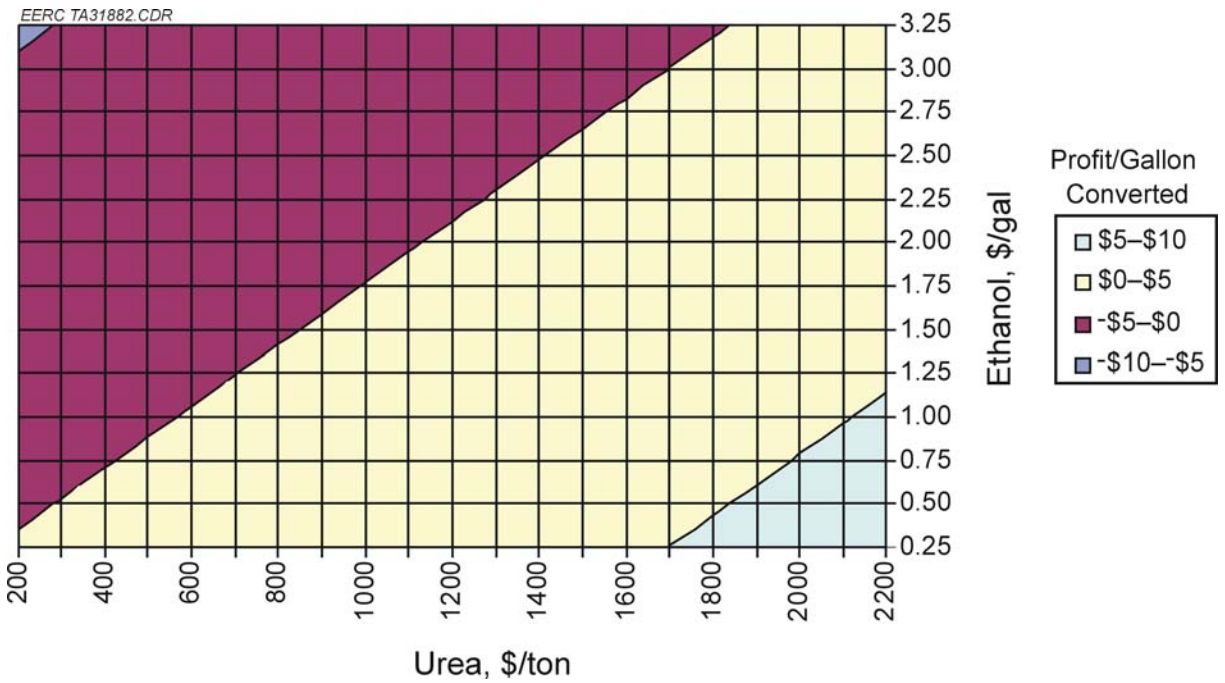


Figure 47. Profit per gallon of ethanol converted to urea as a function of ethanol value and sale price of urea.

to \$0.55/gal to make an anhydrous ammonia process profitable and \$0.75/gal to make a urea process profitable.

In general, a decrease in ethanol prices coupled with an increase in fertilizer prices would favor the economics of a fertilizer production process collocated at a corn-based ethanol plant. Figures 46 and 47 can be used to predict the profitability of a fertilizer production process at multiple intersections of ethanol and fertilizer prices.

Economics of On-Site Hydrogen Production

Hydrogen from ethanol is estimated to cost about \$3.80/kg, including a potential savings of \$0.33/kg from integration. High fossil fuel prices increase savings potential and allow ethanol to be more competitive with other feedstocks for hydrogen production.

The hydrogen cost is currently 7% lower than previously estimated, with a 10% increase in integration savings. Dramatic changes in the prices used for economic calculations of ethanol–hydrogen integration, as shown in Table 32, warranted revision from the previous EERC analysis (5). Prices for corn, ethanol, electricity, natural gas, petroleum diesel, dried distiller’s grains with solubles (DDGS), and hydrogen production from ethanol were updated to 2007 averages. Growth in utility and corn prices has increased the cost of ethanol production (6). Despite the higher cost, however, technological improvements have resulted in a decrease of 6% in commercial hydrogen production cost from ethanol (7).

As prices for fossil fuels continue to rise, energy savings from an integrated process will grow as well and hydrogen production from ethanol will be more viable. Transportation of ethanol, heating of the reforming feedstock, and ethanol distillation contribute significantly to the savings potential of integration (Figure 48). Thus high natural gas and diesel prices make integration of hydrogen and ethanol production more economically feasible. Compared with other feedstocks for hydrogen production (Figure 49), ethanol is also now as competitively attractive as natural gas and is more economical than other forms of renewable hydrogen.

Table 32. Change in Economics for the Estimation of Ethanol-to-Hydrogen Integration Savings

Component/Year	2005 (5)	2007	Change
Ethanol Production			
Corn	\$1.88/bushel	\$4.00/bushel (8)	113%
Ethanol	\$1.50/gal	\$2.50/gal (6)	67%
Electricity	\$0.048/kWh	\$0.064/kWh (9)	33%
Natural Gas	\$6.88/MMBtu	\$7.38/MMBtu (10)	7%
Petroleum Diesel	\$1.90/gal	\$2.86/gal (11)	51%
DDGS	\$97/ton	\$174/ton (12)	79%
Hydrogen Production from Ethanol			
Hydrogen from Ethanol	\$4.36/kg ^a	\$4.09/kg ^b	–6%
Integration Savings	\$0.30/kg H ₂	\$0.33/kg H ₂	10%
Hydrogen Price	\$4.06/kg	\$3.76/kg	–7%

^a 1 kg H₂ = 1 gge = gallon gasoline equivalent.

^b Thomas, 2006; adjusted to account for higher 2007 ethanol prices (7).

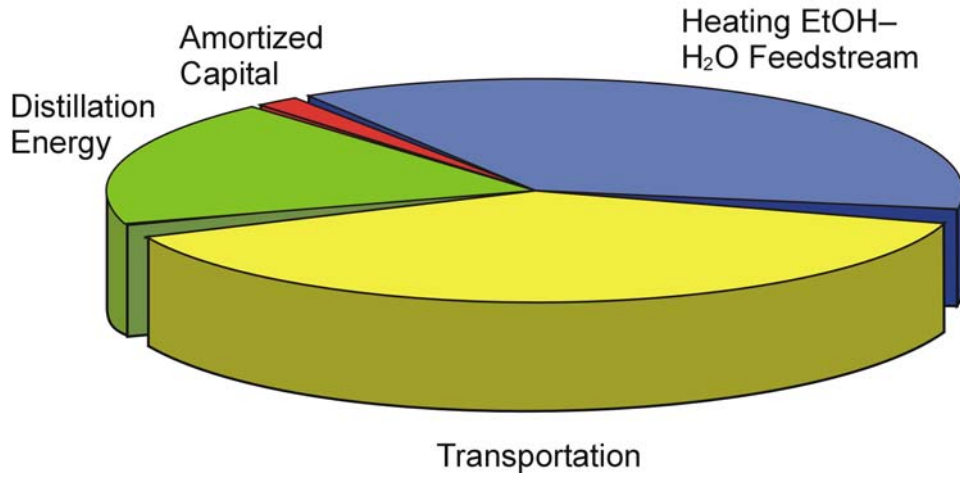


Figure 48. Contributing factors to savings from ethanol-to-hydrogen integration.

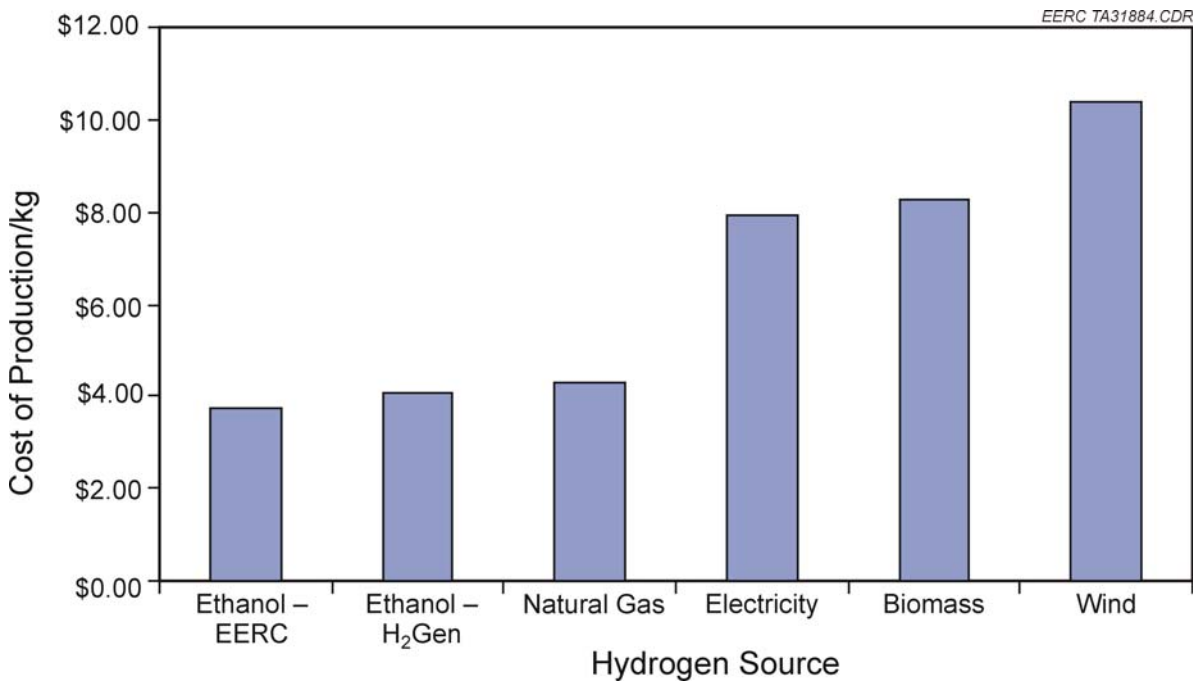


Figure 49. Cost of H₂ production from various feedstocks for comparable system size (adjusted to account for 2007 feedstock costs) (7, 13).

Conclusions

A continuous catalytic reactor system converted ethanol into a hydrogen-rich reformat. Reformat hydrogen concentration was nominally 45 mol%, with the best operating conditions yielding 60 mol% hydrogen. The maximum theoretical hydrogen yield for ethanol reforming is 75 mol%. Experiments varied catalyst amount, reactor temperature, reactor pressure, and water-to-ethanol mass ratio. It was found that, while the first reactor was operated over the ranges studied, maximum hydrogen yield was achieved at high catalyst amount, low pressure, low temperature, and high water-to-ethanol mass ratio.

A modified reactor was constructed in an attempt to improve hydrogen yields while reforming ethanol at high pressure (>5000 psi). The original reactor produced a product gas with only 10 mol% hydrogen when operating above 3200 psi and 374°C. While the modified reactor was operated, typical product gas concentrations were as follows: hydrogen – 50 mol%, carbon dioxide – 23 mol%, and methane – 18 mol%. These results show promise for a high-pressure hydrogen-dispensing system that would not require expensive gas compression.

The reforming catalyst did not show a loss of activity, and minimal operational issues were encountered when a partially distilled ethanol feedstock was reformed. This operational stability suggests that complete distillation and mole sieve operations may not be required upstream of an ethanol-reforming process collocated at an ethanol production facility.

The economic viability of converting ethanol into fertilizer products via reforming was also investigated. Calculations showed that the price of anhydrous ammonia and urea would have to increase 260% and 200%, respectively, for a fertilizer production process to break even at a foregone ethanol price of \$1.50/gallon. In general, decreasing ethanol prices coupled with increasing fertilizer prices favor the economics of a collocated fertilizer production process.

The cost per kg of hydrogen produced from ethanol has decreased 6% from 2005 estimates because of dramatic changes in the prices used for ethanol–hydrogen integration calculations. Hydrogen produced from ethanol is now cost-competitive with hydrogen produced from natural gas.

References

1. National Hydrogen Association. Hydrogen Production Overview. www.hydrogenassociation.org/general/factsheet_production.pdf (accessed Jan 2008).
2. National Research Council and National Academy of Engineering. *The Hydrogen Economy: Opportunities, Costs, Barriers and R&D Needs*; 2004; p 199.
3. Ahmed, S.; Lee, S.; Ahluwalia, R. *High-Pressure Distributed Ethanol Reforming*; FY2005 Progress Report of U.S. Department of Energy Hydrogen Program; Argonne National Laboratory.

4. Molburg, J.C.; Doctor, R.D. Hydrogen from Steam-Methane Reforming with CO₂ Capture. Argonne National Laboratory. Argonne, IL. Presented at the 20th Annual International Pittsburgh Coal Conference, Sept 15–19, 2003.
5. Leroux, K.M.B.; Wocken, C.A. *CBU 2004, Process Integration for Economic Hydrogen Production from Ethanol*; Energy & Environmental Research Center: Grand Forks, ND, 2005.
6. Cooke, R. What Is the Real Cost of Corn Ethanol? *The Cultural Economist*, Feb 2, 2007, www.financialsense.com/editorials/cooke/2007/0202.html (accessed Jan 2008).
7. Thomas, C. Low-Cost Hydrogen from Ethanol: A Distributed Production System, H2Gen Innovations, Inc. Presented at the BioDerived Liquids to Hydrogen Distributed Reforming Working Group KickOff Meeting, BWI Baltimore, MD, Oct 24, 2006; www1.eere.energy.gov/hydrogenandfuelcells/pdfs/biliwg06_thomas_h2gen.pdf (accessed Jan 18, 2008).
8. May, A. Corn Market Review. Extension Economics, South Dakota State University, <http://econ.sdstate.edu/Extension/corn.htm> (accessed Jan 2008).
9. Energy Information Administration. Average Retail Price of Electricity to Ultimate Customers by End-Use Sector. www.eia.doe.gov/cneaf/electricity/epa/epat7p4.html (accessed Feb 2008).
10. Energy Information Administration. Natural Gas Prices. http://tonto.eia.doe.gov/dnav/ng/ng_pri_sum_dcu_nus_m.htm (accessed Feb 2008).
11. Energy Information Administration. Retail Gasoline and Diesel Prices. http://tonto.eia.doe.gov/dnav/pet/pet_pri_gnd_dcus_r20_a.htm (accessed March 2008).
12. USDA-MO Dept Ag Market News. Corn Belt Feedstuffs. SJ_GR225, St. Joseph, MO, Jan 17, 2008, www.ams.usda.gov/mnreports/sj_gr225.txt (accessed Jan 2008).
13. National Academy of Engineering. The Hydrogen Economy: Opportunities, Costs, Barriers, and R&D Needs. Board on Energy and Environmental Systems, 2004, www.nap.edu/catalog.php?record_id=10922 (accessed Jan 2008).

YEAR 2005 – ACTIVITY 6 – BIOJET FUEL COLD-FLOW IMPROVEMENT

Introduction

With the exception of hydroelectricity and nuclear energy, the majority of the world's energy resources are based on fossil fuels such as petroleum, coal, and natural gas. All of these natural reserves are finite, and at current usage rates may be consumed by the end of the next century (1). The depletion of world fossil fuel reserves and increasing environmental concerns have stimulated recent interest in alternative sources for petroleum-based fuels. Biodiesel, made

by transesterification of crop oil, has been successfully introduced into the motor transportation fuel pool as an alternative diesel fuel. Just as biodiesel has similar critical properties to diesel fuel, it is postulated that a biojet fuel, an aviation fuel made from crop oil and/or its derivatives (biodiesel), could be developed as a substitute for petroleum-based jet fuel.

The University of North Dakota has conducted an extensive project to generate a biojet fuel from soybean/canola oil and/or its derivatives (soy/canola methyl ester), which most fully complies with aviation fuel (JP-8) specifications. Preliminary emissions and performance testing on a commercial aviation turbine indicated that development of an aviation fuel from biodiesel was feasible (2). However, the cold-flow properties of biodiesel limit utilization at high altitude and cold temperature climate conditions (2, 3).

A literature review has shown that there are four main solutions to overcome these cold-flow limitations: winterization, additives, branched-chain esters, and chemical manipulation. The latter solution was believed to hold the greatest long-term promise for development of an acceptable crop oil-derived aviation fuel product: biojet fuel. Thermal separation coupled with mild thermal/catalytic cracking has become the focus of this project in order to modify the chemical structure of crop oil and its derivatives with subsequent purification. By this modification, organic compounds present in the fuel feedstock are transformed into lighter organic compounds, and thus a fuel is produced that is amenable to cold conditions. Preliminary experimental results demonstrated that the thermal approach can be used to overcome the cold-flow limitations of crop oil and its derivatives (4).

This study investigated the major operating variables affecting conversion and product composition. Using a design of experiment methodology, we identified the significant reaction conditions as well as potential interaction factors that have the greatest impact on the cracking product (crackate). An analytical procedure that quantified the product and extent of conversion represents the single most important requirement of this study. Nevertheless, developing an analytical procedure that routinely provided trustworthy and reproducible results, presented a significant hurdle which consumed the major part of this research.

Bench experiments typically took 4 hours to conduct; analytical preparations took approximately 12 hours. This limited the total number of experiments and samples that could feasibly be conducted and analyzed in the period available.

Environmental Issues

Besides being independent from the imported commodity petroleum and not depleting natural resources, health and environmental concerns are the driving forces for alternative fuel demands. These concerns are manifested in various regulatory mandates of pollutants, particularly the Clean Air Act Amendments of 1990 (CAAA) and the energy security provisions of the Energy Policy Act of 1992 (EPAAct). Currently, one of the most important concerns is global warming.

Legislation, such as the CAAA and EPAAct, has created markets for alternative fuels that can be produced from renewable resources and are more environmentally benign than petroleum-

based fuels. The CAAA requires the U.S. Environmental Protection Agency (EPA) to identify and regulate air emissions from all major sources. In October 1996, EPA certified B20 (a biodiesel blend with 20% biodiesel and 80% petroleum-based diesel), used in combination with a catalytic converter, as a particulate matter (PM) control device (5). Fuel emission control programs for motor vehicles have increased the need for alternative fuels. Provisions of EPAct mandate federal, state, and alternative fuel providers to increase their purchases of alternative-fueled equipment. The regulation is to encourage the use of alternative fuels that could help reduce dependence on foreign oil in transportation applications.

Global warming refers to the increases in the average temperature of the Earth's atmosphere and oceans in the recent decades. According to the National Academy of Sciences, the Earth's surface temperature has risen by about $0.6 \pm 0.2^{\circ}\text{C}$ ($1.1 \pm 0.4^{\circ}\text{F}$) in the past century, with accelerated warming during the past 25 years. There is strong evidence that most of the warming over the last 50 years is likely attributable to human activities. The increased volumes of carbon dioxide and other greenhouse gases released by the burning of fossil fuels, land clearing, and agriculture are the primary sources of the human-induced component of warming. The combustion of fuels is responsible for about 98% of U.S. carbon dioxide emissions (6). Therefore, shifting from fossil fuels to alternative fuels may be a significant mitigation of global warming.

Crop Oil

The use of crop oil as an alternative fuel has been around since 1900 when the inventor of the diesel engine, Rudolph Diesel, first tested it in his compression engine. The first International Conference on plant and vegetable oils as fuels was held in Fargo, North Dakota, in August 1982 (7).

Most crop oils are primarily water-insoluble, hydrophobic substances commonly referred to as triglycerides (7). Figure 50 shows a typical triglyceride molecule. Triglyceride has a glycerol "backbone" to which is attached three fatty acids (FAs). These FAs differ by the length of the carbon chains, as well as the number, orientation, and position of double bonds in these chains. There is a substantial amount of oxygen in the structure.

The FAs which are most commonly found in crop oils are palmitic, stearic, oleic, linoleic, and linolenic (8). The chemical structures of these FAs are given in Table 33. Table 34 summarizes the common FA composition of canola and soybean oils. The degree of unsaturation is dictated by the number of double bonds in the FAs. Thus C18:1 (oleic acid), for example, denotes a carbon length of 18 with one double bond.

To date, there have been many problems found with using crop oil directly in diesel engines (especially in direct injection engines) for longer periods of time. These problems include (7):

1. Injector coking and trumpet formation to such an extent that fuel atomization does not occur properly or is even prevented as a result of plugged orifices.

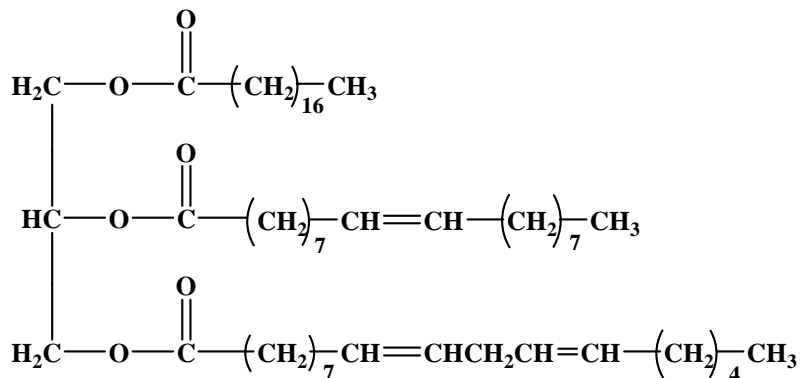


Figure 50. Structure of a typical triglyceride molecule (9).

Table 33. Chemical Structure of Common Fatty Acids (8)

Fatty Acid	Formula	Structure
Palmitic	$\text{CH}_3(\text{CH}_2)_{14}\text{COOH}$	16:00
Stearic	$\text{CH}_3(\text{CH}_2)_{16}\text{COOH}$	18:00
Oleic	$\text{CH}_3(\text{CH}_2)_7\text{CH}=\text{CH}(\text{CH}_2)_7\text{COOH}$	18:1
Linoleic	$\text{CH}_3(\text{CH}_2)_4\text{CH}=\text{CHCH}_2\text{CH}=\text{CH}(\text{CH}_2)_7\text{COOH}$	

Table 34. Fatty Acid Composition of Soybean Oil (10)

Fatty Acid	Canola Oil (wt%)	Soybean Oil (wt%)
Palmitic C16:0	4.0–5.0	2.3–11.0
Stearic C18:0	1.0–2.0	2.4–6.0
Oleic C18:1	55.0–63.0	22.0–30.8
Linoleic C18:2	20.0–31.0	49.0–53.0
Linolenic C18:3	9.0–10.0	2.0–10.5

2. Oil ring sticking.
3. Carbon deposits.
4. The lubricating oil thickening and gelling as a result of contamination by crop oils.

The major causes are the high viscosity and oxidative instability of crop oils. The high viscosity of these oils is due to large molecular mass and chemical structure. Crop oils have high molecular weights in the range of 600 to 900, which is three or more times higher (8) and viscosities 10 to 20 times greater than petroleum diesel fuel (11). This results in the formation of deposits in engines because of incomplete combustion and incorrect vaporization characteristics. Unsaturated fatty acids are very susceptible to polymerization and gum formation caused by oxidation during storage or by complex oxidation and thermal polymerization at the higher temperatures and pressures experienced during combustion (7).

JP-8 and Its Specifications

The single fuel concept was conceived after World War II in order to simplify the logistic supply chain for petroleum products. In 1988, the North Atlantic Treaty Organization (NATO) nations decided to move toward the use of a single fuel, jet propellant 8 (JP-8), for both aircraft and ground equipment (12). The logic behind such a decision comes not only from the gain of big logistical advantages in war time, but also from the more pragmatic fact of being able both to simplify and to make better use of NATO's extensive and expensive pipeline systems in times of peace. The current estimates of the worldwide use of JP-8 are approximately 60 billion gallons per year (43% in the United States) (13).

JP-8 is a kerosene-based aviation fuel with a minimum gross heat of combustion of 42.6 MJ/kg (14) and has additives to improve performance. The detailed specifications of JP-8 are listed in Table 35. It has a complex hydrocarbon mixture containing over four hundred hydrocarbons. The actual composition varies from batch to batch.

JP-8 mainly comprises four classes of compounds: n-alkanes and isoalkanes, olefins, naphthenes, and aromatics. About 18% of this fuel (Table 36) is aromatic hydrocarbons, while the remaining components are aliphatic alkanes and their isomers (9% C8–C9, 65% C10–C14, and 7% C15–C17) (14).

Table 35. Typical Properties of JP-8 Aviation Fuel (6)

Fuel Type	JP-8	Method
Molecular Weight	180 (average)	*E/M 1999
Density (g/mL, 15°C)	0.795	ASTM D1298
Viscosity (cSt, -20°C)	3.87	ASTM D455
Freezing Point (°C)	-47	ASTM D2386
Flash Point (°C)	41	ASTM D93
Conductivity (pS/m)	375	ASTM D2624
Sulfur (wt%)	0.23	ASTM D4294
Nitrogen (ppm)	14	
Aromatics (vol%)	15.3	ASTM D1319
Olefins (vol%)	0.3	ASTM D1319
Water (ppm)	23	ASTM D1744-83
Copper Strip Cor.	1?	ASTM D130
Lubricity		CEC F-06-A-90
Initial Measurement (μm)	754	
Repeated Measurement (μm)	758	
Distillation (°C)	145	ASTM D86
IBP	174	
10%	181	
20%	200	
50%	233	
90%	250	
FBP	251	

* EM = Exxon/Mobile.

Table 36. Typical JP-8 Composition

Component	Concentration, mg/mL
Aliphatic	
Undecane	48.4
Dodecane	36.1
Decane	30.2
Tridecane	21.9
Tetradecane	14.6
Nonane	9.2
Pentadecane	8.4
Aromatic	
Trimethylbenzene	9.7
Methylnaphthalenes	9.9
Dimethylnaphthalenes	6.3
Dimethylbenzene (xylene)	4.8
Naphthalene	2.1
Ethyl benzene	1.2
Methylbenzene (toluene)	0.5

Cold-Flow Impacts/Cold-Flow Properties

Cold-flow properties measure the ability of a fuel to function in cold temperature. One of the major issues associated with the use of crop oil and biodiesel is poor cold-flow properties, indicated by relatively high freezing points (FPs), cloud points (CPs), and pour points (PPs) compared to petroleum fuels. FP is the temperature or temperature range in which a pure compound or mixture freezes. Pure compounds freeze at a specific temperature, while mixtures freeze over a range (5). For complex mixtures, such as petroleum fuels, crop oils, and biodiesel blends, FP may be characterized by a range of temperatures reflecting the freezing point of the individual components. In order to better describe flow characteristics of these complex mixtures, the CP and PP are routinely used (15), which are the key cold-flow properties for winter fuel specification.

Crop oil is here used as an example to describe the freezing process. Almost all crop oils are made primarily from a mixture of different triglycerides. These triglycerides are made up from a molecule of glycerin linked to three FAs, which solidify at different temperatures. As the oil is cooled toward its freezing point (or PP), the different triglycerides solidify in turn causing the oil to become cloudy and increasingly thick before it finally solidifies completely. The temperature at which an oil begins to solidify is known as the CP. When the temperature drops to the oil PP, the oil will become solid and no longer flow. Eventually, it will block any fuel system components in which it lies (16).

CP (ASTM D2500) is the temperature at which the first formation of wax crystals appear as the fuel is cooled. As the temperature decreases below the CP, wax crystals rapidly grow and agglomerate until they are large enough to clog fuel filters and supply lines and, eventually, lead

to major operability problems (17). With further decreasing temperature, the fuel can gel up and cease to pour, approaching its PP.

PP (ASTM D97) is the temperature at which the fuel is no longer pumpable (5). Thus PP is very useful for characterizing the suitability of a fuel for large storage and pipeline distribution (9). The CP is always equal to or higher than the PP. It is recommended by engine manufacturers that the CP be below the temperature of use and not more than 6°C above the PP (10).

Cold-flow properties are critical for aviation fuels because aircraft often operate at high altitudes where temperature is extremely low. If fuel tanks are not heated or insulated, only the thin tank metal wall separates the fuel from air temperatures that decrease as altitude increases. Military specifications require JP-8 fuel to resist the formation of solid crystals (CP) at temperatures as low as -47°C, which corresponds to an altitude of 9500 meters (31,000 feet) (3).

Most biodiesel fuels have CPs and PPs near 0°C and -5°C, respectively (17). When blended with JP-8, the fuel's CP and PP exceed the specification value. Freezing point increases with increasing volume fraction of biodiesel in the fuel blends, as shown in Table 37. This less desirable cold-flow property limits aircraft operation to lower altitudes and land-based equipment operation to warmer conditions, which is unacceptable for both commercial and military applications.

Goals and Objectives

The overall objective of this work was to develop and optimize a thermocatalytic process for production of a viable jet fuel blendstock from crop oils. In Year 1, which was funded by DOE, the North Dakota State Board of Agricultural Research and Education (SBARE), and the North Dakota Soybean Council (NDSC), concept feasibility was studied by 1) operating a commercial-scale aviation turbine with 2%, 10%, and 20% SME (soy methyl ester) in JP-8 fuel blends and 2) determining how closely these fuel blends met JP-8 specifications.

In Year 2, which was funded by DOE, SBARE, NDSC, and the North Dakota Agricultural Products Utilization Committee (APUC), a 1-L lab-scale cracking reactor apparatus was built and used to evaluate the technical feasibility of a cracking-based process for biojet fuel production.

Year 3 activities were funded by DOE, SBARE, NDSC, APUC, and the National Science Foundation (NSF) and included 1) building infrastructure for product development, 2) fuel

Table 37. ASTM D5972 Freezing Point of JP-8 Biodiesel (SME) Blends (4)

Fuel Blend (% biodiesel)	Freezing Point, °C
2	-50
10	-27
20	-19

prototype turbine testing, 3) process optimization, 4) fuel characterization, 5) commercial feasibility, and 6) business model development.

Preliminary research by University of North Dakota (UND) researchers has shown that esterified crop seed oils (specifically, SME, one of a class of fuels labeled as “biodiesel”) can be utilized as an aviation fuel at low altitude conditions. The primary impediment for high-altitude utilization is the cold-flow properties of these oils and esters. Biodiesel complies with many, but not all, of the specifications required for a JP-8 fuel. Non-compliance generally falls into two categories: those due to the presence of glycerol (a by-product of the esterification process) in the biodiesel and those related to cold-flow properties of the heavier esters present in the biodiesel.

UND developed a process to produce a fuel from crop oil or animal fat oils that operates at very cold temperatures and is suitable as an aviation turbine fuel, a diesel fuel, a fuel blendstock, or any fuel having lower CPs, PPs, or freeze points. The process is based on the cracking of crop oil FAs or their associated esters, known as biodiesel, to generate lighter chemical compounds that have lower freeze, cloud, and/or PPs than the original oil or biodiesel. Cracked oil is processed using separation steps together with analysis to select fractions with low-temperature stability by removing undesirable compounds that raise temperature properties.

The process utilizes thermal or catalytic cracking methods coupled with separation technologies selected by chemical analysis to produce crop oil-based fuels that can be utilized at high-altitude conditions and/or very cold temperatures. A simplified block diagram of the biofuel process is shown in Figure 51. The crop oil or animal fat feedstock, **10** (see figure for bolded numbers), is fed to the cracking reactor, **12**. When the time, temperature, and pressure under which a particular feedstock remains under cracking conditions are varied, the desired degree of cracking (conversion) can be controlled. Temperature and time (residence time) are the more important process variables, with pressure playing a secondary role. The products of the cracking process are dependent upon the conditions of cracking and the original composition of the feedstock oil (2). The cracking conditions are varied based on detailed chemical analysis and evaluation of their low-temperature stability of the feedstock and cracking products in order to produce an acceptable biojet fuel. The presence of a catalyst can be used to improve the yield of desirable products, decrease the formation of unwanted products, or increase the efficiency of the cracking reaction because of lower pressure, temperature, or residence time requirements.

The cracking output is subjected to a variety of processing steps, **14**, dependent upon the material generated. Material generated in the cracking reactor consists of four general classes: 1) light ends; 2) biojet fuel chemical components, **26**; 3) unreacted raw materials; and 4) residual materials or residue, **16**.

The light ends consist of the unreacted vapor-phase material that was added to the reactor to manipulate the cracking reaction, such as hydrogen plus small molecular weight organic chemicals and hydrocarbons generated in the cracking reactor. The small molecular weight organic chemicals and hydrocarbons have chemical and physical properties that are undesirable

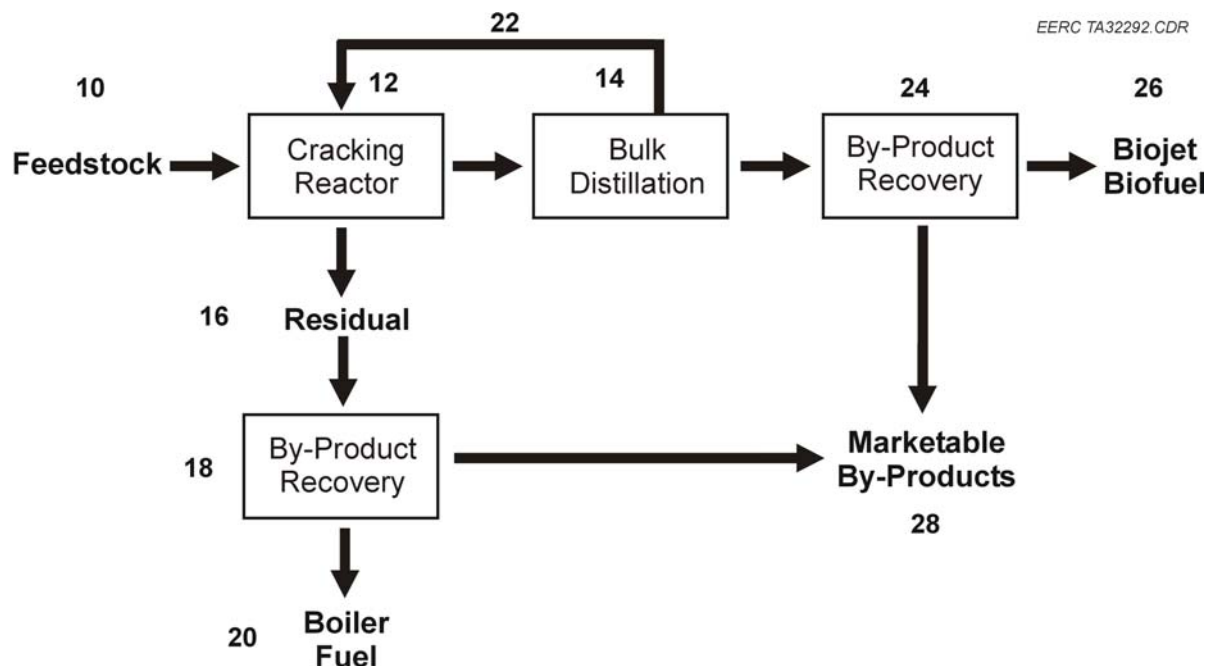


Figure 51. Biojet fuel process (simplified block flow diagram).

in an aviation turbine or cold-flow diesel fuel such as being too volatile. Light ends are separated from the other material that exits the reactor, **24**.

The biojet fuel chemical components, **26**, are those portions of the material generated in the cracking reactor that contribute to desirable chemical and physical properties of the biojet fuel. For example, jet and diesel fossil fuels such as those that meet the fuel specifications for JP-8 are primarily made up of C6–C12 straight-chain alkane hydrocarbons, where “C” refers to carbon and the number (6 or 12) refers to the number of carbon atoms in the molecule. Typical desirable compounds generated in the cracking reactor include C4 to C12 FA methyl esters, C4 to C12 FAs, and C6–C16 alkanes.

Unreacted raw materials are chemicals that entered the cracking reactor but, for some reason, did not experience cracking reactions. These materials have some chemical and physical properties that are undesirable in an aviation turbine or cold-flow diesel fuel. Unreacted raw materials are separated from the biojet fuel chemical components, **14**. These unreacted or uncracked raw materials, **22**, can then be returned to the cracking reactor.

Residual, **16**, consists of chemicals produced during cracking reactions that have a higher molecular weight and/or lower volatility and/or lower heating value than is desirable for the biojet fuel product. Some of the residual components can be separated, **16**, from the biojet fuel chemical components along with the unreacted raw materials and processed with these unreacted raw materials. Other residue components, typically those of higher molecular weight, will be in the form of solid material after the cracking reaction. These compounds are typically known as

“coke.” The “coke” may contain valuable chemical compounds, such as boiler fuel, **20**, or other by-products, **28**, that can be extracted from the residue, **18**.

Experimental

Materials

In this study, coconut methyl ester (CME), SME, canola oil, and soybean oil were used as thermal cracking feedstocks. CME was obtained from the NDSU North Central Research Station in Minot, North Dakota. Canola oil was a super degummed variety purchased from Archer Daniel Midlands (ADM) in Velva, North Dakota. Refined soybean oil and SME were purchased from Ag Processing Inc, a cooperative located in the state of Minnesota. Compositional analysis of the CME–SME and canola–soybean oil are given in Table 38.

Several standard mixtures were used for GC identification and quantification of all samples used in this study. The alkane standard was formulated using Protocol Analytical, LLC – TX-HC-18, which contained 18 alkane compounds as listed in Table 39. The fatty acid methyl esters (FAMES) standard was obtained from RESTEK – Food Industry Fame Mix, which consisted of 37 FAME compounds as listed in Table 40.

The alkene, fatty acid, and BTEX (benzene, toluene, ethylbenzene, *o*-xylene, and *p*-xylene) standard mixtures were internally prepared. These mixtures were formulated by mixing individual compounds with a specific carbon number at the same concentration together. The alkene individual compounds included C9, C11, C13, C14, C16, C17, C18, C19, and C23. The fatty acid individual compounds were saturated C4, C5, C6, C7, C8, C9, C10, and C12.

Equipment

All experimental runs were carried out in a 1-L bench-scale thermal cracking reactor (4). Three critical factors were taken into consideration while selecting and designing this reactor: homogeneous heat distribution, minimization of coke formation, and temperature/pressure rating.

Figures 52 and 53 are a schematic and a picture of the thermal cracking apparatus used for the thermal cracking of CME, SME, canola oil, and soybean oil. The system consists of an

Table 38. Key Components of CME/SME and Canola/Soybean Oil

Component	CME, wt%	SME, wt%	Canola Oil	Soybean Oil
Palmitic C16:0	4.3	8	4	12
Stearic C18:0	2.1	4	2	3
Oleic C18:1	62.3	21	60	23
Linoleic C18:2	19.1	60	20	56
Linolenic C18:3	9.2	7	10	6
Eicosenoic C20:1	11.2	0	1.6	0
Erucic C22:1	1.8	0	2.4	0

Table 39. Composition of Alkane Standard

Compound	Carbon Number	Final Concentration, $\mu\text{g/mL}$
Hexane	C6	1000.0
Heptane	C7	1000.0
Octane	C8	1000.0
<i>n</i> -Nonane	C9	1000.0
Decane	C10	1000.0
Undecane	C11	1000.0
Dodecane	C12	1000.0
<i>n</i> -Tridecane	C13	1000.0
<i>n</i> -Tetradecane	C14	1000.0
<i>n</i> -Pentadecane	C15	1000.0
Hexadecane	C16	1000.0
Heptadecane	C17	1000.0
Octadecane	C18	1000.0
Nonadecane	C19	1000.0
Eicosane	C20	1000.0
Pentacosane	C25	1000.0
Octacosane	C28	1000.0
<i>n</i> -Pentatriacontane	C35	1000.0

autoclave reactor, condenser, flash traps, residual drum, vacuum pump, pressure transducer, Fluke Hydra Logger, and computer.

The thermal cracking reactor was made of stainless steel with 14.0-cm (5.5-inch) diameter and 26.7-cm (10.5-inch) height. This 1-L autoclave reactor was rated for a pressure of up to 37,200 kPa (5400 psi) and was compatible with hot-charge reactant injection and the removal of reaction-temperature volatile materials at reaction pressure. The reactor was externally heated by an electrical ceramic heater and was fitted with a magnetic stirrer to provide uniform heat distribution inside during experiments in order to avoid coke formation on the reactor walls.

The reactor contains four ports. One is the sample port at the bottom of the reactor through which heavy cracked oil (residual) was collected after thermal cracking was completed. The other three ports were used for thermocouples (both liquid and vapor), collection of overhead products, and introduction of feedstock/hydrogen. Additionally, careful control of the heating protocol allowed the exploration of various thermal cracking scenarios. A condenser was used to cool down the overhead vapor product (crackate). Also included are two flash traps (300 mL each) in which overheads are collected. All connections were made with 0.32-cm (1/8-inch) or 0.64-cm (1/4-inch) stainless steel tubing (Swagelok).

The thermal cracking system was tested for leaks before use. The parts for testing include the reactor, two flash traps, the condenser, and the residue drum. The first step in the test was isolating the thermal cracking reactor from the flash traps, condenser, and residue drum. Then the autoclave was initially pressurized with nitrogen to approximately 4100 kPa (600 psig) and left for 30 minutes. After 30 minutes, the pressure was measured in the autoclave and compared

Table 40. Composition of FAME Standard

Compound	Carbon Number	Composition, wt%
Methyl Butyrate	C4:0	4.0
Methyl Hexanoate	C6:0	4.0
Methyl Octanoate	C8:0	4.0
Methyl Decanoate	C10:0	4.0
Methyl Undecanoate	C11:0	2.0
Methyl Laurate	C12:0	4.0
Methyl Tridecanoate	C13:0	2.0
Methyl Myristate	C14:0	4.0
Methyl Myristoleate (cis-9)	C14:1	2.0
Methyl Pentadecanoate	C15:0	2.0
Methyl Pentadecenoate (cis-10)	C15:1	2.0
Methyl Palmitate	C16:0	6.0
Methyl Palmitoleate (cis-9)	C16:1	2.0
Methyl Heptadecanoate	C17:0	2.0
Methyl Heptadecanoate (cis-10)	C17:1	2.0
Methyl Stearate	C18:0	4.0
Methyl Elaidate (trans-9)	C18:1	2.0
Methyl Oleate (cis-9)	C18:1	4.0
Methyl Linoelaidate (trans-9, 12)	C18:2	2.0
Methyl Linoleate (cis-9, 12)	C18:2	2.0
Methyl Linolenate (cis-9, 12, 15)	C18:3	2.0
Methyl Gamma-linolenate (cis-6, 9, 12)	C18:3	2.0
Methyl Arachidate	C20:0	4.0
Methyl Eicosenoate (cis-11)	C20:1	2.0
Methyl Eicosadienoate (cis-11, 14)	C20:2	2.0
Methyl Eicosatrienoate (cis-8, 11, 14)	C20:3	4.0
Methyl Eicosatrienoate (cis-11, 14, 17)	C20:3	2.0
Methyl Arachidonate (cis-5, 8, 11, 14)	C20:4	2.0
Methyl Eicosapentaenoate (cis-5, 8, 11, 14, 17)	C20:5	2.0
Methyl Heneicosanoate	C21:0	2.0
Methyl Behenate	C22:0	2.0
Methyl Erucate (cis-13)	C22:1	2.0
Methyl Docosadienoate (cis-13, 16)	C22:2	2.0
Methyl Docosaheptaenoate (cis-4, 7, 10, 13, 16, 19)	C22:6	2.0
Methyl Tricosanoate	C23:0	2.0
Methyl Lignocerate	C24:0	4.0
Methyl Nervonate (cis-15)	C24:1	2.0

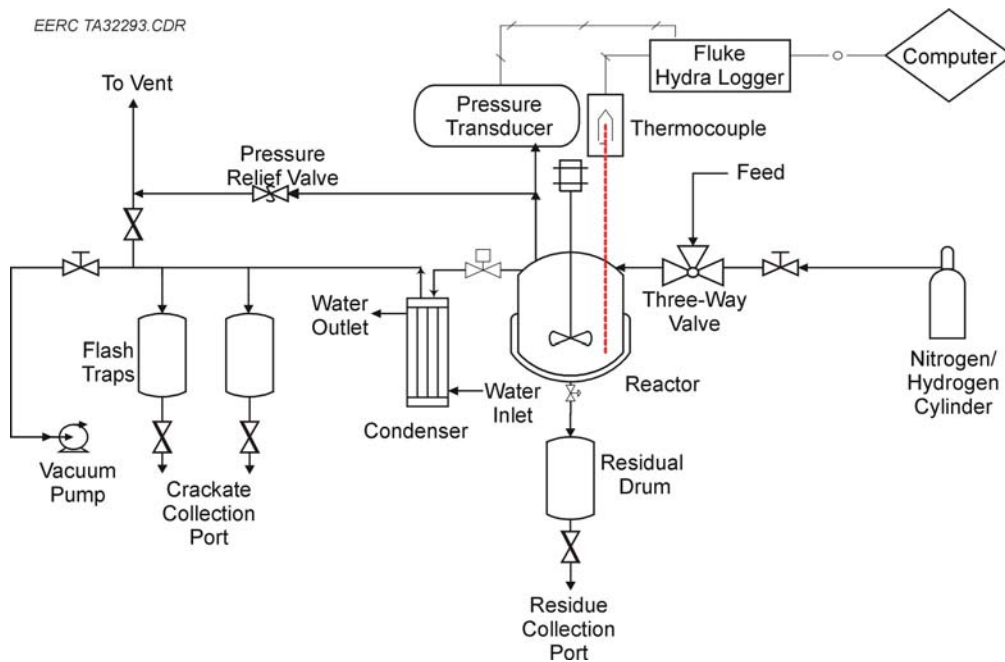


Figure 52. Schematic of thermal cracking apparatus.



Figure 53. Photo of thermal cracking apparatus.

with the initial pressure. If the pressure difference was greater than 10 psig, a leak was assumed to exist.

All of the gas lines and reactor fittings were tested for leaks by allowing nitrogen to flow through the system at high pressures 1400 kPa (approximately 200 psig) and holding it for 5–10 minutes in the system. Soapy water was sprayed on all the joints and fittings to test for leaks.

Sample Characterization Procedure

A biojet fuel was generated by removing the heavy components via separation from the crackates of CME, SME, canola oil, and soybean oil. The separation process was carried out using an Orbis PAM Distillation unit (ASTM D86). In order to more fully comply with JP-8 specification, the distillation cut was set at 300°C. The samples (crackates and distillates) obtained from thermal cracking/distillation units were characterized by their properties and chemical compositions. Three properties measured by analyzer systems were CP, PP, and FP. The compositions of samples were obtained by GC–mass spectrometry (GC–MS) and GC–flame ionization detector (GC–FID).

A ISL CPP 5Gs analyzer (PAC, Houston, TX, USA) was used to measure CP (ASTM D2500) and PP (ASTM D97). Flash point (ASTM D93) tests were conducted by a Setaflash Series 3 FP tester. Samples were analyzed with an Agilent 6890 N GC equipped with a flame ionization detector and an Agilent 7683 series autosampler. A Hewlett-Packard 5890 GC equipped with an MS detector was also used for identification purposes. Data collection and basic analysis were performed by GC Chemsation software.

Two different GC columns and conditions were employed in this study. Column 1 was 30 m long, with 0.25-mm i.d., film thickness of 0.25 μm , and coated with a 5% phenyl-methylpolysiloxane stationary phase film (DB-5, J&W Scientific, town, USA). Column 1 operating conditions were injector temperature at 300°C, 1.0- μL injection volume in splitless mode with splitless time of 0.3 min, detector temperature 320°C, hydrogen as carrier gas, and total flow rate of 68.7 mL/min. The temperature program for Column 1 started at 30°C for 1 min, then ramped at 30°C/min to 80°C, followed by the gradient of 3°C/min to 300°C, and maintained for 5 min.

Column 2 was 100 m long, with 0.25-mm i.d., film thickness of 0.5 μm , and coated with a 100% dimethylpolysiloxane stationary phase film (DB-PETRO, 122-10A6, Agilent Technologies, USA). Column 2 operating conditions were injector temperature at 300°C, 1.0- μL injection volume in splitless mode with splitless time of 0.3 min, detector temperature 325°C, hydrogen as carrier gas, and linear flow rate of 2.3 mL/min. The temperature program for Column 2 started at 35°C for 1 min, then ramped at 30°C/min to 90°C with 5 min hold, followed by the gradient of 4°C/min to 320°C, and maintained for 10 min.

O-terphenyl (C₁₈H₁₄) was used as an internal standard. An internal standard stock solution of methylene chloride (CH₂Cl₂) with a known amount of o-terphenyl was prepared prior to sample preparation and used for analysis in this study. Samples were prepared for the analysis by adding approximately 100 mg of crackates to 10 mL of methylene chloride and then by

mixing 0.8 mL of this mixture with 0.8 mL of the internal standard stock solution. The mixture was then injected into the GC injection port. One μL of the sample was injected into the column. The alkane (C6–C35), alkene (C9–C23), BTEX, FAs (C4–C12), and FAME (C4–C24) standards were used as standard samples to determine the retention times of alkanes, alkenes, BTEX, FAs, and FAMEs. The method of preparation of the samples and standard samples were the same for all samples of cracked soybean/canola oil and SME/CME.

Results and Discussion

A series of experimental runs and tests were conducted to optimize the operating conditions to produce biojet fuel from canola oil or CME. In this study, multiple predicted variables including yield, CP, PP, FP, and chemical compositions were used to determine these optimal operating conditions. In order to use biojet fuel as a substitution for JP-8, the properties of biojet fuel must mostly meet JP-8 specifications. Performance specifications of JP-8 used in this study were boiling point (500°F, 260°C), FP (41°C), CP (–47°C), and PP (–50°C).

Experimental Design

In the bench-scale thermal cracking unit, six major variables (i.e., reaction conditions, also called factors) were considered which could affect the yield, CP, PP, and chemical compositions (i.e., predicted variables, also called responses) of the product. Thus it was decided to determine which of these factors were significant in the formation of the product. As the six factors would require 64 runs for a full-factorial design, or 32 for a half-factorial design, a twelve-run Plackett–Burman design was employed, as shown in Table 41.

The “+” stands for one setting of a factor (the high-level setting if the factor is quantitative) and the “–” stands for another setting of the factor (the low-level setting if the factor is quantitative). Each of the rows corresponds to a set of experimental conditions that were run. Any number of responses can be measured in each experiment. At the end of the experimental program, each response was analyzed separately. The 12 experimental runs were also done in random order so that no “order” bias would be introduced.

A Plackett–Burman design is an economical design with the run numbers (n) a multiple of 4 rather than a power of 2. When only the main effects are of interest, as in this study, it is an extremely efficient design. However, in a Plackett–Burman design, main effects are, in general, heavily confounded with 2-factor interactions. In order to use the Plackett–Burman design, all interactions must be assumed to be negligible (18).

The six factors considered in thermal cracking were reaction temperature, initial pressure, heating rate, residence time, amount of feedstock, and stirring rate. Tables 42 and 43 show the factors and the levels studied. For canola oil, when cracking at a reaction temperature of 440°C and/or residence time of 30 min, the thermal cracking unit was frequently blocked because of canola’s higher viscosity than CME. Therefore, the range of these 2 factors was selected differently for canola oil than for CME.

Optimization results are presented in Tables 44 and 45. Because the probe of the ISL CPP 5Gs analyzer (testing for CP and PP) was broken during the study, tests for CP and PP of canola

Table 41. Design of Experimental Matrix for Thermal Cracking Optimization

Random No.	Run No.	Assigned						Unassigned				
		A X ₁	B X ₂	C X ₃	D X ₄	E X ₅	F X ₆	X ₇	X ₈	X ₉	X ₁₀	X ₁₁
9	1	+	+	-	+	+	+	-	-	-	+	-
11	2	+	-	+	+	+	-	-	-	+	-	+
4	3	-	+	+	+	-	-	-	+	-	+	+
2	4	+	+	+	-	-	-	+	-	+	+	-
6	5	+	+	-	-	-	+	-	+	+	-	+
12	6	+	-	-	-	+	-	+	+		+	+
3	7	-	-	-	+	-	+	+	-	+	+	+
8	8	-	-	+	-	+	+	-	+	+	+	-
10	9	-	+	-	+	+	-	+	+	+	-	-
5	10	+	-	+	+	-	+	+	+	-	-	-
7	11	-	+	+	-	+	+	+	-	-	-	+
1	12	-	-	-	-	-	-	-	-	-	-	-

Table 42. Parameters in Experimental Matrix for the Cracking of CME

Factor	Definition	Label	Range of Factors	
			Low Level (-)	High Level (+)
A	Reaction Temperature, °C	X1	430	440
B	Heating Rate, °C/min	X2	1	2
C	Stirring Rate, rpm	X3	192	395
D	Amount of Feedstock, g	X4	180	260
E	Initial Pressure, kPa	X5	-420	2200
F	Residence Time, min	X6	20	30

Table 43. Parameters in Experimental Matrix for the Cracking of Canola Oil

Factor	Definition	Label	Range of Factors	
			Low Level (-)	High Level (+)
A	Reaction Temperature, °C	X1	420	430
B	Heating Rate, °C/min	X2	1	2
C	Stirring Rate, rpm	X3	192	395
D	Amount of Feedstock, g	X4	180	260
E	Initial Pressure, kPa	X5	-420	2200
F	Residence Time, min	X6	20	20

oil could not be done after each experimental run until 1 month later. Three tested CME crackates were analyzed again for calibration purposes for the analyzer, and the results were almost the same as before. However, for most canola oil crackates, CP and PP could not be found by the analyzer. Although CP of two canola oil crackates was found, which were -1° and -4°C , the results were suspicious. Repeating the whole 12 runs of canola oil cracking was not possible. Thus only three runs were replicated, and the results are listed in Table 45. The cause of

Table 44. Results from Experimental Matrix Tests for the Cracking of CME

Run No.	Random Order	Label No.	Project No.	Yield, %	CP, °C	PP, °C
1	9	Y35-1	Bio No. 54	80.23	-21	-23
2	11	Y37-1	Bio No.56	85.61	-18	-20
3	4	Y30-1	Bio No.49	83.85	-14	-17
4	2	Y67-1	Bio No.84	82.06	-19	-23
5	6	Y32-1	Bio No.51	79.89	-23	-29
6	12	Y38-1	Bio No.57	73.74	-19	-20
7	3	Y29-1	Bio No.48	75.10	-17	-20
8	8	Y34-1	Bio No.53	79.89	-13	-14
9	10	Y68-1	Bio No.85	72.24	-8	-14
10	5	Y27-1	Bio No.46	83.80	-21	-26
11	7	Y33-1	Bio No.52	82.97	-13	-14
12	1	Y66-1	Bio No.83	71.30	-15	-16

Table 45. Results from Experimental Matrix Tests for the Cracking of Canola Oil

Run No.	Random Order	Label No.	Project No.	Yield, %	CP, °C	PP, °C
1	9	Y52-1	Bio No.70	63.12	-	-
2	11	Y53-1	Bio No.71	69.92	-	-
3	4	Y48-1	Bio No.66	59.70	-1	-
4	2	Y47-1	Bio No.65	67.60	-17	-
5	6	Y49-1	Bio No.67	62.78	-17	-
6	12	Y75-1	Bio No.88	67.20	-26	-34
7	3	Y44-1	Bio No.62	61.36	-4	-
8	8	Y57-1	Bio No.75	55.56	-	-
9	10	Y58-1	Bio No.76	47.71	-	-
10	5	Y73-1	Bio No.86	70.70	-15	-31
11	7	Y55-1	Bio No.73	59.78	-	-
12	1	Y74-1	Bio No.87	54.90	-18	-28

this phenomenon might be the formation changes in the canola oil crackates due to the existence of gum, glycerol, or polymer. Stability issues for products generated from canola oil might be an area for future study.

Statistical Analysis

In order to determine which factors are important, data analysis was performed which means which factors had the greatest impact on yield, CP, and PP, respectively, when factors were changed. To calculate the effect of any factor, the average of the results at the low level of that factor was subtracted from the average of the results at the high level of the same factor. In this work, effects were calculated per the following equation:

$$E_{x_i} = \frac{1}{6} \times [\sum (+) - \sum (-)]$$

The calculated effects of the unassigned factors were used to estimate the standard deviation of the effects.

$$s_E = \sqrt{\frac{1}{M}(E_{X_7}^2 + E_{X_8}^2 + E_{X_9}^2 + E_{X_{10}}^2 + E_{X_{11}}^2)}$$

where E_{X_7} is the average effect for column X_7 , etc., and M is the number of unassigned factors used to assess experimental error.

The statistical significance of each effect and interaction is judged by comparing its t value (without negative sign) to the tabulated critical t value (also called Student's t). If the t value of an effect exceeds the critical t value, the effect is statistically significant, and the factor is important. The critical t value is based on the appropriate confidence level and the M degrees of freedom. In this case, degrees of freedom used was 5, and the critical t value was 2.571 at the 95% confidence level.

For thermal cracking of CME, the results indicate that reaction temperature had the greatest impact on all responses (yield, CP, and PP). The higher reaction temperature resulted in higher yield and better cold-flow properties of crackates. Hydrogen, feedstock quantity, and heating rate did not play an important role on these responses. Better cold-flow properties were obtained under vacuum conditions and/or a longer residence time. The stirring rate had a positive impact on yield and PP.

For thermal cracking of canola oil, the results show that reaction temperature was the only factor having significant effect on the yield of crackates. Because of the lack of CP and PP data, calculation of effects for CP and PP could not be performed.

Separation to Biojet Fuel

A distillation column was used to separate light components (biojet fuel) from heavier ones in the crackates in order to achieve JP-8 cold-flow specifications. The distillation cut was 300°C. Tables 46 and 47 present results of the biojet fuels.

The results indicate that the optimal results determined in the cracking study are the overall optimal after separation is considered. The higher reaction temperature of cracking gave a higher yield and better cold-flow properties of biojet fuel. In general, nearly 57% of biojet fuel could be obtained by CME process (cracking and distillation), while 47% of biojet fuel was generated from canola oil. If the differences of variable levels for CME and canola oil are taken into account, the yield of biojet fuel can be conservatively estimated as 50% of feedstocks for a single reactor, single separation process.

The CP and PP were greatly improved after the separation process. CP, PP, and FP of the biojet fuel were comparable to those in JP-8 specifications. The biojet fuel from the CME process gave better results than that from the canola oil process. It is believed if we manipulate the temperature of the distillation cut, further-improved CP, PP, and FP can be obtained for biojet fuels.

Table 46. Cold-Flow Properties of Biojet Fuel Produced from CME

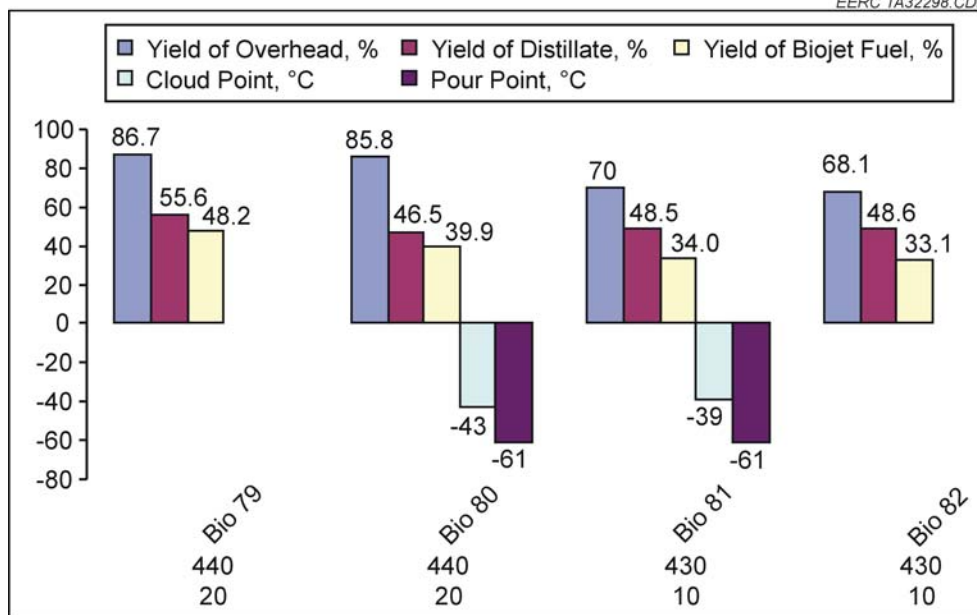
GC Label No.	Y20-1	Y35-1	Y27-1	Y39-1	Y29-1
Project No.	Bio No. 84	Bio No. 54	Bio No. 46	Bio No. 56	Bio No. 48
Temperature, °C	440	440	440	440	430
Heating Rate, °C/min	2	2	1	1	1
Residence Time, min	20	30	30	20	30
Stirring Rate, rpm	395	192	395	395	192
Amount of Feedstock, g	180	260	260	260	260
Initial Pressure, kPa	-420	2200	-420	2200	-420
Yield of Overhead, %	82.1	80.2	83.8	85.6	75.1
CP, °C	-21	-21	-21	-17	-17
PP, °C	-23	-26	-26	-17	-20
Yield of Distillate, %	71.2	67.5	67.5	64.2	62.8
Yield of Biojet Fuel, %	58.5	56.6	56.6	55.0	47.2
CP, °C	-38	-38	-39	-37	-36
PP, °C	-62	-62	-60	-62	-56
FP, °C	68	68	53	>80	58

Table 47. Cold-Flow Properties of Biojet Fuel Produced from Canola Oil

GC Label No.	Y50-1	Y53-1	Y52-1	Y44-1	Y58-1
Project No.	Bio No. 86	Bio No. 71	Bio No. 70	Bio No. 62	Bio No. 76
Temperature, °C	430	430	430	420	420
Heating Rate, °C/min	1	1	2	1	2
Residence Time, min	20	10	20	20	10
Stirring Rate, rpm	395	395	192	192	192
Amount of Feedstock, g	260	260	260	260	260
Initial Pressure, kPa	-420	2200	2200	-420	2200
Yield of Overhead, %	70.7	69.9	63.1	61.4	47.7
CP, °C	-15	-25	-18	-17	-
PP, °C	-31	-33	30	-28	-
Yield of Distillate, %	67.4	66.2	72.3	69	70.5
Yield of Biojet Fuel, %	47.7	46.3	45.6	42.4	33.6
CP, °C	-36	-36	-36	-33	-21
PP, °C	-43	-41	-43	-40	-32
FP, °C	34	44	40	42	36

Soybean Oil/SME

A study was performed to determine the optimal conditions for thermal cracking of soybean oil or SME in a 1-liter batch reactor. Figure 54 shows the results of cracking and distillation for SME and soybean oil.



T: Reaction Temperature, °C; SR: stirring rate, rpm.

Figure 54. The generation of biojet fuel from soybean oil and SME. Bio Nos. 79 and 80 are from SME feedstock, while Bio Nos. 81 and 82 are from soybean oil feedstock.

GC Characterization Results

MS identification and GC-FID quantification were used to define the chemical compositions of the samples (crackates or biojet fuels). Each sample included identified and unidentified components. The unidentified components are composed of small amounts of hundreds of hydrocarbons that cannot be analytically separated well enough to be identified by GC.

For thermal cracking and distillation from SME, the results from GC analysis are presented in Table 48. Identified compounds account for approximately 67% of the mass of both crackates and biojet fuels. The other 33% is unidentified components. Of the total mass of identified compounds of crackates, about 18% were alkanes (17% C7–C15), 2.5% BTEX, 1.2% dimer fatty methyl esters (DFMEs), 75% saturated FAMES (53% C4–C15), and 3.3% unsaturated C18 FAMES. Of the total mass of the identified compounds in the final biojet fuel sample, around 24% were alkanes (almost all C7–C15), 5% BTEX, 70% saturated FAs (67% C4–C15), and 1% alkenes.

For thermal cracking and distillation from soybean oil, the results are listed in Table 49. Identified compounds account for approximately 55% of the mass of crackates and 65% of the mass of biojet fuels. The other 45% of crackates and 35% of biojet fuel are unidentified components. Of the total mass of identified compounds of crackates, around 45% were alkanes (38% C7–C15 for crackates and 47% C4–C15 for biojet fuel), 3% BTEX, and 48% saturated FAs (47% C4–C15 for crackates and 49% C4–C15 for biojet fuel).

Table 48. The Composition of Crackates and Final Biojet Fuel Samples Generated from SME

GC Label No. Project No.	Y61-1 Bio No. 79	Y62-1 Bio No. 80	DY61-1	DY62-1
Alkanes C7–C15	11.2	11.5	15.9	15.4
Total Alkanes	12.2	12.3	16.1	15.5
Saturated FAMES C4–C15	34.9	36.2	43.8	44.3
Saturated FAMES C16–C24	14.6	13.5	2.7	1.6
Unsaturated FAMES C18:x (x = 1, 2, 3)	49.5	49.7	46.5	45.9
Total Saturated FAMES	3.4	2.8	–	–
Total of Alkenes	0.0	0.0	0.3	0.5
Total of BTEX	1.7	1.9	2.9	3.0
Total of DFMEs	0.7	0.8	–	–
Unidentified	32.5	32.5	34.1	35.1

Table 49. The Composition of Crackates and Final Biojet Fuel Samples Generated from Soybean Oil

GC Label No. Project No	Y64-1 Bio No. 81	Y65-1 Bio No. 82	DY64-1	DY65-1
Alkanes C7–C15	18.9	22.0	25.7	29.1
Total Alkanes	23.2	25.8	27.8	30.6
Saturated FAs C4–C15	25.6	25.1	33.9	32.3
Saturated FAs C16–C24	3.2	2.1	0.3	0.3
Total Saturated FAs	28.8	27.2	34.2	32.7
Unsaturated FAMES C18:x (x = 1, 2, 3)	0.1	0.0	0.0	0.0
Total of Alkenes	0.0	0.0	1.1	0.8
Total of BTEX	1.5	1.9	1.1	2.0
Unidentified	46.5	45.1	35.8	33.9

For the analysis of crackates and biojet fuel from canola oil and CME, two separate GC columns were used. GC analysis using Column 1 was only performed on samples of crackates produced from CME under vacuum conditions. These are shown in Table 50. Identified compounds in Table 50 account for approximately 55% of the mass of the crackates. The other 45% is unidentified components. Of the total identified compounds, there were about 22.5% alkanes (20% C7–C15), 1.5% alkenes, 3.6% BTEX, 61.4% saturated FAMES (56% C4–C15), and 11% unsaturated FAMES (6.8% C16–C22).

The chemical compositions of crackates generated from CME and analyzed using Column 2 are listed in Table 51. Identified compounds account for approximately 60% of the mass of the crackates. The other 40% is unidentified components. Of the total identified compounds of crackates, there were about 22% alkanes (20.5% C7–C15), 2% alkenes, 3% BTEX, 3% DFMEs, 60% saturated FAMES (48% C4–C15), and 10% unsaturated FAMES C16–

Table 50. Results and GC Analysis of CME Crackates Using Column 1

GC Label No.	Y16-1	Y17-1	Y18-1	Y19-1	Y20-1	Y22-1	Y15-1
	Bio	Bio	Bio	Bio	Bio	Bio	
Project No.	No. 40	No. 41	No. 42	No. 43	No. 44	No. 45	CME
Temperature, °C	440	440	430	440	440	430	
Heating Rate, °C/min	2	1	4	2	1	1	
Residence Time, min	30	30	20	20	20	20	
Stirring Rate, rpm	192	395	192	192	395	395	
Amount of Feedstock, g	260	180	180	260	180	260	
Initial Pressure, kPa	w/o H ₂	w/o H ₂	w/o H ₂	w/o H ₂	w/o H ₂	w/o H ₂	
Yield of Overhead, %	79.5	84.4	59.8	72.4	82.3	80.1	
CP, °C	-23	-21	-15	-21	-19	-13	-2
PP, °C	-25	-30	-16	-23	-23	-15	-10
Alkanes C7–C15	11.9	11.8	5.6	9.6	11.5	6.7	0.0
Total Alkanes	12.8	12.8	6.2	10.4	12.4	7.3	0.0
Saturated FAMES C4–C15	30.4	29.0	22.4	28.8	30.6	24.0	0.1
Saturated FAMES C16–C24	3.2	6.0	4.7	3.8	4.3	6.1	7.5
Total Saturated FAMES	33.6	35.0	27.1	32.6	34.9	30.1	7.7
Unsaturated FAMES C4–C15	2.0	2.3	5.6	2.8	2.4	3.5	0.0
Unsaturated FAMES C16–C22	3.5	3.5	14.1	5.8	4.8	11.6	89.6
Unsaturated FAMES C18:x (x = 1, 2, 3)	3.5	3.5	14.1	5.8	4.8	11.6	89.6
Total Unsaturated FAMES	5.6	5.8	19.7	8.7	7.2	15.0	89.6
Total FAMES	39.2	40.9	46.8	41.3	42.1	45.1	97.3
Total of Alkenes	0.8	1.1	2.7	1.1	0.4	0.7	0.0
Total of BTEX	2.1	2.1	0.6	1.5	2.0	0.8	0.0
Unidentified	45.1	43.1	43.8	45.7	43.2	46.1	2.7

Table 51. Results and GC Analysis of CME Crackates Using Column 2

GC Label No.	Y20-1	Y35-1	Y27-1	Y39-1	Y29-1
	Bio No. 84	Bio No. 54	Bio No. 46	Bio No. 56	Bio No. 48
Temperature, °C	440	440	440	440	430
Heating Rate, °C/min	2	2	1	1	1
Residence Time, min	20	30	30	20	30
Stirring Rate, rpm	395	192	395	395	192
Amount of Feedstock, g	180	260	260	260	260
Initial Pressure, kPa	-420	2200	-420	2200	-420
Alkanes C7–C15	12.3	12.8	13.0	12.4	10.1
Total Alkanes	13.1	13.5	13.4	13.1	10.8
Saturated FAMES C4–C15	29.9	29.6	30.1	28.8	28.5
Saturated FAMES C16–C24	8.1	6.9	6.8	7.6	9.8
Total Saturated FAMES	38.0	36.4	36.9	36.4	38.3
Unsaturated FAMES C16–C22	6.4	4.5	4.9	5.7	9.1
Unsaturated FAMES C18:x (x = 1, 2, 3)	6.1	4.2	4.7	5.4	8.6
Total of Alkenes	1.4	1.3	1.5	1.2	1.6
Total of BTEX	1.7	1.9	1.9	1.7	1.3
Total of DFMEs	2.9	2.3	3.0	2.2	4.0
Unidentified	36.4	40.1	38.4	39.7	35.0

C22. Comparing these GC analysis results to those in Table 50, the chemical compositions are equivalent for each component, except DFME composition and saturated C4–C15 FAMES. The anticipated advantage of using Column 2, better resolution of unidentified compounds, did not appear as expected in this study. On the contrary, the retention time for alkanes and FAMES were too close to each other; thus the chromatograms were not shown well, and the identification became more difficult.

Table 52 shows the composition of biojet fuels generated from CME. Identified compounds account for approximately 60% of the mass of the biojet fuel. The other 40% is unidentified components. Of the total identified compounds of biojet fuels, there were about 26.5% alkanes (25.4% C7–C15), 2.8% alkenes, 3.7% BTEX, 3.5% DFMEs, 61.5% saturated FAMES (58% C4–C15), and 2% unsaturated FAMES (C16–C22). The heavy components were removed by the separation process, especially saturated and unsaturated C16–C22 FAMES, which might be CME uncracked during the cracking process.

The chemical compositions of crackates generated from canola oil are presented in Table 53. Identified compounds account for approximately 55% of the mass of the biojet fuel. The other 45% is unidentified components. Of the total identified compounds of crackates, there were about 32% alkanes (27% C7–C15), 2.3% alkenes, 2.7% BTEX, and 63% saturated FAs. Apparently, crackates generated from canola oil yield more desired alkanes than from CME. This is because components removed by the transesterification process can also be cracked into small molecular compounds like alkanes by thermal cracking. Therefore, using canola oil to generate biojet fuel might be more economical than using CME because the transesterification process can be eliminated.

Table 54 shows the chemical compositions of biojet fuels generated from canola oil. Identified compounds account for approximately 64% of the mass of the biojet fuel. The other 36% is unidentified components. Of the total identified components of biojet fuels, there were about 33% alkanes (30% C7–C15), 2.4% alkenes, 3.6% BTEX, and 61% saturated FAs.

The results from the GC analysis confirmed that reaction temperature was the most important variable in biojet fuel generation. The alkanes and desired C7–C15 yield increased as the cracking temperature was raised from 430° to 440°C. Hydrogen did not impact the yield of alkanes and the desired C7–C15. Canola oil and CME crackates have a higher concentration of alkane compounds present in them compared to soybean oil and SME at the same cracking conditions. This is because of their difference in fatty acid/ester profile. It is believed since the canola oil and CME consist of 60%–63% oleic acid–ester (one double bond), it facilitates the production of alkanes in thermal cracking.

CME and SME produce higher yields compared to canola oil and soybean oil. However, the yield of alkane and C7–C15 are higher from canola oil and soybean oil than CME and SME. It is believed that components, which were not removed by the transesterification process, facilitated the formation of alkane and C7–C15 in thermal cracking. Distillation was used to remove heavy compounds from the crackates so that biojet fuel more comparable to JP-8 specifications was produced.

Table 52. Results and GC Analysis of CME Biojet Fuel Using Column 2

GC Label No.	DY20-1	DY35-1	DY27-1	DY39-1	DY29-1
Alkanes C7–C15	15.0	15.4	15.1	15.2	13.5
Total Alkanes	15.5	15.8	15.5	15.6	14.1
Saturated FAMES C4–C15	34.5	34.7	33.9	34.3	36.3
Saturated FAMES C16–C24	2.1	1.8	1.8	2.1	2.7
Total Saturated FAMES	36.6	36.5	35.6	36.4	39.0
Unsaturated FAMES C16–C22	1.6	1.1	1.1	0.8	2.0
Unsaturated FAMES C18:x (x = 1, 2, 3)	1.5	1.1	1.1	0.8	2.0
Total of Alkenes	1.7	1.6	1.7	1.5	2.1
Total of BTEX	2.2	2.3	2.3	2.1	1.7
Total of DFMEs	2.1	1.6	2.1	1.6	3.0
Unidentified	40.4	41.1	41.7	42.1	38.1

Table 53. Results and GC Analysis of Canola Oil Using Crackates Using Column 2

GC Label No.	Y50-1	Y53-1	Y52-1	Y44-1	Y58-1
Project No.	Bio No. 86	Bio No. 71	Bio No. 70	Bio No. 62	Bio No. 76
Temperature, °C	430	430	430	420	420
Heating Rate, °C/min	1	1	2	1	2
Residence Time, min	20	10	20	20	10
Stirring Rate, rpm	395	395	192	192	192
Amount of Feedstock, g	260	260	260	260	260
Initial Pressure, kPa	–420	2200	2200	–420	2200
Alkanes C7–C15	21.6	16.0	14.1	17.1	11.4
Total Alkanes	25.3	18.8	16.3	20.5	13.3
Saturated FAs C4–C15	28.7	37.1	35.5	33.2	42.5
Total of Alkenes	1.2	1.3	1.4	1.2	1.4
Total of BTEX	1.7	1.5	1.5	1.4	1.2
Unidentified	43.1	41.3	45.2	43.8	41.4

Table 54. Results and GC Analysis of Canola Oil Biojet Fuel Using Column 2

GC Label No.	DY50-1	DY53-1	DY52-1	DY44-1	DY58-1
Alkanes C7–C15	23.4	18.6	19.4	19.2	36.0
Total Alkanes	25.7	20.7	21.5	21.9	36.0
Saturated FAs C4–C15	31.3	40.5	38.8	36.2	11.3
Total of Alkenes	1.3	1.5	1.9	1.4	6.6
Total of BTEX	1.9	1.8	2.1	1.5	4.5
Unidentified	39.8	35.6	35.9	38.9	41.5

Conclusions

1. A high yield (50% for a single-pass reaction/single-pass separation and around 86% with recycle) of biojet fuel can be obtained that meets the required CP, PP, and FPs analogous to

those in JP-8 specifications. The biojet fuel consists of approximately 15% alkanes, 2% alkenes, 2% BTEX, and 34% C4–C15 saturated fatty compounds.

2. The optimal operating conditions for cracking in a 1-L bench-scale cracking reactor are stirring rate at 395 rpm, heating rate at 1°–2°C/min, initial pressure under vacuum, reaction temperature at 440°C for SME and 430°C for soybean oil, and residence time at 20–30 minutes for SME and 10–20 minutes for soybean oil. The distillation cut point of 300°C is optimal.
3. Hydrogen does not play an important role in the cracking process and formation of products but helps minimize polymerization, especially for oil as a feedstock.
4. A higher yield of crackates can be obtained from biodiesel than its feedstock oil, but the quality (defined as percentage of C4–C15 content) is less from biodiesel than its feedstock oil.
5. Canola oil and CME crackates have a higher concentration of alkane compounds present in them compared to soybean oil and SME produced at the same cracking conditions.
6. Reaction temperature is the most important variable for the yield and quality of biojet fuel generation. A higher reaction temperature of cracking near the feedstock's boiling point results in a higher yield and better cold-flow properties of crackates.

References

1. Aksoy, H.A.; Becerik, I.; Karaosmanoglu, F.; Yatmaz, H.C.; Civelekoglu, H. Utilization Prospects of Turkish Raisin Seed Oil as an Alternative Engine Fuel. *Fuel* **1990**, 69, 600–603.
2. Larson, V. Emission Analysis of Biodiesel in a Commercial Aircraft Engine. Master's Thesis, University of North Dakota, 2004.
3. Dunn, R.O. Alternative Jet Fuels from Vegetable Oils. *American Society of Agricultural Engineers* (ISSN 0001-2351) **2001**, 44 (6), 1751–1757.
4. Ahmed, I. Cold-Flow Biojet Fuel from Soybean Oil. Master's Thesis, University of North Dakota, 2005.
5. Duffield, J.; Shapouri, H.; Graboski, M.; McCormick, R.; Wilson R. U.S. Biodiesel Development: New Markets for Conventional and Genetically Modified Agricultural Fats and Oils. 1998, <http://usda.mannlib.cornell.edu/usda/reports/general/aer/aer770.pdf> (accessed May 20, 2006).
6. EPA. <http://yosemite.epa.gov/oar/globalwarming.nsf/content/climate.html> (accessed June 20, 2006).

7. Ma, F.; Hanna, M.A. Biodiesel Production: A Review. *Bioresource Technology* **1999**, *70*, 1–15.
8. Srivastava, A.; Prasad, R. Triglycerides-Based Diesel Fuels. *Renewable & Sustainable Energy Reviews* **1999**, *4*, 111–133.
9. Chiu, C.W.; Schumacher, L.G.; Suppes, G.J. Impact of Cold-Flow Improvers on Soybean Biodiesel Blend. *Biomass & Bioenergy* **2004**, *27*, 485–491.
10. Knothe, G.; Dunn, R.O.; Bagby, M.O. Biodiesel: The Use of Vegetable Oils and Their Derivatives as Alternative Diesel Fuels. <http://journeytoforever.org/biofuellibrary/VegetableOilsKnothe.pdf> (accessed June 14, 2006).
11. Lang, X.; Dalai, A.K.; Bakhshi, N.N.; Reaney, M.J.; Hertz, P.B. Preparation and Characterization of Bio-Diesels from Various Bio-Oils. *Bioresource Technology* **2001**, *80*, 53–62.
12. Arkoudeas, P.; Kalligeros, S.; Zannikos, F.; Anastopoulos, G.; Karonis, D.; Korres, D.; Lois, E. Study of Using JP-8 Aviation Fuel and Biodiesel in CI Engines. *Energy Conversion & Management* **2003**, *44*, 1013–1025.
13. Ritchie, G.D.; Bekkedal, M.Y.V.; Bobb, A.J.; Still, K.R. Biological and Health Effects of JP-8 Exposure. U.S. Army Petroleum Center, <http://usapc.army.mil/miscellaneous/JP-8HazardsStudy.doc> (accessed June 4, 2006).
14. Dietzel, K.D.; Campbell, J.L.; Bartlett, M.G.; Witten, M.L.; Fisher, J.W. Validation of a Gas Chromatography/Mass Spectrometry Method for the Quantification of Aerosolized Jet Propellant 8. *Journal of Chromatography A* **2005**, *1093*, 11–20.
15. Petroleum HPV Testing Group. www.petroleumhvp.org/Product_Categories/Kerosene&Jet-Fuel/jetfuel_robsumm_final_123103.pdf (accessed July 1, 2006).
16. <http://vegburner.co.uk> (accessed July 1, 2006).
17. Knothe, G. Dependence of Biodiesel Fuel Properties on the Structure of Fatty Acid Alkyl Esters. *Fuel Processing Technology* **2005**, *86*, 1059–1070.
18. Lawson, J.; Erjavec J. *Modern Statistics for Engineering and Quality Improvement*. Wadsworth Group, 2001; pp 421–431.

YEAR 2005 – ACTIVITY 7 – UREA FERTILIZER PRODUCTION FROM ETHANOL COPRODUCT CARBON DIOXIDE

Introduction

Urea is the most widely produced nitrogen-based fertilizer. The commercial production of urea is based on the reaction of carbon dioxide and ammonia at high pressure and high temperature to form ammonium carbamate, which in turn is dehydrated into urea and water, with the ammonia feedstock produced via a well-known heterogeneous reaction of nitrogen and hydrogen on an iron-based catalyst at high pressure and high temperature (Haber process) (1). However, low conversion efficiency (~10%–15%) of hydrogen gas and nitrogen gas to ammonia gives rise to cost-intensive, large-scale chemical plants and to costly operating conditions in order to produce commercially viable hundreds to thousands of tons per day of ammonia in an ammonia synthesis plant.

Therefore, it is of industrial interest to develop a one-step urea production process which can be operated at decreased temperature and pressure. Only recently has the feasibility of using electrochemical processes for urea synthesis been investigated. Shibata et al. published a series of articles that disclosed electrochemical synthesis of urea at ambient temperature and atmospheric pressure by utilizing carbon dioxide, nitrate or nitrite, and hydrogen (2, 3). Several challenges exist, however, for industrial consideration of the reported electrochemical process for the preparation of urea. The biggest challenge is the high cost of the nitrogen source, as both nitrite and nitrate are typically employed.

Both carbon dioxide and nitrogen oxide are main components of greenhouse gases. Corn-based ethanol plant coproduct CO₂ represents approximately 30% by weight (and cost) of the feedstock cost input to the ethanol process. As more and more ethanol plants come online, increasing amounts of clean CO₂ are generated and emitted into the atmosphere. Therefore, a low-temperature and low-pressure electrochemical process that can utilize CO₂ as the carbon source and nitrogen from NO_x emissions of a power plant or separated N₂ from the air as the nitrogen source to produce urea is of academic and industrial importance in terms of the control of greenhouse gases and the innovation of the urea process. As envisioned on a commercial scale, the urea production route comprises 1) CO₂ recovery from an ethanol plant, 2) nitrogen oxide extraction from coal-fired utility boiler emissions, 3) hydrogen production, and 4) the simultaneous reduction of CO₂ and nitrogen oxides to generate urea. To ensure optimal economics and renewability, Steps 3 and 4 of the process would be driven by wind-generated electricity. Since the electrochemical process is compatible with operation on intermittent electrical power, it represents a high potential-viability method for deriving value from remote wind energy resources without the need for expanding expensive and hard-to-permit transmission capacity.

The proposed work was for the EERC to investigate a low-temperature and low-pressure electrochemical urea process by utilizing ethanol coproduct CO₂ as the carbon source, nitric oxide (NO) extracted from flue gases as the nitrogen source, and hydrogen gas as the hydrogen source.

Goals and Objectives

The overall goals and objectives of the proposed research were to optimize an electrochemical process that utilizes wind-generated electricity, ethanol plant-generated CO₂, NO recovered from coal-fired utility boiler emissions, and hydrogen (ideally produced via wind-powered water electrolysis, biomass gasification, or other renewable technology) to produce urea. Specific objectives included:

- Optimizing the electrochemical urea production process via evaluation of process inputs and conditions, including catalysts, reaction media, and reactant form.
- Identifying technical and economic challenges associated with the urea process and developing strategies to overcome the challenges.
- Evaluating the commercial potential of the process.

Experimental

Electrolysis Cell and Electrolysis

Preparative electrolysis was performed in an electrolytic cell (shown in Figure 55 with numbered chambers), which comprises two gas chambers (Nos. 3, 12) and one liquid chamber (Nos. 7). Two E-TEK[®] gas diffusion electrodes (Nos. 4, 11) were used to separate the liquid chamber and gas chambers. A range of transition metals, alloys, and metal phthalocyanines were studied as the cathode catalysts by depositing their inks onto the gas diffusion electrodes, while 10 wt% carbon-supported platinum (E-TEK) was used as the anode catalyst for the oxidation of hydrogen. Aqueous electrolyte of 100 mL was pumped through the electrolysis cell at 5 mL/min using a liquid pump. The mixture of CO₂ and NO at an appropriate ratio was fed to the cathode gas chamber at controlled flow rates while high-purity H₂ was fed to the anode chamber at 60 sccm (standard cubic centimeters/minute). During electrolysis, reaction currents or potentials were controlled using a potentiostat/galvanostat (Princeton Applied Research). In a constant potential mode, a solid Ag/AgCl electrode was used as the reference electrode. Steady-state polarization curves were measured at 5 mVs⁻¹ using the above-mentioned potentiostat/galvanostat.

Analysis of Products

The moles (M_{ammonia}) of ammonia produced during the electrolysis were determined using an ammonium-selective electrode (Cole-Parmer Instrument Company). Urea, (NH₂)₂CO, was decomposed by urease into CO₂ and two ammonia molecules. After the decomposition, the total moles (M_{urease}) of ammonia in the electrolyte were measured by the ammonia electrode and shown as $2M_{\text{urea}} + M_{\text{ammonia}}$, where $2M_{\text{urea}}$ represents the moles of ammonia coming from the decomposition. Therefore, the moles of urea (M_{urea}) produced were calculated by $(M_{\text{urea}} - M_{\text{ammonia}})/2$.

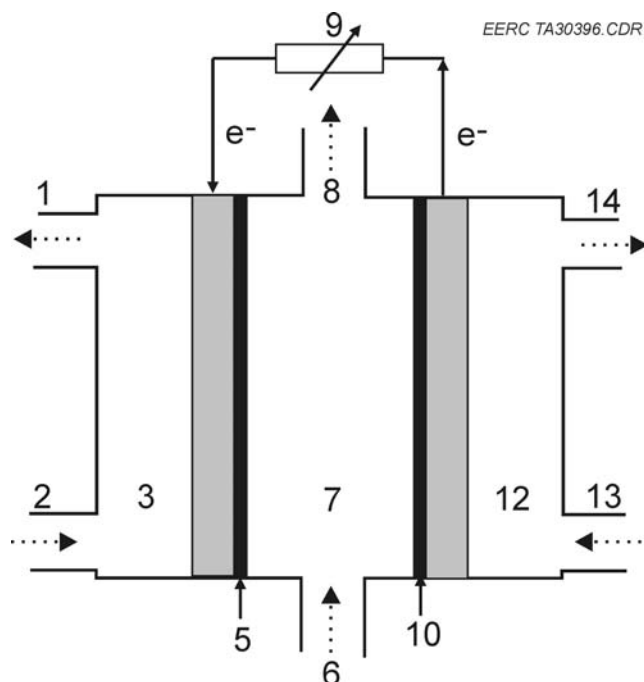


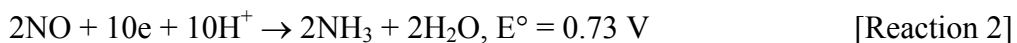
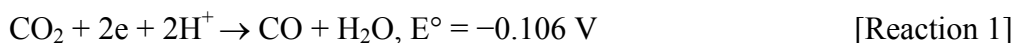
Figure 55. Schematic diagram of an electrolysis cell: 1 – gas outlet at cathode side, 2 – gas inlet at anode side, 3 – gas chamber at cathode side, 4 – gas diffusion layer at cathode side, 5 – cathode catalyst, 6 – liquid electrolyte inlet, 7 – electrolyte chamber, 8 – liquid electrolyte outlet, 9 – current or potential controller, 10 – anode catalyst, 11 – gas diffusion layer at anode side, 12 – gas chamber at anode side, 13 – gas inlet at anode side, and 14 – gas outlet at anode side.

Current efficiency was calculated from the ratio of the theoretical charge required by the formation of measured product to the total charge input, assuming the electron numbers transferred per molecules corresponding to the formation of ammonia and urea are 5 and 10, respectively.

Results and Discussion

Investigation of Electrochemical Coreduction of CO₂ and NO

The electrochemical urea process involves the simultaneous reduction of carbon dioxide and nitrogen-containing compounds. However, electrochemical reduction reactions of CO₂ and electrochemical reduction reactions of nitrogen-containing compounds are thermodynamically and kinetically different (4).



The difference of the standard electrode potential (E°) for Reactions 1 and 2 is around 0.84 V. To achieve coreduction of CO_2 and NO, two approaches may be used: a) change the form of NO and CO_2 to make their standard electrode potential the same or very close or b) alter the reaction kinetics to make $E_1^\circ + \Delta\eta_1$ close to $E_2^\circ + \Delta\eta_2$, where $\Delta\eta_1$ and $\Delta\eta_2$ are overpotentials for Reactions 1 and 2, respectively. Moreover, Reaction 2 must proceed much faster than Reaction 1 since the formation of one urea molecule requires more electrons transferred in Reaction 2 than in Reaction 1.

At the cathode, hydrogen evolution is assumed to be the main competitive reaction:



The above information could be drawn from the measured steady-state polarizations curves. One example is given in Figure 56.

The main results as a function of reaction conditions were collected as follows.

Catalysts

A wide range of catalysts including 1) single-metal catalysts Ag, Cu, Au, Zn, Cd, Hg; 2) cobalt phthalocyanine; 3) carbon; 4) CuZn alloys with varied compositions; and 5) semiconductors CdSe, CdTe, and ZnTe have been evaluated. Several of the tested catalysts showed good activity for both the electrochemical reduction of CO_2 and NO and low hydrogen evolution activity.

Temperatures

The temperature effect of electrochemical reduction of CO_2 and NO was studied. Decreasing temperature can increase the reduction current of CO_2 , but the reaction current of NO has no obvious change with decreasing temperature. Another advantage is that the hydrogen evolution could be suppressed at lower temperatures. Therefore, decreasing temperature may favor the coreduction of CO_2 and NO and inhibit the hydrogen evolution.

Surface Poisons

Several methods were evaluated for efficacy in suppressing the reduction of NO by introducing surface absorbates.

Transformations of NO

Three methods were evaluated for efficacy in transforming NO to an alternative oxidation state to enable lower energy coreduction of CO_2 and NO.

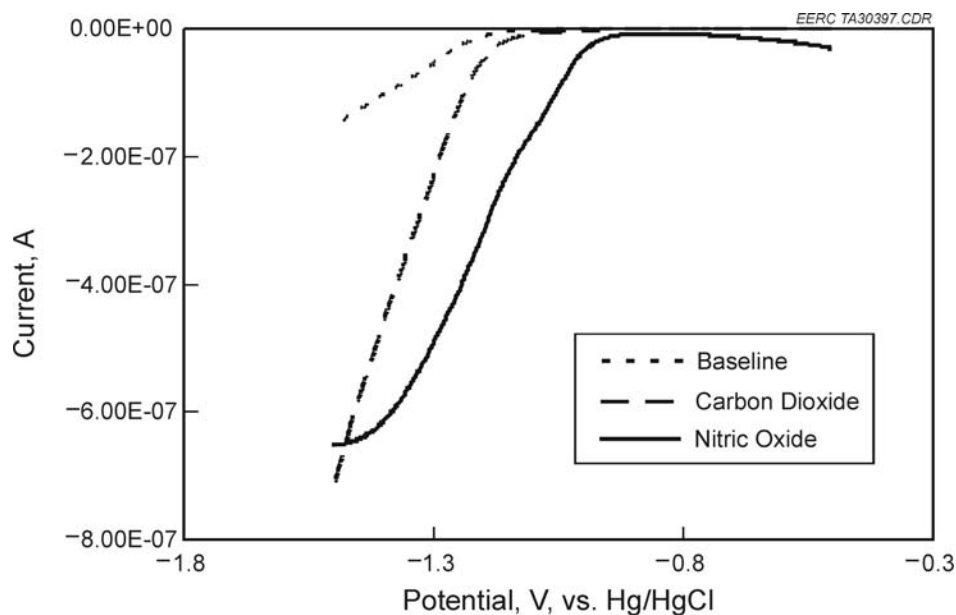


Figure 56. Polarization curves measured at 5 mV s^{-1} for a gold microelectrode (diameter: $58 \text{ }\mu\text{m}$) in 0.5 mol dm^{-3} saturated with high-purity nitrogen (dotted line), CO_2 (dashed line), or NO (solid line).

Cation Effects

At potentials where the coreduction may happen, it is likely that the electrode surface is negatively charged, resulting in the adsorption of cations from the solution. Several cations were studied for their effect on coreduction promotion, including Li^+ , K^+ , NH_4^+ , and Cs^+ .

Preparative Electrolysis and Process Optimization

Process optimization work has been focused on improving process efficiency and selectivity for urea production via the following efforts:

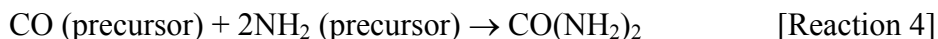
- Evaluating catalyst systems based on promotion of CO_2 and NO coreduction.
- Assessing the impact of varying concentrations of CO_2 and NO on urea yield.
- Assessing the impact of NO transformation to an alternative oxidation state on reaction rate and urea yield.
- Assessing the impact of electrode configuration and components on conversion efficiency and urea selectivity.
- Evaluating the impact of electrode potential, reaction temperature, reactant feed rate, and electrolyte system configuration on process efficiency and urea selectivity.

Key results of the process optimization work are summarized in Table 55.

Table 55. Electrolysis Results for the Coreduction of NO and CO₂ (V_{NO}/V_{CO₂} = 1/1) as a Function of Experimental Conditions with Pure H₂ Fed to the Anode at Room Temperature and Atmospheric Pressure

Catalyst	Electrolyte	Electrolysis Model	Molar Composition of Ammonia and Urea Measured in the Solution		Total Current Efficiency for the Formation of Ammonia and Urea
			Urea	Ammonia	
CA	EA	Constant current, 20 mA cm ⁻²	0%	100%	68%
CB	EA	Constant current, 20 mA cm ⁻²	8%	92%	65%
CC	EA	Constant current, 20 mA cm ⁻²	20%	80%	49%
CD	EB	Constant potential, -1.6 V vs. Ag/AgCl	21%	79%	50%
CE	EB	Constant potential, -1.6 V vs. Ag/AgCl	14%	86%	55%

Further optimization of the electrochemical process for the urea synthesis requires better understanding of the reaction mechanism of the urea formation via the simultaneous reduction of CO₂ and NO_x inputs. Shibata et al. proposed that the electrochemical production of urea via coreduction of CO₂ and nitrites (or nitrates) was caused by the reaction between intermediate CO-like and ammonialike precursors on catalyst surfaces as follows:



The ability of urea formation at various catalysts depends on the current efficiencies of both CO and NH₃ formation in the simultaneous reduction. The catalysts with a high ability for both CO and NH₃ formation would form large amounts of the CO- and ammonialike precursors and have a high ability for urea formation. However, there are some questions regarding Shibata's mechanism. First, the CO- and ammonialike precursors were not experimentally detected. Second, both CO- and ammonialike precursors have a sufficient residence time on the catalysts to form urea. Third, a mechanism exploration that was only based on the values of measured current efficiencies is hardly convincible, since the current efficiency was strongly dependent upon a competitive reaction—hydrogen evolution.

Based on the results obtained and the literature (5–7), we theorized a new mechanism for the electrochemical formation of urea via the simultaneous reduction of CO₂ and NO_x. It is totally different from Shibata's mechanism above and comprises nine steps.

Conclusions

An electrochemical process which utilizes CO₂, NO, and H₂ to produce urea has been proven technically feasible. This feasibility demonstration provides an important way to simultaneously utilize CO₂ from ethanol plants and NO extracted from emission of coal-fired

plants for the production of the widely used nitrogen fertilizer urea. The status of the electrochemical urea process developed at the EERC is characterized by a product comprising approximately 70% ammonia and 30% urea. It has been suggested that the low selectivity for the urea formation in aqueous solutions is caused by the hydrolysis of the reaction intermediate isocyanic acid to ammonia and CO₂, which is formed by the simultaneous coreduction of CO₂ and NO. A new mechanism for the production of urea from CO₂ and NO has been proposed, and several strategies on the further development of the electrochemical urea process have been suggested. The economic competitiveness of the electrochemical urea process strongly depends upon the cost of hydrogen gas and the cost of electricity, as described in Appendix B.

References

1. European Fertilizer Manufacturers Association. *Production of Urea and Urea Ammonium Nitrate*; Brussels, Belgium, 1997.
2. Shibata, M.; Yoshida, K.; Furuya, N. Electrochemical Synthesis of Urea at Gas-Diffusion Electrode III. *J. Electrochem. Soc.* **1998**, *145*, 595–600.
3. Shibata, M.; Yoshida, K.; Furuya, N. Electrochemical Synthesis of Urea at Gas-Diffusion Electrode IV. *J. Electrochem. Soc.* **1998**, *145*, 2348–2353.
4. *Standard Potentials in Aqueous Solutions*; Bard, A.J., Parsons, R., Jordan, J., Eds.; Marcel Dekker Inc.: New York, 1985.
5. Azuma, M.; Hashimoto, K.K.; Hiramoto, M.; Watanabe, A.; Sakata, T. Electrochemical Reduction of Carbon Dioxide on Various Metal Electrodes in Low-Temperature Aqueous KHCO₃ Media. *J. Electrochem. Soc.* **1990**, *137*, 1772–1778.
6. De Vooy, A.C.A.; Koper, M.T.M.; Van Santen, R.A.; Van Veen, J.A.R. Mechanistic Study on the Electrocatalytic Reduction of Nitric Oxide on Transition-Metal Electrodes. *J. Catal.* **2001**, *202*, 387–394.
7. Cant, N.W.; Chambers, D.C.; Liu, I. O.Y. The Amplification of Ammonia by Reaction with NO and CO over Dual-Function Platinum and Palladium Catalyst Systems with Isocyanic Acid as an Intermediate. *Appl. Catal., B: Environ.* **2005**, *60*, 57–63.

YEAR 2005 – ACTIVITY 8 – CHEMICAL FEEDSTOCKS FROM LIGNOCELLULOSIC PYROLYSIS

Introduction

Biomass pyrolysis products have been rarely used as chemical intermediates, owing to difficulties in producing and separating the bio-oils containing the desired constituents in sufficient quantities. These difficulties have been largely solved for hydroxyacetaldehyde (HA) production (1) in the commercial Red Arrow and Ensyn process employing a fast entrained-flow pyrolysis method (2).

HA exists mainly in dimeric forms that are water-soluble. Its main current market is in the Red Arrow technology for making flavor and cooking enhancement products. Having two functional groups, HA is also potentially an ideal platform chemical intermediate for preparing a variety of polymeric materials that can compete with existing petroleum-derived materials.

Goals and Objectives

The project's goal is to investigate the reactions of HA with primary, secondary, and tertiary amines to determine potential routes to useful commercial monomeric, dimeric, or polymeric products.

Experimental

A 60 wt% of hydroxyacetaldehyde (glycolaldehyde) was obtained from Ensyn. This material was produced from wood fast pyrolysis at the Red Arrow Plant in Wisconsin. High-performance liquid chromatography (HPLC) analysis indicated the purity was about 90% and was present in mostly in the dimer form.

Preparation of Polymers

A mixture of 60 wt% glycolaldehyde (20 g, 0.2 mole), ammonium chloride (10.7 g, 0.2 mole) were placed in a round-bottomed flask equipped with reflux condenser. The flask was heated in an oil bath at 60°C for 24 hours. The suspension was magnetically stirred during the course of reaction. A dark solution was formed which gave a tacky black solid on cooling to room temperature. Similar reactions using methylamine hydrochloride and triethylamine hydrochloride gave dark viscous oils.

In another test, reactions of ammonium chloride and hydroxy acid aldehyde were carried out using 10% solution in water. These reactions were carried out by stirring at room temperature for 48 hours in acidic (HCl), basic (NaOH), and neutral conditions.

Preparation of Polyacrylamide Solution

A 1% solution of polyacrylamide (PAM) $[-CH_2CH(CONH_2)-]_n$ (Av. MW = 5000,000) was formed by dissolving 10 g of the polymer in 1000 cm³ deionized water. To this solution, a small amount (1 g) of sodium hydroxide was added and heated at 60°C for 30 min. A viscous solution of partially hydrolyzed PAM was formed.

Preparation of Amine-Glycolaldehyde Polymer Solution

A series of solutions containing 0.4, 0.8 and 1.6 wt% of amine-glycolaldehyde polymer in deionized water were prepared. For ammonium chloride solutions, the amount of ammonium chloride was adjusted to reflect the same number of moles as used in the preparation of ammonium chloride-glycolaldehyde polymer. The actual concentration of ammonium chloride solution was 0.19, 0.38, 0.76 wt%, respectively. PAM solution (100 g) and amine-glycolaldehyde solution (100 g) were mixed thoroughly to produce solutions containing PAM

(0.5 wt%) and amine-glycolaldehyde (0.2, 0.4, and 0.8 wt%). For ammonium chloride and PAM solutions, the concentrations were PAM (0.5 wt%) and ammonium chloride (0.095, 0.19, and 0.38 wt%).

Viscosity Measurements

Viscosity measurements of the above solutions were carried out using a Brookfield Synchro-Lectric Viscometer, Model RVT. Viscosities were measured at ambient temperature.

Results and Discussion

Polymer Synthesis

Reactions of HA with several aliphatic amines were investigated with and without the addition of hydrogen to determine the potential for formation of ethanolamines (with hydrogen addition), ethanolamines (without hydrogen addition), and other products. Studies included the reactions of diethylamine, ethylamine, triethylamine, and ammonia with HA in the presence of acidic and basic catalysts. Formation of monomeric and dimeric products from diethylamine and HA is shown in Figure 57. As described above, HA normally exists in dimeric forms (I, II), but can be converted to the monomer under acid conditions. Reaction of the monomer with the amine produces the iminium ion intermediate (V), which it was hoped could be hydrogenated to diethylethanolamine (DEEA) (III), a useful commercial dispersant, currently produced from ethylene oxide. Similar reactions were reported previously for 2-hydroxypropanal and 1-hydroxy-2-propanone (3). In the absence of hydrogen, the iminium ion intermediate was hoped to dimerize to the cyclic ether dimer (VI).

The initial reactions with or without hydrogen and Pd present showed complete conversion of the HA. However, neutralization and vacuum distillation produced no ethanolamines or dimer products. When the reactions were conducted at ambient or cold (ice bath) conditions, the amine was consumed but none of the expected monomer and dimer products were produced. When the reactions were heated, intense dark-colored solutions resulted, indicative of the occurrence of the Maillard reaction. In fact, little hydrogen was taken up by the reaction in the presence of Pt, Ni, and Pd catalysts. Thus the condensations in Figure 57 did not occur as proposed. The major product in both conditions was a polymeric ammonium compound. The structures of the polymers are not known. The structures could be represented by the ammonium-substituted polyethylene glycol structure (VII) shown in Figure 58 for the reaction of diethylamine, with HA using HCl catalyst. This tertiary ammonium structure has the pendant diethylammonium groups. Alternatively, the quaternary ammonium structure would have nitrogen in the backbone, as represented by the polyalkyleneimine structure (VIII). Or the polymer could contain both types of structures. Similar polycation structures can be written for the reactions of primary amines and ammonia. The reaction of triethylamine, a tertiary amine can only form structures analogous to structure VII, since the nitrogen already has four bonds and cannot become a part of the backbone as in structure VIII. All of the HA-amine polymers were highly water-soluble.

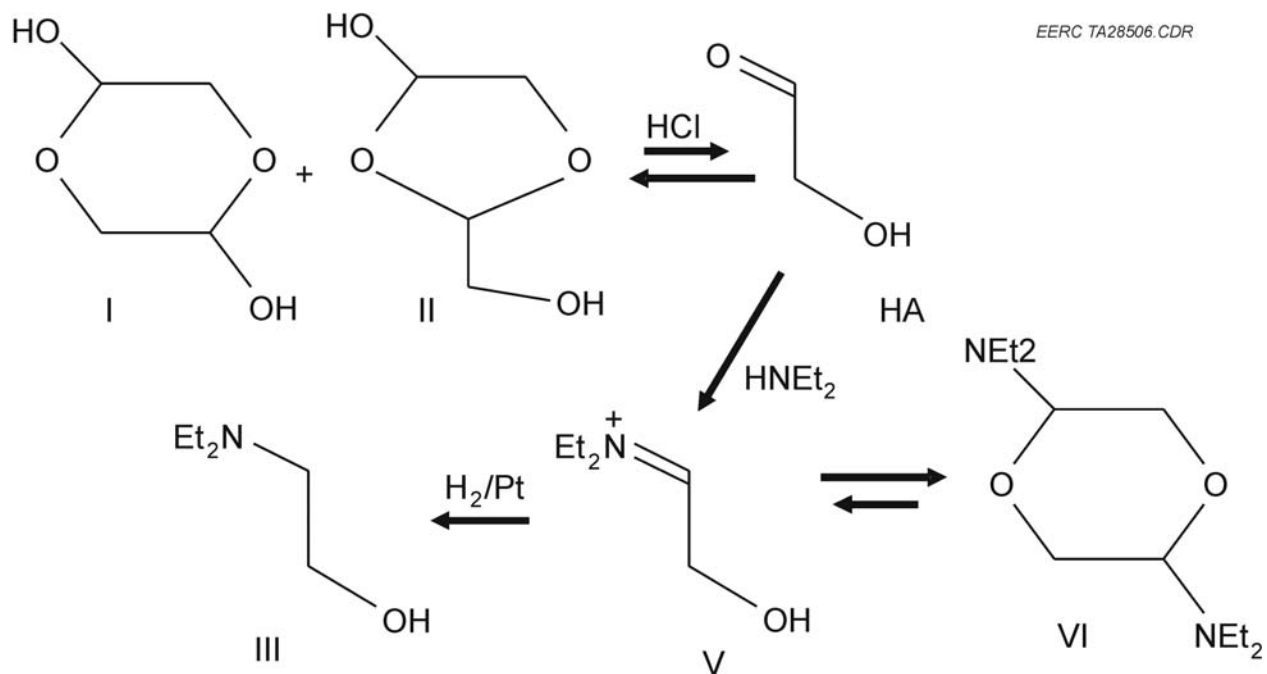


Figure 57. Proposed conversion of HA to dialkylethanamines.

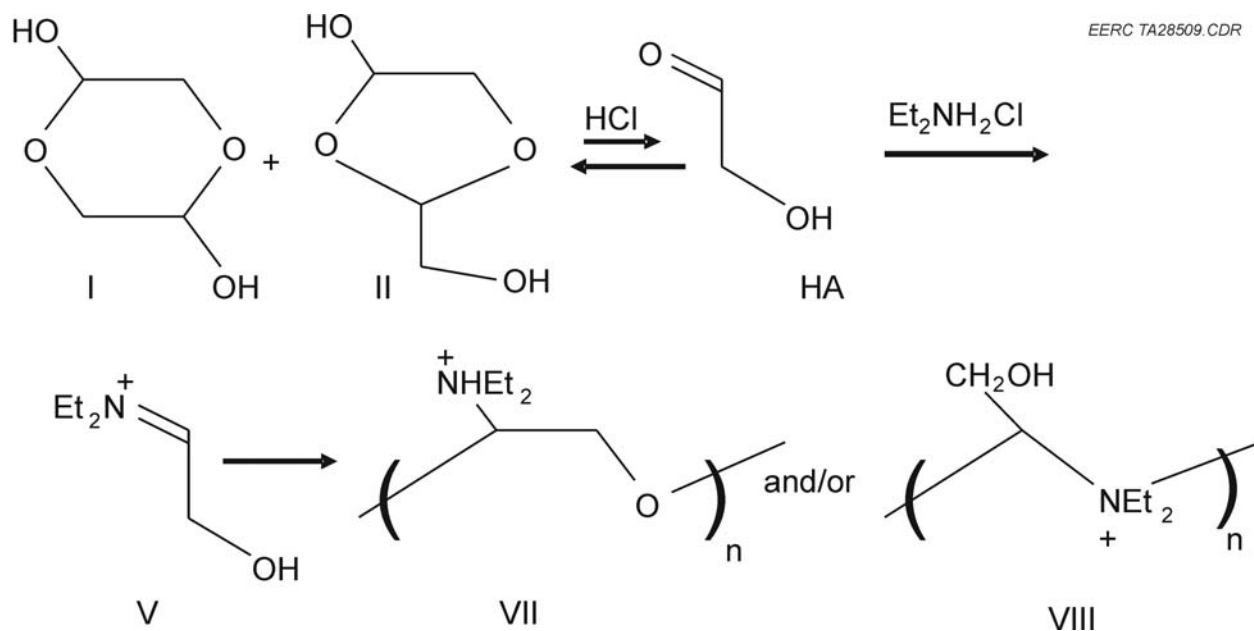


Figure 58. Conversion of HA to poly(N,N-diethylammoniummethylene glycol)(VII) and/or poly(hydroxymethyl-N,N-diethylethyleniminium)(VIII).

Heating the polymers results in their degradation via cleavage of the C–C bonds and subsequent cyclization reactions leading to the typical Maillard reaction products. These products are highly colored and still polymeric, although some are small and volatile.

Hydroxylamine was also reacted with HA with and without hydrogen (Raney nickel catalyst) under a variety of conditions. However, no hydroxylaminoethanol, ethanolamine, or oxime could be isolated. The products are likewise polymeric and decompose on heating via the Maillard reaction or, possibly, dehydration reaction in this case. The reaction is illustrated in Figure 59, but the pendant hydroxylamine structure analogous to structure VII could also be formed. As with the HA–amine polymers, the HA–hydroxylamine polymers were highly water-soluble.

Polyamine Viscosity Properties

One of the uses of polymeric ammonium salts in enhanced oil recovery (EOR) is to inject a mixture of polymers, a polyanion, for example, polystyrenesulfonate, or partially hydrolyzed polyacrylamide, with a very high-viscosity effect at a concentration of 0.1 wt% or less, combined with another polymer that modulates the viscosity of the first (4). The modulator is a soluble quaternary ammonium polymer (polyquat) that partially coagulates or contracts the first polymer when they are injected so that the viscosity is actually low. The lowered viscosity allows the aqueous mixture to be pumped without shearing the polymer, and the mixture can easily move into the reservoir. Then the polyquat adsorbs out on mineral surfaces when it reaches the reservoir and leaves the polyanion by itself in the aqueous solution. The polyanion then extends out, returning the solution to a very high viscosity. A relatively expensive polyquat in combination with a relatively inexpensive polyanion was investigated and reported by Borchardt (4). This combination decreased the viscosity of the polyanion solution from 18.1 to 7.6 cPs (42%). Other examples are described in the Borchardt patent (5).

With the view to conducting polymer flooding using a low-cost polyquat rather than the high-cost compounds used by Borchardt (4), the EOR application with the polyammonium salts discussed above was tested with the compounds that were prepared by room-temperature reaction of HA with simple amines. The series of polyquats prepared from HA and the amines or ammonia were mixed with partially hydrolyzed polyacrylamide, and the viscosity-lowering effect was determined. Partial hydrolysis of the polyacrylamide (av MW = 5,000,000) was conducted with dilute NaOH to give a very high-viscosity solution. The initial polyacrylamide was soluble in water and base. The hydrolysis converted 1%–2% of the amide groups to carboxylate anion groups giving a polyanion. The repulsion of the negative charges causes the polymer to elongate to a maximum extent in the aqueous solution, producing a very high viscosity. Other polymers (polyacrylic acid and copolymers) were less soluble or gave lower viscosities.

The partially hydrolyzed PAM solution was diluted to low concentration (0.5 wt%) which is appropriate for demonstrating the viscosity-lowering effect and is in the application's economically useful range. This solution was mixed with a series of polyquat solutions (0.2, 0.4, and 0.8 wt%) of each polymer, so that equal amounts of the polyanion were present, and the viscosities of the solutions were measured at room temperature with a

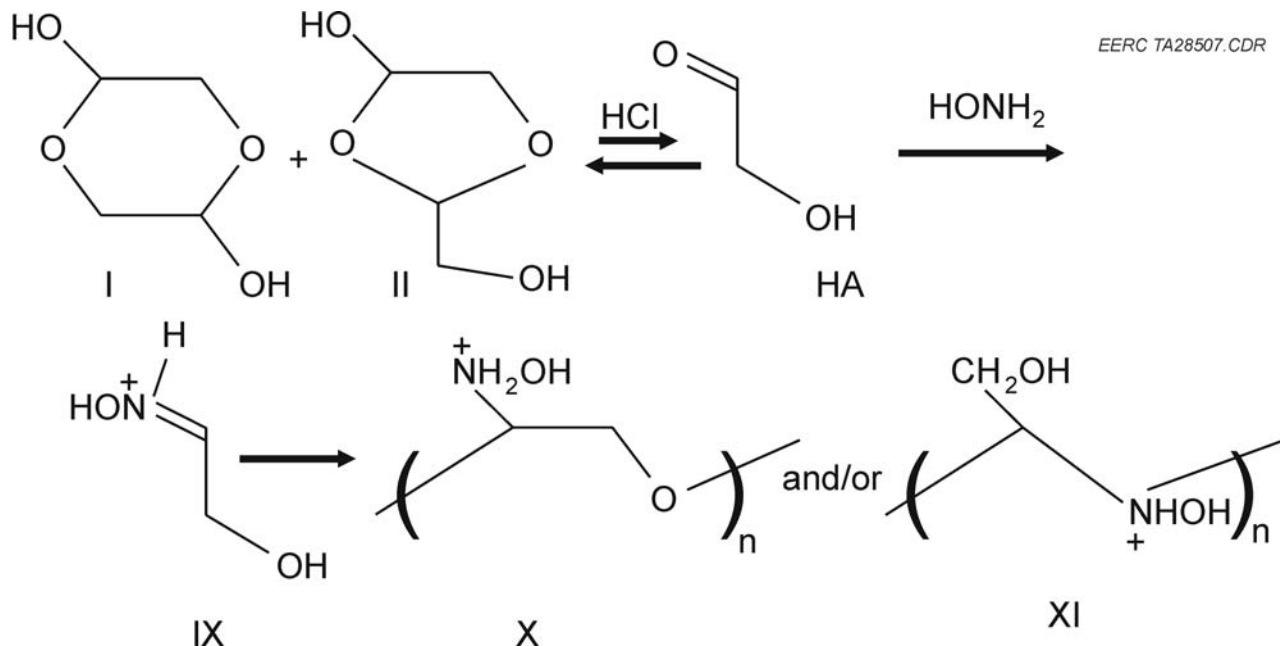


Figure 59. Conversion of HA to poly(N-hydroxyethanolamine).

Brookfield viscometer. The results are shown in Table 56. For comparison, the viscosity of the original polyanion solution at the same concentration and the viscosity of a mixture with unpolymerized ammonium chloride (same number of moles of nitrogen) are also shown.

A series of polymers prepared from ammonium chloride and HA were prepared under different conditions (acidic, basic, and neutral) at ambient temperature for 48 hr. The viscosities of the mixtures with partially hydrolyzed PAM were determined. The results are shown in Table 57.

The results showed that the introduction of unpolymerized ammonium cations produced a significant lowering of the viscosity. Thus neutralization of the charges on the polyanion resulted in a considerable contraction or agglomeration of the polyanion. The ammonium polymers, however, lowered the viscosity to a much greater degree at concentrations of 0.4 to 0.8 wt%. Thus not only are the charges neutralized, but neutralized in a way that forces additional constraints on the polyanion configuration. The largest effect was for the quaternary ammonium salt or polyquat prepared from triethylamine. So perhaps the constraints imposed on the polyanion are larger for the polycations in the polymer backbone of the polyquat compared to the mixed polymer structures obtained from the primary and ammonium-derived polymers.

Cation concentration did have a significant effect on the viscosity lowering. The effects were large only for the case where the polycation concentrations exceeded the polyanion concentration, unfortunately. The polymer from the reaction of diethylamine with HA has not yet been tested. The polymers used by Borchardt were the quaternary type; however, they did not achieve as great an effect in lowering the viscosity.

Table 56. Viscosities (cPs) of Partially Hydrolyzed PAM Solutions (0.5 wt%) Combined with Ammonium and Polyquat Solutions

Cation	Cation Concentration, wt%			
	0	0.2	0.4	0.8
NH ₄ Cl	23.0	15.1	10.1	7.0
NH ₄ Cl + HA (60°C – 24 hr)	23.0	10.9	8.1	4.8
CH ₃ NH ₃ Cl + HA (60°C – 24 hr)	23.0	15.0	7.8	4.0
(C ₂ H ₅) ₃ NHCl + HA (60°C – 24 hr)	23.0	17.7	7.5	2.5

Table 57. Viscosities (cPs) of Partially Hydrolyzed PAM Solutions (0.5 wt%) Combined with Polyquats Prepared under Different Conditions

Cation	Cation Concentration, wt%			
	0	0.2	0.4	0.8
Neutral NH ₄ Cl + HA (25°C – 48 hr)	23.0	12.6	8.4	5.0
Acidic NH ₄ Cl + HA (25°C – 48 hr)	23.0	11.8	7.9	3.5
Basic NH ₄ Cl + HA (25°C – 48 hr)	23.0	13.2	8.3	5.5

The preparation method for the ammonium polycation was shown to have a small effect on the results. The lower temperature for a longer reaction time was more effective. Higher temperatures may have promoted the Maillard reaction, causing bond cleavage after the condensation reactions. The acidic conditions also favored the viscosity-lowering effect, possibly due to greater cross-linking of the polycation and subsequently greater constraints on the polyanion structure in the mixture.

Measurements of the dilute polycation solutions were determined in the absence of the polyanions in order to better understand the effects on the physical properties of these systems. The viscosities of the dilute polycation solutions are not high, indicating that they are likely not high-molecular-weight polymers. In fact, the viscosities are only slightly higher than an ammonium chloride solution (see Table 58). The molecular weights have not been measured. The degree of cross-linking of the polycations is also unknown.

Polymer Separation – Viscosity Restoration

To demonstrate the field applicability of the method, separation of the polyanion–polycation mixture on a clay phase was investigated. The solution containing 0.5 wt% partially hydrolyzed PAM and 0.8 wt% polycation (from ammonium chloride and HA) was stirred with sodium montmorillonite (a smectite clay) for 1 hour. The clay took up the polycation from the mixture, giving an expanded or swelled clay phase. The viscosity of the solution was determined before and after the clay treatment, and the results showed an increase in viscosity from 4.8 to 14 cPs. The weight change in the clay was not indicative of the polymer adsorption because of the water release. However, viscosity increase is consistent with removal of about 90% of the polycation. This experiment demonstrates the viscosity can be returned to its nearly original high value for use in preventing fingering of the aqueous phase in the reservoir.

Table 58. Viscosities of Polycation Solutions

Cation	Concentration, wt%	Viscosity, cPs
NH ₄ Cl	0.38	0.20
NH ₄ Cl + HA	0.8	0.25
CH ₃ NH ₃ Cl + HA	0.8	0.30
(C ₂ H ₅) ₃ NHCl + HA	0.8	0.25

Formation Damage Control

The success of this separation experiment utilizing a smectite clay indicates that the polycation may be useful for preventing formation damage (6, 7). Clays typically swell to many times their original volume when in contact with injected aqueous polymer solutions. This not only can constrict the flow channels in a formation, but also can cause fine particles to release and eventually plug the channels. The polycations in an injected solution strongly adsorb and bind to the clays and other mineral phases in the reservoir, resulting in a stabilization of the layer structures which prevents swelling and release of the fine particles.

Another effect of the polycations used in formation damage control is that the water/oil ratio is lower. Because of the organic content of the polymers, the adsorption of polycations on the mineral phases results in decreased permeability to aqueous phases in the formation but does not alter the permeability of the petroleum phase. Thus the oil migrates more easily through the formation to the well.

Hydrophobically Associating Polyamines

The introduction of numerous alkyl chains into a water-soluble polymer produces polymers that self-aggregate in polar media as a result of micellelike behavior of the attached chains. These polymers are called hydrophobically associating polymers and have a number of uses such as controlling the rheology of water-based paints, controlling release of drugs, and reducing drag in water-based fluids.

The reaction of HA with dodecylamine was investigated to determine whether hydrophobically associated polymers can be easily prepared using HA condensations. The reaction produced layers of a separate water and organic polymer phase. When the pH was lowered, the polymer layer agglomerated into small balls of polymer suspended in the aqueous phase. Thus it appeared that production of more cations at the lower pH resulted in greater intramolecular interactions of the long-attached chains, giving a subsequent change in the morphology of the phases (Figure 60). Further studies of these easily prepared polymers are under consideration. These studies will be conducted at various pH and ionic strengths and will utilize various amine mixtures to give lower concentrations of the long chains in the resulting copolymers.

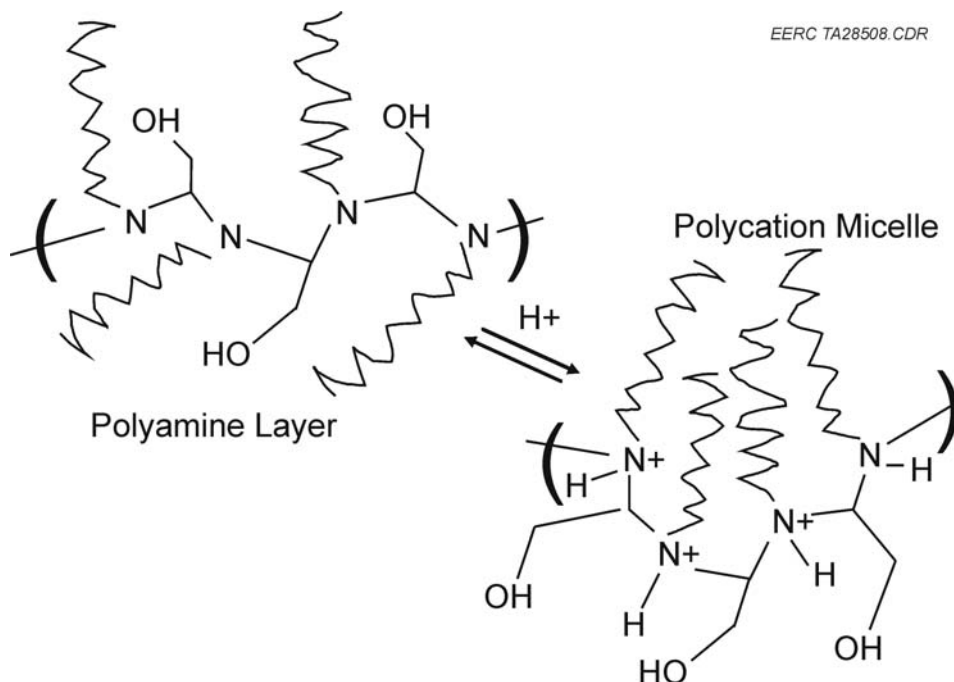


Figure 60. Interconversion of hydrophobically modified polymers.

Conclusions

Ionic polymers were easily prepared from the HA dimers by condensation with inexpensive amines. Introduction of the desired charged groups during polymerization resulted in polycations, with the charged groups being part of the polymer backbone. Several polycations were prepared from various amines under neutral, basic, and acidic conditions. The polycations had the unique property of lowering the viscosity of polyanions via an agglomeration effect. Thus applications in the field of polymer flooding or alkaline-surfactant-polymer flooding for EOR were suggested. This viscosity-lowering effect facilitates pumping and mobility in the reservoir, but is reversed when the polycations in the mixture are selectively adsorbed on clay surfaces. The result was to increase the viscosity of the aqueous phase, which prevents fingering of the aqueous phase into the oil phase and facilitates extraction of the oil phase. The clays were thereby stabilized by adsorption of the polycations. The solution properties of these polymers can be adjusted by varying the type and amount of comonomer and can be further adjusted by changing the temperature, pH, ionic strengths, and counterions in the solution. Thus a variety of uses in viscosification, suspension or flocculation, adhesion, and stabilization are proposed.

References

1. Stradal, J.A.; Underwood, G.L. U.S. Patent 5,393,542, 1995.
2. Freel, B.A.; Graham, R.G. U.S. Patent 5,792,340, 1998.

3. Felder, E.; Romer, M.; Bardonner, H.; Hartner, H.; Fruhstorfer, W. U.S. Patent 5,023,379, 1991.
4. Borchardt, J.K. Viscosity Behavior and Oil Recovery Properties of Interacting Polymers. *ACS Symposium Series* **1991**, 467 (Water-Soluble Polym.), 446–65.
5. Borchardt, J.K.; Brown, D.L. U.S. Patent 4,409,110, 1983.
6. Borchardt, J.K. Cationic Organic Polymer Formation Damage Control Chemicals. A Review of Basic Chemistry and Field Results. *ACS Symposium Series* **1989**, 396 (*Oil-Field Chem.*), 204–21.
7. Borchardt, J.K. Chemicals Used in Oil-Field Operations. *ACS Symposium Series* **1989**, 396 (*Oil-Field Chem.*), 3–54.

YEAR 2005 – ACTIVITY 9 – LANDFILL METHANE FOR MICROTURBINE POWER

Introduction

Landfill gas (LFG) is composed of approximately 50% methane, 40% carbon dioxide, and 10% other gases and is produced by the decomposition of organic waste under anaerobic conditions. The U.S. Environmental Protection Agency (EPA) estimates that there are about 6000 landfills in the United States, mostly made up of municipal solid waste (MSW), that are producing methane. This is assumed to be the largest source of anthropogenic methane emissions in the United States and is speculated to contribute an estimated 450–650 billion cubic feet of methane to the atmosphere each year (U.S. Department of Health and Human Services, 2001).

LFG recovery has the potential to significantly reduce the risk of global climate shift. LFG is one of the largest sources of anthropogenic methane emissions in the United States, contributing almost 40% of these emissions each year. Reducing methane emissions is considered critical in the fight against global climate shift because each ton of methane emitted into the atmosphere has as much global thermal impact as 21 tons of carbon dioxide over the same time period (U.S. Environmental Protection Agency, 1996). In addition, methane cycles through the atmosphere about 20 times more quickly than carbon dioxide, which means reducing methane emissions now can improve the chances of mitigating global climate change in the future.

The use of LFG can offer economical energy for the on-site landfill operations; clean, complete combustion of waste gas; decreased emissions to the environment by reducing the need for traditional electrical generation sources; public relations opportunities for the local community; and educational opportunities for local school students, all as a result of this state-of-the-art gas-to-energy microturbine system being located within the community.

This study completed a preliminary energy assessment of the Grand Forks Landfill and its ability to produce biogas for energy production by determining the physical characteristics of the

landfill site; the biogas generation potential for a 40-year old landfill in a far northern climate; the quality, quantity, and constituents of the potential fuel source; the power generation potential in this region; the requirements for biogas pretreatment technology; and the local parameters for using microturbine technology for continuous electricity and heat generation.

Currently, landfills are considering microturbine technology relative to piston engines as the energy recovery system of choice. Microturbines generally provide lower maintenance and improved emission over piston engines; however, gas treatment systems for use in microturbines remain expensive because of the lower levels of gas contaminants permitted.

The application of microturbines presents a new technology relative to piston engines for the generation of electricity. Manufacturers of microturbine technology are becoming increasingly aware of landfill applications for this equipment. As a result, microturbine manufacturers are designing turbines that have a high tolerance to sulfur (7%), require low maintenance (no oil lubrication), produce lower emissions, and can be more cost-competitive in smaller size ranges (30–65 kW) with traditional internal combustion engines (ICEs) (Capstone, 2008; U.S. Environmental Protection Agency, 2008).






The Grand Forks Landfill

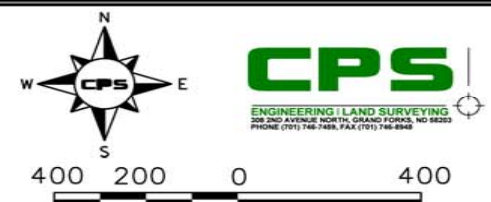
The 180-acre Grand Forks municipal landfill (Figure 61) began operation in the early 1960s as an open regional dump receiving all types of industrial and residential waste. During the early 1990s, this municipal dump became a managed landfill site. At this time, basic sorting and baling practices began separating MSW, yard waste, and inert items. However, immediately following the catastrophic flood in 1997, the landfill received most of the local cleanup and reconstruction debris.

Presently, the City of Grand Forks MSW landfill is a regional facility which serves approximately 110,000 people in northeastern North Dakota and northwestern Minnesota. In 2006, the city MSW landfill accepted approximately 93,000 tons of MSW, of which approximately 37,000 tons was from the city and 56,000 tons was from outside the city. The MSW acceptance rates vary monthly, taking in less in the winter and slightly more in the summer months. The most recent values indicate the average MSW rate is around 7500 tons/month or about 250 tons/day. With a current tipping fee of \$33.50/ton, the approximate annual gross revenue for this site is approximately \$3,000,000 (Amundson, 2007).

The city also owns and operates an inert landfill that accepted approximately 26,000 tons in 2006. This inert landfill eliminated the following materials from entering the MSW landfill, effectively reducing the overall gas generation potential of the MSW site (Feland, 2008):

- Recyclables – 1720 tons
- Metal/appliances – 178 tons
- Tires – 100 tons
- Yard waste – 3015 tons
- Ash – 7389 tons
- Sawdust – 273 tons

Legend	
	MSW Disposal Limits
	Inert Waste Disposal Limits
	Compost Working Area
	Compost Contract Water Pond
	Closure-Phase Boundaries



City of Grand Forks Landfill
LFG for Microturbine Power
Facility Layout



Figure 61. Facility layout. This figure details the main MSW disposal limits, the inert waste disposal area (east end), composting area within the inert area, and the boundaries of the main Closure Phases I through IX. This plan also shows the location of the three piezometer wells and the existing passive gas-venting system. Note the baling facility in the upper northeast corner of the site, across from the inert waste site.

- Brush – 2549 tons

Biogas Generation Based on Site Characterization

Based on assumptions made for the waste-in-place estimates, age, location, and water levels in the wells of the four closure cells, it was determined that we would use one representative venting well from each closure phase to conduct the sampling for the gas constituent analyses. Since the wells used for sampling are part of a simple passive network, no formal well identification numbers exist. Because of the basic nature of this preliminary investigation, the wells were simply referred to as Phase I, Phase II, Phase III, and Phase IV, corresponding to the planned closure phases (Figure 61).

It is likely that the best candidates for energy recovery will have the following characteristics (U.S. Environmental Protection Agency, 1996):

- At least 1 million tons of waste in place
- Either still receiving waste or closed for not more than a few years
- Landfill depth of 40 feet or more

Since the Grand Forks landfill site began operation as an open dump in the early 1960s and began closure phases in the early 1990s, it is very difficult to estimate the amount of waste in place for each closure phase. This makes an estimation of potential energy recovery difficult as well. However, if we base the energy recovery potential on the entire site, which is projected to have almost 3.5 million tons of solid municipal waste in place by the time of final closure in 2009, it is possible to estimate some general gas generation rates. However, considering the previously open nature of this site combined with the high water table and loosely managed waste disposal practices for most of the life of the landfill, all of the approximations presented in this study could be unrealistically biased toward the high end.

Industry guidelines suggest economically viable gas generation rates are about 1 Mcf/day. However, successful energy recovery projects are presently working at landfills with as little as 50,000 tons of waste in place, gas flows of 20,000 scf/day, and depths around 10 feet. In addition, a fairly large percentage of existing and planned projects are at landfills that closed during the 1980s (Solid Waste Association of North America, 1997).

Biogas Contaminants

Digester and landfill biogases are widely used as fuel to produce electricity, drive heat pumps, and fire boilers. Unlike natural gas, these gases are normally saturated with moisture and carry varying quantities of compounds that contain sulfur, chlorine, and silicon. Manufacturers of combustion turbines and reciprocating engines are becoming more interested in siloxane controls as a way to possibly lower maintenance costs and extend the operation run time between major maintenance overhauls. There is no doubt that some maintenance cost benefit can be realized by siloxane removal and through the incidental removal of other biogas contaminants that will occur during siloxane removal; however, at this time most siloxane removal methods are extremely costly.

Siloxanes are organosilicon molecules that also contain mostly carbon, hydrogen, and oxygen but can also contain nitrogen and halogens. Their primary use for the consumer market is in toiletries and cosmetics of all types, including deodorants, hair sprays and gels, lipsticks and glosses, lotions, shaving products, and others. These molecules are a problem in biogas because they form silicon dioxide, SiO_2 , upon combustion. SiO_2 is a white, powdery substance that accumulates on the heated surfaces in combustion equipment, especially in the cylinders of ICE generators. For example, an ICE generator burning biogas containing just 1 ppmv of siloxane D5 will generate approximately 130 lb of SiO_2 a year if operated continuously. Not all of this SiO_2 will remain in the engine; however, what does remain can cause considerable damage and add greatly to the cost of operating the generation equipment (Tower, 2004).

Basic LFG Applications

Since landfill sites decompose and generate LFG continuously and because LFG storage is not economically practical, a continuous use of LFG normally is required. Ideally, the end use will be such that the city could take advantage of the biogas stream 24 hours/day and 7 days/week in a year-round operation. The most economical options for LFG utilization are direct uses such as heat and on-site electrical use, where the end users are in close proximity (no more than 1 mile) to the landfill, and whose energy needs closely match production at the landfill. Any electricity buyback at this site will require interconnection with the local power utility (Nodak Electric Cooperative) to be part of the local transmission/distribution system. On-site displacement costs of \$0.03–\$0.06 per kWh and grid-avoided costs \$0.01–\$0.02 per kWh with negotiations up to \$0.04/kWh may be possible.

The most viable options for the direct use of the medium-heating-value LFG at this site (about 550 Btu/scf) would include use as fuel in microturbines or ICEs to produce electricity, heat, or both for the landfill site and/or the wastewater treatment plant (WWTP). In the case of the Grand Forks landfill site, utilizing the gas on-site for electrical generation or heat production appears to be the most economical use of this “free” gas. After an extensive gas collection, treatment, and energy generation system was complete, the on-site energy utilization would offset the cost of power purchase at the current retail rate. At the Grand Forks site, this retail rate varies between \$0.037 and \$0.062/kWh for the landfill site and between \$0.03 and \$0.0385/kWh for the WWTP (Amundson, 2007, 2008; Tucker, 2008).

Electrical Generation

Generally, there are two proven applications for LFG electricity generation: ICE and gas turbines (microturbine). Most of the larger operating landfill energy recovery projects (>1200 scfm of biogas) can economically sell excess electricity under contract to a power utility. A large percentage of the LFG recovery facilities in the United States generate electricity, which is then sold to a local electric utility company. Several of these facilities use some of their generated electricity on-site.

ICEs used to generate electricity are most commonly “lean burn” turbocharged designs that burn fuel with excess air. When operated on LFG, engine power ratings are commonly reduced

by 5% to 15% compared to operation on natural gas. The overall heat rate (after reduction for parasitic loads) ranges from 11,000 to 14,000 Btu/kWh.

Microturbines used to generate electricity at landfill sites take large quantities of atmospheric air, compress the air, burn fuel to heat the air, and then expand the air in the power turbine to develop shaft horsepower. Microturbines are most efficient when operated at full capacity to optimize performance and limit operational problems (Thorneloe, 1992).

Upgrade to High-Btu Pipeline-Quality Gas

Out of thousands of LFG sites in the United States, less than a dozen upgrade their LFG to pipeline-quality natural gas. These projects generally were implemented in the early 1980s when gas prices on a heating value basis were comparable with oil. These sites have an average LFG flow rate of 5 Mcf/day with a range from 1.1 to 9.5 Mcf/day (Thorneloe, 1992; Gould, 1992). High-capital-cost technology is required to purify the gas to pipeline quality by removing the water, hydrogen sulfide, chlorinated hydrocarbons, and other trace constituents as well as separating out the CO₂. The high-Btu gas must meet pipeline specifications that normally require the following (Koch, 1986):

- A minimum heating value of 950 Btu/scf
- Water levels less than 0.7 lb of water/Mscf
- Hydrogen sulfide less than ¼ grain/100 scf
- Total sulfur less than 9 grains/100 scf
- Interchangeability with natural gas (acceptable heating value, relative density, and oxygen level limits) and must contain no toxic, harmful, or foreign materials

Upgrading to pipeline-quality natural gas was determined not to be economically viable at this site because of low gas quantity and because the required infrastructure is similar to that of a natural gas refinery. In addition, the buyback details require extensive negotiations with the local utility company (Xcel Energy) at usually 40%–80% of the current wholesale gas value.

Goals and Objectives

The goal for this activity is to evaluate the Grand Forks landfill site for gas production and determine the most cost-effective and efficient method to prepare and utilize the biogas for microturbine use. The following objectives were recognized as those that would meet the goal of this prefeasibility energy assessment:

- Preliminary assessment of the landfill site for gas production
 - Determine if the proposed energy recovery project will work at this site. Apply basic screening criteria to determine the landfill characteristics that are general to

successful LFG energy recovery projects. Use a first-order decay equation to estimate the quantity of LFG that could be collected under ideal conditions, as gas quantity is a critical factor in determining whether LFG energy recovery is a viable option.

- Develop a methane gas profile
 - Use the existing passive well network in an attempt to develop a gas extraction site plan, sample the gas, and develop a gas quantity and quality profile for the landfill site. Utilize basic screenings to estimate gas quantity and determine the most effective methods for estimating gas flow, correcting for collection efficiency, and analyzing gas flow rates.
- Investigate more cost-effective, efficient, and aggressive means to prepare the gas for microturbine use (moisture, volatile organic contaminants [VOC]/siloxane, and hydrogen sulfide removal)
 - The removal of moisture from LFG is the single-most important factor in yielding a stable operation for the microturbines. Microturbines are also sensitive to siloxane contamination. The LFG supplied to microturbines is generally expected to require more pretreatment than LFG used to power other electrical generation sources. As a result, additional research into more aggressive cleaning methods is needed.
- Develop a preliminary, simple return-on-investment analysis for this site
 - Presently, the Grand Forks City landfill site has potential benefits to the community, including turning the landfill into a good neighbor, helping the environment, and utilizing a local energy source that would otherwise be wasted. A close working relationship with the city must be established that will focus on developing a comprehensive program for the city's immediate needs (energy) while keeping its future (biosolid waste digesters at the wastewater treatment plant) in sight. This will be achieved by outlining the basic steps required to move forward with a power generation or a combined heat and power (CHP) system and clearly presenting the potential environmental, economic, and energy benefits.

Experimental

Performance of this project was divided into four subtasks.

Subtask 1 – Develop the Basic Landfill Site Parameters

Using basic screening techniques, the landfill site specifications were developed by determining the amount of waste in place and the waste acceptance rates. An initial gas quantity profile was developed, along with a generation potential assessment based on the collected

details of the site. Potential project environmental, economic, and energy benefits were also evaluated.

Subtask 2 – Develop the Basic LFG Characteristics

The most cost-effective and efficient methods to collect, analyze, and determine quality of the LFG were determined. Equivalent air emissions and the maximum expected LFG generation and recovery potential from the landfill site were calculated.

Subtask 3 – Investigate New and Innovative Gas Treatment Systems

More cost-effective and potentially more efficient gas preparation practices and treatment methods for moisture, VOCs and siloxanes, and H₂S removal from the LFG recovered at this site were investigated.

Subtask 4 – Develop the Microturbine Power Generation Plan

A very preliminary concept for an overall energy recovery and generation system was developed that could be used to produce electricity using microturbine technology. Recovery and use of the LFG at this site in a CHP generation system to include biogas extraction, collection, and pretreatment systems were investigated. Also identified were the potential end users and also developed was a best-case cost scenario for the possible biogas-to-energy system project.

The scope of this activity required that samples of biogas be taken from four 4-inch polyvinyl chloride (PVC) vent risers at the Grand Forks landfill site within the existing passive venting system (Figure 61). The LFG samples were taken from all four of the closure phases. A sampling kit for siloxane capture and subsequent analysis, a total biogas VOC sampling bag (to determine the presence and concentration of contaminants typically found in landfill biogas), and a major fuel components kit (for analyzing major gas components and nonmethane organic contaminants) were supplied by Applied Filter Technology (AFT), Inc., in Snohomish, Washington. All sampling protocols, chain-of-custody forms, and analytical results were also supplied by AFT (Tower, 2002).

In addition to determining the baseline biogas composition and contaminants, the flow rates and sustainability of the gas stream were evaluated. However, the methodologies for performing these tests using the existing passive vent system as a low-cost collection system did not provide realistic results. As anticipated, the nature of the existing passive biogas venting system did not allow for accurate gas flow rates and sustainability values at this site. Several attempts were made to direct gas flows in the system toward a single vent riser by closing off all of the vent risers in a network except for one that would be used to determine the flow rates by measuring gas velocities in the vent pipes to approximate the sustainability of the gas in the system. However, all of these attempts yielded values that were determined not to be an accurate representation based on calculated approximations using known landfill site parameters. An actual sample LFG well would need to be installed in a closed phase, or several wells would need to be installed in several closed phases, to obtain the actual flow rates and gas constituents because of variability in waste properties and the environmental conditions in that phase.

All of the cost data presented in this study are intended to illustrate the nature of cost items that may be included when project economics are evaluated. The actual costs of a specific project are dependent on project configuration, design, equipment selection, location of equipment, and other site-specific factors. Thus it is strongly recommended that an engineering firm be consulted when any large investment in a LFG energy recovery project is considered.

Basic Assessment of the Landfill Site

Estimating Biogas Generation

Using data compiled from the City of Grand Forks Annual Waste Management Logs and the Manufacturing or Processing Equipment Annual Emission Inventory Report (Amundson, 2006), the landfill site had 3.0 to 3.1 million tons of waste in place at the end of 2006 (Method 25-C, 2006), with approximately 3.5 million tons of total projected waste in place by site closure in 2009.

Two methods of calculating gas production and recovery potential can be used (U.S. Environmental Protection Agency, 1996):

- Simple approximation calculation method
- First-order decay calculation method

These calculations are based on the following known and derived data:

- Amount of waste in place (2,788,060 million gallons [Mg] or 3,073,936 tons of MSW, 1963–2006) (Method 25-C, 2006)
- Age of landfill (40 years and still accepting waste; 2009 expected closure; 3,174,500 Mg or 3,500,000 tons of MSW at closeout)
- Waste acceptance rates (84,624 Mg or 93,300 tons in 2006 and average annual rate of 69,700 Mg/year or 76,848 tons/year)
- Methane generation rate ($k = 0.02/\text{year}$)
- Methane generation potential ($L_0 = 170 \text{ m}^3/\text{Mg}$ or $2.723 \text{ ft}^3/\text{lb}$) from the site

The simple approximation calculation method gives a rough approximation of LFG production that can be estimated easily using the amount of waste in place as the only variable, but this does not accurately reflect the type of waste, climate, and other characteristics present at a specific landfill:

$$\text{Annual LFG Generation (ft}^3\text{)} = 0.10 \text{ ft}^3/\text{lb} \times 2000 \text{ lb/ton} \times \text{Waste-in-Place (tons)}$$

The first-order decay calculation model can be used to account for changing gas generation rates over the life of the landfill of a proposed project. Understanding the rate of gas flow over time is critical to evaluating project economics. The first-order decay model is more complicated than the rough approximation described above and requires knowledge or estimates for the following five variables:

- Average annual waste acceptance rate
- Number of years the landfill has been open
- Number of years the landfill has been closed, if applicable
- Potential of the waste to generate methane
- Rate of methane generation from the waste

The first-order decay model is given as:

$$LFG = 2 L_0 R (e^{-kc} - e^{-tf})$$

Where

- LFG = total amount of LFG generated in current year (ft³ or m³)
- L₀ = total methane generation potential of the waste (ft³/lb or m³/Mg)
- R = average annual waste acceptance rate during active life (lb or Mg)
- k = rate of methane generation (1/year)
- t = time since landfill opened (years)
- c = time since landfill closure (years)

After substituting the known and derived values into the above equation, approximately 875 scfm of gas production potential was calculated. However, the uncertainty associated with LFG production in this estimate should be accounted for by subtracting 25% to 50% to assume an actual potential recoverable gas flow of 400 to 600 scfm (575,000 to 865,000 scf/day) for this site.

The methane generation potential, L₀, represents the total amount of methane that 1 pound of waste is expected to generate over its lifetime. The decay constant, k, represents the rate at which the methane will be released from each pound of waste. The values for L₀ and k are dependent in part on local climatic conditions and waste composition.

In 1996, EPA established regulations under Title V Annual Compliance Certification for the control of LFG at new and existing MSW landfills with design capacities in excess of 2.5 million metric tons. Affected landfills, like Grand Forks, model their gas emissions using the first-order decay model. These calculations utilize a combination of default and derived values as well as a concentration of nonmethane organic compounds (C_{NMOC}) equal to 261.53 ppmv as hexane.

The gross power generation potential represents the installed power generation capacity that the gas flow can support. It usually does not account for parasitic loads from auxiliary systems and equipment like gas cleanup systems or for system downtime. Gross power

generation potential can be estimated using an equation such as the following (U.S. Environmental Protection Agency, 1996):

$$kW = LFG \text{ Flow } (ft^3/d) \times \text{Energy Content } (Btu/ft^3) \times 1/\text{Heat Rate } (kWh/Btu) \times 1 \text{ d}/24 \text{ hr}$$

Where

- LFG flow is the net quantity of LFG per day that is captured by the collection system, processed, and delivered to the power generation equipment. This is usually 75% to 85% of the total gas produced in the landfill.
- Energy content of LFG is approximately 500–600 Btu/ft³.
- Heat rates can be given at 12,000 Btu/kWh for ICEs and combustion turbines above 5 MW and 8500 Btu/kWh for combined-cycle combustion turbines.

A simple substitution of values yields a 1.5- to 2.0-MW gross power generation capacity for the total gas flow calculated above.

The net power generation potential is given as the gross power generation potential less parasitic loads from compressors and other auxiliary equipment. Parasitic loads can be estimated to range from 7% for ICEs to 17% or higher for combustion turbines. Applying this to the gross power generation potential from above, we get 1.25- to 1.66-MW net power generation potential after parasitic loads are accounted for (U.S. Environmental Protection Agency, 1996).

The annual capacity factor can be explained as the share of hours in a year that the power-generating equipment is producing electricity at its rated capacity. Typical annual capacity factors for LFG projects can range between 80% and 95% and are usually based on generator outage rates (4% to 10% of annual hours), LFG availability, and overall plant design. An assumed annual capacity factor is usually 80% or 90% (U.S. Environmental Protection Agency, 1996).

The annual electricity generated is the amount of electricity generated in a year, measured in kWh, taking into consideration the possibility of energy recovery equipment downtime. This value is calculated by multiplying the net power generation potential by the number of operational hours in a year. Annual operational hours are estimated as the number of hours in a year multiplied by the annual capacity factor (U.S. Environmental Protection Agency, 1996). Thus:

$$\text{Annual Electricity Generated } (kWh) = \text{Net Power Generation Potential } (kW) \times 24 \text{ hr}/\text{day} \times 365 \text{ days}/\text{yr} \times 80\%$$

For the Grand Forks landfill site, this equation yields 8700- to 11,500-MWh annual electricity generation potential, assuming 80% annual capacity.

Overall, the first-order decay equation is an acceptable approximation of the energy generation potential at a landfill site. However, because of specific site conditions that cannot be

accurately taken into consideration in this equation, the power generation results of this model approximation tend to be higher than are historically achieved in practice. Nevertheless, being an approximation, it offers a starting point to begin further investigations into any energy recovery project.

Biogas Sampling

As part of evaluating economical approaches to harvesting LFG at small municipal sites, part of this task investigated using the existing passive venting system already installed in seven closed phases at the Grand Forks landfill site (Figure 61). The Grand Forks LFG site currently utilizes a branched collection system to control the buildup of biogases at the site under the landfill cover. This vent system uses a series of 4-inch PVC vent risers spaced 100 feet apart above the contour level at 850 feet above mean sea level (MSL). The vents are interconnected by a perforated 4-inch PVC pipe surrounded by washed pea gravel sitting on top of the waste layer just below the cover. This network interconnects and links all of the current seven closure phases and will eventually connect the entire site after final closure in 2009.

The Grand Forks municipal landfill site is undergoing a planned closure (Orr-Schelen-Mayeron, 1990). Following completion of the 10-foot vertical expansion over a small portion of the overall site (Closure Phase IX) (Figure 62), the landfill is now scheduled to close approximately 1 year later than the originally planned closure in 2008. At the time this report was completed, seven closure phases were completed, with two more planned by the time the site actually closes in 2009.

During the gas-sampling phase of this project, only Closure Phases I through IV were complete. Phase I closed and was capped in 1993, Phase II in 1994, Phase III in 1999, and Phase IV closed in 2003, with the cap finished in early 2004. Since the gas-sampling part of this task concluded, Phase V was closed in 2005, Phase VI was closed in 2006, Phase VII was closed in 2007 with the final cap planned to be complete in early 2008, and Phase VIII is scheduled to be closed and capped by the end of 2008.

Closure Phases V, VI, and VII were completed in 2005, 2006, and 2007, respectively, just after the samples for this investigation were taken. Additionally, in October of 2006, three 5-inch-diameter piezometer wells were installed and became operational (Figure 63). These wells range between 14 and 28 feet deep, extend to within 2 feet of the landfill bottom, have the lower 10 feet screened, and are primarily designed to monitor leachate levels at the site. However, by their design and optimal locations within Closure Phases I, III, and IV, the wells would make excellent gas-sampling locations for future monitoring or remediation investigations.

The current passive biogas collection system at the site is a simple passive collection network of 4-inch perforated PVC piping that sits between the cap and the uppermost layer of the waste. It was anticipated that such a shallow interconnected system could be used as an economical approach to collecting a significant portion of the biogas being produced by this site. This would warrant not installing numerous collection wells along with their requisite header and lateral systems. During the period of performance of this project, gas samples were taken and

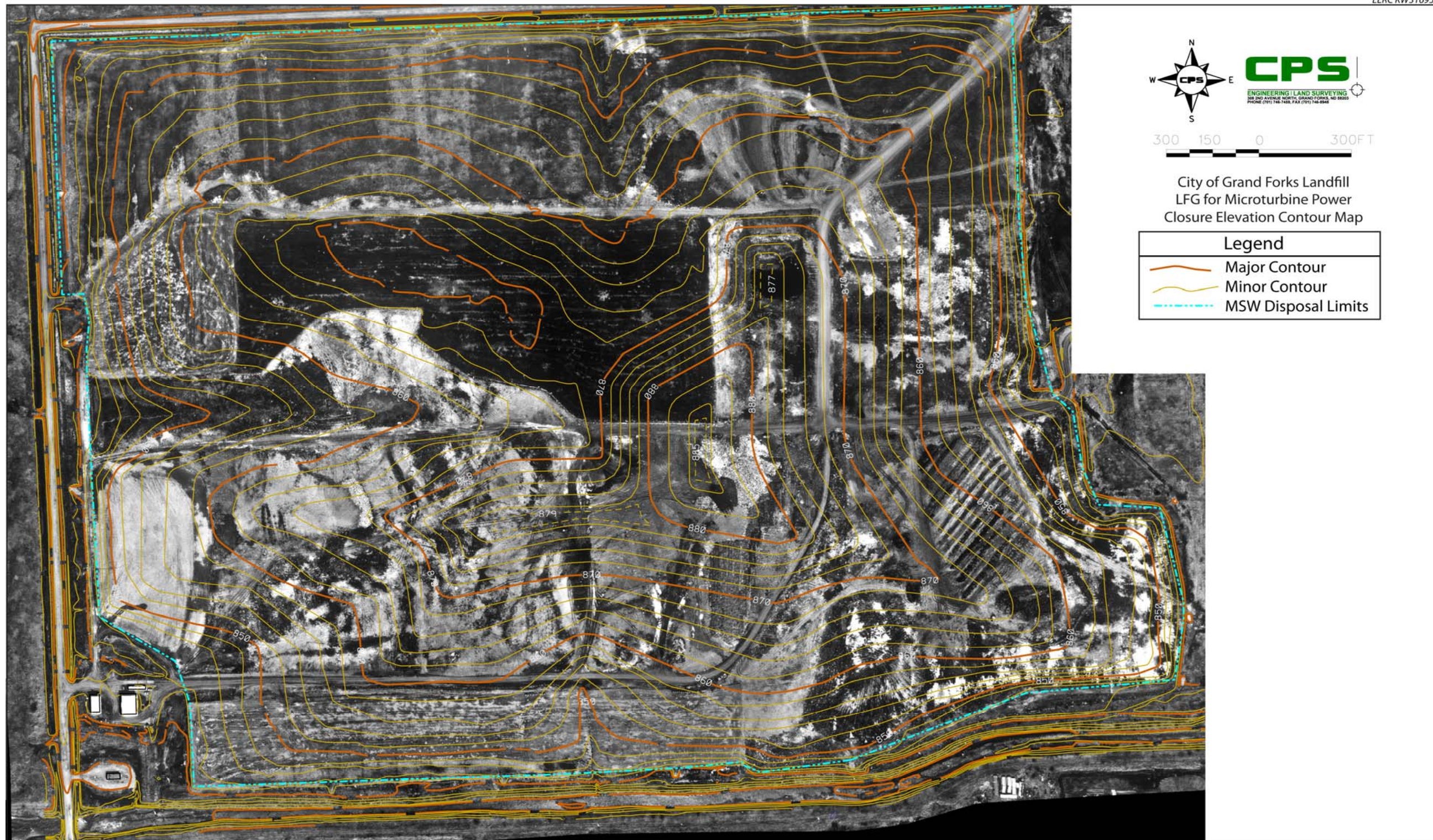


Figure 62. Closure elevation contour map. This aerial view of the waste facility shows the planned elevations across the site. Note the 885 foot above MSL contour lines in the central part of the landfill indicating the location of the planned vertical expansion for the final Closure Phase IX. The MSW disposal limits are shown as the blue line.

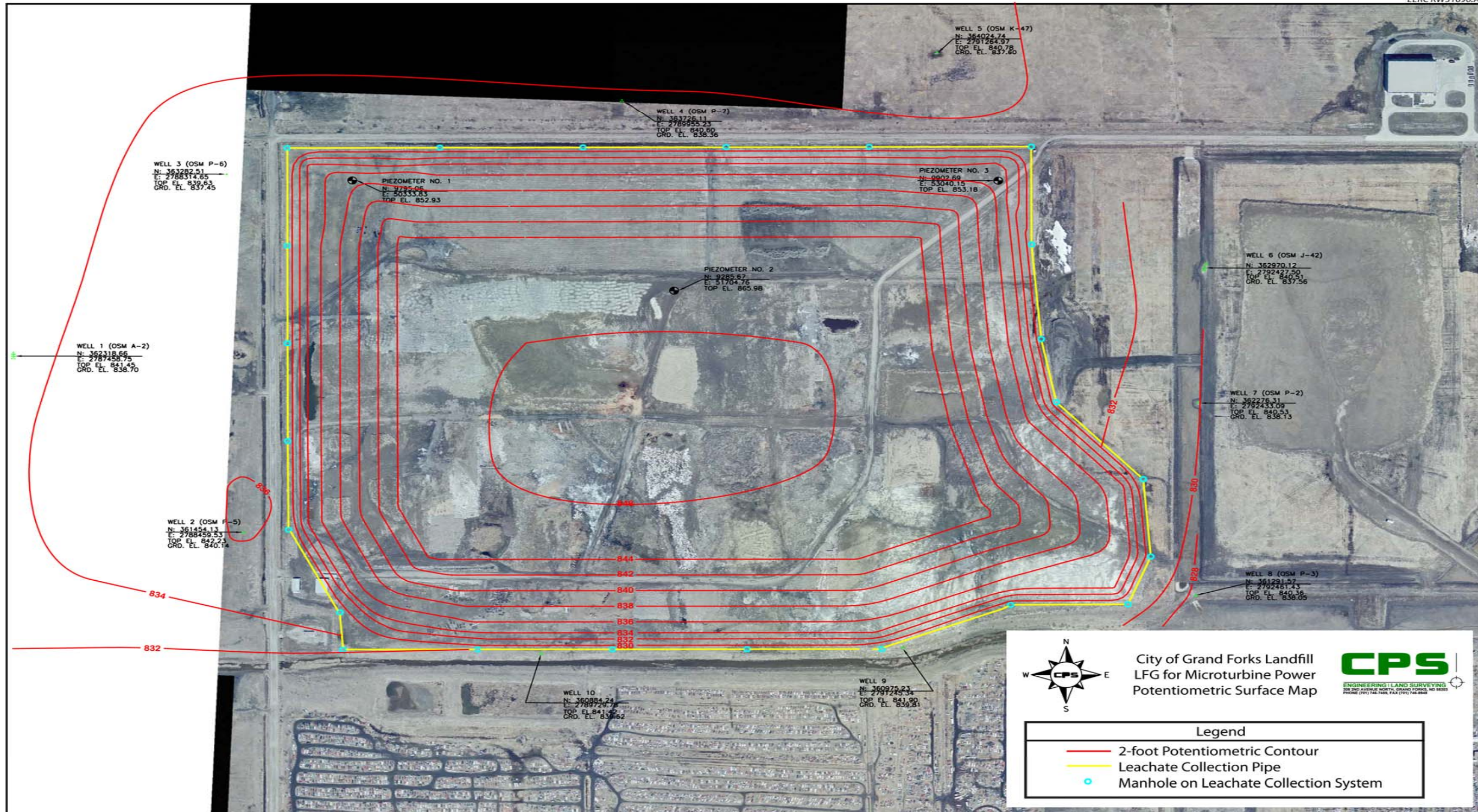


Figure 63. Potentiometric surface map. Detail of the 2-foot potentiometric surface contour map of the groundwater within the landfill site developed by observation wells on site. Note the location of the piezometer wells and the perimeter leachate collection pipe (yellow perimeter line). Note the 16-foot rise in groundwater elevation from the perimeter to the center of the site. This compares to a ground surface elevation of 840 feet above MSL toward the center of the site. The bottom elevation of the landfill site is assumed to be between 820 and 825 feet above MSL.

flow velocity measurements attempted at designated vent risers in Closure Phase I, II, III, and IV. The sample locations were selected because of the elevation of the riser (high point in the network) or location (end of run). The gas samples taken were used to determine gas constituents (total VOCs, siloxanes, CO₂, and moisture) and methane content (in Btu). In each case, however, the flow velocity could not be accurately determined. A simple hand-held mechanical vane anemometer was used to record velocity of the gas through the vent pipe. After numerous attempts at blocking off risers in isolated sections of the network to allow a directed flow to a single riser, it was concluded the design of the passive venting system does not appear to be conducting enough gas through the pipes to be measured.

By installing biogas demonstration extraction wells in a single closed phase or several wells in several closed phases, it may be possible to get the actual flows and gas constituents that would be due to variability in waste properties and the environmental conditions in any given phase. Thus from the entire site (400–600 scfm) utilizing an active collection system under ideal conditions, it may be possible to generate 576,000–864,000 scf/day of biogas, which is equivalent to 315–475 MMBtu/day.

Existing Passive Gas Collection System

Passive gas collection systems use existing variations in landfill pressure and gas concentrations to vent LFG into the atmosphere. The existing passive vent system at the city landfill site is a simple system of slotted PVC pipes installed just below the cap (Figure 61). This existing venting system was examined as a possible low-cost, alternate collection network; however, as described above, no biogas flow rates were recorded from the network.

In mid-2007, biogas velocity measurements (Table 59), using the handheld anemometer as described above, were conducted at the three piezometer well locations in Closure Phases I, III, and IV as described above. These measurements represent the maximum velocity and corresponding energy value at each well.

As can be seen by the variable velocity measurements from these three wells located in different parts of the landfill site, the waste-in-place models are still needed to estimate the range of flows from the entire site based on amount of waste, depth of waste, moisture content, and time.

These measurements yield a combined average instantaneous velocity of about 345 ft/min or about 47 scfm from the three 5-inch-diameter pipes that were installed only to monitor and extract leachate water. These simple velocity measurements indicate raw biogas is passively venting from the existing piezometer wells at about 66,000 scf/day, or about 22,000 scf/day per well on average. Thus each well is venting the equivalent of about 12 MMBtu/day (at 550 Btu/scf) of lost energy production potential. This represents a revenue loss of about \$110/day or about \$40,000/year at the city's current natural gas value of \$9.48/MMBtu.

Extrapolating the venting estimates from the piezometer wells, it is possible to apply this information to the entire landfill site and speculate the biogas production potential and revenue from the entire site using the collected biogas data.

Table 59. Piezometer Biogas Velocity Measurements for Wells in Closure Phases I, III, and IV Taken Mid-2007

Piezometer Well No.	Velocity, m/s	Velocity, f/m	Flow, 5-in pipe scfm	Flow, 5-in pipe scf/d	Energy Value, MMBtu/day
1	0.3	59	8	11,500	6.3
2	0.6	118	16	23,000	12.7
3	1.7	334	45	64,800	35.6
Total	2.6	511	69	99,300	54.6

Assuming an on-site well field installation of fifty-three 250-foot zone-of-influence biogas extraction wells, each produces an estimated average 22,000 scf/day, for a total of 1,166,000 scf/day of biogas (Figure 64). This is the equivalent of about 640 MMBtu/day (at 550 Btu/scf) of energy potential and about \$6000/day or \$2,190,000/year revenue at \$9.48/MMBtu. However, since LFG sites do not produce gas uniformly, we can apply an approximate correction factor of 65%–70% to the annual production and revenue estimates. This lowers the overall biogas production to about 795,000 scf/day, reduces the energy potential from the biogas estimation for the site to around 435 MMBtu/day, and decreases the annual revenue from the biogas to around \$1,500,000 at \$9.48/MMBtu.

VOC and Siloxane Analysis Methods

In order to develop an accurate profile of any LFG, comprehensive biogas testing must be performed. A complete battery of the necessary tests includes major gas components, complete identification and speciation of the VOCs, measurement of the hydrogen sulfide and organic sulfur contaminant concentration, and siloxanes. All of the gas analyses of the LFG for this study were conducted by Air Toxics in Folsom, California, under contract to AFT.

Biogas testing for VOCs involved collecting the gas samples from each sampling point in one or two Tedlar bags, about 1 liter each. These samples were sent directly to Air Toxics where the samples were analyzed for contaminants by GC–MS methods.

The next group of VOCs addressed during a comprehensive LFG analysis were the siloxanes. The siloxanes were determined by the SIL-1TM sampling method (Modified Dow Procedure or chilled-methanol impinger approach) and then by direct injection of the methanol into a GC–MS for species identification and quantification of the targeted siloxanes (Tower, 2004).

The method used for analyzing the methanol from the impingers for siloxanes is by GC coupled with MS. With this technique, not only is the total mass of siloxanes determined but also the individual species and their masses. By knowing the volume of gas passed through the sampling train and the mass of siloxanes measured, their concentrations can be calculated. Although this was the method used to determine the gas constituents for this study, it should be noted that, until recently, this was the most common commercially available analysis for siloxane; however, this technique is no longer popular because of its high cost and lack of repeatability. Current analytical procedures utilize a Tedlar bag to capture the gas from the



Figure 64. Planned biogas collection system. This schematic shows the relative distance between the landfill site, the baling facility (northeast corner of landfill, across from the composting site), and the wastewater treatment plant (upper center). The image shows 53 gas extraction wells, the 250-foot zone of influence for each well, the collection system, and the biogas treatment and power generation package. The possible scenario given here places the cogeneration package at the WWTP and assumes only electricity would be sent to the baling facility over a city-owned transmission system, while both electricity and heat would be utilized at the WWTP.

landfill collection system and directly analyze the gas in a GC–MS. This technique is faster, less subject to sample variability, and more accurate. Most importantly, it is repeatable (Wetzel, 2007).

The concentration of siloxane in the methanol, in mg/m^3 , and the ppbv in the gas can be calculated from the volume of methanol and the volume of the gas quantity passed through the impingers. The stated reporting limit is 16 to 49 ppbv for individual siloxanes, but in practice, limits of detection vary from 19 ppbv to 189 ppbv. Previously, only cyclical siloxanes up through decamethylcyclopentasiloxane (D5) were reported at a detection limit of $0.03 \text{ mg}/\text{m}^3$. Recently, dodecamethylcyclohexasiloxane (D6) was added to this list. Table 60 shows the present detection limits of the siloxanes normally encountered in LFG (Tower, 2004).

Damage inflicted by siloxanes can be profound, causing more frequent maintenance and lowering power generation capacity. During combustion of the LFG, siloxanes are oxidized to SiO_2 , the main ingredient in sand and glass. Analysis of deposits from engines burning LFG containing siloxanes shows that additional reactions occur to form silicates, or chemicals containing the SiO_3 group, and more complex silicates. ICE deposits are mainly silicates, and silicates can contain metals such as sodium, potassium, magnesium, calcium, and aluminum or iron or manganese.

Basic Capital Cost Estimates

The capital equipment costs for any LFG system are dependent on numerous factors, including gas contaminants, amount of gas produced, size of the project, and the end use of the energy produced. Some of the more common estimated costs associated with a LFG system are given in Table 61 along with the percentage that cost represents of the total capital amount. Similar values to the typical capital costs were used to determine the simple payback approximation for this investigation.

Typical LFG recovery projects have an estimated economic life of 15 years—or 20 years for dry climate projects. Typical contracts with the landfill owners range from 15 to 25 years; however, the economic life for debt service is often estimated at 10 years for the recovery of the investment.

Initial Economic Energy Production Profile

Preliminary studies of the Grand Forks municipal landfill site indicate good potential for biogas recovery and use leading to electricity production. The Grand Forks landfill is currently undergoing plans for a 10-foot vertical extension that can give the site another 1 year of accepting waste, thereby increasing its power generation potential and extending the duration of power generation. The City of Grand Forks is considering that any power or CHP generated would be utilized on-site by the baling facility and/or the wastewater treatment facility, and this electrical generation would be accomplished by either a piston engine generator or a microturbine. Since methane gas is an extremely powerful greenhouse gas, utilization of this biogas to generate supplemental power for either site makes good sense for the environment, plus it can help offset some energy costs associated with site operation. By keeping the power

Table 60. Common Siloxane Species and Their Current Detection Limits by GC-MS

Siloxane Species	Detection Limit, mg/m ³	Detection Limit, ppbv/v
Pentamethyldisiloxane	0.03	48.78
Hexamethyldisiloxane (MM)	0.03	44.58
Octamethyltrisiloxane (MDM)	0.03	30.61
Octamethylcyclotetrasiloxane (D4)	0.03	24.41
Decamethylcyclopentasiloxane (D5)	0.03	19.53
Dodecamethylcyclohexasiloxane (D6)	0.03	16.27

Table 61. Estimated Common Capital Costs for LFG Systems

Item	Range	Typical	Percent
Collection System	\$300,000–\$1,000,000	\$400,000	11
Engineering	\$30,000–\$1,000,000	\$200,000	6
Gas Treatment System	\$250,000–\$1,200,000	\$750,000	22
Interconnect Cost	\$50,000–\$250,000	\$100,000	3
Generating Equipment	\$500,000–\$2,000,000	\$1,600,000	46
Contingency	15% of equipment costs	\$425,000	12
TOTAL	\$1,130,000–\$5,450,000	\$3,475,000	100

generated by the biogas off the electrical grid, issues involving avoided costs and interconnection fees for this power could be eliminated.

In recent years, a significant amount of attention was focused on siloxanes in LFG and the costly problems they create for operators of power generation equipment. While it is important to focus on siloxanes, it is equally important to focus on the overall gas-conditioning systems. Generally, gas-conditioning packages lower both total VOCs and organosilicon species below the current detectable limits and can exponentially increase power generation equipment efficiency and lifetime while lowering downtime and maintenance costs. However, the overall costs for these systems can be quite high considering the relatively low gas flows of a typical landfill site. For sites with greater than 3-MW potential (higher gas flows), the cost of gas collection, cleanup and preparation, and power generation can be more than \$2,000,000 per MW. For sites with less than 3-MW potential (lower gas flows), the costs can be similar because current technology for gas cleanup and power generation are not scalable to gas flow rates (Tower, 2006).

While LFG can be considered a “free” fuel, the gas pretreatment requirements for its utilization in any combustion system can significantly add to the costs associated with LFG utilization for energy recovery. The next generation of VOC and siloxane removal technology should be scaled to the gas flow rates and contaminants, such that maintenance costs are lower and not cost-prohibitive for smaller-volume biogas generation sites including small landfill sites, that have a generation potential of less than 3 MW (<60 scfm) and wastewater treatment plants (<60 scfm).

Summary Economic Feasibility Considerations

Based on our findings, supported by current literature, the following considerations are offered regarding the economic feasibility of the Grand Forks LFG energy project:

- The capital and operating costs associated with LFG pretreatment systems can add significantly to any project costs. Typically these costs are seen to be between \$900/kW and \$1500/kW, or \$400–\$1000/cfm. Thus when considering the EPA Landfill Methane Outreach Program (LMOP) estimate of \$2000–\$2500/kW systems, the nonturbine costs for most pretreatment systems appear to account for about 60%–65% of the total system costs.
- Power generation equipment service life could require ongoing capital investments. The service life goal for the current and next-generation combustion systems, including major overhauls every 11,000 operating hours, is 45,000 hours, or about 5 years. This suggests that additional significant capital investments, up to and including power generation and/or gas treatment equipment replacement, may be required about every 5 years (Wheless and Wiltsee, 2001).
- The overall success of a municipal project may ultimately depend on higher avoided retail energy costs, extended renewable energy credits (REC), and/or continued governmental grant funding. Most of the projects that were reviewed under this project received some degree of grant funding in addition to reduced cost or donated equipment. The most successful projects appear to have been implemented in service areas where the avoided electricity costs were relatively high, \$0.14 to \$0.16/kWh. The economic feasibility of any LFG project will be hampered in service areas with lower avoided electricity costs, lower REC revenues, and/or where grant funding is difficult to obtain or simply not available (Nagl, 2008; U.S. Environmental Protection Agency, 2002a).

Overall project economics will improve with increased experience and innovation. The application of microturbine systems in LFG recovery projects is less than 5 years old. Given the significant benefits associated with these systems, it is likely that the economic feasibility of these systems will continue to improve as a result of ongoing research and development programs at the federal and state level.

Results and Discussion

Geology of Grand Forks County

Grand Forks County in northeastern North Dakota is underlain by glacial drift, westward-dipping Paleozoic and Mesozoic sedimentary rocks and Precambrian igneous and metamorphic rocks. Glacial drift covers the bedrock to a maximum thickness of 455 feet. This drift can be differentiated into five specific drift sheets; each sheet can be separated into till units, lake clay and silt units, and sand and gravel units. Relief on the bedrock surface is observed to be greater than the relief on the present glacial topography.

Eastern Grand Forks County is mainly a lake plain underlain by clay and silt and, in places, sand and gravel. Northwest of the city of Grand Forks, saline soils occur above the shallow subcropping Dakota Group sandstones. An extensive, discontinuous bed of silt underlies the lake plain in the eastern part of the county. Lake Agassiz originated as a small proglacial lake which expanded in area and rose to the maximum level of the Herman beaches. Later, as the glacial ice receded, the lake receded and drained in a number of steps marked by strandlines. The Agassiz Lake Plain district includes a large area of eastern North Dakota and northwestern Minnesota. It is a flat area that slopes almost imperceptibly toward the Red River of the North. Modifications on the lake plain include short segments of end moraine, beach ridges and scarps, and tree-lined river valleys. The westernmost boundary of the Agassiz Lake Plains district is on the west side of the Herman strandline except in northwestern Grand Forks County where it is along the west edge of an outwash plain. The lake plain slopes from an elevation of 1060 to 1070 feet above sea level in western Grand Forks County northeastward to an elevation of about 800 feet above sea level in northeastern Grand Forks County (Hansen and Kume, 1970).

Landfill Site Geologic and Hydrologic Conditions

The Grand Forks landfill is located in eastern Grand Forks County, about 4 miles west of Grand Forks in TWP 152 North, Range 51 West N ½, Section 35 (Figure 65). This site encompasses about 180 acres. Previous site investigations determined the site is located in fine-grained lacustrine sediments in a saline discharge area. Numerous hydraulic wells installed in the area have depths from 5 to 42 feet and have revealed that the lacustrine sediments are saturated to near the ground surface, with the groundwater flow regime dominated by vertical hydraulic gradients instead of horizontal gradients. The vertical gradient fluctuates seasonally with a downward movement during the spring and summer months and upward during the winter months. The upward movement is the result of regional discharge from the underlying bedrock aquifers. The water quality in the shallow groundwater flow system is mixed chlorides characterized by high total dissolved solids concentrations with pH near 6.5. It was shown the Grand Forks landfill does not endanger groundwater supplies because of the slow horizontal flow velocities and strong upward flow gradient (Olson and Greer, 1994).

Landfill Biogas-to-Energy System Overview

The most common types of landfill treatment facilities for smaller landfill sites utilize blower/flare or energy generation systems. Other common treatment or disposal options may include the following:

- Free vent to atmosphere (because the methane is a powerful greenhouse gas, this option is becoming regarded as unacceptable and soon may no longer be an option)
- Venting through activated carbon
- Destruction by flare (open flame) combustion
- Utilization in an energy recovery process (power, heat, or a combination) using combustion as the primary method of LFG use

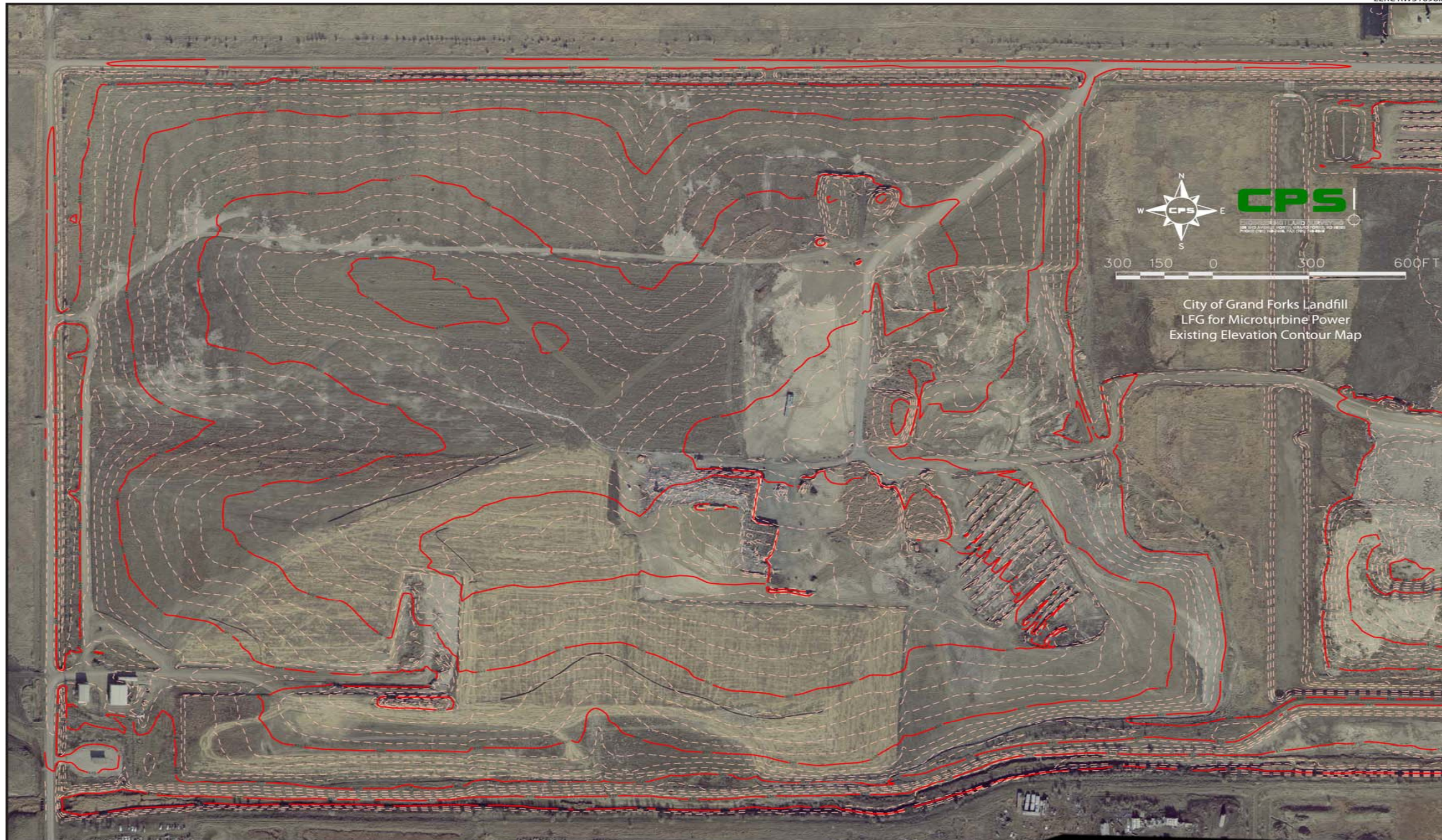


Figure 65. Existing elevation contour map. This schematic represents an aerial view of the city MSW facility, showing the current elevation contour lines within the MSW disposal limits.

LFG Well Field System

The typical LFG well field system consists of a network of LFG extraction wells, including flow control valves and monitoring ports, and LFG collection piping, including condensate water collection points (sumps and/or knockouts), isolation valves, and monitoring ports used to transport the LFG to the treatment or disposal (combustion) facility (Solid Waste Association of North America, 1997).

LFG Well Field

LFG is collected by means of wells or collectors installed in the landfill. The system of wells and collectors is referred to as the well field. As a result of the variability in the LFG production because of the basic landfill site characteristics, the collection system requires constant balancing of the wells to achieve a smooth, steady-state system operation for effective biogas recovery and control.

LFG Collection System

The active LFG collection system consists of piping for collection and transport of the extracted LFG to a blower/flare facility or other treatment, disposal, or energy recovery process. Common collection piping can be PVC or high-density polyethylene (HDPE). Condensate is removed from the LFG collection system by a separate handling system. This system consists of a series of traps, drains, sumps, pumps, knockouts, storage tanks, and treatment equipment. The condensate is then removed, treated, and disposed.

Header and Lateral System

LFG is transported under vacuum to gas pretreatment and end-use equipment through a network of collection piping. The main pipe from the well field to the blower facility is called the header. The secondary pipes that connect the wells in the field to the headers are called laterals. The entire collection network can be buried beneath the cap and routed around the landfill. Header piping may be arranged in a branched, looped, or matrix configuration. LFG collection systems can be categorized as basic vertical wells and horizontal trenches.

Vertical Well System

The most common system for LFG collection is the vertical well system. Vertical wells are installed within the landfill for emission control and energy recovery projects. Typical well depths range from 25 to 75 feet, but may exceed 100 feet, depending on landfill depth. Wells are typically drilled to the depth of the liquid level in the landfill, or to approximately 75% of the landfill depth, whichever is less. Well drilling requires careful monitoring to avoid affecting the bottom of the landfill. The well spacing is dependent upon landfill characteristics (landfill depths, refuse type, compaction rates, and cover materials). Well spacing generally ranges from 50 to 300 feet (U.S. Environmental Protection Agency, 1991b). The vertical well system uses a blower or compressor to extract the LFG under vacuum from the landfill through the piping network.

Passive Collection System

Passive gas collection systems use existing variations in landfill pressure and gas concentrations to vent LFG into the atmosphere or a control system. Passive collection systems can be installed during active operation of a landfill or after closure. Passive systems use collection wells, also referred to as extraction wells, to collect the LFG. The collection wells are typically constructed of perforated or slotted plastic and are installed throughout the landfill to depths ranging from 50% to 90% of the waste thickness or just under the cap layer. If groundwater is encountered within the waste, wells end at the groundwater table. The vertical well system is typically installed after the landfill, or a portion of a landfill, has been closed. At some smaller sites, the collection wells vent directly to the atmosphere or convey the biogas to treatment or control systems such as a flare.

Active Collection System

Active collection systems are considered the most effective means of LFG collection (U.S. Environmental Protection Agency, 1991a). Active gas collection systems can include vertical and horizontal gas collection wells similar to passive collection systems. Unlike the gas collection wells in a passive system, however, wells in the active system should have valves to regulate gas flow and to serve as a sampling port. Sampling allows the system operator to measure gas generation, composition, and pressure. Active gas collection systems include vacuums or pumps to move gas out of the landfill and piping that connects the collection wells to the vacuum. Vacuums or pumps pull gas from the landfill by creating low pressure within the gas collection wells. The low pressure in the wells creates a preferred migration pathway for the LFG. The size, type, and number of vacuums required in an active system to pull the gas from the landfill depend on the amount of gas being produced. With information about LFG generation, composition, and pressure, the landfill operator assesses gas production and distribution changes to actively modify the pumping system and collection well valves to most efficiently run an active gas collection system.

LFG Treatment System

A typical landfill biogas system consists of an extraction well and gas collection system to direct the gas to the treatment skids before being sent to the microturbine or ICE for heat and/or power generation. Any combustion system must deal with fouling, corrosion, excessive wear of components, and potential failure from silica or other constituents found in LFG. The level of required fuel pretreatment, which dictates the number of treatment steps, varies depending on the characteristics of the LFG and the power generation package manufacturer. New biogas technologies and innovative processes are used to pretreat LFG prior to introduction to any energy generation equipment and typically cost around \$750/cf biogas produced and are usually designed to remove moisture, H₂S, and total VOCs and siloxanes. Siloxanes represent the most significant problem in biogas because they form SiO₂ upon combustion. SiO₂ is a white, powdery substance that accumulates on the heated surfaces in the combustion equipment, especially in the cylinders of IC generator engines and combustion chambers of microturbines. An ICE burning biogas containing just 1 ppmv of a common siloxane known as D5, for example, will generate approximately 130 lb of SiO₂ per year if operated continuously. Not all of this SiO₂

will remain in the engine; however, what does remain can cause extensive damage, causing more frequent maintenance, and lowering overall power generation capacity (Tower and Wetzel, 2004).

AFT in Snohomish, Washington, developed a nonmechanical process to remove siloxanes from biogas in 1996. The basis of this process is sequential removal of siloxanes and other contaminants in what is termed a Selective Active Gradient™, or SAG™. The SAG process utilizes gas-sieving media called PMG™ or PolyMorphous Porous Graphite™. Siloxanes are removed and trapped by the PMG, which requires easy periodic replacement. The SAG process has proven to be the most effective siloxane removal method available. The SAG process uses a novel form of polymorphous graphite developed by AFT to remove siloxanes from methane containing many types of organics. The SAG PMG media uses a novel application of physical sieving to remove the siloxanes in the presence of other organics in the gas, thereby allowing the beneficial fuel constituents to pass through (Tower, 2003).

In early 2004, AFT introduced the SWOP™ process for heavily contaminated biogas (50 ppmv, or in some cases lower, depending on what makes up the bulk of the VOCs). The SWOP process utilizes media that is regenerated on a continuous basis to prevent siloxanes, halogenated VOCs, and other harmful VOCs from entering combustion equipment or being released into the atmosphere. The SWOP process has a low pressure drop and has just a few moving parts. It is compact, small, relatively inexpensive to use, and fully automated and can remove virtually all organosilicons and VOCs that can foul boilers, IC engines, turbines, microturbines, and emission catalysts (Tower et al., 2006).

LFG Cogeneration System

The Capstone CR65-ICHP (65 kW) is a renewable energy microturbine system from Capstone Turbine Corporation. This generation package is a biogas-fueled 65-kW power/heat generator that can be arrayed without switchgear or other external hardware to serve power loads ranging from several kilowatts to more than a megawatt. The Capstone microturbine engine has no mechanical subsystems and uses no oil, lubricants, coolants, or other hazardous materials. These generators achieve extremely low emissions without any exhaust treatment devices or chemicals and emit no ammonia, mercury, carcinogenic soot, or other toxics common to other power plants. The CR65 engine also destroys methane and nonmethane organic compounds far more effectively and with far lower pollutant emissions than flaring. This microturbine achieves 64% total fuel efficiency in combined power and water-heating efficiency because of its stainless steel heat exchanger. For biogas applications, this microturbine requires between 325 and 875 Btu/scf and has a standard biogas treatment package that will remove moisture, VOCs and siloxanes, CO₂, and H₂S to <400 ppm with an inlet fuel pressure of 75 psig for a cost of around \$71,500 (Capstone Turbine Corporation, 2008a). The benefits of combining the thermal and electrical outputs of a system are widely recognized. Extracting the exhaust energy that would otherwise be wasted increases the total system efficiency far beyond that of fossil-fueled cogeneration plants. This means more useful work from limited natural resources and less greenhouse gas emissions than using conventional energy conversion technologies (Gillette, 2004).

Comprehensive LFG Gas Analyses

Volatile Organic Compounds

Sampling LFG for VOC analysis involved the use of one or two 1-liter Tedlar bags filled by the use of a small electronic pump. These were sent for analysis by direct GC–MS injection. More than 250 different VOCs can be found in landfill and digester biogas. Normally, most LFG will contain at least 20 to 80 of these, usually commensurate with the total VOC content of the gas. Some LFG contaminants have been found at levels over 100 ppmv. While this test is useful for environmental reasons, it has limited applicability in total LFG quality management. A total VOC survey can detect, identify, and measure the concentration from 50 ppbv to 250 ppmv of all VOCs in a biogas sample. While it may not be necessary to remove all of the detected VOCs from the biogas to meet a particular engine manufacturer's specification, it is important to know what these contaminants are and their concentrations because they can impact the design and overall performance of the gas treatment system as well as impact air emissions (Tower, 2004).

Part of the total VOC survey is measurement of the major gas components: methane, carbon dioxide, nitrogen, and oxygen. The total VOC content is also reported as “NMOC (nonmethane organic contaminants) as hexane.” The comprehensive analysis of the biogas contaminants also reveals hydrogen sulfide and organic sulfur species such as the mercaptans, sulfides, and disulfides. Most power plant manufacturers limit the hydrogen sulfide level in the fuel gas to around 100 ppmv or even lower. High-sulfur-containing VOC contaminant levels in the LFG can result in corrosion and in SO_x emissions to the atmosphere (Tower, 2004).

Biogas properties can vary considerably because of a number of factors: seasonal temperature changes, rainfall, gas withdrawal volume vs. LFG production volume, and pulling from different landfill cells. A complete VOC profile is required to assess the impact of any or all of these factors. Otherwise, any gas treatment system may or may not function properly all of the time. Regardless of how the landfill is managed, the produced LFG needs to have a complete VOC profile analysis to determine its complete characteristics. Known concentrations of methane, CO₂, oxygen, and nitrogen are critical to the design of gas treatment equipment, which serves as the pretreatment to the siloxane removal equipment and other contaminant removal equipment that may be downstream in the entire process. It is also critical to the optimum performance of generator engines and maintenance of air emission levels.

Four basic types of biogas composition data are required for the design of a siloxane removal system:

1. Complete biogas as a volume percent
2. Complete VOC profile, including the individual species and their concentrations
3. Inorganic and organic sulfur contaminants and their concentrations
4. Individual siloxane species and their concentrations

Biogas samples were taken from three different locations at the landfill site using two different types of wells. One set of samples was collected from three passive venting wells, while the second set of samples was collected from three piezometer wells almost 1 year later.

Although the first round of sampling yielded inconclusive analytical results, the second round indicated the fuel components and other constituents could be considered nominal for a 40-year-old upper Midwest landfill. In any case, because of the outdated method of collection and analysis for VOCs and siloxanes, these data cannot be duplicated and must be confirmed by resampling and reanalyzing samples collected from proper extraction wells or, at the very least, a sampling port that extends into the waste above the water surface.

Gas Analysis Results

During the performance of this project, gas samples were collected, and data were generated from four of the closure phases at the landfill site. The samples were analyzed for the complete siloxane series, total VOCs, sulfur species, gas composition, and heating value by AFT in Snohomish, Washington.

As provided by AFT, the following is a summary of the overall gas analyses for the combined Closure Phases I through IV, including siloxane determination, total VOC scan, and major fuel components:

- 50% to 60% methane (with a heating value of 500 to 600 Btu/scf)
- Trace H₂
- 35% to 45% CO₂
- 2% to 5% N₂
- 2% to 5% moisture
- 400 to 500 ppmv total VOCs
- 2.5 to 6 ppmv total siloxanes

Until further gas sampling and analyses are conducted on the gas produced at this site, we will assume these values to be a general cross-sectional representation of the biogas for the entire landfill site through final closure in 2009.

Siloxane Discussion

A major problem with the use of LFG for heat and power production has been silicate deposits. The primary cause of silicate-based material deposition is the increased use of siloxanes in consumer and industrial products over the past 30 years. Siloxanes are a family of man-made organic compounds that contain silicon, oxygen, and methyl groups. During combustion of biogas containing siloxanes, silicon is released and can combine with free oxygen or various other elements in the combustion gas. Deposits are formed containing mostly silica and silicates (SiO₂ and SiO₃), but they can also contain calcium, copper, sodium, sulfur, and zinc. Most deposits caused by combustion of siloxanes are off-white to light brown in color and are of varying texture; some are very smooth with a powdery-looking surface, while others are coarse and grainy. These deposits can ultimately build to a surface thickness of several millimeters and are difficult to remove by chemical or mechanical means. The tendency for silica/silicate deposits appears to vary based on flame front, heated surface area, rotation/tip speed, and postcombustion equipment such as heat recovery and catalysts. These deposits result in higher stack temperatures and poor heat transfer in heat exchangers. In power generation equipment,

silicate-based material is deposited on pistons and in cylinder heads of reciprocating IC engines. In turbines, silicates can cause severe abrasion of impeller blades. These phenomena result in lower power production, reduced heat recuperation and, sometimes, catastrophic failure. As a result, many manufacturers are now requiring removal of siloxanes from the biogas before it enters their equipment. All LFG biogas contains siloxanes and, unless the gas stream is treated in some way before combustion, silicates will form and poison exhaust catalysts, which impedes their ability to reduce CO and NO_x emissions (Tower, 2004).

The use of siloxanes is predicted to increase into the future because of their highly desirable product enhancement characteristics. Siloxanes are manufactured nontoxic additives that improve personal care product properties such as color dispersion, uniformity, and ease of use. Siloxanes are released in landfills during biodegradation and become incorporated in the biogas produced. Siloxanes are difficult to remove from biogas, and once oxidized to form silicates, they become strongly bonded to the heated metal surfaces in reciprocating engines, boilers, and turbines, requiring frequent and expensive maintenance.

Numerous industrial applications for treating siloxane-laden biogas exist. Most involve expensive and sometimes very exotic processes to try and remove or reduce the levels to below the lower detection limits. Because of the cost of these treatment options, the overall cost of utilizing the biogas can also be very high. A typical LFG-to-power system includes the gas collection system and some type of gas pretreatment to remove H₂S, moisture, and most of the total VOCs (including siloxanes). This is followed by use of a compressor, a dryer, and CO₂ removal before the gas stream enters the power or heat generation package. Other applications for LFG sites can have more involved and more expensive processes. One fact remains clear: current biogas treatment technologies and power generation packages typically require very large capital investments.

Major Gas Contaminant Removal Systems

Moisture Removal

The removal of moisture from LFG is the single-most important factor in yielding a stable operation for the microturbines. The literature indicated that early experimentation with desiccants, coalescing filters, and deliquescent filters yielded poor results. The addition of an absorption chiller to cool LFG and a subsequent reheat of the compressed gas yielded better results. Such a system includes a chiller to reduce the gas temperature to 40°F and a gas-to-gas heat exchanger to reheat the gas to near-ambient temperature. Removal of the water also removes calcium, iron, silicon, and other metals. These materials cause a buildup in small orifices of the fuel system.

Carbon Dioxide Removal

For LFG to be used, it must be of a suitable quality for the selected application. One of the largest hindrances to using LFG from landfill sites is gas dilution by air. To enhance the LFG Btu value of the biogas, the CO₂ must be removed.

Liquid absorption processes are available for the simultaneous removal of H₂S and CO₂. These technologies are further characterized by employing chemical or physical absorbents. Chemical absorbents selectively remove acidic compounds by reacting with them to form weakly bonded compounds, which disassociate upon the application of heat. Physical absorbents rely on the solubility of the acidic components in the absorbent, which are then released by merely reducing the pressure. When acidic gases constitute a major portion of the gas stream to be treated, physical absorbents become more attractive because of their lower energy requirement.

Acid gases can also be separated from LFG by utilizing membrane separation techniques. For LFG applications, CO₂ and H₂S have high permeabilities and will pass through a membrane, while CH₄ has a very low permeability and will remain outside of the membrane.

VOC and Siloxane Removal

Traditional treatment systems for the removal of siloxanes and VOCs were found to have several drawbacks. First, they are often expensive to operate. Second, they do not eliminate much, if any, of the VOC contamination. Third, and most importantly, they often do not remove all of the organosilicons, as some are not siloxanes and are much more difficult to remove.

With desiccant-based treatment systems or deep chilling, the siloxanes and VOCs that are removed from the system are either vented to the atmosphere or disposed of on-site as a liquid waste stream. Among the latest types of these treatment systems used for LFG are the following:

- SAG carbonaceous adsorbent media systems
 - SAG is a proprietary process developed by AFT. Although this technology is effective in removing both siloxanes to nondetectable levels and VOCs, it is best suited for gas streams with a low-to-moderate total VOC burden. These systems generate spent media that must be disposed of (Tower, 2004).
- Deep chilling
 - The deep chilling process (–10°F) claims to remove greater than 95% of all siloxanes and VOCs. It produces a liquid waste stream of condensed VOCs that must be disposed of. This process also reduces the moisture level in the gas prior to VOC removal.
- Regenerable desiccant media-based systems
 - It is claimed that the regenerable desiccant system removes greater than 95% of the siloxanes. It is unknown if the desiccant system removes the VOCs and to what extent. The regenerable desiccant system is not normally preceded by a gas-conditioning package, except for a coalescing filter, and removes moisture from the gas until it becomes saturated. Desiccant media regeneration is based on siloxane breakthrough rather than moisture breakthrough.
- The SWOP process
 - A relatively new proprietary biogas treatment system developed and marketed by AFT is the SWOP Process. Five separate process operations comprise this process.

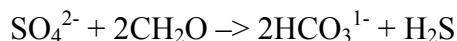
The first of these is the process whereby the biogas contaminants are concentrated onto regenerable media in a concentrator vessel. The second process is the pneumatic conveyance of the media from the concentrator to the stripper and back to the concentrator vessel. The third process is thermal stripping of regenerable media containing the removed and concentrated contaminants. The fourth process is the production of hot regenerant gas by the inert gas generator for use by the stripper. The fifth process is the destruction of the spent regenerant gas stream in a small enclosed ground flare, followed by the SAG final VOC polishing process (Tower, 2004).

Hydrogen Sulfide Removal

More than 350 commercial LFG recovery operations in the United States generate electricity on-site, and historically, very few have required H₂S treatment. Many landfills are now accepting large quantities of construction debris, which can lower LFG quality and increase O&M costs through the postclosure period. Gypsum (CaSO₄ · 2H₂O) wallboard, for example, can generate H₂S gas. In sufficient amounts, this can result in the need for sulfur abatement systems, which can be expensive and complex. Fortunately, the technology for such systems is well-developed and has been in commercial use for the last 30 years.

Hydrogen Sulfide Generation

Under anaerobic landfill conditions, sulfate-reducing bacteria produce H₂S from the sulfate (SO₄²⁻) in gypsum and the organic carbon in waste material as follows:



From the above reaction, if 100 tons of sulfate is placed in a landfill, there is the potential of producing 35 tons of H₂S; most will be released during the active LFG production phase (Phase 4).

Increasing concentrations of H₂S in LFG can have the following negative effects:

- Onset of odor problems
- Corrosion of gas recovery hardware
- Increasing SO_x emissions from flaring or other combustion processes
- Possible health consequences for workers

The level at which gas-quality specifications are exceeded and sulfur removal is required will vary by application, equipment, and vendor. ICEs for LFG projects can tolerate levels as high as 1000–1500 ppmv (total sulfur in gas). Properly specified turbine generators can tolerate in excess of 10,000 ppmv. Gas specifications for microturbines have a very wide range, depending on the manufacturer. However, the sulfur limit for gas turbine systems is often determined by the gas compressor upstream of the turbine, which may tolerate only 75–100 ppmv because a highly corrosive liquid condensate can form during the higher compression required for turbines. Thus many landfills generating electricity require sulfur limits

to be restricted to 75–100 ppmv. However, for sites such as this study site, with relatively low sulfur concentrations and gas flow (<1 million scf/day and 50 ppmv H₂S), the recommended sulfur treatment would typically be a low capital investment scavenger (nonregenerable) system and be simple to operate. The costs of removing the sulfur, while small in total capital expense, can be quite large in terms of cost per unit of sulfur removed (Heguy and Bogner, 2008).

H₂S Removal Systems

A scavenger can be a liquid or solid system. The solid system has several advantages for landfill applications:

- No operators are needed to treat the gas (although the H₂S concentration at the outlet of the system will need to be monitored).
- Media changeout can often be done by contractors.
- Disposal of spent solid media is often easier than liquid waste.
- The system can easily be expanded by additional media.

On the downside, the part of the solid system that is undergoing the media changeout is out of service during that time, and the media changeout process can be messy and allow noxious odors into the surrounding environment. The most common forms of solid scavengers used for treating smaller landfill sites are iron sponge and iron-based systems.

The decision between a simple scavenger system and a more capital-intensive liquid regenerable system are determined by long-term comparison of projected capital vs. operating costs. A payback of just this removal system could occur in 2–3 years at about 400 pounds of sulfur removed per day. Although this payback requirement is an industry standard, municipalities often have a longer payback period, which could make the regenerable system more attractive at lower sulfur removal levels.

Basic Solid Scavenger System

The process description when hydrogen sulfide is converted to iron pyrite is as follows:

- Raw gas is saturated with water.
- Saturated gas passes over the media bed; iron pyrite is formed.
- Treated gas exits the system.

Overall system cost: \$40,000–\$45,000

Operating cost: \$3.00/lb of sulfur removed

Media cost for 1 Mscf/day of biogas is as follows:

- 50 ppm: \$3800/year
- 100 ppm: \$8000/year
- 500 ppm: \$40,000/year
- 1000 ppm: \$80,000/year

Basic Liquid Iron Reduction/Oxidation System

Process description when hydrogen sulfide is converted to elemental sulfur is as follows:

- Raw gas is scrubbed with catalyst solution, sulfur is formed, and the treated gas exits the column.
- Catalyst is regenerated using air and returned to scrubber.
- Sulfur is separated from catalyst.

Overall system cost: \$1M–\$2M

Operating cost: \$0.10/lb of sulfur removed

Economic switching point (scavenger to regenerable system) is as follows:

- 1 Mscf/day: 4500 ppm
- 2 Mscf/day: 2300 ppm
- 5 Mscf/day: 1000 ppm

Gas Pretreatment Costs

The following represents the basic cost estimates for generalized biogas cleanup systems (Wetzel, 2007):

- \$900–\$1000/cfm for complete gas cleanup system, with \$750/cfm being typical
- \$300/cfm for fundamental moisture removal
- \$400/cfm for overall VOC/siloxane removal
- \$200–300/cfm for basic H₂S removal (can be higher depending on amount of H₂S in gas stream)

Energy Losses Due to Parasitic Loads

Another important factor to consider when evaluating the overall LFG gas treatment strategy is the power consumption by fans, compressors, and chillers. Chilling below a certain

point does not usually make sense from a cost/benefit perspective. For example, chilling to remove moisture can also remove from 10% to 60% of the siloxanes, depending on the species present and other gas constituents. Chilling the biogas to temperatures much below 38°F (3° to 4°C) produces little benefit. At lower temperatures, a little more of the siloxanes might be removed, but some of the methane can become hydrated and lost with the condensate. Additionally, with chillers that operate below 32°F (0°C), the coalescers routinely freeze up and need to be thawed. Redundant chillers that cycle back and forth are used to maintain adequate performance through these freeze–thaw campaigns. However, the parasitic load required chilling the gas below 30°F, and this coupled with installing redundant chillers, deicing routines, and the potential of lost methane usually does not justify deep chilling methods (Tower, 2004; Wetzel, 2007).

Basic LFG Economics

Operation and Maintenance Cost Estimates

- Overall life-of-the-project rates are estimated between \$0.015–\$0.018/kWh (U.S. Environmental Protection Agency, 2008).
- Scheduled and unscheduled maintenance for the power generation equipment (microturbines and ICEs) rates are estimated between \$0.015 and \$0.018/kWh (U.S. Environmental Protection Agency, 2008).
- Operation and maintenance costs for the VOC removal system are estimated to be between \$0.03/kWh and \$0.035/kWh (Wetzel, 2007).
- Overall facility operation and maintenance costs are estimated to be between \$0.02 and \$0.025 per kWh (U.S. Department of Energy, 2005).

Economics of Electrical Generation

ICEs appear to be more economical where the supply of LFG is able to produce 1 to 3 MWh, while microturbines with their higher capital costs (between \$1100 and \$1500/kW) appear to be the most efficient at sites with a net power output over 3 or 4 MWh, although there are numerous examples across the nation where this is not the practice.

Advantages of ICEs include comparatively low capital costs (between \$800 and \$1000/kW), a high degree of standardization, and ease of transportation from one landfill site to another. Two of the most significant disadvantages with ICEs are higher combustion emissions and overall lower combustion efficiency.

There are several economic disadvantages to using microturbines. Microturbines typically have parasitic energy losses of 17% (of gross power output) as compared to only 7% for ICEs. Microturbine turndown performance (ability to maintain efficiency at lower operating loads) is also considered poor when compared to ICEs, and difficulties may occur when they are operated at less than a full load (Energy Nexus Group, 2002).

Other problems that are shared by either combustion system fired with LFG are combustion chamber corrosion and accumulation of deposits on internal combustion chamber moving parts.

Because of their robust designs, lower O&M costs, and proven operational records, ICEs are currently the most favorable option for LFG energy projects and have been applied in greater numbers than any other option. However, at the Grand Forks landfill site, the use of microturbines could be the more favorable option because of the flexibility of adding more energy generation potential as more gas becomes available and there becomes a greater need for large amounts of heat at either the landfill baling facility or the WWTP. Microturbines are more efficient in applications that require cogeneration because of the large amounts of waste heat than can be easily and economically recovered.

Investigation of the technologies to prepare LFG for use in a microturbine or ICE has determined that at LFG sites with a power generation potential of less than 3–4 MW, no economical systems are currently available to efficiently remove siloxanes and total VOCs from the gas stream. For sites with greater than 3-MW potential, the initial capital cost of gas collection, cleanup and preparation, and power generation equipment can be \$2,000,000–\$3,000,000/MW (depending on the extent of gas treatment required).

Microturbine Economics

Economic considerations regarding microturbine technology include the following (Energy Nexus Group, 2002; Capstone, 2008b; U.S. Environmental Protection Agency, 2008):

- The current total installed costs for LFG microturbine systems (including fuel pretreatment equipment) are the following:
 - \$4000–\$5000 per kW for smaller (65 kW and less) systems
 - \$2000–\$2500 per kW for larger (200 kW and above) systems
- Nonfuel operation and maintenance costs are approximately \$0.015–\$0.020/kWh.
- LFG microturbines are most economical under an electrical cost-saving scenario, where purchased electric power is replaced by power generated by the microturbine.
- In most cases, the cost to generate electricity with microturbines will be higher than the price for which it can be sold back to the utilities.
- Detailed information is not yet available regarding the long-term reliability details for O&M costs associated with LFG microturbines and those costs associated with the required extensive LFG cleanup systems.

Project Revenues

The following are projected revenues for either using the generated energy on-site or selling the energy off-site.

Electricity

Many states have special schedules for the purchase of power from small-quantity generators. These schedules detail the contract terms, capacity and energy payment terms, adjustment factors, etc. For the Grand Forks LFG site, the pathway for off-site sale would require interconnection with the local utility company transmission/distribution system. The following items represent the various costs that could be applied to on-site usage or off-site sale:

- On-site displacement costs
 - The most economical use of the electricity generated by this LFG site would be for the site itself: the baling facility and, perhaps, the wastewater treatment facility.
 - At the time this report was prepared, the cost of on-site electrical demand at the landfill site was \$0.037/kWh and \$0.062/kWh, and it was \$0.030 and \$0.0385/kWh at the WWTP.
- Offset costs
 - The Grand Forks LFG site may receive peak or off-peak rates for the avoided cost of electricity from qualifying facilities in the range of \$0.03–\$0.04/kWh (Schmidt, 2007).
- Grid-avoided cost
 - The cost for the fuel that the local power supply utility would incur to generate the electricity is in the range of \$0.01–\$0.02/kWh.
- REC
 - Current revenue rates for these credits are typically around \$0.01/kWh but have been negotiated as high as \$0.03/kWh depending on the utility company.

Medium-Btu Use

Revenues are usually based on the prices of equivalent energy sources. Typical revenues range from 75% to 90% of the price on a Btu basis for the fuel replaced (usually natural gas or fuel oil). The greatest difficulty is locating potential users in close proximity to the LFG site. For the city LFG site, this would be the landfill site and the city-owned and -operated wastewater treatment facility less than a mile to the north of the LFG site.

Pipeline-Quality Gas (high-Btu use)

Revenues are based on the price for natural gas (\$6–\$7/MMBtu at the wellhead). The gas is often sold at 90% of the current wellhead price and requires infrastructure similar to that of a natural gas refinery. The buyback details usually require extensive negotiations with the local utility company. Since the capital investment is significant and the estimated biogas production is determined to be low, this option was not considered reasonable and was, therefore, not pursued.

Federal Programs

The Energy Policy Act of 1992 included several provisions which may have a positive impact on the LFG recovery industry (U.S. Environmental Protection Agency, 1991b).

Section 29 – Credits for Producing Fuel from a Nonconventional Source

The Section 29 (Internal Revenue Code) tax credits were initiated in 1979. A \$3.00 credit per barrel of oil equivalent (5.8 MMBtu) is available for the production and sale of certain qualified fuels to unrelated parties. The credit is adjusted each year for inflation (subject to limitation dependent upon the wellhead price of oil). The credit is phased out as the price per barrel of oil exceeds \$29.50. The estimated value of the tax credits (1993 dollars) were approximately \$0.979 MMBtu or approximately \$490/Mcf of LFG (U.S. Department of Treasury, 1993).

This availability of tax credits usually results in a second or third party being brought into the project. The tax credit is only available if the gas which is produced is sold to an “unrelated party” and is only of benefit if the producer can use the tax credits (Pierce, 1992). With this tax credit extension, a strong economic incentive exists for the future development of LFG utilization projects.

Inflation Adjustment Factor and Reference Price

The inflation adjustment factor for calendar year 2004 is 2.1853. The reference price for calendar year 2004 is \$36.75. These amounts were published in the Federal Register on April 6, 2005.

Phaseout Calculation

Because the calendar year 2004 reference price does not exceed \$23.50 when multiplied by the inflation adjustment factor, the phaseout of the credit provided for in Section 29 Part (b) Subpart (1) does not occur for any qualified fuel sold in calendar year 2004.

Renewable Energy Credits

The nonconventional source fuel credit under Section 29 Part (a) is \$6.56 per barrel-of-oil equivalent of qualified fuels ($\$3.00 \times 2.1853$). This amount was also published in the Federal Register on April 6, 2005.

Section 1212 – Renewable Energy Production Incentive (REPI)

The Renewable Energy Production Incentive (REPI) is managed by DOE and provides financial incentive payments for electricity generated and sold by new qualifying renewable energy generation facilities (solar, wind, biomass, or geothermal sources). Qualifying facilities are eligible for annual incentive payments of 1.5 cents per kilowatt hour (1993 dollars and

indexed for inflation) for the first 10-year period of their operation, subject to the availability of annual appropriations in each federal fiscal year of operation by Congress and DOE.

To qualify for the program, the owner/operator must meet the following requirements (Congressional Record, 1992):

- Generate electricity from solar, wind, biomass, or geothermal sources (burning MSW for energy is not included)
- Be a public entity or nonprofit electric cooperative
- Use the facility for the first time in 1993 or later (excludes existing facilities)
- Petition DOE for payments

REPI was originally authorized under Section 1212 of the Energy Policy Act of 1992 and was amended in 2005 with Section 202 of the Energy Policy Act of 2005 (H.R. 6). Section 202 reauthorized appropriations for fiscal years 2006 through 2026 and expanded the list of eligible technologies and facilities owners. The regulations for the administration of the REPI program are contained in Title 10 of the Code of Federal Regulations, Part 451 (10 CFR 451).

Site Energy Demand

When the 2006 historical electrical usage for the entire landfill site obtained from billing records was examined, it was determined the electrical demand for this site is about 400 MWh annually. Approximately 35 MWh was billed at \$0.062/kWh, and 365 MWh was billed at \$0.037/kWh. After estimating summer demand charges and facility charges, the total electrical expense at this site for 2006 was estimated at more than \$18,000.

Electrical demand for the WWTP was not as straightforward to determine because of inconsistent electrical usage from month to month over the past several years. It was therefore necessary to estimate peak usage values from the billing history across several years (2003–2006) in an attempt to estimate a full 12 months of electrical use. This technique yields an annual electrical demand between 7000 and 8000 MWh annually. Like the landfill facility, two billing rates apply (\$0.03 and 0.0385/kWh); however, unlike the landfill, each of these rates cannot be applied to a specific usage amount. Thus the higher rate will be applied to the greater estimated demand. This estimation gives a total annual electrical expense at the WWTP of around \$310,000. A combined energy demand estimate for the two facilities is about 8500 MWh and just less than \$330,000.

The heating demand for either facility can be much greater during the colder winter months of September through May. Therefore, two possible scenarios exist for the location of the energy production package. The first would be to send raw biogas to the treatment skid and the cogeneration package at the WWTP, which would be in close proximity for heat and electrical utilization, and send the electrical energy to the baling facility by city-owned transmission equipment. The second scenario would be to locate the cogeneration and treatment package at

the baling facility and send the electricity to the WWTP. However, we have assumed the heating need for the WWTP would be greater than the baling facility requirement because of the operational environment of the digesters; thus the second scenario does not represent the most practical use of the energy produced from biogas on this site and was considered to be an option.

Taking this into consideration, the daily heating demand for the WWTP can be estimated from the natural gas usage history records provided by the city Public Works Department. Using a similar approach for estimating the natural gas use that was used for estimating the electrical demand, it can be shown the WWTP annual demand is about 70,000 Mscf (or about 70,000 MMBtu annually). Presently, the cost of natural gas is \$0.948244/therm (gas plus distribution) or about \$9.48/Mscf. This equates to an annual natural gas cost of about \$665,000. Because of the upper Midwest climate, most of this heating demand occurs during the colder part of the year, and it can be estimated the WWTP annual demand is about 42,000 Mscf for the 6-month winter peak (or about 42,000 MMBtu). Thus the WWTP demand is about 230 MMBtu/day during the 6-month winter peak (180 days), or about 230,000 scf/day (230 Mscf/day). This equates to a 6-month natural gas cost of about \$395,000.

If we presume the LFG from this site can sustain 22 Capstone CR65-ICHP microturbines, then they can produce around 24,000 MMBtu over a 6-month period for a heat value of about \$227,000 or around 36,000 MMBtu over a 9-month period for a heat value of \$341,000, which is equivalent to a waste heat generation capacity of about 133 MMBtu/day. If this is compared to the demand of 230 MMBtu/day, it can be seen the WWTP demand is about 100 MMBtu/day more than the 22 generators can produce for each day of operation during the 6 months of peak demand. However, over the 3 additional months, the demand is more in-line with the heat production of the generator array, leading to a more economic use of the heat from the microturbines.

For this site, the revenue would be in the form of cost savings. If we assume an electrical value of \$0.062/kWh and a natural gas value of \$9.48/Mscf, then under ideal conditions, this site could produce enough biogas to generate a revenue stream of almost \$1,020,000/year that could be applied to on-site energy utilization to reduce operating costs.

Preliminary Economic Assessment

A preliminary economic assessment was conducted to evaluate typical LFG-to-energy system costs and potential revenue generated. The economic evaluation (Table 62) assumes Capstone CR65-ICHP (65-kW) microturbines would be utilized at this site. These microturbines utilize a heat exchanger, or recuperator, to capture exhaust heat for space heating or other heating uses, such as heating a digester or baling facility. This feature allows significant economical utilization of waste heat energy produced during the electrical generation process.

Total annual energy costs of the landfill operation and wastewater treatment facility were compared to the estimated total annual revenue (represented as cost savings) derived from electricity production (gross production less parasitic load) and waste heat recovery. Based on preliminary estimates, the Grand Forks landfill is projected to be capable of producing about 792,000 scf/day of medium-Btu biogas that could, under ideal operating conditions, support

Table 62. Preliminary Economic Assessment of the Grand Forks Landfill Methane Collection and Energy Generation System

Capital Cost	
Gas Extraction and Collection System	\$400,000
Gas Treatment for 792,000 scfd (H ₂ O, VOC, H ₂ S, siloxane removal)	\$750,000
Interconnect	\$100,000
Capstone CR65-ICHP Microturbine Electrical Generators (22 at \$71,420 each)	\$1,573,000
Engineering	\$200,000
Contingency (15% of equipment costs)	\$423,450
Total Capital Cost	\$3,446,450
Capital Amortization	
Principal	\$3,446,450
Interest Rate	6%
Life of Loan (years)	6
Annual Payment	\$704,809
Total Cost of Loan	\$4,200,661
O&M Cost	
Labor (1 staff year)	\$75,000
Parasitic Electricity at 17% of Electrical Output	\$139,091
Siloxane Removal System Maintenance	\$50,000
Parts	\$50,000
Annual O&M Cost	\$314,091
Total Annual Cost (Capital + O&M)	\$1,018,900
Revenue	
Total Biogas Production, scf/day	792,000
Methane Content of Biogas, %	55%
Methane, scf/day	435,600
Btu/scf, LHV (lower heating value)	913
Btu/day	397,702,800
Fuel Flow Requirement LHV, Btu/hr	765,000
Generators (maximum supported)	21.7
Length of Operation (days/year)	365
Total Annual Methane, scf/year	158,994,000
Generator Heat Rate, Btu/kWh	11,000
kWh/day	36,155
Electricity Value, \$/kWh	\$0.062
Electricity Value, \$/year	\$818,183
Net Electrical Production (gross – parasitic)	\$679,092
Heat Production – Hot Water Recovery, Btu/hr/generator	251,000
Total Heat Recovery for 9-months Cold Weather, Btu	35,753,741,656
Natural Gas Equivalent of Heat Recovery, Mscf	35,754
Natural Gas Unit Value, \$/Mscf	\$9.48
Heat Value, \$/year	\$339,033
Total Revenue, \$/year	\$1,018,125

operation of approximately 22 Capstone CR65-ICHP microturbines. A LFG extraction and collection system is estimated to cost \$400,000, and a basic biogas treatment system is estimated to cost \$750,000. If an interconnect system is required, the cost is estimated at \$100,000. A contingency cost of approximately 15% of the equipment costs represents about \$424,000. A nonequipment engineering cost estimate of about \$200,000 is included to cover siting and design costs for the system. The bank of 22 CR65-ICHP microturbines is estimated to cost \$1,573,000. This represents a total capital investment of about \$3,450,000, with an annual system O&M cost around \$314,000. This corresponds to an annual system cost of about \$1,020,000. If a microturbine heat recovery system is utilized, an estimated 133 MMBtu/day of waste heat could heat the wastewater treatment plant buildings and the landfill baling facility for 9 months of the year. The estimated payback period is about 6 years when capital costs are amortized at a 6% annual interest rate.

Capital Costs for Siloxane Removal

The capital cost for gas cleanup technology is not scalable to the flow rate of the biogas at the LFG site. Currently, several biogas treatment packages are commercially available; however, all are designed to efficiently treat a gas flow greater than 1200 scfm. Any LFG-to-energy design that is currently constrained by gas flow rates in the range between 60 to 600 scfm are typically forced to use equipment that was designed for the larger systems. Therefore, the capital required by the smaller sites is similar to that of the cost of the larger systems, with a significantly lower rate of return because of the smaller volume of biogas to be processed. In some cases, certain individual components of a typical gas treatment package cannot be designed for the lower gas volumes; thus the cost remains similar. Hence, biogas treatment at a LFG site that produces 2500 scfm raw biogas would share similarly designed equipment that would be used at a site that only produced 60 scfm of raw biogas. Gas collection systems and power generation equipment are directly scalable to the raw fuel generation potential: the higher the flow volume, the more collection wells are required and the larger the power generation equipment required to utilize all of the available gas. As discussed above, because of current technology constraints, the cost of a LFG-to-energy facility is not usually cost-efficient below 1500 scfm of biogas production. Depending on the landfill characteristics and biogas parameters, the volume would be equivalent to 3–4 MW of untapped power generation potential. New technologies in biogas pretreatment and innovative approaches to power generation are needed to take advantage of the thousands of aging landfill sites and wastewater treatment plants in the United States that lie within this range.

Two Business Options

Current biogas treatment technologies and power generation packages typically require very large capital investments. There are two business approaches for biogas pretreatment: either one can result in significant expense either in up-front capital or in annual maintenance agreements. The first option places a highly efficient biogas pretreatment package as upfront capital included with the cost of the overall system. This gas-conditioning package lowers both total VOCs and organosilicon species below the currently detectable limits and can exponentially increase power generation equipment efficiency and lifetime, while lowering downtime and maintenance costs. The second option lowers the initial gas pretreatment and power generation costs by spreading and substituting these costs as a high-cost O&M package that shifts the responsibilities of the engine/generator to the supplier or manufacturer and off of the

owner/operator. This option significantly reduces equipment lifetime and efficiency. Because of the high frequency of maintenance cycles, the equipment damage caused by inadequate gas pretreatment is not apparent because the heavy maintenance is performed routinely. The nature of the O&M contract specifies, depending on the constituents of the raw biogas, after every few thousand hours of operation, major maintenance be performed on the engine and generator to try to minimize the effects of the silica damage. Our investigation suggests that either option requires a fairly significant capital investment, either mostly up-front as in the first option or planned over the life of the project as in the second.

LFG Production Barriers

Several conditions exist at this site that could reduce the projected flow of biogas and thus lower the overall efficiency of the LFG production. These include, but may not be limited to, the following:

- Decomposition phasing
 - Most LFG is produced by bacterial decomposition, which occurs when organic waste is broken down by bacteria naturally present in the waste and in the soil used to cover the landfill.
 - Bacteria decompose landfill waste in four phases, and the composition of the gas produced changes with each of the four phases of decomposition. Since landfills can accept waste over a long period, a landfill may be undergoing several phases of decomposition at once. This means that older waste in one area might be in a different phase of decomposition than more recently buried waste in another area. This difference in phasing will affect the sustainability of the gas production.
 - ▶ During Phase I decomposition, aerobic bacteria consume oxygen while breaking down the organic waste. This decomposition can last for days or months, depending on how much oxygen is present.
 - ▶ Phase II decomposition starts after the oxygen in the landfill has been used up. Using an anaerobic process, bacteria convert compounds created by aerobic bacteria into alcohols.
 - ▶ Phase III decomposition starts when anaerobic bacteria consume the organic acids produced in Phase II and form a more neutral environment in which methane-producing bacteria become established.
 - ▶ Phase IV decomposition begins when both the composition and production rates of LFG remain relatively constant. Gas is produced at a fairly stable rate in this phase, typically for 15–20 years.

- Because of the age and type of landfill, we are assuming the older closure phases are in decomposition Phase IV, while the newer closure phases could be somewhere between decomposition Phases I and III.
- Even though it could be speculated that most of the landfill site is in Phase IV decomposition because of its historical structure, without installing extraction wells, it cannot be known with any certainty where in the 20-year window of methane production any specific area currently is.
- Static leachate water level
 - Following the installation of the three piezometers in October 2006, the water surface elevations in each well were measured as shown in Table 63.
 - This indicates the leachate levels at the landfill site are rising nonuniformly with the center of the site more than 9 feet above the elevation of the water surface at the perimeter. Figure 63 illustrates the potentiometric contours around the site. Note the higher water surface toward the center of the landfill, which may be because of the leachate collection system around the perimeter.
 - Extraction wells installed in this location can lower the water surface to establish a more uniform water elevation across the landfill site. The results of this dewatering may have undetermined effects on the biogas production in this part of the landfill system.
 - Installation of several biogas collection wells in this area is highly recommended to gain a better understanding of what will occur as the water level is lowered to a uniform elevation across the site.
 - The amount of water in the system can affect how much of the waste is under the appropriate conditions for optimum methane production. A high water level can decrease the amount of waste that is able to generate gas, thus leading to possibly lower gas estimates.
 - The water surface levels represented in Figure 63 should be regarded as preliminary because the contour lines are based on data from only three piezometer wells across the entire site. It is strongly suggested that additional monitoring be conducted and further data collected before drawing a final conclusion about the elevation of the water surface within the site.

Table 63. Measured Water Surface Elevations in the Three Piezometer Wells

Piezometer Well No.	October 2006 Feet, MSL	October 2007 Feet, MSL	Difference, feet
1	839.00	837.70	+1.30
2	845.30	845.40	+0.10
3	835.60	836.10	+0.50

- Estimated landfill bottom
 - Since this site initially started receiving waste as an open municipal dump in the early 1960s, the bottom elevation was not accurately recorded. The elevation is estimated between 820 and 825 ft above MSL.
 - Although this difference seems relatively minor, this estimation can affect the total depth of the waste in place as well as affect the overall depth of water. This can affect the accuracy of the calculations for estimating gas production values.
- Maximum waste elevation
 - As a result of the vertical elevation extension, the maximum waste elevation will be 880 ft above MSL. However, this elevation will only represent a peak near the center (Closure Phase IX) and will not be uniform across the entire landfill site. After completing the cap, the finish grade will follow the waste elevation at 885 ft above MSL (Figure 62).
- Amount of biodegradable waste in place
 - Although few formal waste logs exist for a good portion of the landfill history, it is known that there is a significant amount of inert waste in the landfill. The most recent influx of inert waste occurred following the 1997 flood. For a period of time following this event, large quantities of debris from the citywide cleanup effort were disposed of in the landfill. The presence of this material will reduce both the estimated and actual gas production values.
- Methods used for gas generation determination
 - Although a good representation of gas generation, the first-order decay equation tends to overestimate the production values because there are no terms in the equation that consider all of the details that can occur at every landfill site.
 - The first-order decay model has two recognized faults as it is applied to methane gas generation in landfills (Anderson, 2008):
 - ▶ Gas emissions from a landfill will usually follow a bimodal function that reflects the reality of a second wave of gas generation following any breach of the cap when rainfall and runoff reenter the site. Thus this model only traces one decay function.
 - ▶ The model does not adequately account for the sensitivity of gas generation due to sufficient moisture in the system (which can be a governing, albeit limiting, condition). Incoming wastes can have an average of 20% moisture content, while complete decomposition requires between 45% and 70% moisture that is equally distributed throughout the deposited waste.

The above discussion suggests that the speculated results regarding the LFG production may not be as straightforward as even the first-order decay estimation may appear. Therefore, this study recommends that several gas extraction wells be strategically located in several of the closed phases to determine the actual gas flow rates, sustainability over time, and constituents due to variability in waste properties and subsurface environmental conditions in any given phase.

Follow-Up Project Concepts

With the conclusion of this preliminary energy assessment study, it was determined this site does have the potential to help offset some energy costs for the city-run landfill and wastewater treatment plant. However, before a large capital improvement project is begun, an additional investigation should be conducted. This next study should develop the site engineering plans and cost analysis for the following:

- Installation of a demonstration biogas extraction and collection well in a strategic order or such that the zone of influence is either 250 or 500 feet in diameter to determine actual gas flow rate and constituents such that a more accurate design of the gas treatment and power generation packages can be completed.
- Determination of the appropriate level of gas recovery based on flow and sustainability investigation.
- Making an informed decision to do nothing, flare the biogas, or produce energy as heat, electricity, or both.
- Development of a detailed site plan analysis and cost analysis to determine feasibility of a full-scale project and the design of the project based on the results of this next feasibility study.

Future Research Directions

Total VOCs, specifically siloxanes, potentially remain a large challenge to economical power generation from landfill or digester biogases. Several future research directions that the EERC would like to pursue would address the alternatives to the current combustion practices and biogas treatment technology for LFG and could include the following.

Organic Rankine Cycle (ORC) Technologies

- The ORC engine is a process that uses an organic fluid in a closed cycle to convert thermal energy, such as an engine or flare burning LFG, into mechanical energy resulting in essentially no air emissions. The ORC may represent a technically feasible alternative for electrical generation using LFG (Ormat, 2007).

- As part of heat generation for this cycle, development of an economical biogas combustor/heat exchanger could eliminate the need for siloxane removal because of an advanced combustion chamber design.
- OCR technologies should continue to be examined; however, there is a high cost to demonstrate this engine with no large commercial-scale units being designed or demonstrated.
- Ormat Technologies, Inc. (Schmidt, 2007)
 - Costs \$1000/kW for full-cycle technology
 - Costs \$2000/kW for complete package design
- Turboden
 - Costs are unknown at this time

Microturbine Materials Development

- Antistick coating development for internal microturbine components that may be prone to siloxane damage.

Innovative Gas Pretreatment Technologies

- Explore options of using a low parasitic load biogas preheater (electric or biogas feed) to control silica formation on removable plates prior to combustion of biogas in any ICE or microturbine.
- Develop an economical and nontoxic liquid scrubber system to remove the siloxane from the biogas stream ahead of the combustor for any ICE or microturbine. Liquid must be inexpensive and environmentally friendly before and after exposure to siloxane.

Future Project Financial Resources

Funding any size LFG project can be a monumental challenge for a municipality. Since most potential governmental funding sources consider any aspect of a LFG-to-energy project to be mature technology, assistance will be minimal. Most current governmental assistance is in the form of RECs or, possibly, in the form of future carbon credit-trading programs.

One government organization, however, that is leading the pursuit for utilizing LFG in energy production is the EPA. The EPA's LMOP is a voluntary assistance program that helps to reduce methane emissions from landfills by encouraging the recovery and use of LFG as an energy resource. LMOP forms partnerships with communities, landfill owners, utilities, power marketers, states, project developers, tribes, and nonprofit organizations to overcome barriers to project development by helping them assess project feasibility, find financing, and market the benefits of project development to the community. EPA launched LMOP to encourage productive use of this resource as part of the U.S. commitment to reduce greenhouse gas emissions under the United Nations Framework Convention on Climate Change. More

information about how LMOP could offer assistance to the City of Grand Forks for this LFG-to-energy project can be found at the LMOP Web site at www.epa.gov/lmop/index.htm.

Conclusions

This activity completed a preliminary feasibility study for distributed power generation at the City of Grand Forks landfill site that quantitatively and qualitatively established the physical characteristics of the biogas and supports the potential for a power generation demonstration.

Based on the average annual acceptance rate obtained from city reports and utilizing the estimate calculated from the first-order decay equation, utilizing an active collection system under ideal conditions, it may be possible to generate 576,000–864,000 scf/day of biogas, which is equivalent to 315–475 MMBtu/day.

The duration of this level of generation potential is estimated to be about 20 years, considering the age, moisture, depth, and quantity of waste at this site. Under favorable conditions and based on the calculated waste in place and an average projected total gas flow of almost 800,000 scf/day, this landfill site has a gross power generation capacity of 1.5 to 2.0 MW with an annual electricity generation potential between 8700 and 11,600 MWh after parasitic loads are accounted for and assuming an 80% capacity factor.

Based on preliminary estimates, the Grand Forks landfill is projected to be capable of producing enough medium-Btu biogas that it could, under ideal operating conditions, support operation of approximately 22 Capstone CR65-ICHP microturbines. A landfill biogas extraction and collection system is estimated to cost \$400,000; a basic biogas treatment system is estimated at \$750,000; the bank of 22 CR65-ICHP microturbines is estimated to cost \$1,573,000; this plus additional engineering and equipment contingency costs of almost \$725,000 represents a total capital investment of about \$3,450,000, with an annual system O&M cost around \$314,000 for an annual system cost of about \$1,020,000. If a microturbine heat recovery system were utilized, an estimated 133 MMBtu/day of waste heat could heat the WWTP buildings and the landfill baling facility for 9 months of the year, meaning the estimated payback period for this landfill energy recovery project is about 6 years when capital costs are amortized at a 6% annual interest rate.

Assuming these estimations are reasonably accurate, this site appears to have a projected capacity to generate enough energy to offer a moderately reasonable source of electricity and heat to help offset the energy costs at the landfill baling facility and the WWTP which, combined, were determined to use less than 9000 MWh annually. The revenue stream from this project would be in the form of on-site operating expense savings. If we assume an overall electrical value as high as \$0.062/kWh and a natural gas value of \$9.48/Mscf, this site, under ideal conditions, could produce enough biogas to generate a revenue stream of almost \$1,020,000/year that could be applied to on-site energy utilization and reduce operating costs.

As discussed above, the most reasonable option for utilizing any energy produced on-site would be for heat and power at the baling facility or the WWTP. The most economical method of producing this heat and power would be by a microturbine. Since methane gas is an extremely

powerful greenhouse gas (more than 20 times that of CO₂), utilization of this biogas to generate supplemental energy for either facility makes good environmental sense, plus it can facilitate the offset of some energy costs associated with operations at both facilities.

Investigation of the current technologies available to remove the contaminants of the LFG before use in a microturbine or ICE indicates power generation at LFG sites that have a potential greater than 3 or 4 MW, the initial capital cost of gas collection, cleanup and preparation, and power generation equipment can be \$2–\$3M per MW (depending on the extent of gas treatment). For sites with less than 3 MW potential, no economical systems are available or scalable to efficiently remove siloxanes and VOCs from the gas stream. By comparison, several proposed EERC biogas pretreatment systems expect to target landfill or WWTP sites with less than 3 MW potential for an expected total per-MW cost that could be less than the current rate.

Although this investigation concludes that the Grand Forks landfill site appears to have the potential to offset some of the on-site energy costs, a more detailed investigation into the sustainability of the gas would be required to make a more informed decision. Before any detailed plans for a waste-to-energy facility are begun, it is recommended the city install several extraction wells in strategic locations to conduct tests that would determine the sustainability and quantity of the gas flow rate to determine the exact amount of energy production potential possible. This quantity determination would also be used to more accurately design an extraction and collection system as well as the most economical LFG pretreatment system. Known biogas flow rates would assist in the design of the gas recovery and help determine the best use for the captured gas, to flare, generate power and/or heat, or do nothing. A detailed economic evaluation of the system based on the actual gas values obtained from the wells would follow a site plan layout that would help with the financial and economic analysis.

Further investigations at the Grand Forks landfill site need to be completed in close combination with the final closure phases and efforts of the new City of Grand Forks Green 3 Environmental Initiative. This program represents cities around the country that have taken the position that they will work in partnership with federal and state government in addressing energy and environmental concerns but also have the ability to assume a leadership role at the local level.

Several of these innovative technologies could be developed to economically treat the biogas and produce energy from this site and other comparably sized landfill sites across the nation. In addition to the continuation steps described above, alternatives to the current combustion practices and biogas treatment for LFG must be more economical and should be examined in more detail. Several areas for future technologies could include the following.

ORC Technologies

- Use ORC technologies as part of the power generation package utilizing a newly developed, economical biogas combustor/heat exchanger that could eliminate the need for siloxane removal because of its innovative combustion chamber design.

Microturbine Materials Development

- Development of new materials for an antistick coating for the internal microturbine components that are prone to repeated siloxane damage.

Innovative Gas Pretreatment Technologies

- Explore economical gas pretreatment technologies for using a low parasitic load biogas preheater (electric or biogas feed) to control silica formation on removable plates prior to combustion of biogas in any ICE or microturbine.
- Develop an economical liquid scrubber system to remove the siloxane from the biogas stream ahead of the combustor in any ICE or microturbine. The liquid must be inexpensive and environmentally friendly before and after exposure to siloxane.

Current federal law requires all landfills to monitor their air emissions, and many must collect the gas and dispose of it in one of two ways: either flare the gas or install a LFG-to-energy system. According to EPA, under ideal conditions, every 1 million tons of waste deposited in landfills has the potential to produce enough LFG to generate at least 8600 MWh of electricity a year, enough to power almost 800 homes. Using this gas for energy purposes, rather than expelling it into the atmosphere, is equivalent to removing more than 9000 cars from the road or planting 13,000 acres of trees (U.S. Environmental Protection Agency, 1996).

A quick examination of direct and avoided equivalent emissions reduced by implementing a landfill energy project at this site indicates almost 2500 tons of methane a year and almost 7400 tons of carbon dioxide would not be vented to the atmosphere. This has an environmental benefit of removing the emission equivalent of more than 10,500 vehicles, planting almost 15,000 acres of forest, or offsetting the use of 267 railcars of coal (U.S. Environmental Protection Agency, 2006).

This preliminary energy assessment determined that this site, under ideal conditions, could produce enough energy to offset the electrical costs at the baling facility as well as provide heat and power for the WWTP on a fairly regular schedule. This ability to produce this energy from a free gas could have been enhanced by some advanced planning early in the life of the landfill. As the city stands on the threshold of siting and designing a new landfill, this message should not be ignored. This study should provide an avenue for the continuation of these findings and consider implementing some of the recommendations for a proper gas extraction and collection system, energy production package, and nearby end use for the produced electricity and/or heat.

References

Amundson, L., February 2006, City of Grand Forks Public Works Department Annual Waste Management Logs and the Manufacturing or Processing Equipment Annual Emission Inventory Report.

Amundson, L., March 2007, City of Grand Forks Public Works Department, Personal communication.

- Amundson, L., January 2008, City of Grand Forks Public Works Department, Personal communication.
- Anderson, P., 2008, Center for a Competitive Waste Industry: www.competitivewaste.org.
- Capstone Turbine Corporation, accessed February 2008a, Capstone announces launch of ultra low emissions product to operate on digester and LFG: www.microturbine.com/news/story.asp?id=456.
- Capstone Turbine Corporation, 2008b, www.capstoneturbine.com.
- Congressional Record, October 1992, No. 142, Part V Energy Policy Act of 1992: Washington, D.C.
- Energy Nexus Group, 2002, Technology characterization—microturbines: U.S. Environmental Protection Agency Climate Protection Partnership Division, Washington, DC.
- Feland, T., January 2008, City of Grand Forks Public Works Department, Personal communication.
- Gillette, S.F., 2004, CHP case studies—saving money and increasing security: Presented at the West Coast Energy Management Conference, 2004.
- Gould, R., ed., 1992, 1991–92 methane recovery from landfill yearbook: New York, Governmental Advisory Associates, Inc.
- Hansen, D.E., and Kume, J., 1970, County Ground Water Studies 13 North Dakota State Water Commission, Geology and Ground Water Resources of Grand Forks County Part I Geology: Prepared by the North Dakota Geological Survey in cooperation with the North Dakota State Water Commission, the United States Geological Survey, and the Grand Forks Water Management District.
- Heguy, D., and Bogner, J., 2008, Cost-effective hydrogen sulfide treatment strategies for commercial LFG recovery—role of increasing C&D (construction and demolition) waste: Merichem Company, www.gtp-merichem.com/support/technical_papers/municipal_landfills.php, accessed January 2008.
- Koch, W.R., 1986, A new process for the production of high Btu gas: in GRCDA 9th Annual International Landfill Gas Symposium, Newport Beach, CA, 1986, Proceedings: Newport Beach, CA, GRCDA/SWANA.
- Method 25-C Analytical Results, 2006, Triangle Environmental Services, Inc.
- Nagl, G.J., accessed January 23, 2008, Technical analysis of landfill gas recovery systems for the production of high Btu gas: www.gtp-erichem.com/support/technical_papers/landfill_gas_recovery/index.php.

- Olson, J., and Greer, P.L., 1994, Site suitability review of the Grand Forks landfill: ND Landfill Site Investigation No. 45, North Dakota State Water Commission and the North Dakota Geological Survey.
- Ormat Technologies, Inc., www.ormat.com/businesses.php?did=26, 2007.
- Orr–Schelen–Mayeron & Associates, Inc., 1990, Engineering plan Grand Forks sanitary landfill: Grand Forks, North Dakota.
- Pierce, J.L., 1992, Alternative contractual and financial arrangements for implementation of landfill gas power generation projects, in SWANA 15th Annual Landfill Gas Symposium, Silver Spring, MD, 1992, Proceedings: Silver Spring, MD, GRCDA/SWANA.
- Schmidt, D., 2007, University of North Dakota Energy & Environmental Research Center, personal communication.
- Solid Waste Association of North America (SWANA), 1997, Landfill gas operation and maintenance, manual of practice: U.S. Department of Energy National Renewable Energy Laboratory.
- Thorneloe, S., 1992, Landfill gas utilization—options, benefits, and barriers: Presented at the Second United States Conference on Municipal Solid Waste Management, Arlington, VA, 1992.
- Tower, P., February 2002, Methane Sampling Instructions: Applied Filter Technology, Inc.
- Tower, P.M., 2003, New technology for removal of siloxanes in digester gas results in lower maintenance cost and air quality benefits in power generation equipment: Applied Filter Technology, Inc., Presented at the WEFTEC 2003 78th Annual Technical Exhibition and Conference, October 2003.
- Tower, P., 2004, Siloxanes and other harmful contaminants—their importance in total LFG quality management: Applied Filter Technology, Inc.
- Tower, P., July 2006, Applied Filter Technology, Inc., Personal communication.
- Tower, P.M., and Wetzel, J.V., 2004, Reducing biogas power generation costs by removal of siloxanes: Applied Filter Technology, Inc., Snohomish, Washington.
- Tower, P., Wetzel, J., Lombard, X., 2006, New Landfill gas treatment technology dramatically lowers energy production costs: Applied Filter Technology, Inc., Snohomish, Washington, and Verdesis, Brussels, Belgium.
- Tucker, D., January 2008, City of Grand Forks Public Works Department, Personal communication.

- U.S. Department of Energy, Climate Change Technology Program, 2005, Technology options for the near and long term: www.climatechange.gov/library/2005/tech-options/index.htm.
- U.S. Department of Health and Human Services, Agency for Toxic Substances and Disease Registry, Division of Health Assessment and Consultation, November 2001, Landfill gas primer—an overview for environmental health professionals.
- U.S. Department of Treasury, April 1993, Description of the Modified Btu Tax.
- U.S. Environmental Protection Agency, March 1991a, Air emissions from municipal solid waste landfills—background information for proposed standards and guidelines: EPA-450/3-90/011a.
- U.S. Environmental Protection Agency, October 1991b, Federal Registry 40 CFR, Parts 257 and 258, Solid Waste Disposal Facility Criteria, Final Rule: Washington, D.C.
- U.S. Environmental Protection Agency, 1996, Turning a liability into an asset—a landfill gas-to-energy project development handbook: EPA 430-B-96-0004.
- U.S. Environmental Protection Agency, Landfill Methane Outreach Program (LMOP), 2002b, Landfill gas utilization feasibility study Rocky Face Landfill, Dalton, Georgia: Dalton–Whitfield Regional Solid Waste Management Authority, Eastern Research Group.
- U.S. Environmental Protection Agency, Landfill Methane Outreach Program (LMOP), accessed November 2006, Landfill gas calculator—emission reductions and environmental and energy benefits for landfill gas energy projects: www.epa.gov/lmop/res/lfge_benefitscalc_022806.xls.
- U.S. Environmental Protection Agency, Landfill Methane Outreach Program (LMOP), 2008, www.epa.gov/lmop.
- U.S. Environmental Protection Agency, October 2002a, Powering microturbines with landfill gas: Office of Air and Radiation (6202J), EPA 430-F-02-012.
- Wetzel, J., October 2007, Applied Filter Technology, Inc., Personal communication.
- Wheless, E., and Wiltsee, G., 2001, Demonstration test of the Capstone microturbine on landfill gas: Presented at the SWANA 24th Annual LFG Symposium, Dallas, TX, March 2001.

YEAR 2005 – ACTIVITY 10 – BIODIESEL EDUCATION AND OUTREACH

Introduction

The EERC, in collaboration with the North Dakota Division of Community Services, the North Dakota Department of Agriculture, and the South Dakota Soybean Research and Promotion Council (SDSRPC), conducted several biodiesel education workshops in South Dakota and North Dakota. An increased interest and profile for biodiesel has created an opportunity for outreach to a spectrum of interested parties from growers to end users, particularly in the transportation sector.

Acceptance of biodiesel is gaining momentum in the northern Great Plains. As a result of the education and marketing efforts of the North Dakota Soybean Council (NDSC), biodiesel is now used in 96 school buses in 11 North Dakota school districts. The Red River Valley Clean Cities Coalition, coordinated by the EERC and formally designated by DOE, has worked to promote biodiesel through demonstrations using government fleets in the cities of Grand Forks, North Dakota, and Winnipeg, Manitoba, Canada, and presentations to fleet managers and the public. SDSRPC is developing activities to promote the use of biodiesel in South Dakota. Two biodiesel facilities near Minot, North Dakota, have also begun production in 2007 to accommodate the growing market in the Dakotas.

Goals and Objectives

The goal of this project was to promote biodiesel education and outreach for production and utilization of biodiesel. Objectives were, therefore, to conduct education workshops in the region as follows:

- South Dakota Biodiesel Workshops – to promote utilization of biodiesel in transportation.
- North Dakota Biodiesel Workshop – to provide information on biodiesel issues from production to end use.
- A biodiesel education session at a regional conference.

Experimental

A total of three biodiesel workshops were held: two in South Dakota and one in North Dakota, and a biofuel session was included in the fourth annual Biomass '06: Power, Fuels, and Chemicals Workshop. The EERC coordinated the logistics for each event.

The EERC held two half-day workshops targeting fleet managers in South Dakota in collaboration with the SDSRPC. Limiting efforts to only two workshops provided the opportunity to locate in higher-population areas, generating a larger audience and providing a bigger impact to state efforts. The South Dakota workshops focused on the implementation of biodiesel fuel in vehicles and were targeted toward managers of city and school bus, private,

state, and GSA fleets. The registration fee for the South Dakota workshops was \$10 per person to help cover expenses.

A full-day biodiesel education workshop was conducted in North Dakota, in collaboration with the North Dakota Department of Agriculture and the North Dakota Division of Community Services. The North Dakota Soybean Council sponsored a presenter. This workshop targeted a general audience and addressed the full spectrum of biodiesel production and utilization, including feedstocks, processing, marketing, and usage. The registration fee of \$25 per person was implemented to assist with workshop expenses.

A Transportation Biofuels session was held as part of the Biomass '06: Power, Fuels, and Chemicals Workshop. The Biomass Workshop targeted a general audience and the session provided an overview of biofuels, such as biodiesel, hydrogen, and ethanol, as well as the status of chosen biofuel facilities and processes.

The EERC coordinated all workshop logistics. This included mailing lists, brochure development and subsequent mailing, registration, and meeting accommodations, food and refreshments, and handout materials. The EERC also solicited speakers and developed the program agenda and technical materials. The events were open to the public, and the media were invited.

Results and Discussion

Over 300 individuals were presented with biodiesel education and outreach materials and presentations during the workshop and session events conducted from this effort, covering issues such as fleet utilization, feedstocks through general end use, and current industry status. At least 80% of feedback evaluations rated the events as *Good* or better.

South Dakota Biodiesel Workshops

The South Dakota workshops were held March 27, 2007, in Rapid City and March 28, 2007, in Sioux Falls, both as 4-hour half-day sessions. Topics included an overview of biodiesel and facts concerning biodiesel usage in fleets. Presentation materials were provided by SDSRPC and the National Biodiesel Board (NBB), presented by EERC staff. A short NBB video describing methods to ensure biodiesel quality was also shown. In addition, Cenex representatives offered a brief summary of biodiesel distribution in the area. A small group from Ellsworth Air Force Base also attended the Rapid City workshop and provided an account of experiences using biodiesel. Copies of the presentations were provided as well as packets containing fuel supplier and equipment dealer information, supplied by the SDSRPC. The registration fee included workshop materials, a continental breakfast, and midmorning refreshment.

The workshops attracted 25 attendees total and four media outlets. The attendees represented 14 organizations from the local area, a majority of which were end users, sellers, or government-affiliated. Two-thirds of the participants provided feedback on the workshops.

About 90% of those who responded rated the workshop as *Good* or better, 80% giving a score of at least “8” on a scale where “10” was considered *Excellent*.

North Dakota Biodiesel Workshop

The North Dakota workshop was held March 29, 2007, in Fargo, North Dakota, as an 8-hour all-day session. The workshop focused on the growing biodiesel industry, crop oil grower issues, the refining process, transportation issues, marketing and incentives, and user experience. Presentations were made by the EERC; the North Dakota State University (NDSU) Department of Plant Sciences; Northern Canola Growers Association; NDSU Ag & Biosystems Engineering; Kadrmas, Lee, & Jackson; North Dakota Department of Agriculture; the NBB; the city of Brooklyn Park (MN); and the city of Fargo (ND). Copies of the presentations were supplied. Panel discussions were also allowed at the conclusion of the late morning and afternoon sessions, giving the audience an opportunity to discuss biodiesel issues with the presenters. The registration fee included course materials along with a continental breakfast, lunch, and morning and afternoon refreshments.

This workshop hosted 101 attendees and attracted two media outlets. The attendees hailed from the tristate area of North Dakota, South Dakota, and Minnesota, representing 63 organizations, a majority of which were research- or academia-affiliated, sellers, government-affiliated, and potential investors. Half the participants provided feedback on the workshop. About 90% of those who responded rated the workshop as *Good* or better, 80% giving a score of at least “8” on a scale where “10” was considered *Excellent*.

Biofuel Session at a Regional Conference

The Transportation Biofuels session occurred during the Biomass Workshop held at the EERC, July 18–19, 2006. Specific biodiesel topics included updates on vegetable oil-derived fuels from Archer Daniels Midland Company (ADM), biofuel production in Canada from Ag-West Bio Inc., a proposed biodiesel facility in Minot, North Dakota, from Dakota Skies Biodiesel. Copies of the presentations were provided to all workshop attendees.

Through the workshop, the Transportation Biofuels session reached an audience of nearly 200 representing four countries and over 100 organizations, primarily industry, research or academia, and government-affiliated. One-third of the participants provided feedback on the session. About 80% of those who responded gave the biodiesel presentations a score of at least “4” on a scale where “5” was considered *Excellent*.

Conclusions

The South Dakota and North Dakota Biodiesel Workshops and the Biomass Workshop biofuels session were successful endeavors, receiving numerous positive comments from participants. All attendees gained useful information from industry and peers that will enable them to make well-founded decisions on biodiesel production, utilization, and investment.

References

None.

APPENDIX A
DETAILED GAS SAMPLING AND ANALYSIS

Table A-1. Detailed Gas Sampling and Analysis

Date	3/25/2008	3/26/2008	3/26/2008	3/26/2008	3/27/2008	3/27/2008	3/27/2008	3/27/2008	3/27/2008	3/27/2008
Time	11:20	10:00	11:00	12:13	10:15	11:00	11:36	12:25	13:00	13:43
Gas Bag Sample #	1	3	4	5	6	7	8	9	10	11
Fuel	Wood Chips	Wood Pellets	Wood Pellets	Sawdust	Sawdust (char)	Wheat Straw	Wheat Straw	Com Silage	Sawdust	Sawdust
Hydrogen	1.42%	10.77%	14.81%	13.88%	14.70%	11.94%	12.25%	14.50%	9.58%	12.84%
Carbon Dioxide	14.75%	15.20%	14.59%	19.02%	10.98%	9.06%	14.80%	15.74%	15.37%	16.11%
Propylene		0.07%	0.07%	0.19%	0.08%	0.05%	0.06%	0.15%	0.28%	0.16%
Acetylene		0.30%	0.04%							
1-butene				0.02%					0.02%	0.01%
iso-butene				0.02%					0.01%	
t-2-butene				0.02%					0.01%	
c-2-butene				0.01%						
1,3 butadiene			0.03%	0.04%					0.03%	
Ethylene	0.05%	0.46%	0.69%	0.59%	0.20%	0.04%	0.11%	0.22%	0.44%	0.30%
Ethane		0.06%	0.13%	0.33%	0.08%		0.06%	0.08%	0.20%	0.12%
Oxygen	5.86%	1.19%	1.21%	1.24%	1.77%	1.55%	2.01%	2.14%	5.64%	3.59%
Nitrogen	74.30%	54.16%	46.11%	45.43%	51.63%	54.95%	57.26%	53.98%	56.53%	54.42%
Methane	1.05%	2.86%	3.67%	4.70%	2.40%	1.13%	1.69%	1.73%	3.18%	2.64%
Carbon Monoxide	2.57%	14.93%	18.65%	14.51%	18.16%	21.28%	11.76%	11.46%	8.71%	9.81%
MW	30.11	27.36	26.12	27	25.74	26.29	27.08	26.66	27.89	27.11
HHV (Btu/scf)	24.3	126.4	161.6	162.3	136.9	120.4	98.9	109.9	110.6	110.9
Sp. Gravity	1.04	0.94	0.9	0.93	0.89	0.91	0.94	0.92	0.96	0.94

APPENDIX B

PRELIMINARY ECONOMIC ANALYSIS

PRELIMINARY ECONOMIC ANALYSIS OF ELECTROCHEMICAL NITROGEN FERTILIZER PRODUCTION USING NO RECOVERED FROM COAL-FIRED POWER PLANT FLUE GAS

Junhua Jiang, Paul Pansegrau, and Ted Aulich
Energy & Environmental Research Center

FERTILIZER PRODUCTION COST PROJECTIONS BASED ON NO-COST NITRIC OXIDE

Preliminary estimates were developed for the cost of producing nitrogen fertilizers via three different electrochemical processes. All three processes are conducted at low temperature and pressure, utilize an aqueous liquid electrolyte, and utilize electricity and nitric oxide (NO) recovered from coal-fired utility emissions as inputs. Cost projections were developed for electrochemical production of:

1. Ammonium nitrate (AN) from NO.
2. Ammonia from NO and hydrogen.
3. Urea from NO, carbon dioxide, and hydrogen.

As shown in Tables B-1–B-3, based on these preliminary estimates, only AN production offers potential market viability, primarily because of the high cost of hydrogen required for the other two processes. The viability of the ammonia and urea processes will improve with lower-cost options for renewable hydrogen production. Assuming an electricity cost of \$0.04 per kilowatt hour (kWh), the projected cost of electrochemical AN production is \$166/ton, which translates to a margin of \$144/ton versus the April 2007 AN market price of \$310/ton. Also as shown in the tables, all cost projections are based on the availability of no-cost NO. Although there will undoubtedly be a cost associated with power plant emission-extracted NO, its value was set at zero to enable easy cost comparison between the three fertilizer production processes. In order to derive a more realistic cost of NO, it is necessary to consider NO recovery in the context of national and state air quality regulations, which in many cases necessitates the use of emission control technologies to meet standards for power plant stack emissions of “oxides of nitrogen” (NO_x), of which NO typically comprises about 95%.

NO_x FORMATION AND EMISSION MITIGATION

NO_x formation as a result of coal combustion can be controlled by 1) limiting excess oxygen in the combustion zone and 2) limiting flame temperature. Although limiting oxygen to an excess of only 2% results in a dramatic decrease in NO_x production, an undesired consequence may be the formation of soot, indicating that a certain amount of fuel value (and fuel cost) is not being utilized for power production. Limiting flame temperature is also effective. This can be easily achieved with “low-NO_x” combustion technology, which involves the use of specially designed burners that spread the flame out over a greater volume of the combustion

Table B-1. Per-Ton AN Electrochemical Production Cost Projections(AN production reaction: $8\text{NO} + 7\text{H}_2\text{O} + 2\text{NH}_3 \rightarrow 5\text{NH}_4\text{NO}_3$)

	\$0.05/kWh ¹	\$0.04/kWh	\$0.03/kWh
Electricity Price	\$0.05/kWh ¹	\$0.04/kWh	\$0.03/kWh
Cost of Electricity ²	\$100	\$80	\$60
Cost of Ammonia ³	\$38	\$38	\$38
Capital Cost ⁴	\$24	\$24	\$24
O&M Cost ⁵	\$24	\$24	\$24
Cost of NO	\$0	\$0	\$0
Total Cost	\$186	\$166	\$146
Total Revenue ⁶	\$124	\$144	\$164

¹ Kilowatt hour.² Cell voltage of 1.2 V and current efficiency of 75%.³ Based on anhydrous ammonia price of \$450/ton.⁴ Based on capital cost for comparably sized water electrolysis system.⁵ Based on operating and maintenance cost for comparably sized water electrolysis system.⁶ April 2007 AN market price of \$310/ton minus total cost.**Table B-2. Per-Ton Ammonia Electrochemical Production Cost Projections**(ammonia production reaction: $2\text{NO} + 5\text{H}_2 \rightarrow 2\text{NH}_3 + 2\text{H}_2\text{O}$)

	\$0.05/kWh	\$0.04/kWh	\$0.03/kWh
Electricity Price	\$0.05/kWh	\$0.04/kWh	\$0.03/kWh
Hydrogen Price	\$3/kg ¹	\$2/kg	\$1/kg
Cost of Electricity	\$10	\$8	\$6
Cost of Hydrogen	\$882	\$588	\$294
Capital Cost	\$57	\$57	\$57
O&M Cost	\$56	\$56	\$56
Cost of NO	\$0	\$0	\$0
Total Cost	\$1005	\$709	\$413
Total Revenue ²	-\$555	-\$259	\$37

¹ Kilogram.² April 2007 ammonia price of \$450/ton minus total cost.**Table B-3. Per-Ton Urea Electrochemical Production Cost Projections**(urea production reaction: $2\text{NO} + \text{CO}_2 + 5\text{H}_2 \rightarrow \text{CO}(\text{NH}_2)_2 + 3\text{H}_2\text{O}$)

	\$0.05/kWh	\$0.04/kWh	\$0.03/kWh
Electricity Price	\$0.05/kWh	\$0.04/kWh	\$0.03/kWh
Hydrogen Price	\$3/kg	\$2/kg	\$1/kg
Cost of Electricity	\$513	\$410	\$308
Cost of CO ₂	\$13	\$13	\$13
Cost of Hydrogen	\$535	\$357	\$178
Capital Cost	\$35	\$35	\$35
O&M Cost	\$34	\$34	\$34
Cost of NO	\$0	\$0	\$0
Total Cost	\$1130	\$849	\$568
Total Revenue ¹	-\$815	-\$534	-\$253

¹ April 2007 urea price of \$315/ton minus total cost.

chamber, resulting in fewer hot spots and, therefore, less NO_x. Another method involves injection of water into a flame, reducing the temperature of the flame. Both temperature-reduction measures have the consequence of increasing fuel consumption and cost by reducing the amount of coal energy content converted to steam or power. While the above-described strategies for limiting NO_x are useful, they are not good enough for many power producers to meet U.S. Environmental Protection Agency (EPA) emission requirements.

The two currently available commercial methods for removal of NO_x from stack gases are selective catalytic reduction (SCR) and selective noncatalytic reduction (SNCR). Both methods have in common the requirement that anhydrous ammonia be injected into the flame zone of the combustion chamber. A chemical reaction occurs between ammonia and NO_x, resulting in the formation of elemental nitrogen (N₂)—which is present in air at a concentration of approximately 78%—and water. Both technologies incur operating expenses of \$2100 to \$2500 per ton of NO_x removed (assuming 80% removal), which could translate to an electricity rate increase of at least \$0.004 per kWh based on a 30-year power generation facility lifetime. A NO_x control technology that may represent an economic alternative to SCR or SCNR is a process currently being developed by Cansolv Technologies, Inc., of Montreal, Quebec, Canada. The Cansolv process comprises solvent extraction of NO_x from a stack gas, followed by electrolytic solvent regeneration to yield solvent for recycle and a 99.5% pure NO stream, which can then be converted to N₂ in a “reduction” burner—or used as a feedstock for fertilizer production. Not only is the Cansolv process (as configured with NO reduction to N₂) projected to be significantly cheaper than SCR and SNCR on a per-ton-NO_x mitigation basis, it also offers the potential of yielding an NO stream with value as a chemical feedstock, which would further reduce the cost of mandated NO_x control versus SCR and SNCR.

AN PRODUCTION INTEGRATED WITH POWER PLANT NO RECOVERY

Because of the favorable projected economics of electrochemical AN production (based on the use of no-cost NO), a more in-depth analysis was conducted to enable projecting the economics of integrating AN production with NO_x control at a power plant required by EPA or other regulatory agency to control NO_x emissions. But rather than achieving NO_x control via SCR or SNCR, which requires spending money to convert NO_x to N₂ that then goes up the stack and away, NO_x control would be achieved via an integrated process comprising 1) NO_x removal from stack emissions via the Cansolv solvent extraction process, 2) Cansolv solvent regeneration and generation of NO, and 3) electrochemical conversion of NO to AN fertilizer.

Tables B-4–B-7 show anticipated business costs for a series of NO_x control scenarios. All scenarios are based on the need to control NO_x emissions from the Great River Energy Coal Creek Station power plant at Underwood, North Dakota. The plant includes two power generation units with a total capacity of about 1200 megawatts. EPA-reported data for 1998 cite total annual NO_x emissions from the Coal Creek facility at 26,312 tons, which translates to an AN production of 56,132 tons/year based on 80% NO_x recovery and conversion. Tables B-4 and B-5 project the annual cost of NO_x control using SCR and integrated Cansolv-based NO_x control–AN production, respectively, for the first 5 years of operation. Tables B-6 and B-7

Table B-4. Projected Cost of NO_x Control via SCR for Years 1–5

Sales			Assumptions
1	Cash	\$0	Note 1
2	Credit	\$0	
	Total sales (1+2)	\$0	
Variable Costs			
3	Utilities, services, and feedstocks	\$19,678,400	
4	Wages and salaries	\$1,400,000	Note 2
	Total variable costs (3 + 4)	\$21,078,400	
	Gross profit as a percentage of sales (c% <i>a</i> x 100)	\$0	
Fixed Costs			
5	Production/operation	\$0	Calculated
6	Other fixed costs	\$9,900,000	5% FCI (Note 3)
7	Selling and distribution	\$0	10% of sales
8	Administration	\$280,000	20% of wages and salaries
9	Other expenses	\$100,000	Contingency
10	Finance charges	\$19,800,000	10% of FCI
11	Depreciation	\$39,600,000	5 years to pay down
	Total fixed costs	\$69,680,000	
	Total cost	\$90,758,400	

Notes: 1) Coal Creek Units 1 and 2.

2) Four technicians/shift at \$40/h (\$28.60/h wage x 1.4).

3) Fixed-capital investment of \$198 million.

project the annual cost of SCR and integrated NO_x control–AN production, respectively, for Year 6 and beyond. As shown in these preliminary projections, integrated NO_x control–AN production offers the potential to:

- Significantly reduce the annual cost of commercial utility NO_x control versus SCR by approximately \$50 million for Years 1–5 and by about \$21 million for Year 6 and beyond.
- Establish a new, economically viable fertilizer industry that can optimally utilize wind-generated and other intermittent/low-cost sources of electricity without the need for increased transmission capacity, thereby enabling widespread rural economic growth.
- Provide an affordable, domestic, reliable source of fertilizer for U.S. farmers.

Based on current total U.S. coal-fired electricity generation capacity, AN fertilizer production from emission-extracted NO has the potential to reach about 7–10 million tons/year. Current U.S. nitrogen fertilizer consumption is about 15–19 million tons/year, of which about 6–9 million tons/year is AN. In addition to the economic projections described here, it is important to consider that most current AN production utilizes hydrogen derived from natural gas as a process input and that the economic competitiveness of electrochemical fertilizer production will increase along with any increase in natural gas price.

Table B-5. Projected Cost of Integrated NO_x Control–AN Production for Years 1–5

Sales			Assumptions
1	Cash	\$17,401,000	Note 1
2	Credit	\$0	
A	Total sales (1+2)	\$17,401,000	Note 2
Variable Costs		\$0	
3	Utilities, services, and feedstocks	\$18,742,388	Calculated
4	Wages and salaries	\$2,276,000	Note 3
B	Total variable costs (3 + 4)	\$21,018,388	
C	Gross profit (A – B)	-\$3,617,388	
D	Gross profit as a percentage of sales (C%A x 100)	-\$20.79	
Fixed Costs			
5	Production/operation	\$0	Calculated
6	Other fixed costs	\$5,145,000	5% FCI (Note 4)
7	Selling and distribution	\$870,050	5% of sales
8	Administration	\$522,744	20% of wages and salaries
9	Other expenses	\$200,000	
10	Finance charges	\$10,290,000	10% FCI
11	Depreciation	\$20,580,000	5 years to pay down
E	Total fixed costs	\$37,607,794	
	Net profit before tax (C – E)	-\$41,225,182	
	Total cost	\$41,225,182	

Notes: 1) Coal Creek Units 1 and 2 (1998).

2) 56,132 tons of AN at \$310/ton, assuming 80% NO_x capture and conversion.

3) Two technicians/shift at \$50/h (\$35/h wage x 1.4).

4) Fixed-capital investment of \$102,900,000 includes cost of Cansolv unit and AN plant.

Table B-6. Projected Cost of SCR for Year 6 and Beyond

Sales			Assumptions
1	Cash	\$0	Note 1
2	Credit	\$0	
Total sales (1+2)		\$0	
Variable Costs			
3	Utilities, services, and feedstocks	\$19,678,400	Note 2
4	Wages and salaries	\$1,400,000	Note 3
Total variable costs (3 + 4)		\$21,078,400	
Gross profit as a percentage of sales (C%A x 100)		\$0	
Fixed Costs			
5	Production/operation	\$0	Calculated
6	Other fixed costs	\$9,900,000	5% FCI
7	Selling and distribution	\$0	10% of sales
8	Administration	\$280,000	20% of wages and salaries
9	Other expenses	\$100,000	
10	Finance charges	\$0	Plant paid off
11	Depreciation	\$0	Plant paid off
Total fixed costs		\$10,280,000	
Total cost		\$31,358,400	

Notes: 1) Coal Creek Units 1 and 2 (1998).

2) Projected cost from confidential source.

3) Four technicians/shift at \$40/h (\$28.60/h wage x 1.4).

Table B-7. Projected Cost of Integrated NO_x Control–AN Production for Year 6 and Beyond

Sales			Assumptions
1	Cash	\$17,401,000	Note 1
2	Credit	\$0	
A	Total sales (1+2)	\$17,401,000	Note 2
Variable Costs			
3	Utilities, services, and feedstocks	\$18,742,388	Calculated
4	Wages and salaries	\$2,276,000	Note 3
B	Total variable costs (3 + 4)	\$21,018,388	
C	Gross profit (A – B)	–\$3,617,388	
D	Gross profit as a percentage of sales (C/A x 100)	–\$20.79	
Fixed Costs			
5	Production/operation	\$0	Calculated
6	Other fixed costs	\$5,145,000	5% FCI (Note 4)
7	Selling and distribution	\$870,050	5% of sales
8	Administration	\$522,744	20% of wages and salaries
9	Other expenses	\$200,000	
10	Finance charges	\$0	Plant paid off
11	Depreciation	\$0	Plant paid off
E	Total fixed costs	\$6,737,794	
F	Net profit before tax (C – E)	–\$10,355,182	
	Total cost	\$10,355,182	

Notes: 1) Coal Creek Units 1 and 2 (1998).

2) 56,132 tons of AN at \$310/ton, assuming 80% NO_x capture and conversion.

3) Two technicians/shift at \$50/h (\$35/h wage x 1.4).

4) Fixed-capital investment of \$18.9 million.